

**SHEAR RESISTANCE OF OIL PALM SHELL CONCRETE
BEAMS WITH AND WITHOUT SHEAR
REINFORCEMENT**

MEI YUN CHIN

**Thesis submitted to the University of Nottingham
for the degree of Doctor of Philosophy**

August 2014

Abstract

In recent years, the use of Oil Palm kernel Shell (OPS) aggregate as coarse aggregate in concrete has received increasing attention due to its environmental and economic benefits. To date, considerable amount of research have been carried out to aid the understanding of its concrete mixture designs and its material properties, but, only limited amount of works have been carried out to aid the current understanding with respect to its shear resistance.

The main objective of this research was to investigate the shear resistance of Oil Palm kernel Shell Concrete (OPSC), and to compare with the conventional Normal Weight Concrete (NWC) through experimental and analytical study. The experimental work carried out in this research involved destructive testing of forty-five numbers of beam specimens, of which twenty-nine beams (24 casted with OPSC and 5 casted with NWC) were casted without shear reinforcement while the remaining sixteen beams (11 casted with OPSC and 5 casted with NWC) were casted with shear reinforcement. The main variables for beams casted without shear reinforcement were the concrete strength (f_{cu}), overall section depth (h), longitudinal reinforcement (ρ), and span to depth ratio (a/d). Whilst the main variables for beams casted with shear reinforcement were concrete strength (f_{cu}), shear reinforcement (ρ_s) and inclination of shear cracks (θ).

For beams casted without shear reinforcement, three distinct failure mechanisms were observed from the tests: the shear compression mechanism (associated with $a/d < 2.5$); the diagonal tension mechanism (associated with $a/d = 2.5$ and $\rho = 0.88\%$); and the shear mechanism (associated with $a/d \geq 2.5$ and $\rho > 0.88\%$). Whilst for OPSC

beams casted with shear reinforcement, shear compression failure was observed for the tests.

A comparative study was carried out to investigate if there are any differences on the ultimate shear resistance and the shear failure mechanism between the OPSC beams and NWC beams. In general, all specimens (OPSC and NWC) were found to fail in similar failure mechanism; however, some variations have been noted in the ultimate resistance with respect to span to depth ratio, concrete strength, and longitudinal steel ratio (for beams without shear reinforcement) and concrete strength (for beams with shear reinforcement).

An analytical study was carried out using the upper bound approach to evaluate the observed shear failure mechanisms, and hence, to predict the failure loads. A theoretical model was developed for each of the casting condition. In addition, design models based on Eurocode 2 (EC2) and BS8110 have been developed. In all cases, the proposed models achieved good agreement with the test results.

Publications

CHIN, M.Y. and LAU, T.L., *Shear Resistance of Non-Reinforced Oil Palm Shell Concrete Beams*, Advance Materials Research. Vol.587, 2012, pp. 130-143.

Acknowledgements

I would like to express the deepest gratitude to my supervisor, Associate Professor Dr. Teck Leong Lau, for his advice, support, and interest in the work. Through him I have greatly improved my understanding on reinforced concrete beams. Without his guidance and patience, the present work would not be possible.

I would like to thank the University of Nottingham Malaysia for the scholarship, which provided me the opportunity to undertake the research programme.

I would like to express my gratitude to the technical staff of Department Civil Engineering's laboratory for their friendly assistance during the period of research.

I would like to express my appreciation and gratitude to my family, especially my parents, for their financial support and encouragement for my education. Without them, I won't be who I am today. I would also like to thank my brothers, sister in laws, and nephews for their support.

Table of Contents

	Page No.
Abstract	i
Publications	iii
Acknowledgments	iv
Table of Contents	v
List of Tables	xi
List of Figures	xiv
Notations	xxiv
Chapter 1 Introduction	1
1.1 Introduction	1
1.2 Problem Statement	2
1.3 Objectives and scope	3
1.3.1 Objectives	3
1.3.2 Scope	3
Chapter 2 Literature Review	7
2.1 Introduction	7
2.2 Shear for Normal Weight Concrete (NWC) beams	8
2.2.1 Shear for NWC beams without shear reinforcement	10
2.2.1.1 Shear transfer mechanism	10
2.2.1.2 Empirical Approach	13
2.2.1.3 Concrete Plasticity Approach	25
2.2.1.4 Building Code Approach	27
2.2.1.4.1 BS8110 Code	27
2.2.1.4.2 Eurocode 2	28
2.2.1.4.3 ACI Code	29
2.2.2 Shear for NWC beams with shear reinforcement	29
2.2.2.1 Shear transfer mechanism	30
2.2.2.2 Empirical Approach	31
2.2.2.3 Concrete Plasticity Approach	39
2.2.2.4 Building Code Approach	41
2.2.4.1 BS8110 Code	41

2.2.4.2	Eurocode 2	42
2.2.4.3	ACI Code	44
2.3	Size effect	45
2.3.1	Beams without shear reinforcement	45
2.3.2	Beams with shear reinforcement	49
2.4	Oil Palm Shell Concrete (OPSC)	51
2.4.1	Properties of Oil Palm Shell (OPS) aggregates	51
2.4.2	Oil Palm Shell Concrete (OPSC) mix design	52
2.4.3	Flexural strength of OPSC	55
2.5	Shear strength of OPSC beams	55
2.5.1	Shear strength of OPSFC beams	56
2.5.2	Shear behaviour of reinforced palm kernel shell concrete beams	57
2.6	Flexural behaviour of OPSC beams	58
2.6.1	Flexural behaviour of reinforced Lightweight Concrete Beams made with OPS	58
2.6.2	Ductility behaviour of reinforced Palm Kernel Shell Concrete beams	59
2.7	Summary	60
Chapter 3	Experimental Work	80
3.1	Introduction	80
3.2	Concrete Material Properties	81
3.2.1	Oil Palm Shell Concrete (OPSC)	81
3.2.2	Normal Weight Concrete (NWC)	82
3.3	Reinforcement	82
3.3.1	Specimens cast without shear reinforcement	82
3.3.2	Specimens cast with shear reinforcement	83
3.4	Beam specimens cast without shear reinforcement	83
3.4.1	OPSC beam specimens	83
3.4.2	NWC beam specimens	84
3.5	Beam specimens cast with shear reinforcement	85
3.5.1	OPSC beam specimens	85
3.5.2	NWC beam specimens	85
3.6	Fabrication of specimens	86
3.6.1	Mould	86

3.6.2	Casting and curing	86
3.7	Test setup	87
3.7.1	Beam specimens cast without shear reinforcement	88
3.7.2	Beam specimens cast with shear reinforcement	88
3.8	Central deflection	88
3.9	Testing procedures	89
Chapter 4	Failure Mechanisms and Test Results	108
4.1	Introduction	108
4.2	Specimens cast without shear reinforcement	109
4.2.1	Overall behaviour of OPSC beams and NWC beam specimens	109
4.2.2	Central deflection	115
4.2.3	Ultimate Failure Loads	116
4.2.3.1	Span to depth ratio	117
4.2.3.2	Longitudinal steel ratio	119
4.2.3.3	Concrete strength	121
4.2.3.4	Section depth	123
4.3	Specimens cast with shear reinforcement	124
4.3.1	Overall behaviour of OPSC beams and NWC beam specimens	124
4.3.2	Central deflection	127
4.3.3	Ultimate Failure Loads	128
4.3.3.1	Shear reinforcement spacing	129
4.3.3.2	Inclination angle of shear cracks	130
4.3.3.3	Concrete strength	131
4.4	Summary	133
Chapter 5	Theoretical Plastic Models	172
5.1	Introduction	172
5.2	Beams cast without shear reinforcement	173
5.2.1	Theoretical plastic model for concrete beam without shear reinforcement (CP-I Model)	173
5.2.2	Modification on parameters	175
5.2.2.1	Shear span to height ratio, a/h	175
5.2.2.2	Longitudinal steel ratio, ρ	176

5.2.2.3	Cylindrical concrete strength, σ_c	177
5.2.2.4	Overall section depth, h	177
5.2.3	Comparisons with test results	178
5.3	Beams cast with shear reinforcement	179
5.3.1	Theoretical plastic model for concrete beam with shear reinforcement (CP-II Model)	179
5.3.2	Modification on parameters	180
5.3.2.1	Cylindrical concrete strength, σ_c	181
5.3.2.2	Shear reinforcement ratio, ρ_s	182
5.3.2.3	Inclination angle of shear cracks, θ	182
5.3.3	Comparisons with test results	183
5.4	Summary	183
Chapter 6	BS8110 Design Models	195
6.1	Introduction	195
6.2	Beams cast without shear reinforcement	197
6.2.1	BS8110 design model for concrete beam without shear reinforcement (BS8110-I Model)	197
6.2.2	Modification on parameters	198
6.2.2.1	Span to effective depth ratio, a/h	198
6.2.2.2	Longitudinal steel ratio, ρ	199
6.2.2.3	Cube concrete strength, f_{cu}	200
6.2.2.4	Beam effective depth, d	201
6.2.3	Comparisons with test results	202
6.3	Beams cast with shear reinforcement	203
6.3.1	BS8110 design model for concrete beam with shear reinforcement (BS8110-II Model)	203
6.3.2	Modification on parameters	204
6.3.2.1	Shear reinforcement ratio, $\frac{A_{sw}}{s}$	204
6.3.2.2	Cube concrete strength, f_{cu}	205
6.3.2.3	Shear to effective depth ratio, a/d	206
6.3.3	Comparisons with test results	206
5.4	Summary	207

Chapter 7 Eurocode 2 Design Models	217
7.1 Introduction	217
7.2 Beams cast without shear reinforcement	217
7.2.1 Eurocode 2 design model for concrete beam without shear reinforcement (EC2-I Model)	219
7.2.2 Modification on parameters	220
7.2.2.1 Span to effective depth ratio, a/d	220
7.2.2.2 Longitudinal steel ratio, ρ	221
7.2.2.3 Cylindrical concrete strength, f_{ck}	222
7.2.2.4 Beam effective depth, d	223
7.2.3 Comparisons with test results	224
7.3 Beams cast with shear reinforcement	225
7.3.1 Eurocode 2 design model for concrete beam with shear reinforcement (EC2-II Model)	225
7.3.2 Modification on parameters	226
7.3.2.1 Inclination angle of shear cracks, θ	226
7.3.2.2 Shear reinforcement ratio, $\frac{A_{sw}}{s}$	226
7.3.3 Comparisons with test results	227
7.4 Summary	228
Chapter 8 Conclusions and Future Work	237
8.1 Summary of current study	238
8.2 Mix design of Oil Palm kernel Shell Concrete (OPSC)	238
8.3 Failure Mechanisms and Effect of Variables on OPSC beams	239
8.4 Comparisons between OPSC and NWC beams	240
8.5 Theoretical models	240
8.5.1 CP-I Model	241
8.5.2 CP-II Model	241
8.6 BS8110 design models	242
8.6.1 BS8110-I Model	243
8.6.2 BS8110-II Model	244
8.7 Eurocode 2 design models	244
8.7.1 EC2-I Model	245

8.7.2 EC2-II Model	246
8.8 Future works	247
References:	248
Appendices	253

List of Tables

	Page No.
Chapter 2	
Table 2.1	Properties of OPS Aggregate and Crushed Granite Aggregate 61
Table 2.2	Material properties of OPSC by researchers ⁶ 62
Table 2.3	Flexural strength of OPSC ⁶ 63
Table 2.4	V_{min} for NWC beams without shear reinforcement based on EC2 ⁴⁸ 63
Chapter 3	
Table 3.1	Mix design of Oil Palm Shell Concrete (OPSC) 90
Table 3.2	Mix design of Normal Weight Concrete Beam (NWC) 90
Table 3.3	Details of OPSC beam specimens cast without shear reinforcement 91
Table 3.4	Details of NWC beam specimens cast without shear reinforcement 91
Table 3.5	Details of OPSC beam specimens cast with shear reinforcement 92
Table 3.6	Details of NWC beam specimens cast with shear reinforcement 92
Table 3.7	Curing and concrete strength for OPSC beam specimens cast without shear reinforcement 93
Table 3.8	Curing and concrete strength for NWC beam specimens cast without shear reinforcement 93
Table 3.9	Curing and concrete strength for OPSC beam specimens cast with shear reinforcement 94
Table 3.10	Curing and concrete strength for NWC beam specimens cast with shear reinforcement 94
Chapter 4	
Table 4.1	Test results of OPSC beam specimens cast without shear reinforcement 136
Table 4.2	Test results of NWC beam specimens cast without shear reinforcement 136

Table 4.3	Cracking load of OPSC beam specimens cast without shear reinforcement	137
Table 4.4	Cracking load of NWC beam specimens cast without shear reinforcement	138
Table 4.5	Span to effective depth ratio, a/d for OPSC beam specimens cast without shear reinforcement	138
Table 4.6	Longitudinal steel ratio, ρ for OPSC beam specimens cast without shear reinforcement	139
Table 4.7	Cube concrete strength, f_{cu} for OPSC beam specimens cast without shear reinforcement	139
Table 4.8	Overall sectional depth, h for OPSC beam specimens cast without shear reinforcement	140
Table 4.9	Test results of OPSC beam specimens cast with shear reinforcement	140
Table 4.10	Test results of NWC beam specimens cast with shear reinforcement	140
Table 4.11	Cracking load of OPSC beam specimens cast with shear reinforcement	141
Table 4.12	Cracking load of NWC beam specimens cast with shear reinforcement	141
Table 4.13	Shear reinforcement spacing, s for OPSC beam specimens cast with shear reinforcement	142
Table 4.14	Angle inclination, θ for OPSC beam specimens cast with shear reinforcement	142
Table 4.15	Cube concrete strength, f_{cu} for OPSC beam specimens cast with shear reinforcement	143
 Chapter 5		
Table 5.1	Comparisons of shear strength predictions with respect to the test results of OPSC beams cast without shear reinforcement	185
Table 5.2	Comparisons of shear strength predictions with respect to the test results of OPSC beams cast with shear reinforcement	187

Chapter 6

Table 6.1 Comparisons of shear strength predictions with respect to the test results of OPSC beams cast without shear reinforcement 208

Table 6.2 Comparisons of shear strength predictions with respect to the test results of OPSC beams cast with shear reinforcement 209

Chapter 7

Table 7.1 Comparisons of shear strength predictions with respect to the test results of OPSC beams cast without shear reinforcement 229

Table 7.2 Comparisons of shear strength predictions with respect to the test results of OPSC beams cast with shear reinforcement 230

List of Figures

		Page No.
Chapter 1		
Figure 1.1	Oil Palm Kernel Shell (OPS) aggregate	5
Figure 1.2	Plantation of palm oil tree	5
Figure 1.3	Cross section of palm oil fruit	6
 Chapter 2		
Figure 2.1	Three combined actions in reinforced concrete beams without shear reinforcement ²⁷	64
Figure 2.2	Hypothesis of systematically failure for beams failed in diagonal tension ³⁰	64
Figure 2.3	Formation of diagonal tension crack for beams without shear reinforcement ³¹	64
Figure 2.4	Shear resistance vs a/d ratio for Mattock's data ³¹	65
Figure 2.5	Reserve shear resistance beyond critical condition (uniform load and no shear reinforcement) ³⁴	65
Figure 2.6	Comparisons of calculated and observed critical shear intensities ³⁴	66
Figure 2.7	Shear stress at failure vs a/d ³⁵	66
Figure 2.8	$\frac{M_u}{M_{f1}}$ vs a/d ³⁵	67
Figure 2.9	Relation between ρ and v_u ³⁶	67
Figure 2.10	Ultimate shear force vs moment shear ratio for $\rho = 1.7\%$ and $\rho = 2.67\%$ for both deformed bars and plain bars ³⁸	68
Figure 2.11	Test results of series a/d=1.5, 2.5 and 3.6 with respect to concrete strength ³⁹	68
Figure 2.12	Test results of theoretical vs experimental shear strength values ⁴¹	69
Figure 2.13	Effect of variables: reinforcement ratio, compressive strength and shear span on cracking and ultimate shear strength ⁴²	70
Figure 2.14	Plastic approach for reinforced concrete beams without shear reinforcement ⁴⁶	70

Figure 2.15	Four combined actions in reinforced concrete beams with shear reinforcement ²⁷	71
Figure 2.16	Diagonal tension cracks crossed one of the shear reinforcement ⁵⁰	71
Figure 2.17	Comparison of test data with proposed formula ⁵¹	71
Figure 2.18	Shear contributions of shear reinforcement ³⁴	72
Figure 2.19	Plastic approach for reinforced concrete beams with shear reinforcement ⁴⁶	72
Figure 2.20	Test results of beams with varying depth ⁵⁵	73
Figure 2.21	Test specimens casted by Kani ⁵⁵	73
Figure 2.22	Test specimens Series C casted by Leonhardt and Walther ⁵⁵	74
Figure 2.23	Test specimens Series D casted by Leonhardt and Walther ⁵⁵	74
Figure 2.24	Test specimens casted by Taylor ⁵⁵	75
Figure 2.25	Illustration of size effect according to theory of linear fracture mechanics and nonlinear fracture mechanics ⁵⁷	75
Figure 2.26	Comparisons of the design formula with literature data ⁵⁷	76
Figure 2.27	Experimental values vs Calculated values of mean nominal shear strength for beams without shear reinforcement ⁵⁸	76
Figure 2.28	Relative nominal shear strength of gravel and lightweight concrete beams as function of the effective cross sectional depth ($a/d=3$) ⁵⁹	77
Figure 2.29	Shear stresses at inclined cracking and failure vs effective depth for short beams with $a/d=1$ ⁵⁹	77
Figure 2.30	Crack patterns in slender beams ($a/d=3$) with various depth ⁵⁹	78
Figure 2.31	Crack patterns in short beams with various depth ⁵⁹	78
Figure 2.32	Experimental values vs Calculated values of mean nominal shear strength for beams without shear reinforcement ⁶⁰	79
Figure 2.33	Shear stresses vs effective depth for short beams with shear reinforcement ⁵⁹	79
 Chapter 3		
Figure 3.1	Grading curves of OPS Aggregate for OPSC beam specimens	95

Figure 3.2	Grading curve of Fine Aggregate for OPSC and NWC beam specimens	95
Figure 3.3	Grading curves of Gravel Aggregate for NWC beam specimens	96
Figure 3.4	General arrangements of beams without shear reinforcement	96
Figure 3.5	General arrangements of OPSC (3A, 3B, 3C) and NWC (NWCA) beams reinforced with 2T14 (compression), 2T16 (tension), and R6@120 mm (shear reinforcement)	97
Figure 3.6	General arrangements of OPSC (4A, 4B, 4C, 4D, 4E) and NWC (NWCB, NWCD, NWCE) beams reinforced with 2T14 (compression), 2T16 (tension), and R6@80 mm (shear reinforcement)	97
Figure 3.7	General arrangements of OPSC (5A, 5B, 5C) and NWC (NWCC) beams reinforced with 2T(14 + 20) (compression), 2T(16+20) (tension), and R6@60 mm (shear reinforcement)	98
Figure 3.8	General arrangements of steel mould for casting of specimens having overall section depth ≤ 200 mm	99
Figure 3.9	Bolting details of steel mould shown in Figure 3.8	100
Figure 3.10	General arrangements of wooden mould for casting of specimens having overall section depth > 200 mm	101
Figure 3.11	Bolting details of steel mould shown in Figure 3.10	102
Figure 3.12	Test setup for OPSC and NWC beam specimens	103
Figure 3.13	Loading rig for OPSC and NWC beam specimens	103
Figure 3.14	Loading arrangement for all beam specimens cast without shear reinforcement	104
Figure 3.15	Location of shear reinforcement were marked to ensure for correct positioning of loads and supports	104
Figure 3.16	Loading arrangement for OPSC and NWC beam specimens cast with shear reinforcement spaced at 120 mm intervals and loaded with 240 mm shear span	105
Figure 3.17	Loading arrangement for OPSC and NWC beam specimens cast with shear reinforcement spaced at 80 mm intervals and loaded with 240 mm shear span	105
Figure 3.18	Loading arrangement for OPSC and NWC beam specimens cast with shear reinforcement spaced at 60 mm intervals and loaded with 240 mm shear span	106
Figure 3.19	Loading arrangement for OPSC and NWC beam specimens cast with shear reinforcement spaced at 80 mm intervals and loaded with 200 mm shear span	106

Figure 3.20	Loading arrangement for OPSC and NWC beam specimens cast with shear reinforcement spaced at 80 mm intervals and loaded with 160 mm shear span	107
Figure 3.21	Position of mechanical dial gauge for measurements of mid span deflection	107
 Chapter 4		
Figure 4.1	Failure mechanism of OPSC beam cast without shear reinforcement, 10A	144
Figure 4.2	Failure mechanism of OPSC beam cast without shear reinforcement, S1	144
Figure 4.3	Failure mechanism of OPSC beam cast without shear reinforcement, 12A	144
Figure 4.4	Failure mechanism of OPSC beam cast without shear reinforcement, 12B	144
Figure 4.5	Failure mechanism of OPSC beam cast without shear reinforcement, 12C	144
Figure 4.6	Failure mechanism of OPSC beam cast without shear reinforcement, 12D	145
Figure 4.7	Failure mechanism of OPSC beam cast without shear reinforcement, 12E	145
Figure 4.8	Failure mechanism of OPSC beam cast without shear reinforcement, 12F	145
Figure 4.9	Failure mechanism of OPSC beam cast without shear reinforcement, 16A	145
Figure 4.10	Failure mechanism of OPSC beam cast without shear reinforcement, 16B	145
Figure 4.11	Failure mechanism of OPSC beam cast without shear reinforcement, 16C	146
Figure 4.12	Failure mechanism of OPSC beam cast without shear reinforcement, 16D	146
Figure 4.13	Failure mechanism of OPSC beam cast without shear reinforcement, 16E	146
Figure 4.14	Failure mechanism of OPSC beam cast without shear reinforcement, 20A	146
Figure 4.15	Failure mechanism of OPSC beam cast without shear reinforcement, 20B	146
Figure 4.16	Failure mechanism of OPSC beam cast without shear reinforcement, 20C	147
Figure 4.17	Failure mechanism of OPSC beam cast without shear reinforcement, 20D	147

Figure 4.18	Failure mechanism of OPSC beam cast without shear reinforcement, 20E	147
Figure 4.19	Failure mechanism of OPSC beam cast without shear reinforcement, AD1	147
Figure 4.20	Failure mechanism of OPSC beam cast without shear reinforcement, AD2	147
Figure 4.21	Failure mechanism of OPSC beam cast without shear reinforcement, F1	148
Figure 4.22	Failure mechanism of OPSC beam cast without shear reinforcement, F2	148
Figure 4.23	Failure mechanism of OPSC beam cast without shear reinforcement, H2	148
Figure 4.24	Failure mechanism of OPSC beam cast without shear reinforcement, S2	148
Figure 4.25	Failure mechanism of NWC beam cast without shear reinforcement, NWC1	148
Figure 4.26	Failure mechanism of NWC beam cast without shear reinforcement, NWC2	149
Figure 4.27	Failure mechanism of NWC beam cast without shear reinforcement, NWC3	149
Figure 4.28	Failure mechanism of NWC beam cast without shear reinforcement, NWC4	149
Figure 4.29	Failure mechanism of NWC beam cast without shear reinforcement, NWC5	149
Figure 4.30	Load (kN) vs Central deflection (mm) for OPSC beam specimens cast without shear reinforcement of $a/d = 1$ and $\rho = 1.08\%$, 1.92% and 2.99%	150
Figure 4.31	Load (kN) vs Central deflection (mm) for OPSC beam specimens cast without shear reinforcement of $a/d = 1.5$ and $\rho = 1.08\%$, 1.92% and 2.99%	150
Figure 4.32	Load (kN) vs Central deflection (mm) for OPSC beam specimens cast without shear reinforcement of $a/d = 2.5$ and $\rho = 1.92\%$	151
Figure 4.33	Load (kN) vs Central deflection (mm) for OPSC beam specimens cast without shear reinforcement of $a/d = 2.5$ and $\rho = 0.75\%$, 1.08% and 2.99%	151
Figure 4.34	Load (kN) vs Central deflection (mm) for OPSC beam specimens cast without shear reinforcement of $a/d = 3$ and $\rho = 1.08\%$, 1.92% and 2.99%	152
Figure 4.35	Load (kN) vs Central deflection (mm) for NWC beam specimens cast without shear reinforcement	152
Figure 4.36	Surface texture at the interface of major diagonal shear cracks of OPSC beams cast without shear reinforcement	153

(Sectional view)

Figure 4.37	Diagonal shear cracks of OPSC and NWC beams cast without shear reinforcement (Side view)	153
Figure 4.38	V_{OPSC} (kN) vs Shear span to effective depth ratio, a/d for OPSC beam specimens cast without shear reinforcement	154
Figure 4.39	V_{Test} (kN) vs Shear span to effective depth ratio, a/d for OPSC and NWC beam specimens cast without shear reinforcement	154
Figure 4.40	Surface texture of diagonal shear interface of OPSC beams cast without shear reinforcement tested at $a/d=1.5$ and $a/d=2.5$ (Sectional view)	155
Figure 4.41	Surface texture of diagonal shear interface of OPSC and NWC beams cast without shear reinforcement tested at a/d ratio = 1 (Sectional view and Isometric view)	156
Figure 4.42	Surface texture of diagonal shear interface of OPSC and NWC beams cast without shear reinforcement tested at a/d ratio = 2.5 (Sectional view and Isometric view)	157
Figure 4.43	V_{OPSC} (kN) vs Longitudinal steel ratio, ρ (%) for OPSC beam specimens cast without shear reinforcement	158
Figure 4.44	V_{Test} kN) vs Longitudinal steel ratio, ρ (%) for OPSC and NWC beam specimens cast without shear reinforcement	158
Figure 4.45	V_{OPSC} (kN) vs Concrete strength, f_{cu} (N/mm ²) for OPSC beam specimens cast without shear reinforcement	159
Figure 4.46	V_{Test} (kN) vs Concrete strength, f_{cu} (N/mm ²) for OPSC and NWC beam specimens cast without shear reinforcement	159
Figure 4.47	V_{OPSC} (kN) vs Overall section depth, h (mm) for OPSC beam specimens cast without shear reinforcement	160
Figure 4.48	V_{OPSC} (N/mm ²) vs Overall section depth, h (mm) for OPSC and NWC beam specimens cast without shear reinforcement	160
Figure 4.49	V_{Test} (kN) vs Overall section depth, h (mm) for OPSC and NWC beam specimens cast without shear reinforcement	161
Figure 4.50	Failure mechanism of OPSC beam cast with shear reinforcement, 3A	161
Figure 4.51	Failure mechanism of NWC beam cast with shear reinforcement, 3B	161
Figure 4.52	Failure mechanism of NWC beam cast with shear reinforcement, 3C	161
Figure 4.53	Failure mechanism of OPSC beam cast with shear reinforcement, 4A	162
Figure 4.54	Failure mechanism of NWC beam cast with shear reinforcement, 4B	162
Figure 4.55	Failure mechanism of NWC beam cast with shear reinforcement, 4C	162

Figure 4.56	Failure mechanism of OPSC beam cast with shear reinforcement, 5A	162
Figure 4.57	Failure mechanism of NWC beam cast with shear reinforcement, 5B	162
Figure 4.58	Failure mechanism of NWC beam cast with shear reinforcement, 5C	163
Figure 4.59	Failure mechanism of OPSC beam cast with shear reinforcement, 4D	163
Figure 4.60	Failure mechanism of OPSC beam cast with shear reinforcement, 4E	163
Figure 4.61	Failure mechanism of NWC beam cast with shear reinforcement, NWCA	163
Figure 4.62	Failure mechanism of NWC beam cast with shear reinforcement, NWCB	163
Figure 4.63	Failure mechanism of NWC beam cast with shear reinforcement, NWCC	164
Figure 4.64	Failure mechanism of NWC beam cast with shear reinforcement, NWCD	164
Figure 4.65	Failure mechanism of NWC beam cast with shear reinforcement, NWCE	164
Figure 4.66	Load (kN) vs Central deflection (mm) for OPSC beam specimens with shear reinforcement of shear reinforcement spacing = 120 mm	165
Figure 4.67	Load (kN) vs Central deflection (mm) for OPSC beam specimens with shear reinforcement of shear reinforcement spacing = 80 mm	165
Figure 4.68	Load (kN) vs Central deflection (mm) for OPSC beam specimens with shear reinforcement of shear reinforcement spacing = 60 mm	166
Figure 4.69	Load (kN) vs Central deflection (mm) for NWC beam specimens with shear reinforcement	166
Figure 4.70	Surface texture of diagonal shear interface of OPSC and NWC beam specimens cast with shear reinforcement (Sectional view)	167
Figure 4.71	Surface texture of diagonal shear interface of OPSC and NWC beam specimens cast with shear reinforcement (Isometric view)	168
Figure 4.72	V_{OPSC} (kN) vs Shear reinforcement spacing, s (mm) for OPSC beam specimens cast with shear reinforcement	169
Figure 4.73	V_{Test} (kN) vs Shear reinforcement spacing, s (mm) for OPSC and NWC beam specimens cast with shear reinforcement	169
Figure 4.74	V_{OPSC} (kN) vs Inclination of shear cracks, θ (degree) for OPSC beam specimens cast with shear reinforcement	170

Figure 4.75	$V_{Test}(kN)$ vs Inclination of shear cracks, θ (degree) for OPSC and NWC beam specimens cast with shear reinforcement	170
Figure 4.76	$V_{OPSC}(kN)$ vs Concrete strength, f_{cu} (N/mm^2) for OPSC beam specimens cast with shear reinforcement	171
Figure 4.77	V_{Test} (kN) vs Concrete strength, f_{cu} (N/mm^2) for OPSC and NWC beam specimens cast with shear reinforcement	171

Chapter 5

Figure 5.1	$f(a/h)$ vs a/h for Existing plastic model (CP-NS Model) and Modified plastic model (CP-I Model)	188
Figure 5.2	$f(\rho)$ vs $\rho(\%)$ for Existing plastic model (CP-NS Model) and Modified plastic model (CP-I Model)	188
Figure 5.3	$f(\sigma_c)$ vs σ_c (N/mm^2) for Existing plastic model (CP-NS Model) and Modified plastic model (CP-I Model)	189
Figure 5.4	$f(h)$ vs h (mm) for Existing plastic model (CP-NS Model) and Modified plastic model (CP-I Model)	189
Figure 5.5	V_{OPSC}/V_{CP} vs Shear span to height ratio, a/h	190
Figure 5.6	V_{OPSC}/V_{CP} vs Longitudinal steel ratio, ρ (%)	190
Figure 5.7	V_{OPSC}/V_{CP} vs Cylindrical concrete strength, σ_c (N/mm^2)	191
Figure 5.8	V_{OPSC}/V_{CP} vs Overall section depth, h (mm)	191
Figure 5.9	$f(\sigma_c)$ vs σ_c (N/mm^2) for Existing CP Model (CP-S Model) and Modified CP Model (CP-II Model)	192
Figure 5.10	$f(\rho_s)$ vs ρ_s (%) for Existing concrete plastic model (CP-S Model)	192
Figure 5.11	$f(\frac{1}{\tan \theta})$ vs θ (rad) for Existing CP Model (CP-S Model)	193
Figure 5.12	V_{OPSC}/V_{CP} vs Cylindrical concrete strength, σ_c (N/mm^2)	193
Figure 5.13	V_{OPSC}/V_{CP} vs Shear reinforcement ratio, ρ_s (%)	194
Figure 5.14	V_{OPSC}/V_{CP} vs Inclination angle of shear cracks, θ (rad)	194

Chapter 6

Figure 6.1	$f(a/d)$ vs a/d for Existing BS8110 design Model (BS8110-NS Model) and Modified BS8110 design Model (BS8110-I Model)	210
------------	--	-----

Figure 6.2	$f(\rho)$ vs ρ (%) for Existing BS8110 design model (BS8110-NS Model)	210
Figure 6.3	$f(f_{cu}^{1/3})$ vs f_{cu} (N/mm ²) for Existing BS8110 design model (BS8110-NS Model)	211
Figure 6.4	$f(d)$ vs d (mm) for Existing BS8110 design Model (BS8110-NS Model) and Modified BS8110 design Model (BS8110-I Model)	211
Figure 6.5	V_{OPSC}/V_{BS8110} vs Shear span to effective section depth ratio, a/d	212
Figure 6.6	V_{OPSC}/V_{BS8110} vs Longitudinal steel ratio, ρ (%)	212
Figure 6.7	V_{OPSC}/V_{BS8110} vs Cube concrete strength, f_{cu} (N/mm ²)	213
Figure 6.8	V_{OPSC}/V_{BS8110} vs Effective section depth, d (mm)	213
Figure 6.9	$f(\frac{A_{sw}}{s})$ vs $\frac{A_{sw}}{s}$ for Existing BS8110 design model (BS8110-S Model)	214
Figure 6.10	$f(f_{cu}^{1/3})$ vs f_{cu} (N/mm ²) for Existing BS8110 design model (BS8110-S Model)	214
Figure 6.11	$f(\frac{a}{d})$ vs a/d for Existing BS8110 design model (BS8110-S Model) and Modified BS8110 design model (BS8110-II Model)	215
Figure 6.12	V_{OPSC}/V_{BS8110} vs Shear reinforcement ratio, $\frac{A_{sw}}{s}$	215
Figure 6.13	V_{OPSC}/V_{BS8110} vs Cube concrete strength, f_{cu} (N/mm ²)	216
Figure 6.14	V_{OPSC}/V_{BS8110} vs Shear span to effective depth ratio, a/d	216
 Chapter 7		
Figure 7.1	$f(a/d)$ vs a/d for Existing EC2 design Model (EC2-NS Model) and Modified EC2 design Model (EC2-I Model)	231
Figure 7.2	$f(\rho^{1/3})$ vs ρ (%) for Existing EC2 design Model (EC2-NS Model)	231
Figure 7.3	$f(f_{ck}^{1/3})$ vs f_{ck} (N/mm ²) for Existing EC2 design Model (EC2-NS Model)	232
Figure 7.4	$f(k)$ vs d (mm) for Existing EC2 design Model (EC2-NS Model) and Modified EC2 design Model (EC2-I Model)	232
Figure 7.5	V_{OPSC}/V_{CP} vs Shear span to effective depth ratio, a/d	233
Figure 7.6	V_{OPSC}/V_{CP} vs Longitudinal steel ratio, ρ (%)	233

Figure 7.7	V_{OPSC}/V_{CP} vs Cylindrical concrete strength, f_{ck} (N/mm ²)	234
Figure 7.8	V_{OPSC}/V_{CP} vs Effective section depth, d (mm)	234
Figure 7.9	$f(\cot \theta)$ vs θ (degree) for Existing EC2 design Model (EC2-S Model)	235
Figure 7.10	$f(\frac{A_{sw}}{s})$ vs $\frac{A_{sw}}{s}$ for Existing EC2 design Model (EC2-S Model) and Modified EC2 design Model (EC2-II Model)	235
Figure 7.11	V_{OPSC}/V_{EC2} vs Inclination angle of shear cracks, θ (degree)	236
Figure 7.12	V_{OPSC}/V_{EC2} vs Shear reinforcement ratio, $\frac{A_{sw}}{s}$	236

Notations

a	Length of that part of a member traversed by a shear failure plane
A_s	Cross sectional area of longitudinal steel reinforcement
A_{sw}	Cross sectional area of shear reinforcement
b	Breadth of section
d	Effective depth
d'	Depth to compression reinforcement
f_{cu}	Cube concrete strength
f_{ck}	Cylindrical concrete strength
f_{yk}	Characteristic yield strength of reinforcement
f_{yw}	Design yield strength of the shear reinforcement
h	Overall depth of beam section
L	Length or span
M	Moment or bending moment
s	Shear reinforcement spacing
v_c	Design cracking stress of the beam
v_u	Design ultimate shear stress of the beam
V	Total shear strength of the beam
V_c	Design cracking load of the beam
V_u	Design shear force due to ultimate load
ρ	Longitudinal steel ratio
ρ_s	Shear reinforcement ratio
θ	Inclination angle of shear cracks
γ_m	Partial safety factor for material strength
γ_c	Partial safety factor for concrete strength

Chapter 1

Introduction

1.1 Introduction

In recent years, the use of Oil Palm kernel Shell (OPS) (see Figure 1.1) as coarse aggregate in concrete, Oil Palm kernel Shell Concrete (OPSC), has increasingly become popular in research [1-16] owing to its environmental and economic benefits. Due to the scale of palm oil production industry in Malaysia, substantial amount of OPS have therefore resulted. However, these OPS were of no economical values and were mostly left to decay [1], but, in recent years, it has become increasing popular as raw burning materials for power production [17].

OPS (see Figure 1.1) is essentially a by-product of palm oil production (see Figure 1.2). OPS has low bulk density, and when it is used in concrete as coarse aggregate, lightweight concrete is produced. The lightweight nature of the concrete reduces the overall dead load in a structure, hence, lead to smaller foundation size, and results in a great amount of saving in the total construction cost [13].

The OPSC constitutes of cement, sand, OPS and water. Since the introduction of OPSC, considerable amount of research [1-16] have been carried out to aid the understanding of its concrete mixture designs [1-6] and its material properties [7-11].

OPS is brown coloured in nature and it is basically the hard endocarps encasing the palm kernel oil from the palm fruit as shown in Figure 1.3. The OPS extracted from

palm oil production take the shape of crescent, where the convex part of OPS were observed to be rougher than the concave part as indicated in Figure 1.1.

1.2 Problem Statement

Previous researchers [1-11] have been focusing on the mix design and material properties of OPSC. However, only limited amount of works have been carried out to aid the understanding of the OPSC structural resistance, such as bending resistance [12-14] and shear resistance [15 & 16]. Hence, due to the OPS promising potential as lightweight aggregates, and OPSC as lightweight structural concrete, it is apparent that more research are required to develop a comprehensive understanding, particularly, in the area of shear transfer mechanism for its structural elements.

Current understanding on shear transfer mechanism, derives from tests on NWC cast using normal granite aggregates, indicates that shear resistance of reinforced concrete elements derives from aggregate interlocking, dowel action of the longitudinal reinforcement, concrete compression zone and concrete tensile strength. Since the OPS aggregate differed from those of normal aggregates in term of aggregate impact strength, specific gravity, aggregate shape, and bulk density, the shear transfer mechanism of OPSC would expected to be different from those of NWC.

The current design procedures by BS8110 [47] and EC2 [48] for shear transfer mechanism of both the Lightweight Aggregate Concrete (LWAC) and the Normal Weight Concrete (NWC) are derived from the understanding of concrete cast using normal aggregates. Hence, it is apparent that, the current design procedures by BS8110 [47] and EC2 [48] may not be suitable to predict the ultimate shear resistance

of the OPSC beams. Since no guidance has been given from the current codes of practice [47 & 48], it is therefore essential that a research investigation to be carried out to aid the current understanding on shear transfer mechanisms of OPSC beams, both cast without shear reinforcements and with shear reinforcements.

1.3 Objectives and scope

The main objective of this research is to explore the shear resistance of OPSC beams through experimental and analytical study.

1.3.1 Objectives

Objectives of the research include:

1. To develop mix design of OPSC for structural applications.
2. To observe from experimental testing, the effect of variables considered on the ultimate shear failure capacities and the shear failure mechanisms.
3. To compare the ultimate shear failure capacities and shear failure mechanisms between the OPSC beams and NWC beams cast with and without shear reinforcements, respectively.
4. To develop theoretical prediction models using upper bound plastic approach [45 & 46] and simple predictive design models, from those based on the current EC2 [47] and BS8110 [48] to predict the shear carrying resistance of OPSC beams cast with and without shear reinforcements, respectively.

1.3.2 Scope

For OPSC cast without shear reinforcements, the variables considered are concrete strength (σ_c), overall section depth (h), longitudinal steel ratio (ρ), and shear span to height ratio (a/h). While for OPSC beams cast with shear

reinforcements, the effect of variables considered include concrete strength (f_{ck}), shear reinforcements ratio (ρ_s) and inclined angle of shear cracks (θ).



Figure 1.1 Oil Palm kernel Shell (OPS) Aggregate.



Figure 1.2 Plantation of Palm Oil Tree.

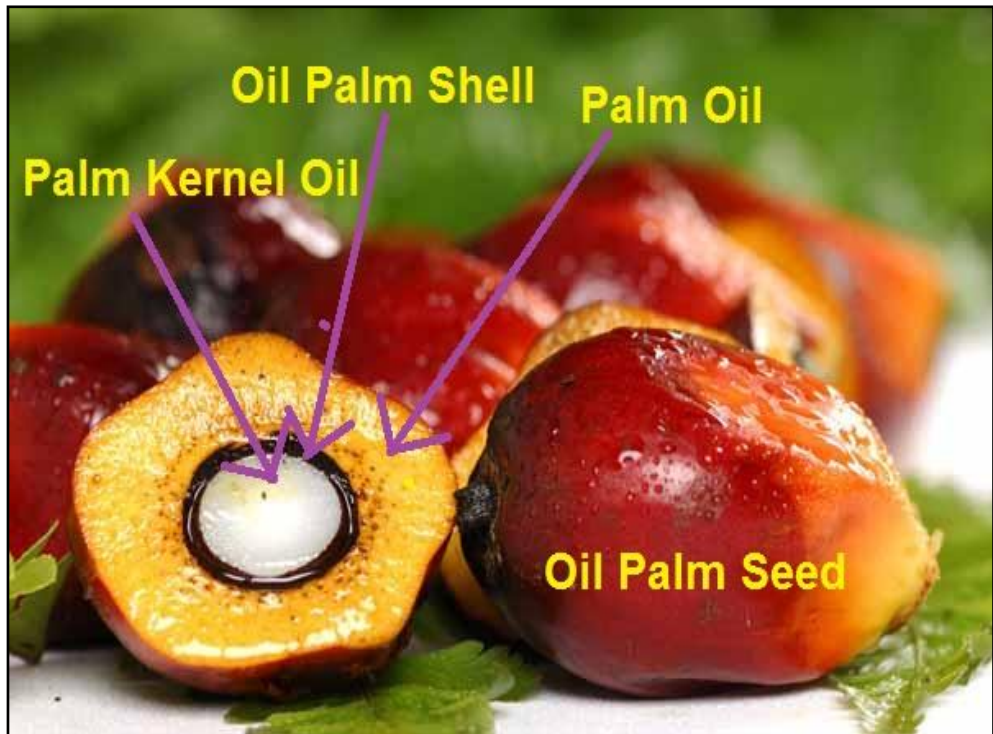


Figure 1.3 Cross Section of Oil Palm Fruit.

Chapter 2

Literature Review

2.1 Introduction

In 1990, Okapala [1] introduced the use of Oil Palm kernel Shell (OPS) aggregates in concrete and subsequently, considerable amount of research have been carried out to aid the understanding of Oil Palm kernel Shell Concrete's (OPSC) mixture design [1-6] and material properties [7-11].

However, the current understanding of OPSC Beam's structural resistance, such as, bending resistance [12-14] and shear resistance [15 & 16] carried out by researchers were found to be limited. In order to improve the current understanding in OPSC beam's shear mechanism, the present understanding about the shear mechanism of reinforced concrete beam elements cast with normal aggregates have been reviewed to form the fundamental understanding for this research. The shear mechanism and effect of variables on the shear strength of normal weight concrete beams without and with shear reinforcement based on various approaches [18-61] were reviewed in Section 2.2 and Section 2.3.

On the other hand, as this research involves the use of Oil Palm Kernel Shell (OPS) as coarse aggregates in concrete, therefore, the present understanding about its mixture design [1-6] were reviewed in Section 2.5 to form the fundamental understanding for the OPS mixture design of this research.

2.2 Shear for normal weight concrete beam

Shear failure mechanism is a rupture and complex failure mechanism; hence, it has received extensive amounts of attentions among the researchers during the last two centuries. Numerous tests have been performed to obtain the experimental data as well as many methods were employed to obtain the shear capacity of both normal weight concrete (NWC) beams with and without shear reinforcement. From which, various understanding and design procedures have been reported.

In 1899, Ritter [18] introduced the concept of truss analogy and proposed the design of shear reinforcement, which was later found to be very similar to that published of the ACI-ASCE 1962's design specifications [19]. Later in 1906-1907, Mörsch [20] presented an explanation to the diagonal tension mechanism, and further supported his theory with data from Von Emperger [21] and Probst [22]. Mörsch [20] introduced the shear strength concept, V_u/bd and reinforced Ritter's concept [18] by stating that contribution from shear reinforcement to the shear resistance of reinforced concrete members by resisting tensile stresses, and not shear stresses. He demonstrated that the effectiveness of shear reinforcement is more pronounced when diagonal crack occurred.

Later in 1909, Talbot [23] disputed the fact that nominal shear strength of the normal weight concrete beams is only dependent on the concrete compressive strength. That is, it was demonstrated apart from the material strength, contributions from the amount of longitudinal steel reinforcement, and the beam length to depth ratios were also noted [23]. Furthermore, it was reported that diagonal tension failure occurred not only due to the stresses from bending, but also due to the shear

stresses. Talbot presented his concept from analytical studies of 106 NWC beams without shear reinforcement. Unfortunately, those findings were not expressed in mathematical terms [18].

According to ACI-ASCE Committee 326 [19], in the years between 1920 and early 1950's, the investigations by Talbot and other pioneers along with the early research carried out on the effects of percentage of reinforcement and the length to depth ratio was forgotten. It was only in the late 1940's that these forgotten fundamentals were recalled when Moretto [24] reported on a series of beam tests and proposed an empirical equation, which considered the variable of percentage of longitudinal steel reinforcement.

Later in the early 1950's, Clark [25] introduced the variable of shear span to depth ratio, a/d ratio into his proposed equation, which was also recognized as a mathematical expression for the effect of length to depth ratio. In addition, Clark's equation also incorporated Talbot's philosophies by inclusion of the three variables: percentage of longitudinal steel reinforcement, ratio of length to depth, and concrete strength [25] into his investigations.

Hence, these pioneer findings had inspired subsequent researchers in realizing the effects of various variables on the shear failure of normal weight concrete (NWC) beams cast without shear reinforcement and with shear reinforcement. The contributions by researchers [18-53] in the prediction of shear capacity of concrete beam are notable for the current understanding of structural concrete beam element for shear strength prediction of NWC beams without and with shear reinforcement (see Section 2.2.1 and Section 2.2.2, respectively).

2.2.1 Shear for NWC beams without shear reinforcement

For NWC beams without shear reinforcement, the approaches presented by researchers consist of basic shear transfer mechanism (see Section 2.2.1.1), empirical approach (see Section 2.2.1.2), concrete plasticity approach (see Section 2.2.1.3), and building code approach (see section 2.2.1.4).

2.2.1.1 Basic shear transfer mechanism

In 1973, the ACI-ASCE Committee 426 [26] reported on the contributions from the concrete shear stress, interface shear transfer (aggregate interlock), dowel action, arch action and shear reinforcement on the basic shear transfer mechanism of reinforced concrete members. However, the development of shear transfer mechanisms in beam was not explained chronologically.

Kong and Evan [27] in 1998 presented the contribution of each internal force on the shear resistance of both structural reinforced concrete beams casted with and without shear reinforcement (see Figure 2.1). Furthermore, Kong and Evan reported on the development of shear transfer mechanism with respect to reinforced concrete beams cast without shear reinforcement and with shear reinforcement. For concrete beam cast without shear reinforcement, the applying shear force, V is believed to be resisted by the combination of three shear actions: (i) the shear force in uncracked concrete compression zone (V_{cz}), (ii) the shear force from dowel action of the longitudinal reinforcement (V_d), and (iii) the vertical component of shear force from aggregate interlock (V_a) (see Figure 2.1). And, the total shear resistance can be computed as indicated below:

$$V = V_{cz} + V_d + V_a \quad (\text{Eqn 2.1})$$

The shear force, V (Eqn 2.1) is carried in the approximate ratios stated below:

Shear V_{cz} in uncracked compression Zone, $V_{cz} = 20 - 40\%$

Shear V_d from dowel action of the longitudinal reinforcement, $V_d = 15 - 25\%$

Shear V_a due to aggregate interlock, $V_a = 35 - 50\%$

It was reported that during testing, with the increment of applied loading, dowel action would first reached its capacity followed by the aggregate interlock and subsequently, by the concrete compression zone before shear failure occurred. The consecutive development of the shear transfer mechanisms **were** described as:

1. The shear cracks were observed to form at the support when the dowel action began to lose its resistance against the shear force and consequently, after the dowel action lost its capacity, shear force are transferred to the aggregate interlock.
2. Upon increment of loading, the shear cracks propagated towards the neutral axis of the beam when the aggregate interlock began to lose its resistance.
3. The aggregate interlock lost its capacity when the shear cracks passed the neutral axis of the beams and the shear force is carried by the concrete compression zone.
4. Upon further loading, the concrete compression zone lost its capacity and finally, the shear failure occurred.

Furthermore, Kong and Evans [27] presented a summary of the variable's contributions towards that shear failure of normal weight concrete beams cast without shear reinforcement. The variables, which influenced the normal weight concrete beam without shear reinforcement, consist of:

1. Concrete strength

The increment of concrete strength results in increased of the dowel action capacity, the aggregate interlock capacity and the compression zone capacity.

It is believed that the bond strength between the tension reinforcement and concrete increased as the concrete strength increased.

2. Aggregate type

The aggregate type influenced the aggregate interlock capacity with different aggregate crushing strength, impact strength and abrasion strength, which in turn affects the shear strength of the beam.

3. Beam size

The increased of beam size results in the ultimate shear stress reduction, which larger beams are weaker than smaller beams. It is believed that the increments of aggregate interlock capacity are not proportional to the beam size.

4. Longitudinal steel ratio

The shear strength is affected by the longitudinal steel ratio as lower longitudinal steel ratio results in the reduction of shear strength with the decreased of dowel shear capacity and increased of crack widths, which in turn reduces the aggregate interlocking capacity.

5. Shear span to effective depth ratio

The increment of shear span to effective depth ratio, a/d would results in the reduction of shear strength. When a beam is loaded with $a/d < 2.5$, it is reported that beam assumed to behave like an arch action, which allows the load to be transferred to the support.

Whilst for normal weight concrete with shear reinforcement, the combination of the shear actions and the consecutive developments of the shear transfer mechanisms are presented in Section 2.2.2.1.

2.2.1.2 Empirical Approach

Moody et.al [28 & 29] in 1954 presented experimental works on 40 NWC beams casted without shear reinforcement and 2 NWC beams casted with shear reinforcement, which were segregated into three series to observe the influence of the variables: (i) percentage of longitudinal and web reinforcement and method of anchorage, (ii) size and percentage of longitudinal reinforcement and cylindrical concrete strength and (iii) concrete mixture and method of curing. The concept of redistribution of internal stresses was introduced for the predictions of shear failure for NWC beams. For each of the 3 series, the sizes of the beams were different and the beams were tested with one or two concentrated load. It was observed that all beams failed in shear. It is observed that the shear capacity of the NWC beam specimens increased with the increment of concrete strength and percentage of longitudinal steel. It was also noted that the test results indicated that the beam strength tested at higher a/d ratio is governed by the first cracking load whilst the beam strength tested at lower a/d ratio is governed by the load, which caused destruction to the concrete compression zone. Hence, it is suggested by Moody et. al that instead of cracking load, ultimate load should be taken as the measured value for shear capacity.

Ferguson [30] in 1956 presented two series of tests on (1) the effect of extra and multiple loads with constant a/d ratio, and (2) variable of shear span to depth ratio

(a/d) with identical loading condition, on the ultimate shear capacity of concrete beams without shear reinforcement. It was found that higher ultimate shear strength were obtained for beams loaded with four point loads compared to two point loads. Furthermore, it was found that the beams loaded with point load near the support (lower a/d ratio) sustained higher ultimate strength compared to beams loaded further away from the support (higher a/d ratio). Further discussions on the development of shear failure for concrete beams without shear reinforcement were indicated systematically, which is shown in Figure 2.2 that:

- (1) Initial diagonal crack formed near mid depth and discontinued within the compression area at 1a, and in tension area somewhere at 1b.
- (2) Discontinuation of cracks propagations from 1a towards the compression zone at 2.
- (3) Cracking in the zone around the steel, which might developed simultaneously with (2).
- (4) Sudden failure by an extension of flexural crack at 4a or the shear-compression failure at 4b, accompanied with a secondary failure in splitting at bond at 4c.

Taub et.al [31] in 1960 reported the shear failure of concrete beam based upon redistribution of internal stresses introduced by Moody et. al [24 & 25] and the effect of each variable considered: (1) types of shear failure and the influence of a/d ratio, (2) shape and proportions of beam, (3) percentage area of main tension and compression reinforcement, (4) size of tension bars, (5) cylindrical concrete strength and (6) arrangement of loading and the magnitude of the bending moment and shearing force applied, on the shear strength of concrete beam without shear

reinforcement. The free body diagram after widening of the diagonal cracks for a beam without shear reinforcement is shown in Figure 2.3. The redistribution of internal forces was presented (see Figure 2.3), which when the diagonal cracks were formed, the force in tension reinforcement, T was assumed to act in horizontal direction. Hence, the redistribution of internal forces occurred when the diagonal tension crack reached section 2-2, where the distribution of forces in tension reinforcement along the beam varied with the distribution of external moment. Upon further increment of loading, the diagonal tension crack extended at either end and ultimately, lead to the failure of the beam.

In addition, Taub et.al [31] categorized shear failure into four distinct types for normal weight concrete beam without shear reinforcement, which are:

1. Shear compression failure, which occurred by crushing at the concrete compression zone when compressive stress in concrete become equal to its ultimate strength due to the extension of diagonal tension cracks followed by the reduction of compressive block size.
2. Shear tension failure accompanied by anchorage failure at the support, which occurred when anchorage was not provided.
3. Shear tension failure by total separation of beam at shear span, which occurred by horizontal splitting of the beam at the shear span tension zone.
4. Crushing of concrete strut connecting the load point with the support, which occurred when shear span is extremely small.

From the studies carried out for NWC beams without shear reinforcement, Taub et.al [31] concluded that:

1. The shear force increased with the reduction of a/d based on Mattock's data (see Figure 2.4), where beams tested at different a/d failed in different type of shear failure: $a/d=0.96$ failed in strut like manner, $a/d=1.45$ failed in shear compression, $a/d=1.93$ failed in balanced failure between shear compression and diagonal tension, $a/d=3.83$ failed suddenly in shear tension when splitting along the main steel occurred, and $a/d=7.79$ failed in flexural failure by yielding of steel at mid span with results.
2. Experimental works carried out indicated that the concrete beam shear strength is not affected by the compression reinforcement.
3. Based on the results, the ultimate shear strength of normal weight concrete beams without shear reinforcement was influenced by concrete strength, which the shear strength increased with the increment of cylindrical concrete strength.
4. The influence of shape and proportions of beams were reported by increment of beam width based on the test results of T beams and rectangular beams by results indicated that shear force were found to be directly proportional to the width of the web.
5. The resistance to bond failure is higher when a larger number of smaller longitudinal bars were used instead of smaller number of larger longitudinal bars for the same longitudinal steel ratio. Hence, the amount of longitudinal bars adopted by Author in this research was reserved as two numbers to avert this influence on the OPSC beams test results.

Apart from normal weight concrete beam without shear reinforcement, the redistribution of internal forces and the observations on the tests conducted on the normal weight concrete beam with shear reinforcement were also reported by Taub et. al [50], which are mentioned in Section 2.2.2.2.

Mathey and Watsein [32] in 1963 presented the findings of the experimental study on the effect of yield strength of longitudinal reinforcement ranging from 275 N/mm² to 690 N/mm² on the shear strength of the beams and a total of 25 NWC beams without shear reinforcement were tested. It was found from the investigations that the shear strengths at the diagonal tension cracking loads were not influenced by the yield strength of the longitudinal reinforcement. A modified empirical formula based on Clark's formula [25] was proposed for a prediction of cracking shear stress, which is given as:

$$v_c = \frac{3.1 V_c d \sqrt{f_{ck}}}{M_{\max}} + 4000 \rho \quad (\text{Eqn 2.2})$$

It was reported that the proposed formula contributes to a lower bound solution and is applicable for beams with wide range of concrete strengths, longitudinal steel ratios, steel stresses, properties of reinforcement, and ratios of external shear to maximum moment in the shear span.

Acharya and Kemp [33] in 1965 reported the contributions of dowel forces on the shear resistance of rectangular beams cast without shear reinforcement with a series of 20 beams. It was reported that the high stresses on the concrete at the top of the diagonal stress were implied with the assumption of zero dowel force. Hence, it was indicated that the size and its point of application are important factors in deciding the mode of shear failure of the beam. Hence, it is understood by Author that Archary and Kemp acknowledged the influence of longitudinal steel reinforcement and shear span to effective depth ratio affecting the type of failure for rectangular beams without shear reinforcement.

Krefeld and Thurston [34] in 1966 reported the tests on 152 reinforced concrete beams without shear reinforcement, in which 78 beam specimens and 74 beam specimens were subjected to concentrated load and uniform load, respectively. The tests carried out took into account for the variables: (1) concrete strength, (2) beam dimensions, (3) longitudinal steel ratios, and (4) span length. All the beams were subjected to concentrated load and it was observed that the shear strength were affected by the span length, L/d ratio, which showed that longer span length, L/d results in lower shear resistance of the beams (see Figure 2.5). It was found that a good agreement with a mean of 0.96 is achieved between the test results and the calculated critical average shearing stress, V_c , when the formula is taken as:

$$\frac{V_c}{b h} = 1.8 \sqrt{f_{ck}} + \frac{2600 \rho d}{(M/Vd) z} \quad (\text{Eqn 2.3})$$

Where, f_{ck} = cylindrical concrete strength (psi)

V = total shear at a section

M = bending moment at a section

However, it was reported that for common beam dimensions, the suggested Eqn 2.3 varied from 0.77 to 0.91 (see Figure 2.6). Therefore, using a mean of 0.86, the shear cracking load, V_c , were taken as the maximum applied resistance for common beam dimensions, which is given as follow:

$$\frac{V_c}{b h} = 1.6 \sqrt{f_{ck}} + \frac{2100 \rho d}{M/V} \quad (\text{Eqn 2.4})$$

In addition, Krefeld and Thurston also presented formulas for the shear strength predictions of normal weight concrete beams casted with shear reinforcement, which are given in Section 2.2.2.2.

Kani [35] in 1966 reported the test results of 133 beams without shear reinforcement to investigate the influence of 3 variables; f_{ck} , ρ and a/d ratio. From the investigations, it was acknowledged that:

1. The change of behaviour for beams tested at $a/d < 2.5$ and $a/d > 2.5$ (see Figure 2.7). It was noted that $a/d = 2.5$ is the minimum point for beam strength, which the “valley of diagonal failure” is greatly reduced at the region of $a/d = 1.5$ and 3.5 . (see Figure 2.8)
2. The contribution of longitudinal steel reinforcement (ρ) on the ultimate shear capacity of NWC beams without shear reinforcement as experiments reported confirmed the effect of percentage of longitudinal steel reinforcement on the shear capacity of the beams when other variables were kept constant.
3. The influence of concrete strength on the so called shear strength was insignificant and could be ignored in the analysis of diagonal failure load.

Rajagopalan and Ferguson [36] in 1968 presented the effect of percentage of longitudinal steel, ρ of the normal weight concrete beams without shear reinforcement. The experimental consist of 10 normal weight concrete beams tested at $a/d=4$ with respect to variable of ρ (%), which the results reported loss of shear strength with the reduction of ρ (%) (see Figure 2.9). An ultimate shear stress formula is proposed based on the test results from the experimental works for beams tested with $a/d > 2.75$ (see figure 2.9) subjected to $\rho \leq 0.012$, and it is given as:

$$v_u = (0.8 + 100 \rho) \sqrt{f_{ck}} \quad (\text{Eqn 2.5})$$

It was noted that the proposed formula gives a lower bound solution when in comparisons to the test results (see Figure 2.9).

Zsutty [37] in 1971 presented a formula for NWC beam without shear reinforcement tested at shear span to effective depth ratio, $a/d < 2.5$ and $a/d \geq 2.5$, respectively, using dimensional analysis and statistical regression analysis of approximately 200 beams test data from different sources. It was reported that beam behaviour should be separated into arch action of short beams and beam actions of slender beams. The arch action of short beams was categorized for beams tested at $a/d < 2.5$, which compressive stress or direct load transfers to support were observed. Whilst for the beam action of slender beams, it was categorized for beams tested at $a/d \geq 2.5$, which combined bending and shear stress were observed. The primary variables considered were the concrete strength, the longitudinal steel ratio and the shear span to effective depth ratio for both NWC beams without shear reinforcement and with shear reinforcement. The proposed empirical formulas are given as:

For slender beam, $a/d \geq 2.5$,

$$v_u = 60 \sqrt[3]{f_{ck} \rho \frac{d}{a}} \quad (\text{Eqn 2.6})$$

For short beam, $a/d < 2.5$,

$$v_u = 150 \sqrt[3]{f_{ck} \rho \left(\frac{d}{a}\right)^4} \quad (\text{Eqn 2.7})$$

However, for value of $a/d = 2.5$, discontinuity were observed, which he acknowledged that the results obtained for short beams were not satisfactory. In addition, another formula for the shear capacity predictions of normal weight concrete beams with shear reinforcement is reported, which is mentioned in Section 2.2.2.2.

Swamy et al. [38] in 1970 reported on the investigations of five series of tests on the internal mechanism of shear failure and load distribution of reinforced beams, which consists of arch action formed in unbonded bar, steel strain distribution of the

rectangular and T-beams under various loading conditions, cracking from compression edge near load points and supports and neutral axis profile throughout each beam, were comprehensively discussed. In addition, one test series were reported to discuss the effect of bond conditions and surface conditions of longitudinal steel on the beam cast without shear reinforcement. It was reported that for rectangular beams, deformed bars provide higher shear resistance compared to plain bars for smaller a/d ratios. Whilst for T beams, plain bars provide higher shear resistance than deformed bars (see Figure 2.10). It was found that the beams cast with unbonded longitudinal steel reinforcement may also failed in shear or at the anchorage similarly to beams casted with bonded longitudinal steel reinforcement. It was also shown that surface conditions of the longitudinal steel, which consists of either plain or deformed bars, did not contribute significantly towards the ultimate shear resistance of both rectangular and T-beams.

In 1984, Mphonde and Frantz [39] presented a shear capacity formula for predicting the ultimate shear capacity of rectangular concrete beams without shear reinforcement of slender beams ($a/d \geq 2.5$) using regression analysis. The variable of cylinder concrete strength, f_{ck} (psi) was considered for the derivations of the formula whilst other variables: the longitudinal steel ratio, the shear span to effective depth ratio and the height of the beams were neglected.

The regression ultimate shear capacity formula obtained is as follow:

$$v_u = 10.10 (f_{ck})^{1/3} + 71 \quad (\text{Eqn 2.8})$$

It was reported that the proposed Eqn 2.8 best predict beams with shear span to effective depth of 3.6 as shown in Figure 2.11.

Kim and White [40] in 1991 presented a cracking shear strength formula using an approximate analytical approach based on schematical variation of cracking load along shear span. Test data of more than 100 beams were used and the results obtained showed good correlation between the measured and predicted values. The variables considered include (1) longitudinal steel reinforcement, (2) shear span to effective depth ratio and (3) concrete strength. However, the variable of beam height is neglected. It was reported that the proposed formula is suitable for all shear span to effective depth ratio, a/d . In addition, the proposed formula is only valid for the prediction of cracking shear strength of NWC beams without shear reinforcement and it is not applicable for the prediction of ultimate shear strength.

$$V_{cr} = 9.4 [\sqrt{\rho} (1 - \sqrt{\rho})^2 \left(\frac{d}{a}\right)]^{1/3} \sqrt{f_{ck}} b d \quad (\text{Eqn 2.9})$$

It was noted that good agreements were achieved between the shear strength predictions (see Eqn 2.9) and the test results with the mean value of 1.009 and standard deviation of 0.148.

Rebeiz [41] in 1999 proposed a formula each for predictions of cracking shear strength and ultimate shear strength of NWC beams without shear reinforcement using multiple regression analysis of original ACI formulas. It was reported that no significant effect was found on v_u and v_c with respect to $\sqrt{f_{ck}}$ (see Figure 2.12). The differences in behaviour between short and long beams were taken into account by using the variable $\sqrt{f_{ck}} \rho \frac{d}{a}$.

For ultimate shear strength predictions for is given as:

$$v_u = \frac{V_u}{b d} = 0.4 + \sqrt{f_{ck}} \rho \frac{d}{a} (10 - 3A_d) \quad (\text{Eqn 2.10})$$

For cracking shear strength predictions is given as:

$$v_c = \frac{V_c}{bd} = 0.4 + \sqrt{f_{ck}} \rho \frac{d}{a} (2.7 - 0.4A_d) \quad (\text{Eqn 2.11})$$

However, for design purpose, the ultimate shear strength prediction is given as:

$$v_u = \frac{V_u}{bd} = 0.28 + \sqrt{f_{ck}} \rho \frac{d}{a} (7 - 21.1A_d) \quad (\text{Eqn 2.12})$$

Where, A_d , shear shape adjustment factor = a/d for $1.0 < a/d < 2.5$

or 2.5 for $a/d \geq 2.5$

It was observed that good agreements were achieved between the proposed theoretical predictions (Eqn 2.12) with the measured test data (see Figure 2.12).

Subsequently, Rebeiz [42] in 2001 carried out an analysis on the effects of the variables: (1) compressive strength (f_{ck}), (2) longitudinal steel ratio (ρ) and (3) shear span to depth ratio (a/d) on the cracking shear strength, v_c and ultimate shear strength, v_u of reinforced concrete beams without shear reinforcement. Literature data of more than 300 beams for normal strength concrete and more than 50 beams for high strength members were used for the analysis (see Figure 2.13), which It was found that a/d ratio has much more significant effect on the ultimate shear strength, v_u than to the cracking shear strength, v_c of the beams. It was presented in Figure 2.12 that for beams tested at $a/d < 2.5$, the ultimate shear strength, v_u reduced as the a/d increased whilst for beams tested at $a/d \geq 2.5$, both the ultimate shear strength, v_u and the cracking shear strength, v_c were not affected with the variations of a/d ratio. Further, it was observed that the compressive strength influenced both the ultimate shear strength, v_u and the cracking shear strength, v_c for beams tested at all a/d ratio. However, the effect of the longitudinal steel ratio on the cracking shear strength, v_c were negligible for beams tested at $a/d < 2.5$.

Russo [43] in 2005 proposed a concrete contribution to shear strength formula, v_{uc} based on mechanical analysis approach by the inclusion of parametric expression for reinforced concrete beams cast without shear reinforcement. Test data of 917 beams from literature data were included for comparisons with the proposed formula and the results obtained showed good correlation between the measured and predicted values with a mean value of 1.00 and a standard deviation of 0.21. The formula is given as:

$$v_{uc} = 1.13 \xi [\rho^{0.4} f_{ck}^{0.39} + 0.5 \rho^{0.83} f_{yl}^{0.89} (\frac{a}{d})^{-1.2-0.45a/d}] \quad (\text{Eqn 2.13})$$

Where, f_{yl} = yield strength of longitudinal steel

$$\xi = \text{size effect function} = \frac{1 + \sqrt{\frac{5.08}{d_a}}}{\sqrt{\frac{1+d}{25 d_a}}}, \text{ where } d_a = \text{maximum aggregate size}$$

Arslan G. [44] in 2007 proposed a cracking shear strength formula for NWC beams without shear reinforcement, which is given as follow:

$$v_c = 0.15 \sqrt{f_{ck}} + 0.02 f_{ck}^{0.65} \quad (\text{Eqn 2.14})$$

However, the formula only took account into the concrete strength, f_{ck} whereas other variables: (1) longitudinal steel ratio, (2) shear span to effective and (3) beam height were omitted in Arslan's formula. Hence, it is believed by Author that the proposed formula is not satisfactory as influence of other variables were neglected and test results from literature data indicated the presence of longitudinal steel ratio, shear span to effective and beam height on the shear strength contribution of normal weight concrete beams without shear reinforcement.

2.2.1.3 Concrete Plasticity Approach

In 1975, Braestrup [45] reported shear tests on rectangular reinforced concrete beams and proposed corresponding work formulas. Using upper bound technique of plasticity theory, he derived a general work formula based on the assumption if a rigid region I move, for a displacement δ , in a given direction, at an angle α to the discontinuity, relative to the rigid region II, the work dissipated in the narrow plastic zone for concrete beam without shear reinforcement (see Figure 2.14), which is given as:

$$W = P\delta = \frac{\delta \sigma_c}{2} (1 - \cos \theta) \left(\frac{b h}{\sin \theta} \right) \quad (\text{Eqn 2.15})$$

Where, σ_c = concrete compressive strength

δ = displacement

θ = angle of plane of discontinuity

The above formula was confirmed by Nielsen et. al [46] in 1978 to be exact solution using the upper bound technique approach. However, it was found that an agreement was only achieved between the theoretical predictions and the test results with the modifications of the theoretical prediction by an effectiveness factor, u . The effectiveness factor was found that approximate average effectiveness factor, u was found to be 0.54 for concrete beams without shear reinforcement mainly because concrete is not a perfectly plastic material as assumed in this approach, where concrete is assumed to exhibit perfectly plastic behaviour and has a compressive strength equal to the peak value on a stress strain curve. It is believed that it is unlikely that the concrete stress would be equal to the maximum compressive strength at all points of the failure surface as concrete is not a homogenous material and has a very limited deformability. However, when in tension, the concrete exhibits brittle behaviour at low stress and displays monotonic

strain softening behaviour at large strain. It was also reported that the value of effectiveness factor for concrete beam without shear reinforcement were lower than the value found for concrete beam with shear reinforcement, which was due to the absence of shear reinforcement. Hence, this led less restraint to concrete could be achieved.

For concrete beams without shear reinforcement, it was found that better agreement with the tests when v was considered to be a function of concrete cylinder compressive strength (σ_c), overall section depth (h), longitudinal steel ratio (ρ) and shear span to height ratio (a/h) as given in the following formula:

$$v = f_1(\sigma_c) f_2(h) f_3(\rho) f_4\left(\frac{a}{h}\right) \quad (\text{Eqn 2.16})$$

$$\text{Where, } f_1(\sigma_c) = \frac{3.5}{\sqrt{\sigma_c}} \quad (\sigma_c \text{ in N/mm}^2) \quad (\text{Eqn 2.16.1})$$

$$f_2(h) = 0.27 \left(1 + \frac{1}{\sqrt{h}}\right) \quad (h \text{ in m}) \quad (\text{Eqn 2.16.2})$$

$$f_3(\rho) = 0.15\rho + 0.58 \quad (\rho < 4.5\%) \quad (\text{Eqn 2.16.3})$$

$$f_4\left(\frac{a}{h}\right) = 1 + 0.17 \left(\frac{a}{h} - 2.6\right)^2 \quad \left(\frac{a}{h} < 5.5\right) \quad (\text{Eqn 2.16.4})$$

The detail of the derivation of these effectiveness factors and the comparisons with the test result for concrete beams without shear reinforcement could be found in Nelsen et. al [46] in 1978. In addition to concrete beam without shear reinforcement, he also derived a work formula and proposed an effectiveness factor for concrete beam with shear reinforcement, which are mentioned in the following Section 2.2.2.3.

2.2.1.4 Building Code Approach

Many codes of practice were introduced for shear strength prediction of normal concrete beam without shear reinforcement. Some of the well-known codes of practice discussed here include BS8110 Code [47], Eurocode 2 Code [48], and ACI Code [49]. However, it is noted by Author that there are variations among the codes regarding the formulas of the shear strength prediction and the considerations of variables affecting the shear strength of the beam. Hence, formulas of the shear strength predictions by the various codes of practice are shown in Section 2.2.1.5.1 to Section 2.2.1.5.2 for BS8110 Code [47], Eurocode 2 Code [48], and ACI Code [49], respectively.

2.2.1.4.1 BS8110 Code

BS8110 [47] developed a formula each for the shear capacity prediction of normal weight concrete beam without shear reinforcement loaded with $a/d \leq 2$ and $a/d > 2$, which are given as follow:

For $a/d \leq 2$,

$$V_{Rdc} = \frac{0.79 \left(\frac{100 A_s}{b_v d}\right)^{1/3} \left(\frac{400}{d}\right)^{1/4} \left(\frac{f_{cu}}{25}\right)^{1/3} \frac{2d}{a}}{\gamma_m} b d \quad (\text{Eqn 2.17})$$

For $a/d > 2$,

$$V_{Rdc} = \frac{0.79 \left(\frac{100 A_s}{b_v d}\right)^{1/3} \left(\frac{400}{d}\right)^{1/4} \left(\frac{f_{cu}}{25}\right)^{1/3}}{\gamma_m} b d \quad (\text{Eqn 2.18})$$

Where, γ_m = partial factor of material = 1.15

The functions of parameters are:

$$f\left(\frac{a}{d}\right) = 2 \frac{d}{a} \quad \left(\frac{a}{d} \leq 2\right) \quad (\text{Eqn 2.19.1})$$

$$f(\rho) = \rho^{1/3} = \frac{100 A_s}{b d}^{1/3} \quad (\rho < 3\%) \quad (\text{Eqn 2.19.2})$$

$$f(f_{cu}) = \left(\frac{f_{cu}}{25}\right)^{1/3} \quad (f_{cu} > 25 \text{ MPa}) \quad (\text{Eqn 2.19.3})$$

$$f(d) = \left(\frac{400}{d}\right)^{1/4} \quad (d \text{ in mm}) \quad (\text{Eqn 2.19.4})$$

2.2.1.4.2 Eurocode 2

For NWC beam without shear reinforcement, Eurocode 2 [48] took into account the parameters: cylindrical concrete strength (f_{ck}), longitudinal steel ratio (ρ), effective section depth (k) and shear span to effective depth ratio (a/d) in the shear strength prediction for normal weight concrete beams without shear reinforcement.

The design shear resistance of a normal weight concrete beam without shear reinforcement is predicted using the formula as follow:

For $a/d \leq 2$,

$$V_{Rdc} = [C_{rd,c} k (100 \rho f_{ck})^{1/3} + k_1 \sigma_{cp}] b_w d \left(\frac{2d}{a}\right) \quad (\text{Eqn 2.20})$$

For $a/d > 2$,

$$V_{Rdc} = [C_{rd,c} k (100 \rho f_{ck})^{1/3} + k_1 \sigma_{cp}] b_w d \quad (\text{Eqn 2.21})$$

Where, $k_1 = 0.15$

$$C_{rd,c} = \frac{0.18}{\gamma_c}, \text{ where } \gamma_c = \text{partial factor of concrete}$$

Hence, the functions of parameters are:

$$f\left(\frac{a}{d}\right) = \frac{2d}{a} \quad \left(\frac{a}{d} \leq 2\right) \quad (\text{Eqn 2.22.1})$$

$$f(\rho) = \rho^{1/3} = \frac{A_s}{b d}^{1/3} \quad (\rho \leq 0.02) \quad (\text{Eqn 2.22.2})$$

$$f(f_{ck}) = f_{ck}^{1/3} \quad (f_{ck} \text{ in MPa}) \quad (\text{Eqn 2.22.3})$$

$$f(k) = 1 + \sqrt{\frac{200}{d}} \quad (d \text{ in mm}) \quad (\text{Eqn 2.22.4})$$

and

The minimum value of V_{Rdc} ,

$$V_{Rdc} = v_{min} b_w d \quad (\text{Eqn 2.23})$$

Where, values of v_{min} is shown in Table 2.4

2.2.1.4.3 ACI code

In 2002, ACI 318 Building code [49] recommended a formula for the prediction of shear strength for normal weight concrete beam without shear reinforcement subjected to shear and flexure, which is given as follow:

$$v_c = \frac{V_c}{b d} = \frac{1}{7} (\sqrt{f_{ck}} + 120 \rho \frac{V_u d}{M_u}) \leq 0.3 \sqrt{f_{ck}} \quad (\text{Eqn 2.24})$$

Where, V_c = cracking shear strength of concrete in MPa

M_u = factored moment occurring simultaneously with the factored shear force, V_u , at section considered

The cracking shear given in (Eqn 2.24) is typically simplified into the formula:

$$v_c = \frac{V_c}{b d} = \frac{1}{6} \sqrt{f_{ck}} \quad (\text{Eqn 2.25})$$

2.2.2 Shear for NWC beams with shear reinforcement

For NWC beam with shear reinforcement, the approaches discussed are basic shear transfer mechanism approach (see Section 2.2.2.1), empirical approach (see Section 2.2.2.2), concrete plasticity approach (see Section 2.2.2.3), and building code approach (see Section 2.2.2.4).

2.2.2.1 Shear transfer mechanism approach

For structural concrete beam cast with shear reinforcement, Kong and Evan [27] in 1998 reported that the shear force, V is resisted by four combined shear action: the shear in uncracked concrete compression zone (V_{cz}), the shear from dowel action of the longitudinal reinforcement (V_d), the vertical component of shear force due to aggregate interlock (V_a) and the shear force carried by the shear links crossed by the diagonal crack (V_s), (see Figure 2.15) which is given as:

$$V = V_c + V_a + V_d + V_s \quad (\text{Eqn 2.26})$$

For concrete beam cast with shear reinforcement, the consecutive developments of the shear transfer mechanisms are reported as:

1. During testing, the shear links would first yielded as the external shear V increased so that the shear force carried by the shear links crossed by the diagonal crack (V_s) remained at the yield value, and subsequently, the increased in V were carried by the shear in uncracked concrete compression zone (V_c), the vertical component of shear force due to aggregate interlock (V_a) and the shear from dowel action of the longitudinal reinforcement (V_d).
2. Consequently, as the applied load increased, the vertical component of shear force due to aggregate interlock (V_a) becomes less effective as the diagonal cracks widens, which the shear in uncracked concrete compression zone (V_c), and the shear from dowel action of the longitudinal reinforcement (V_d) were forced to increase rapidly.
3. Ultimately, as the applied load was further increased, the shear failure of the beam occurred either by dowel splitting of the concrete along the

longitudinal reinforcement or by crushing of the concrete compression zone resulting from the combined shear direct stresses.

Kong and Evan reported that the variables, which influenced the shear strength of normal weight concrete beam without shear reinforcement, would have also contributed to the shear strength of normal weight concrete beam with shear reinforcement. It was stated that the function of shear reinforcement is to resist the diagonal shear failure occurred between point load and support. Hence, the shear resistances of the beam are considerably increased by the increment of shear reinforcement, which increased the ductility of the beam and significantly decreased the possibility of a sudden and catastrophic failure that commonly occurred in concrete beams without shear reinforcement.

2.2.2.2 Empirical Approach

In 1945, Moretto [24] in 1945, reported on the tested beams with welded shear reinforcement, which include studies on the systematically effect of the inclination of shear reinforcement on the shear strength and the investigations of the variables: concrete strength, longitudinal steel ratio, shear reinforcement ratio, and the inclination of the shear reinforcement. He proposed two empirical shearing stress formulas, which are given as follow:

For the load at which the web reinforcement was stressed to the yield point,

$$V_u = (K r f_y + (0.04 f_{ck}) + 5000 \rho) b j d \quad (\text{Eqn 2.27})$$

For ultimate failure load,

$$V_u = (K r f_y + (0.10 f_{ck}) + 5000 \rho) b j d \quad (\text{Eqn 2.28})$$

Where, f_{ck} = cylindrical compressive strength (psi)

f_y = yield strength of shear reinforcement (psi)

$$r = \frac{A_s}{b s} = \text{shear reinforcement ratio, where } s = \text{shear reinforcement spacing}$$

$$K = (\sin \alpha + \cos \alpha) \sin \alpha, \text{ where } \alpha = \text{angle between the inclined Shear reinforcement and axis of the beam}$$

It is observed by Author that given two formulas (Eqn 2.27 and Eqn 2.28) by Moretto [24] provided minimal contributions by the concrete on the shear strength predictions of normal weight concrete beams with shear reinforcement.

Clark in 1951 [25] reported investigations on the normal weight concrete beams with shear reinforcement, which are noteworthy not only because he introduced an expression for that shear span to effective depth ratio, a/d , but another three variables: cylindrical compressive strength, the shear reinforcement ratio, and the longitudinal steel ratio reported by Moretto [24], which affects the shear strength of both concrete beams cast without shear reinforcement and with shear reinforcement, were recognized. It was reported that shear strength of the concrete beams increased with the reduction of shear span to effective depth ratio. Clark's empirical formula was derived from both tests results obtained from investigations and the tested beams, which was proposed for beams failed in diagonal tension failure. The cracking shear stress formula, which aid to express Talbot's philosophies for the variable of shear span to effective depth ratio [18], consist of a mathematical term for the nominal shear strength prediction of four variables: (1) the cylindrical compressive strength, (2) the shear span to effective depth ratio, (3) the shear reinforcement ratio and (4) the longitudinal steel ratio. The cracking shear stress formula is given as follow:

$$v_c = 7000 \rho + (0.12 f_{ck}) \frac{d}{a} + 2500 \sqrt{r} \quad (\text{Eqn 2.29})$$

Where,

f_{ck} = cylindrical compressive strength (psi)

$r = \frac{A_s}{b s} =$ shear reinforcement ratio, where s = shear
reinforcement
spacing

It was reported that Eqn 2.29 is only applicable for the shear strength predictions of beams failed in diagonal tension.

Apart for normal weight concrete beams without shear reinforcement, Taub et.al [50] in 1960 reported the shear failure of the concrete beam based upon redistribution of internal stresses introduced by Moody et. al [28 & 29] and the effect of variables considered which consist of types of shear failure and the influence of a/d ratio, shape and proportions of beam, percentage area of main tension and compression reinforcement, size of tension bars, cylindrical concrete strength and arrangement of loading and the magnitude of the bending moment and shearing force applied on the shear strength of normal weight concrete beams with shear reinforcement. The free body diagram after widening of the diagonal cracks for normal weight concrete beams with shear reinforcement (see figure 2.16) were discussed, which it was reported that with the increment of applied load, the stress in the shear reinforcement increased until the shear reinforcement yielded and subsequently, no further increment of load were resisted by shear reinforcement although the strain continued to increase. With that, the role of shear reinforcement ended and the consecutive redistribution of internal forces of normal weight concrete beams with shear reinforcement are similar to those without shear reinforcement, which are mentioned in Section 2.2.1.2.

For NWC beams with shear reinforcement, he reported three types of shear failure exist, which was also similar to those found for normal weight concrete beams without shear reinforcement. However, the difference is that the failure of normal weight concrete beams with shear reinforcement occurred at higher load compared to normal weight concrete beams without shear reinforcement. The three types of shear failure are by:

1. Crushing of the concrete at the top of the diagonal tension crack.
2. The destruction of the tension zone between the lower end of the diagonal tension crack and the beam support.
3. The opening of a flat-slope crack up to the top surface of the beam.

For normal weight concrete beam with shear reinforcement, Taub et. al [50] concluded that:

1. Full protection from shear failure would not be provided by the presence of shear reinforcement if the required minimum shear reinforcement is not sufficient.
2. The shear capacity of the shear reinforced normal weight concrete beams increased with the reduction of shear span to effective depth ratio (a/d) based on the results
3. The shear capacity of shear reinforced normal weight concrete beams increased with the increment of cylindrical concrete strength of the beam based on the results.
4. The shear reinforced normal weight concrete beams were not influenced by compression reinforcement based on the findings by the University of Manchester.

Bresler and Scordelis [51] in 1963 reported the results of nine normal weight concrete beams with shear reinforcement casted with different concrete strength and shear reinforcement ratio. The beams were tested at $4 \leq a/d \leq 7$ under concentrated loading and it was noted that small amount of shear reinforcement ratio provided increased the shear strength of the beams. The proposed shear strength formula for normal weight concrete beam with shear reinforcement is given as follow:

$$\frac{V_u}{bd} = 1.9 \sqrt{f_{ck}} + 2500 \left(\frac{\rho V d}{M} \right) + r f_{yw} \quad (\text{Eqn 2.30})$$

or
$$\frac{V_u}{bd} = 2 \sqrt{f_{ck}} + r f_{yw} \quad (\text{Eqn 2.31})$$

Where, r = percentage of web reinforcement

f_{yw} = yield point stress of the shear reinforcement steel (psi)

f_{ck} = cylindrical concrete strength (psi)

M = bending moment at a section

It is observed by Author from Figure 2.17 that the proposed Eqn 2.30 and Eqn 2.31 achieved good agreements between the proposed formulas and the test results by researchers.

Apart from the two nominal shear strength formulas proposed for normal weight concrete beam without shear reinforcement mentioned in Section 2.2.1.2, Krefeld and Thurston 1966 [34] also reported the investigations of 44 concrete beams specimens casted with shear reinforcement: (i) 37 beam specimens subjected to concentrated load and (ii) 7 beam specimens subjected to uniform loads. The variables considered were concrete strength, steel ratio, span length and shear reinforcement ratio. It was noted that the additional shear reinforcement provided delayed the horizontal cracking along the bars and the failure by increasing the dowel

resistance. It was reported that the contributions by the shear reinforcement are the most effective when positioned in the vicinity of the critical section, which is at the shear span section. Krefeld and Thurston presented predictions for normal weight concrete beams with shear reinforcement based on the test results of beams with shear reinforcement, which was obtained from the investigations and literature data (see Figure 2.18). The shear strength of a normal weight concrete beam with shear reinforcement is predicted using the formula as follow:

$$\frac{V_{ult}}{b h} = v_c \quad r f_{yw} \leq 30 \quad (\text{Eqn 2.32})$$

$$\frac{V_{ult}}{b h} = v_c + 1.5 r f_{yw} - 45 \quad 30 \leq r f_{yw} \leq 90 \quad (\text{Eqn 2.33})$$

$$\frac{V_{ult}}{b h} = v_c + r f_{yw} \quad 90 \leq r f_{yw} \quad (\text{Eqn 2.34})$$

Where, r = percentage of web reinforcement

f_{yw} = yield point stress of the shear reinforcement steel

It was observed by Author that good agreements were achieved between the above ultimate shear strength predictions and the test results obtained with a mean of 0.99 and standard deviation of 0.10.

Apart from NWC beams without shear reinforcement, Zsutty [34] in 1971 also presented a formula for NWC beams with shear reinforcement using dimensional analysis and statistical regression analysis with approximately 200 beams test data from different sources, which beam behaviour were separated into arch action of short beams and the beam actions of slender beams. The variables considered for normal weight beams cast with shear reinforcement were the (1) cylinder concrete strength, (2) the longitudinal steel ratio and (3) the shear span to effective depth

ratio and shear reinforcement. The proposed empirical formula for NWC beams with shear reinforcement, are given as:

For $a/d < 2.5$,

$$v_u = v_{u2} \left(\frac{2.5}{a/d} \right) + r f_{yw} \quad (\text{Eqn 2.35})$$

$$\text{Where, } v_{u2} = 150 \sqrt[3]{f_{ck} \rho \left(\frac{d}{a} \right)^4}$$

For $a/d \geq 2.5$,

$$v_u = v_{u1} + r f_{yw} \quad (\text{Eqn 2.36})$$

$$\text{Where, } v_{u1} = 60 \sqrt[3]{f_{ck} \rho \frac{d}{a}}$$

However, for value of $a/d = 2.5$, discontinuity were observed by Zsutty and he acknowledged that the results obtained for short beams were not satisfactory.

Regan and Placas [52] in 1971 reported tests on 5 rectangular NWC beams cast without shear reinforcement, 25 rectangular NWC beams cast with shear reinforcement, 2 NWC T-beams cast without shear reinforcement and 30 beams cast with shear reinforcement, which four distinct modes of failure were observed: (i) diagonal tension failure, (ii) shearing failure, (iii) shear compression failure and (iv) web crushing. An expression for shear and shear compression was proposed, respectively, to predict the ultimate shear failure load of rectangular normal weight concrete beams cast with shear reinforcement. The formulas are given as:

For shear failure mode,

$$V_u = 1.5 b d' r f_{yw} + 12.5 \left[\frac{100 A_s}{bd} \frac{Vd}{M} f_{ck} \right]^{1/3} b d \quad (\text{Eqn 2.37})$$

For shear compression mode,

$$V_u = \frac{3}{2} m_s^{2/3} (r f_{yw})^{1/3} \left(\frac{Vd}{M} \right)^{1/3} \left(\frac{b'}{b} \right)^{1/3} b d \quad (\text{Eqn 2.38})$$

Where, d' = depth from compressed surface to lowest layer of main steel

$$r = \frac{A_{sv}}{b s \sin \alpha}$$

f_{yw} = yield point stress of the shear reinforcement steel (psi)

f_{ck} = cylindrical concrete strength (psi)

M = bending moment at a section

$$m_s = 27 \left[f_{ck} \frac{100 A_s}{bd} \right]^{1/3}$$

Using Eqn 2.37 and 2.38, a very satisfactory agreement was achieved with the test results, which for rectangular concrete beams with shear reinforcement; a mean value of 0.91 for $V_{\text{Prediction}}/V_{\text{Test}}$ and standard deviation of 0.058 were obtained whilst for concrete T-beams with shear reinforcement; a mean of mean of 0.91 for $V_{\text{Prediction}}/V_{\text{Test}}$ and standard deviation of 0.007 were obtained.

Apart from the two nominal shear strength formulas proposed for normal weight concrete beam without shear reinforcement mentioned in Section 2.2.1.2, Arslan [53] in 2007 proposed two nominal shear strength formulas for normal weight concrete beams with shear reinforcement, which were categorized into short beams (for $a/d \leq 2.5$) and slender beams (for $a/d > 2.5$). The proposed formulas are as follow:

For slender beams, $a/d > 2.5$:

$$V_n = (0.15 f_{ck}^{1/2} + 0.02 f_{ck}^{0.65}) + \rho_w f_{yw} \quad (\text{Eqn 2.39})$$

For short beams, $a/d \leq 2.5$:

$$V_n = (0.15 f_{ck}^{1/2} + 0.02 f_{ck}^{0.65}) \left(\frac{2.5}{a/d} \right) + \rho_w f_{yw} \quad (\text{Eqn 2.40})$$

Where, $\rho_w f_{yw}$ = nominal shear strength of shear reinforcement in MPa

Arslan [53] achieved good agreement with the test results, which for normal weight concrete beams with shear reinforcement tested at $a/d > 2.55$, a mean of 1.34 for P_{Exp}/P_{Prop} and a standard deviation of 0.31 were obtained, compared to ACI 318 Building Code Provisions, which achieved a mean of 1.41 for P_{Exp}/P_{ACI318} and a standard deviation of 0.33. For normal weight concrete beams with shear reinforcement tested at $a/d \leq 2.5$, a mean of 1.47 for P_{Exp}/P_{Prop} and a standard deviation of 0.22 were achieved compared to ACI 318 Building Code Provisions, which achieved a mean of 1.84 for P_{Exp}/P_{ACI318} and a standard deviation of 0.39. However, it was noted the ratio of experimental to predicted shear strength was not significantly influenced with increasing a/d , $\rho_w f_{yw}$ and f_{ck} .

2.2.2.3 Concrete Plasticity Approach

As mentioned in Section 2.2.1.3, Braestrup [44] in 1975 reported shear tests on rectangular reinforced concrete beams and proposed corresponding work formulas. He derived a general work formula (Eqn 2.40) using upper bound theorem, based on the assumption if a rigid region I move, for a displacement δ , in a given direction, at an angle α to the discontinuity, relative to the rigid region II, the work dissipated in the narrow plastic zone for concrete with shear reinforcement are shown in Figure 2.19.

Upon simplification, for a concrete beam with shear reinforcement, the work required to shear the concrete beam is given as:

$$W = P\delta = \delta \rho_s \sigma_f b h \cot \theta + \frac{\delta \sigma_c}{2} (1 - \cos \theta) \left(\frac{b h}{\sin \theta} \right) \quad (\text{Eqn 2.41})$$

Where, σ_c = concrete compressive strength

α = angle of movement to plane of discontinuity

ρ_s = ratio of shear reinforcement

δ = displacement

θ = angle of plane of discontinuity

σ_f = yield strength of reinforcement

The above formulas were confirmed by Nielsen et.al [45] in 1978 to be an exact solution using the lower bound technique approach. However, it was found that an agreement between the theoretical predictions and test results was achieved only if the theoretical prediction was modified by an effectiveness factor, u . The effectiveness factor, u was found to be 0.74 for concrete beams with shear reinforcement mainly because concrete is not a perfectly plastic material as assumed in this approach, where concrete is assumed to exhibit perfectly plastic behaviour and has a compressive strength equal to the peak value on a stress strain curve. It is believed that it is unlikely that the concrete stress would be equal to the maximum compressive strength at all points of the failure surface as concrete is not a homogenous material and has a very limited deformability. However, when in tension, the concrete exhibits brittle behaviour at low stress and displays monotonic strain softening behaviour at large strain. Hence, it is important to compute the effectiveness of the concrete compressive strength at failure using the effectiveness factor.

For concrete beams with shear reinforcement, it was found that better agreement with the tests when the effectiveness factor, u was considered to be a function of concrete cylinder compressive strength, σ_c , as given in the following formula:

$$u = 0.8 - \frac{\sigma_c}{200} \quad (\text{Eqn 2.42})$$

The details of the effectiveness factor derivation and the comparison with the test results is presented by Neilsen [45] in 1978.

2.2.2.4 Building Code Approach

In addition to the shear strength prediction of normal weight concrete beams without shear reinforcement, codes of practice: BS8110 Code [47], Eurocode 2 Code [48], and ACI Code [49] also presented the shear strength prediction of normal weight concrete beams with shear reinforcement. However, it is noted by Author that there are variations among the codes regarding the formula of shear strength prediction and the considerations of variables affecting the shear strength of the structural beam elements. Hence, the formula for shear strength predictions of normal weight concrete with shear reinforcement are discussed in Section 2.2.2.4.1 to Section 2.2.2.4.3 for BS8110 Code [47], Eurocode 2 Code [48], and ACI Code [49], respectively.

2.2.2.4.1 BS8110 Code

In 1997, BS8110 design code [47] recommended two formulas for the prediction of shear capacity of concrete beam with shear reinforcement, which derived from two components, concrete and shear reinforcement as given as follow:

$$V_n = V_s + V_c \quad (\text{Eqn 2.43})$$

Where, V_c = cracking shear strength of concrete in MPa

V_s = shear strength of shear reinforcement based on yield

The two formulas for the shear strength prediction of a normal weight concrete beam with shear reinforcement are for $\frac{a}{d} \leq 2$ and $a/d > 2$, respectively. The formulas are given as follow:

For $\frac{a}{d} \leq 2$,

$$V_{BS8110-S} = \left[\frac{0.79 \rho^{1/3} \frac{f_{cu}^{1/3}}{25} \frac{400^{1/4}}{d} 2 \frac{d}{a}}{\gamma_m} + 0.87 \frac{f_{yw}}{b} \frac{A_{sw}}{s} \right] b d \quad (\text{Eqn 2.44})$$

For $\frac{a}{d} > 2$,

$$V_{BS8110-S} = \left[\frac{0.79 \rho^{1/3} \frac{f_{cu}^{1/3}}{25} \frac{400^{1/4}}{d}}{\gamma_m} + 0.87 \frac{f_{yw}}{b} \frac{A_{sw}}{s} \right] b d \quad (\text{Eqn 2.45})$$

From Eqn 2.45, the influence of parameters is:

$$f\left(\frac{A_{sw}}{s}\right) = \frac{A_{sw}}{s} \quad (\text{Eqn 2.46.1})$$

$$f(f_{cu}) = \frac{f_{cu}^{1/3}}{25} \quad (f_{cu} > 25\text{MPa}) \quad (\text{Eqn 2.46.2})$$

$$f\left(\frac{a}{d}\right) = \frac{2d}{a} \quad (a/d \leq 2) \quad (\text{Eqn 2.46.3})$$

2.2.2.4.2 Eurocode 2

The shear strength of normal weight concrete beams with shear reinforcement in Eurocode 2 [48] were formed based on the variable strut inclination method to determine the shear capacity of reinforced concrete beams with shear reinforcement.

The design shear resistances of normal weight concrete beam with shear reinforcement are given by Eurocode 2 are given as follow:

$$V_n = V_{rd,s} + V_{ccd} + V_{td} \quad (\text{Eqn 2.47})$$

Where, $V_{rd,s}$ = design value of the shear force which can be sustained by the yielding shear reinforcement

V_{ccd} = Design value of the shear component of the force in the compression area, in the case of an inclined compression chord

V_{td} = Design value of the shear component of the force in the tensile reinforcement, in the case of an inclined tensile chord

The design value of the shear force which can be sustained by the yielding shear reinforcement, $V_{rd,sr}$ for a shear strength prediction of a beam with shear reinforcement is given as the smaller amount of:

$$V_{rd,sr} = \frac{A_{sw}}{s} z f_{yw} \cot \theta \quad (\text{Eqn 2.48})$$

and

$$V_{rd,max} = \frac{\alpha_{cw} b_w v_1 z f_{cd}}{\cot \theta + \tan \theta} \quad (\text{Eqn 2.49})$$

Where, $v_1 = 0.6 \left(1 - \frac{f_{ck}}{250}\right)$ for $f_{ck} \leq 60$ MPa = strength reduction factor for concrete cracked in shear

α_{cw} = coefficient taking account the state of the stress in the compression chord

$f_{cd} = \alpha_{cc} \frac{f_{ck}}{\gamma_c}$ where $\alpha_{cc} = 1$ and $\gamma_c = 1$ for the OPSC shear

strength predictions.

θ = the angle between the concrete compression strut and the beam axis perpendicular to the shear force

From Eqn 2.47, the influence of parameters is:

$$f(\theta) = \cot \theta \quad (\text{Eqn 2.50.1})$$

$$f\left(\frac{A_{sw}}{s}\right) = \frac{A_{sw}}{s} \quad (\text{Eqn 2.50.2})$$

From Eqn 2.48, the influence of parameters is:

$$f(v_1) = v_1 = 0.6 \left(1 - \frac{f_{ck}}{250}\right) \quad (\text{Eqn 2.50.3})$$

The inclination angle of shear cracks, θ given in the prediction of shear strength for normal weight concrete beam with shear reinforcement by Eurocode 2, are not fixed as 45 degree but it was limited to the angle between 22 degree to 45 degree, as given in the Eurocode 2.

2.2.2.4.3 ACI code

In 2002, ACI 318 Building code [49] recommended 2 formulas for the prediction of shear capacity of concrete beam with shear reinforcement, which derived from two components, concrete and shear reinforcement based on experimental results of beam test data and given as:

$$V_n = V_s + V_c \quad (\text{Eqn 2.51})$$

Where, V_c = cracking shear strength of concrete in MPa

V_s = shear strength of shear reinforcement based on yield

The contribution of V_s is derived from basic equilibrium considerations on a 45 degree truss model with constant effective depth and shear reinforcement spacing.

A formula was given each for short beams (beams tested $a/d < 2.5$) and for slender beams (beams tested at $a/d \geq 2.5$), respectively, which are further defined as:

For short beams, $a/d < 2.5$,

$$V_n = (3.5 - 2.5 a/d) \frac{1}{6} \sqrt{f_{ck}} + \rho_s f_{yw} \quad (\text{Eqn 2.52})$$

For slender beams, $a/d \geq 2.5$,

$$V_n = \frac{1}{6} \sqrt{f_{ck}} + \rho_s f_{yw} \quad (\text{Eqn 2.53})$$

Where, f_{yw} = design yield strength of the shear reinforcement

f_{ck} = cylinder concrete strength (psi)

2.3 Size effect

2.3.1 Beams without shear reinforcement

It was reported by researches [54-60] that size effect occurs in normal weight concrete beams, which shear capacity decreases with the size of specimen. Hence, the shear capacity of a concrete beam is affected by the specimen size.

Kani [54] in 1967 presented a series of tests on large beams, in which the beam depth was tested between 150 mm to 1220 mm whilst the width was held constant at 150 mm with longitudinal steel ratio of 2.8%. The variables considered were absolute size and depth to width ratio, which it was observed that the strength of the large beam reduced approximately 40 % of the strength that were expected from the test results on the small beams.

Taylor [55] in 1972 reported the investigations of size effect in beams, which a series of tested beams with varying depth from 150 mm to 1000 mm whilst the width were held constant at 40 mm with longitudinal steel ratio casted at 1.35%. Taylor observed that from the tests from Kani [54] and Leondhart et.al [56], increment of beam size with particle size kept constant results in a decreased of the total shear capacity, which occurred due to the reduction in aggregate interlock contribution. Further, it was reported that the contradict results obtained between Kani [54] and Leondhart et.al [56] were because of the difference in the depth to width ratios considered for each beams and also the aggregate size was not scaled. Hence, a series of tests were carried out and reported to investigate the effect of maximum aggregate sizes on the beams with varying depth from 150 mm to 1000 mm, which slight reductions in the shear strength capacity of large beams occurred, when compared with the relative

strength of small beams. Further, the tests also showed the effect of aggregate scaling with respect to beam depth, which it was found that scaling of aggregate correctly would not cause a loss of strength (see Figure 2.20).

It is observed by Author from Taylor's [55] report that cracks with respect to the beams by Kani [54], Taylor [55] and Leondhart et.al [56] increased with the depth increment (see Figure 2.21) from Kani, Figure 2.22 and 2.23 from Leondhart, and Figure 2.24 from Taylor, which indicate that loss of interlocking strength are more significant in larger beams.

Bazant and Kim [57] in 1984 presented a statistical analysis of normal weight concrete beams without shear reinforcement using data based on nonlinear fracture mechanics approach to represent the size effect in concrete beams. It was noted that nonlinear fracture mechanics approach predicts the test results more accurately than linear fracture mechanics approach as concrete exhibited brittle characteristics in failure (see Figure 2.25). According to Bazant and Kim, size effect in structure occurred due to the release of strain energy from the beam into the cracking zone as the cracking zone lengthens and hence, the increment size of the structure would lead to higher energy released. A cracking shear capacity (Eqn 2.54) were presented by Bazant and Kim to represent the size effect for diagonal shear failure of concrete beams element with longitudinal reinforcement without shear reinforcement, which it is believed that the energy loss due to cracking is a function of both fracture length and of cracking zone area assumed to have a constant width at its front, proportional to the maximum aggregate size. The cracking shear stress of concrete beams without shear reinforcement is predicted as follow:

$$v_c = v_c^0 \left(1 + \frac{d}{\lambda_0 d_a}\right)^{-1/2} \quad (\text{Eqn 2.54})$$

Where, d_a = maximum aggregate size

λ_0 = empirical constants

v_c^0 = material parameter given

The variable formula, v_c^0 in Eqn (2.54) is given as:

$$v_c^0 = k_1 \rho^{\frac{1}{3}} \left(\sqrt{f_{ck}} + 3000 \sqrt{\frac{\rho}{(a/d)^5}} \right) \quad (\text{Eqn 2.55})$$

Where, $k_1 = 10$

f_{ck} = cylindrical compressive strength in psi

In addition, an ultimate shear capacity formula was derived from the analysis and summations of arch action for short beam and the composite beam action for slender beam were proposed, which considered the variables: cylinder concrete strength, steel ratio, shear span to effective depth ratio, effective depth and maximum aggregate size. It was reported that Bazant's law size effect law showed good agreement with 297 test results available with respect to the increase of reinforced concrete depth. (see Figure 2.26)

The proposed formula is given as:

$$v_u = \frac{8 \sqrt[3]{\rho}}{\sqrt{1 + \frac{d}{25 d_a}}} \left(\sqrt{f_{ck}} + 3000 \sqrt{\frac{\rho}{\alpha^5}} \right) \quad (\text{Eqn 2.56})$$

Where, d_a = maximum aggregate size

$\alpha = a/d$ for concentrated load and $\alpha = l/4d$ for uniform load

f_{ck} = cylindrical concrete strength in psi

In 1987, Bazant and Sun [58] generalized the proposed existing formula (Eqn 2.54), which took account into the effect of maximum aggregate size, which the proposed cracking shear strength prediction for concrete beams without shear reinforcement is given as:

$$v_c = v_c^0 \left(\frac{1 + \sqrt{\frac{c_0}{d_a}}}{\sqrt{1 + \frac{d}{\lambda_0 d_a}}} \right) \quad (\text{Eqn 2.57})$$

Where, $c_0 = 0.2$ inch

$\lambda_0 = 25$

$d_a =$ maximum aggregate size

It was reported that good agreements were achieved between the new generalized proposed formulas (Eqn 2.57) with 461 literature data (see Figure 2.27).

Apart from NWC beams without shear reinforcement, Bazant and Sun [58] also presented a formula for NWC beams with shear reinforcement, which are mentioned in Section 2.3.2.

Walvaren and Lehwalter in 1994 [59] reported that size effect occurred in both normal weight concrete and lightweight concrete beams, which comparisons were carried out between normal weight concrete (NWC) and light weight concrete (LWC) beams without shear reinforcement of shear span to effective depth ratio, $a/d = 3$ with respect to variations of depth. It was reported that the ultimate shear capacity obtained by the NWC beams were slightly higher than the LWC beams, which would have due to the difference in aggregate interlocking capacity provided (see Figure 2.28). In Author opinion, NWC beams would have exhibited higher shear capacity due to the higher impact strength provided by the gravel aggregates compared to lightweight aggregates.

Walvaren and Lehwalter [59] also presented the investigations on the size effect of normal weight concrete beams tested with respect to the variables: beam depth, aggregate size, and shear span to effective depth ratio. It was reported that

significant size effect occurred in normal weight concrete beams without shear reinforcement, which were tested at $a/d < 2.5$ (see Figure 2.29). It was noted by Walvaren and Lehwalter [59] that the size effect observed in short and slender beams, of normal weight concrete and lightweight concrete, for effective depths between 150 mm and 1000mm, can be formulated with the Bazant's size effect law.

Walvaren and Lehwalter [59] also noted that smaller size beams exhibited smaller crack widths compared to larger beams, which is believed were due to the substantial amount of tensile stresses transmitted over the crack faces during loading. From Author observations, the amount of cracks exhibited by the beam increased with the increment of beam depth for both short and slender beams tested by Walvaren and Lehwalter (see Figure 2.30 and 2.31).

2.3.2 Beams with shear reinforcement

For concrete beams with shear reinforcement, Bazant and Sun [58] in 1987 proposed an ultimate shear stress formula (Eqn 2.58), which consists of combination of cracking shear stress capacity, v_c and contribution of yield forces in shear reinforcement, v_s . The proposed formula is given as follow:

$$v_u = v_c + v_s \quad (\text{Eqn 2.58})$$

The contribution of yield forces in shear reinforcement, v_s from Eqn 2.58 was obtained from plastic limit analysis, which is given as follow:

$$v_s = \frac{A_{sv} f_{yw}}{b s} (\sin \alpha + \cos \alpha) \quad (\text{Eqn 2.59})$$

Where, α = angle between the shear reinforcement and the longitudinal axis of the beam

f_{yv} = yield strength of reinforcement (psi)

It was reported by Bazant and Sun [58] that good agreement were obtained between the new generalized proposed formula (Eqn 2.58) with 87 test results (see Figure 2.32). However, Bazant and Kazemi in 1991 [60] reported that the scatter of the test results were too large and hence, another formula for the ultimate shear stress of concrete failed in diagonal shear failure were proposed (see Eqn 2.60), which incorporated cracking shear stress formula given by ACI 318 design code with his size effect law. The proposed formula is given as:

$$v_u = B v_c (1 + \beta)^{-1/2} \quad (\text{Eqn 2.60})$$

Where, $v_c = \min \left(1.9 \sqrt{f_{ck}} + 2500 \rho \frac{V_u d}{M_u}, 3.5 \sqrt{f_{ck}} \right)$

B = size effect variable (see Ref [55])

$$\beta = \frac{d}{d_o}$$

It was reported by Bazant and Kazemi [60] that good agreements with the series with different size range variation of 1:16, 2: 16 and 2: 8 were achieved between the new proposed formula (Eqn 2.60) and the experimental results conducted.

In addition to normal weight concrete beams with shear reinforcement, Walvaren and Lehwalter in 1994 [59] also presented the investigations on the size effect of normal weight concrete beams with shear reinforcement tested at $a/d < 2.5$. It was noted by Walvaren and Lehwalter [59] that the significant size effect also observed in normal weight concrete beams with shear reinforcement tested at $a/d < 2.5$ (see Figure 2.33).

2.4 Oil Palm kernel Shell Concrete (OPSC)

Since the introduction of OPS aggregates as coarse aggregates in concrete, extensive amount of research has been carried out in search of the Oil Palm kernel Shell Concrete (OPSC) properties. The core materials to cast OPSC consists of ordinary Portland cement, sand as fine aggregate, Oil Palm kernel shell (OPS) as coarse aggregate and water. Optional material such as admixtures and cementitious materials were added into the OPSC mix to achieve higher compressive strength and workability.

Researchers [1-16] found that OPSC have low bulk densities of 1600 kg/m^3 to 1960 kg/m^3 . Consequently, OPSC is categorized as structural lightweight aggregate, which satisfies the range specified by ASTM C330 [63]. Teo et.al [13] suggested the lightweight density of OPSC results in the reduction of the overall dead load in structures, which in turn significantly reduced the total cost in construction and also reduced the catastrophic impact caused by earthquake in earthquake prone countries.

2.4.1 Properties of Oil Palm Shell (OPS) aggregate

In this research, the types of coarse aggregate used were Oil Palm kernel Shell (OPS) aggregate and crushed granite aggregate. As the material properties of both types of aggregate differ, it would affect the material and structural properties of the concrete produced. Therefore, it is crucial to understand the properties of aggregate prior to mixing.

The physical and mechanical properties of OPS aggregate and crushed granite aggregate obtained from different researchers in the field of OPSC are shown in Table 2.1. It is noted that OPS aggregate is porous in nature, which results in low bulk density and high water absorption. Teo [5] suggested that aggregate with high water absorption is less sensitive to poor curing due to the internal water supply stored by the porous lightweight aggregate. Teo et.al [5] also stated that low aggregate abrasion value and aggregate impact obtained indicate that OPS aggregate is good absorbance to shock.

2.4.2 Oil Palm kernel Shell Concrete (OPSC) mix design

Mannan [3] and Teo et. al [4 & 5] reported that the normal mix design method suggested by Short and Kinniburgh [61] for lightweight concrete is not applicable to obtain the targeted OPSC strength because the properties of OPS aggregate differed with other existing lightweight concrete. Hence, it is suggested that trial mixes should be adopted to obtain the targeted OPSC strength. With these, contributions by Okpala [1], Basri [2], Mannan [3, 7-10], Teo [4 & 5] and Alengaram [11 & 16] on the mix design of OPSC are noteworthy.

In 1990, Okpala [1] proposed 2 mix proportion for OPSC without addition of admixtures, which were 1:1:2 and 1:2:4 in term of volume of cement: river sand: OPS aggregate (C: S: OPS) with water/cement (w/c) ratio in range of 0.5 to 0.8. The highest cube compressive strength achieved at 28 days was 18.9 N/mm² of mix ratio 1:2:4 (C: S: OPS) of w/c = 0.5. The OPSC has a higher noise absorption capacity and a low thermal conductivity compared to NWC.

In 1999, Basri et.al [2] presented the compressive strength of OPSC under 3 curing conditions of water cured, air cured and partial water and air cured over 56 days period and the influence of fly ash as a cement replacement admixture on OPSC strength, which the highest OPSC compressive strength obtained at 28 days was water cured with 23 N/mm² by mix design of 1: 1.71: 0.77 (Cement: Sand: SSD OPS) and w/c ratio =0.41. The results showed that the addition of fly ash as cement replacement admixture had a negative effect on the OPSC compressive strength. He also suggested that as OPS aggregate is hard and organic, it will not contaminate or leach to produce toxic substances once bound in concrete matrix.

Mannan et.al [3, 7-10] proposed a mix proportion of 1: 1.71: 0.77 (Cement: Sand: SSD OPS) by weight with w/c ratio of 0.41 and addition of admixtures, FDN superplasticizer or sikament NN. The highest cube compressive strength obtained at 28 days was 24.2 N/mm². M.A.Mannan [3] reported that the addition of fly ash as cement replacement into the OPSC mix results in the reduction of OPSC cube compressive strength as reported by H.B.Basri [2]. Distinctly, the addition of calcium chloride of 1% in the OPSC mix managed to increase the OPSC cube compressive strength to 29.4 N/mm².

Mannan et.al [7] reported the long term strength of OPSC, which the results obtained show that OPSC strength continue to increase with time as no retrogression in strength present even after 365 days. However, it was reported by Mannan that the increment of rate in OPSC compressive strength is lower than NWC for 365 days curing period.

Teo et.al [4 & 5] proposed a mix proportion for OPSC, which the most suitable mix proportion were found to be 1: 1.66: 0.6 and 1: 2.14: 1.63 by weight and volume respectively, with a w/c ratio of 0.41. Additional admixture, Type F-naphthalene sulphonate superplasticizer (SP) was added into the OPSC mix to improve the workability of the OPSC mix and The OPSC cube compressive strength recorded at 28 days was 28 N/mm².

Teo et.al [4] presented a comparison between OPSC and NWC using the proposed mix proportion of 1: 2.14: 1.60 by volume with a w/c ratio of 0.38 and additional admixture, Type F-naphthalene sulphonate superplasticizer (SP) was added into the OPSC mix. The tests conducted on both concrete include compressive strength, split tensile strength, modulus rupture and modulus of elasticity. The results obtained at 28 days shown that the values obtained for compressive strength, split tensile strength, modulus rupture and modulus of elasticity by OPSC were approximately 0.52, 0.38, 0.58 and 0.27 times lower respectively compared to NWC.

Teo [5] reported on the bond behaviour and durability performance of the OPSC, which the bond test results reported that for plain bars, the bond strength obtained was 10 to 24 % of the cube compressive strength whilst for deformed bars, the bond strength obtained was 24 to 42 % of the cube compressive strength. It was reported that the bond strength of OPSC obtained was much higher than the theoretical bond strength predicted by BS8110.

The durability performance of OPSC was measured by water permeability and water absorption test. The results reported show that relatively high water content of 4.8% to 5.5% was observed for OPSC. Observations by Teo [5] also show that OPSC has a

high water absorption compared to NWC due to the porous nature of OPS aggregate. Teo [5] stated that the lightweight concrete with porous aggregate (high water absorption) are less sensitive to poor curing as compared to normal weight concrete due to the internal water supply stored by the porous lightweight aggregate.

Alengram and Jumaat [11, 14 -16] adapted OPSC mix proportion of 1:1.2:0.8 by weight with the w/c ratio of 0.35. Additional admixture and cementitious material added were 10 % silica fume, 5% fly ash and 1% superplasticizer. The OPSC compressive strength achieved was 36 N/mm².

The mix designs adopted by various researchers stated above are summarized by Alengram [6], which are also shown in Table 2.2 [6].

2.4.3 Flexural strength of OPSC

The flexural strength of OPSC achieved by various researchers was summarized by Alengram [6], which are also shown in Table 2.3. The flexural strength of OPSC without additional admixtures are found to be 10% to 13% of the OPSC compressive strength, in which from Okpala reported 13 %, Teo and Liew reported 11% and Mahmud et al. reported 10% [6].

2.5 Shear strength of Oil Palm kernel Shell Concrete (OPSC) beams

In addition to the shear strength of NWC beams without shear reinforcement, the shear strength of Oil Palm kernel Shell Concrete (OPSC) beams reported by researchers were also reviewed to form the current understanding on the research

development of OPSC as structural beam elements, which were reported by Jumaat et.al [15] and Alengaram et.al [16]. Both researches reported on the comparison between OPSC beams and NWC beams of the shear strength obtained from their investigations.

2.5.1 Shear strength of Oil Palm Shell Foamed Concrete (OPSFC) beams

Jumaat et.al [15] in 2009 presented an experimental study carried out to compare the shear strength of Oil Palm Shell foamed Concrete (OPSFC) beams and normal weight concrete (NWC) beams casted from concrete having cube compressive strength, $f_{cu} = 20 \text{ N/mm}^2$. In this study, a total of eight beam specimens were tested, of which, four cast without shear reinforcement, while the remaining four cast with shear reinforcement. Among these four beam specimens, two of each were OPSFC beams, while the remaining two were NWC beams.

From these investigations, it was found that, in the case of beam cast without shear reinforcement, the shear strength of OPSFC beam specimens out-perform those of NWC beam specimens by 10 %. For shear reinforced beam, the shear strength obtained for both specimens are almost similar. Based on the experimental observations, it was reported, in comparison to NWC beam specimens, the OPSFC beam specimens exhibited profound “zig zag” shear cracks on both sides surface of the beam specimens. Upon further investigations, he found the OPSFC beam specimens exhibited rougher shear failure surface in comparison to those of NWC beam specimens. Therefore, it was suggested that the convex nature of oil palm kernel shell (OPSC) contributed good aggregate interlocking, and hence, a higher shear resistance was mobilised. Further, it was suggested that the convex portion of

the oil palm kernel shell (OPS) allowed for good bonding with the cement mortar, and hence, provided a higher resistance against bonding failure between OPS and cement mortar, if otherwise, would have led to a lower shear resistance.

2.5.2 Shear behaviour of reinforced palm kernel shell concrete beams

Alengaram et.al [16] in 2011 reported the shear behaviour of reinforced palm kernel shell concrete beams and comparisons were carried out between OPSC beams and NWC beams of cube concrete compressive strength of 30 N/mm^2 with respect to the shear behaviour. In this study, a total of eight beam specimens were tested, of which, four cast without shear reinforcement, while the remaining four cast with shear reinforcement. Among these four beam specimens, two of each were OPSC beams, while the remaining two were NWC beams.

From the investigation, it was concluded that the ultimate shear strength to density ratios obtained for non-shear and shear reinforced OPSC beams were 22% and 49% higher than the NWC beams respectively. He further reported that the shear strength ratios between the experiment and prediction by the BS8110, ACI and EC2 code of practice were in the range of 1.57 to 2.83. Hence, it was concluded that all the three codes underestimate the actual shear strength of non-shear and shear reinforced OPSC and NWC beams.

It was mentioned that good aggregate interlocking suggested by Jumaat et. al [15] and enhanced dowel action of OPSC beams, of which contributed from the large tensile stresses in the OPSC between the cracks, produced a higher shear strength of OPSC beam.

2.6 Flexural Behaviour of OPSC beams

The flexural behaviour of concrete beams, which incorporated OPS as coarse aggregates in concrete, were reported by Teo et.al [13] and Alengaram et.al [14]. Both researchers investigated on the flexural behaviour of OPSC beams and comparisons were also carried out between the OPSC beams and NWC beams on the flexural resistance observed.

2.6.1 Flexural Behaviour of Reinforced Lightweight Concrete Beams Made with OPS

In 2006, Teo [13] reported experimental study on the flexural behaviour of OPSC beams. Total six similar sizes of under-reinforced OPSC beam specimens were casted: 3 singly reinforced OPSC beams and 3 doubly reinforced OPSC beams.

All the OPSC beam specimens showed typical structural behaviour in flexure and yielding of the tensile reinforcement occurred before crushing of the compression concrete in the pure bending zone. For beam specimens up to a reinforcement ratio of 3.14%, the experimental ultimate moments of 4 % to 35 % higher compared to the predicted BS8110 moments. For OPSC beam specimens with reinforcement ratio of 3.9%, the experimental ultimate moment obtained are 6 % lower compared to the predicted BS8110 moment.

For singly reinforced beam specimens, the deflections obtained from the experimental are acceptable as the span to deflection ratios ranged from 252 to 263 and satisfied the allowable limit provided by BS8110. For doubly reinforced beam specimens, the span to deflection ratios obtained ranged from 146 to 196 and hence,

beam depths should be increased. All OPSC beam specimens showed considerable amount of deflection, which provides ample warning to the imminence of failure.

2.6.2 Ductility behaviour of reinforced palm kernel shell concrete beams

Alengaram et. al [14] in 2008 reported experimental study on the flexural behaviour of OPSC beams and comparisons were made between OPSC beams and NWC beams of grade 30 with respect to mechanical properties and structural behaviour.

Both OPSC and NWC beams displayed flexural failure with yielding of tension steel occurred prior to crushing of concrete in compression zone. Prior to failure, flexural cracks were observed and extended to the neutral axis for both types of concrete. During failure, OPSC beams failed in ductile manner which allowed sufficient warning whereas NWC beams failed in brittle failure.

The experimental moments obtained by all beams were 5% higher than the theoretical calculations. However, it was noted that the experimental moments obtained by OPSC beams were slightly higher than NWC beams. The experimental deflections obtained at service stage were close to the deflection predicted by BS8110 code compared to the ACI code and were within the permissible limit of 8.4 mm as stipulated by the BS8110 code for structural use.

2.7 Summary

The research carried out in search for the shear transfer mechanism of normal weight concrete beams with and without shear reinforcement had been covered thoroughly since the last two centuries.

However, for OPSC beams, the current understanding about the shear resistance of OPSC beams both cast with and without shear reinforcement were lack and only small amount of study has been carried out due to its novelty, which research on OPSC material properties and mix design only took place for the past two decades.

In addition, the design procedures for design against shear of beam cast with and without shear reinforcement respectively have not been covered in the present design codes. Advice has been given by some researches to adopt the current design code of normal weight concrete beam for the shear strength predictions of OPSC beam. However, the investigations carried out have not been covered adequately to validate that the design codes for normal weight concrete beams is completely suitable to be adopted for the shear strength predictions of OPSC beam.

Therefore, it is considered that there is a need for an experimental study to understand the shear strength of OPSC beams with and without shear reinforcement, respectively, and to determine whether the current design codes for normal weight concrete beams are applicable for Oil Palm kernel Shell Concrete (OPSC) beams.

Table 2.1 Properties of OPS Aggregate and Crushed Granite Aggregate.

Researcher	M.A.Mannan and D.C.L Teo		U.J.Alengaram and M.Z.Jumaat	
Type of aggregate	Crushed granite aggregate	Oil palm shell aggregate	Crushed granite aggregate	Oil palm shell aggregate
Thickness (mm)	12.50	0.50-3.00	15.00	0.70-3.50
Specific gravity (SSD)	2.61	1.17	2.67	1.27
Water absorption for 24 hours (%)	0.76	23.30	<1	24.50
Bulk Density (kg/m ³)	1470	590	1510	620
Fineness Modulus (F.M)	6.33	6.24	6.57	6.24
Aggregate Impact Value (%)	17.29	7.86	16.78	3.91
Aggregate Abrasion Value, L.A. (%)	24.00	4.80	N/A	N/A
Flakiness Index (%)	24.94	65.17	N/A	N/A
Elongation Index (%)	33.38	12.36	N/A	N/A

Table 2.2 Material properties of OPSC by researchers⁶.

Fresh and mechanical properties of concrete (All the mechanical properties reported at the age of 28-day.)								
Author (year)	Code used for mix proportions	W/C ratio	Mix proportions	Slump, (mm)	Compressive strength (MPa)	Flexural strength (MPa)	Splitting tensile strength (MPa)	Young's modulus (GPa)
Abdullah (1984)	-	0.6	1:1.5:0.5-1.0	200-0	10.00-2.50	-	-	-
			1:2.0:0.5-1.0	230-5	11.50-5.00	-	-	-
			1:2.5:0.3-0.75	260-10	15.00-8.00	-	-	-
			1:2.0:6	0-260	20.50-0	-	-	-
Okafor (1988)	-	0.48	1:1.70:2.08	8	~23	6.20	2.40	-
			1:1.88:2.18	28	~22	5.50	2.35	-
			1:2.10:1.12	50	~16	4.30	2.00	-
Okpala (1990)	-	0.5	1:1:2	30	22.20	2.81	-	-
			0.6	63	19.80	2.53	-	
			0.7	Collapse	16.50	2.30	-	
			0.8	Collapse	14.90	2.13	-	
			0.5	1:2:4	3	18.90	-	-
			0.6	28	16.50	-	-	
Mannan and Ganapathy (2001)	ACI	0.53	1:2.73:0.85	0	13.65	-	-	-
			1:2.73:0.85	4	6.30	-	-	
			1:2.73:0.85	0	13.15	-	-	
			0.60	1:1.28:0.55	Collapse	11.80	-	-
			1:1.28:0.55	Collapse	14.35	-	-	
			1:1.13:0.92	-	14.40	-	-	
Olanipekun et al. (2005)	-	-	1:1:2	-	17.50	-	-	-
			1:2:4	-	14.70	-	-	
Teo and Liew (2006)	DOE method	0.41	1:1.12:0.80	13	22	2.30	2.24	-
Teo et al. (2007)	-	0.38	1:1.66:0.60	60	28.00	-	-	5.31
Alengaram et al. (2008)	Specific gravity method	0.35	105	37.41	3.83	2.10	1.15	-
			-	-	36.70	3.50	1.95	10.05
Mahmud et al. (2009)	Specific gravity method	0.35	1:1:0.8	160	26.98	2.79	1.98	7.08
			1:1:0.8 (5%FA; 10%SF)	103	29.49	2.76	1.90	8.57
			1:1:2.8 (5%FA; 10%SF)	65	34.49	3.22	2.00	10.01
			1:1:6.8 (5%FA; 10%SF)	60	37.79	4.10	2.35	10.90
Alengaram et al. (2011)	Specific gravity method	0.30-0.35	1:0.8:1 (5%FA; 10%SF)	-	25.8-30.3	-	-	5.50-7.10
			1:1.0/1.2/1.6:0.8 (5%FA; 10%SF)	-	-	-	-	-
Shafiqh et al. (2011)	-	0.38	1:1.736:0.72 (steel fibers)	-	30.1-37.8 39.34-44.95	5.42-7.09	7.83-5.55	7.93-10.10 15.1-16.1

Table 2.3 Flexural strength of OPSC⁶.

Researcher (Year)	Mix Proportion	w/c ratio	Compressive strength (MPa)	Flexural strength (MPa)	Compressive strength
					Flexural strength (%)
Okpala (1990)	1:1:2	0.50	22.20	2.81	13%
			19.80	2.53	13%
Teo and Liew (2006)	1:1.12:0.80	0.41	22.00	2.30	11%
Mahmud et al. (2009)	1:1:0.8	0.35	26.98	2.79	10%

Table 2.4 V_{min} for NWC beams without shear reinforcement based on EC2⁴⁸.

	d = 200	d = 400	d = 600	d = 800
C20	0.44	0.35	0.25	0.29
C40	0.63	0.49	0.44	0.41
C60	0.77	0.61	0.54	0.50
C80	0.89	0.70	0.62	0.58

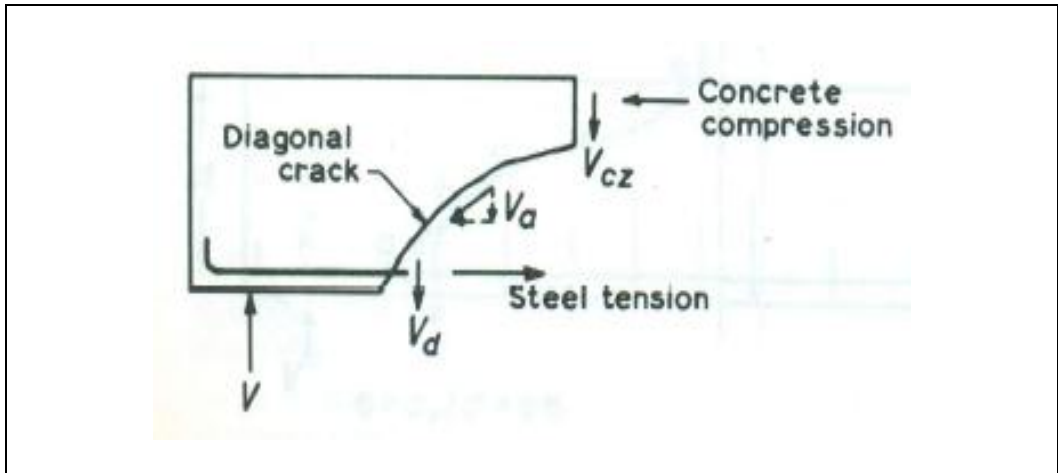


Figure 2.1 Three combined actions in reinforced concrete beams without shear reinforcement²⁷.

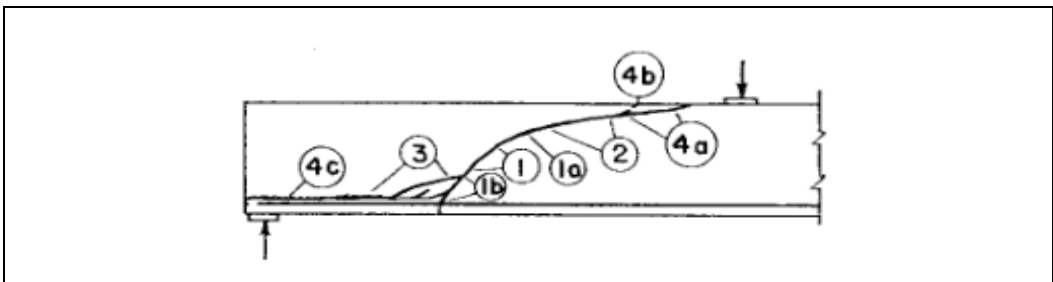


Figure 2.2 Hypothesis of systematic failure for beams failed in diagonal tension³⁰.

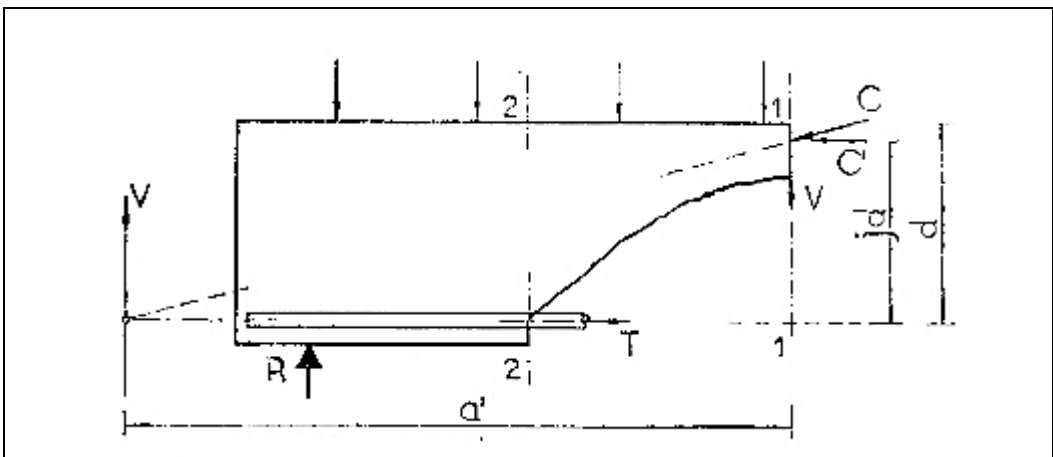


Figure 2.3 Formation of diagonal tension crack for beams without shear reinforcement³¹.

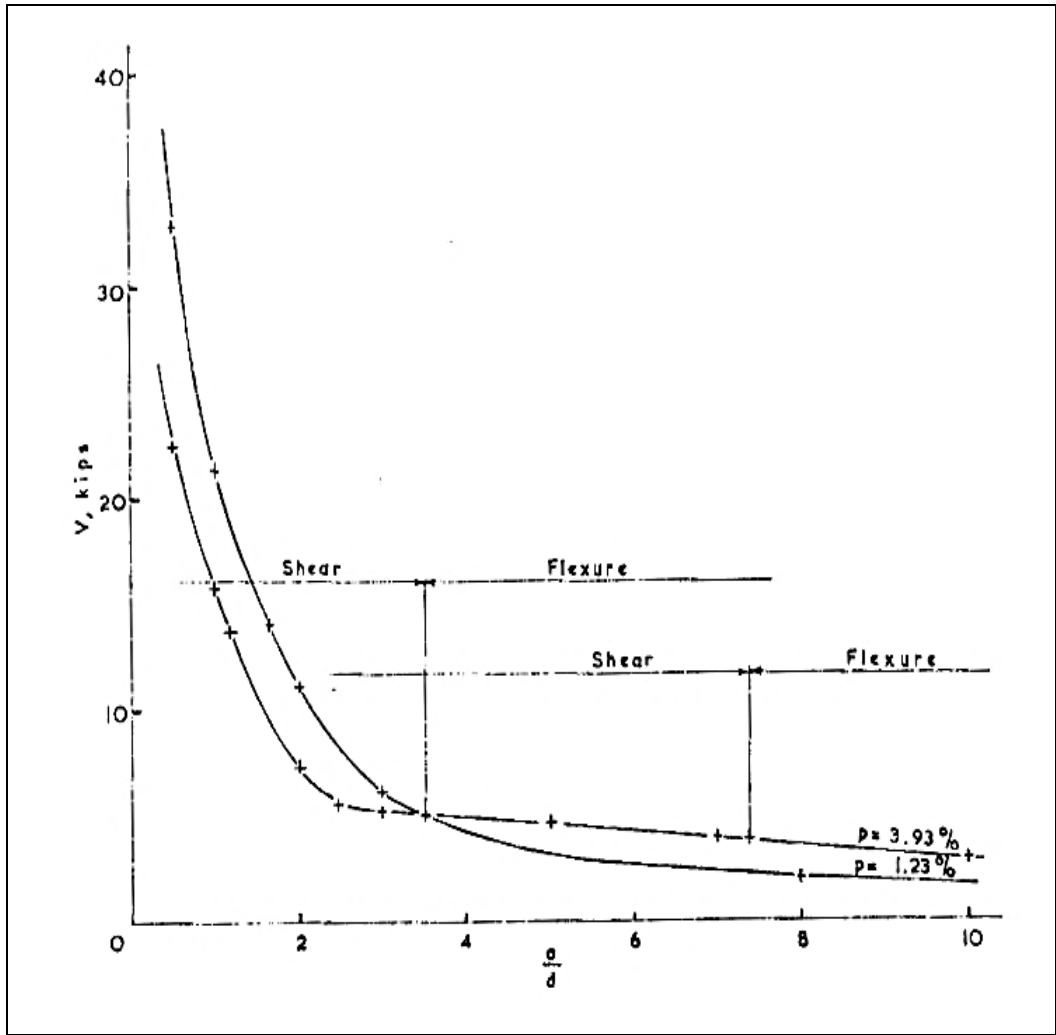


Figure 2.4 Shear resistance vs a/d ratio for Mattock's data³¹.

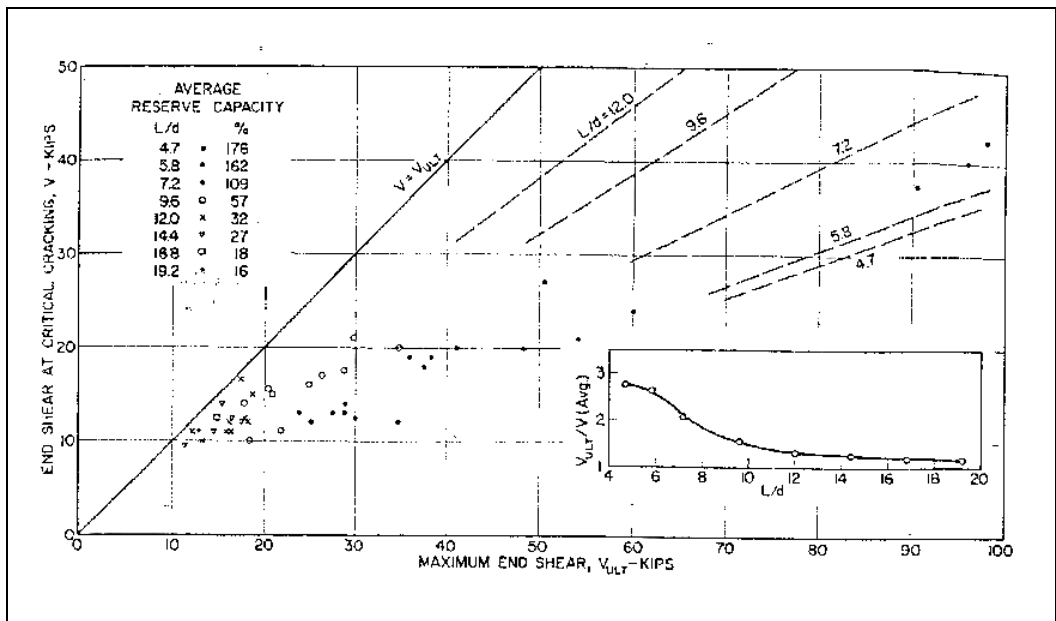


Figure 2.5 Reserve shear resistance beyond critical condition (uniform load and no shear reinforcement)³⁴.

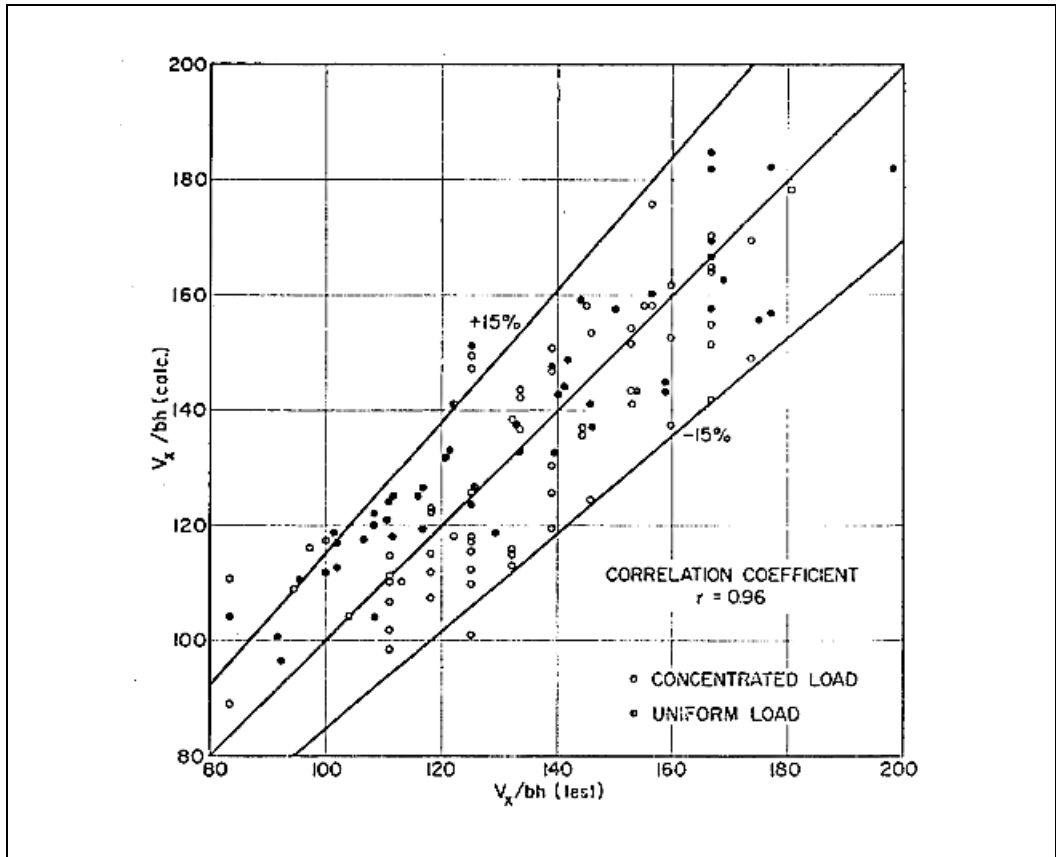


Figure 2.6 Comparisons of calculated and observed critical shear intensities³⁴.

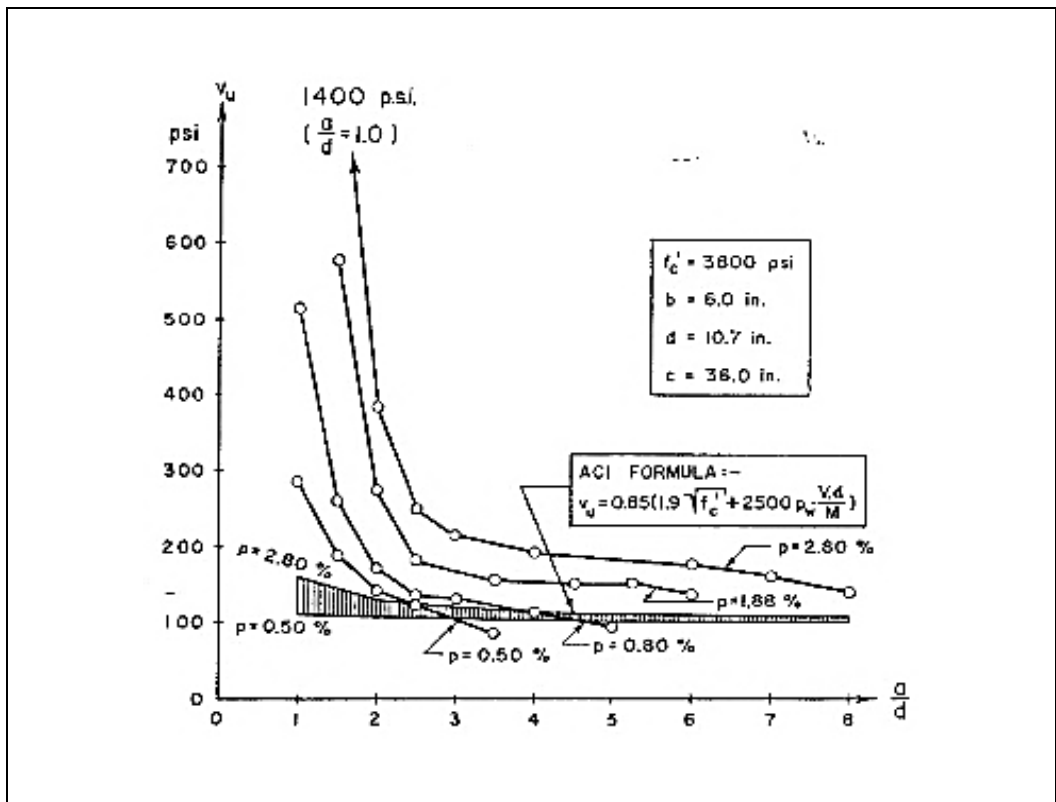


Figure 2.7 Shear stress at failure vs a/d ³⁵.

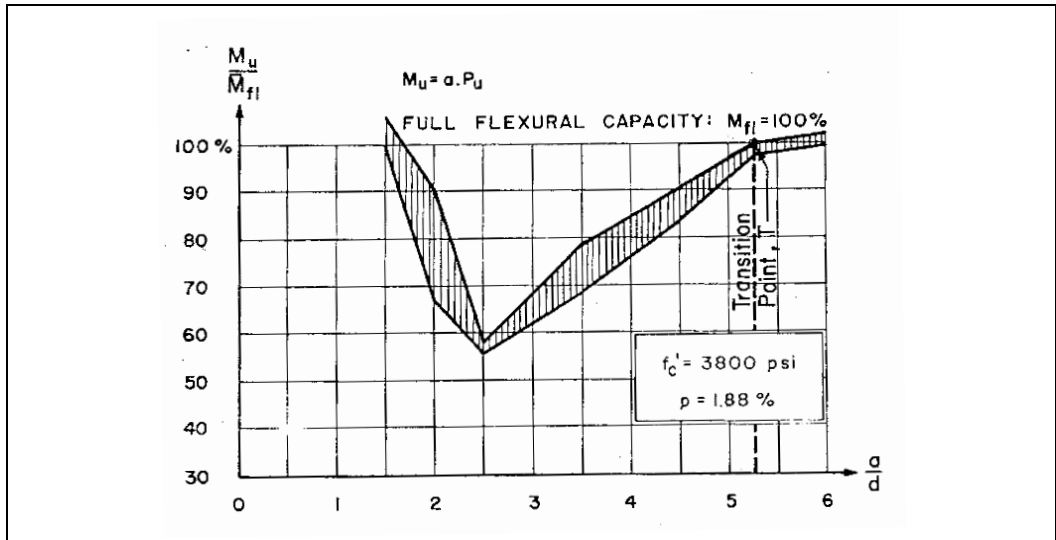


Figure 2.8 $\frac{M_u}{M_{f1}}$ vs a/d ³⁵.

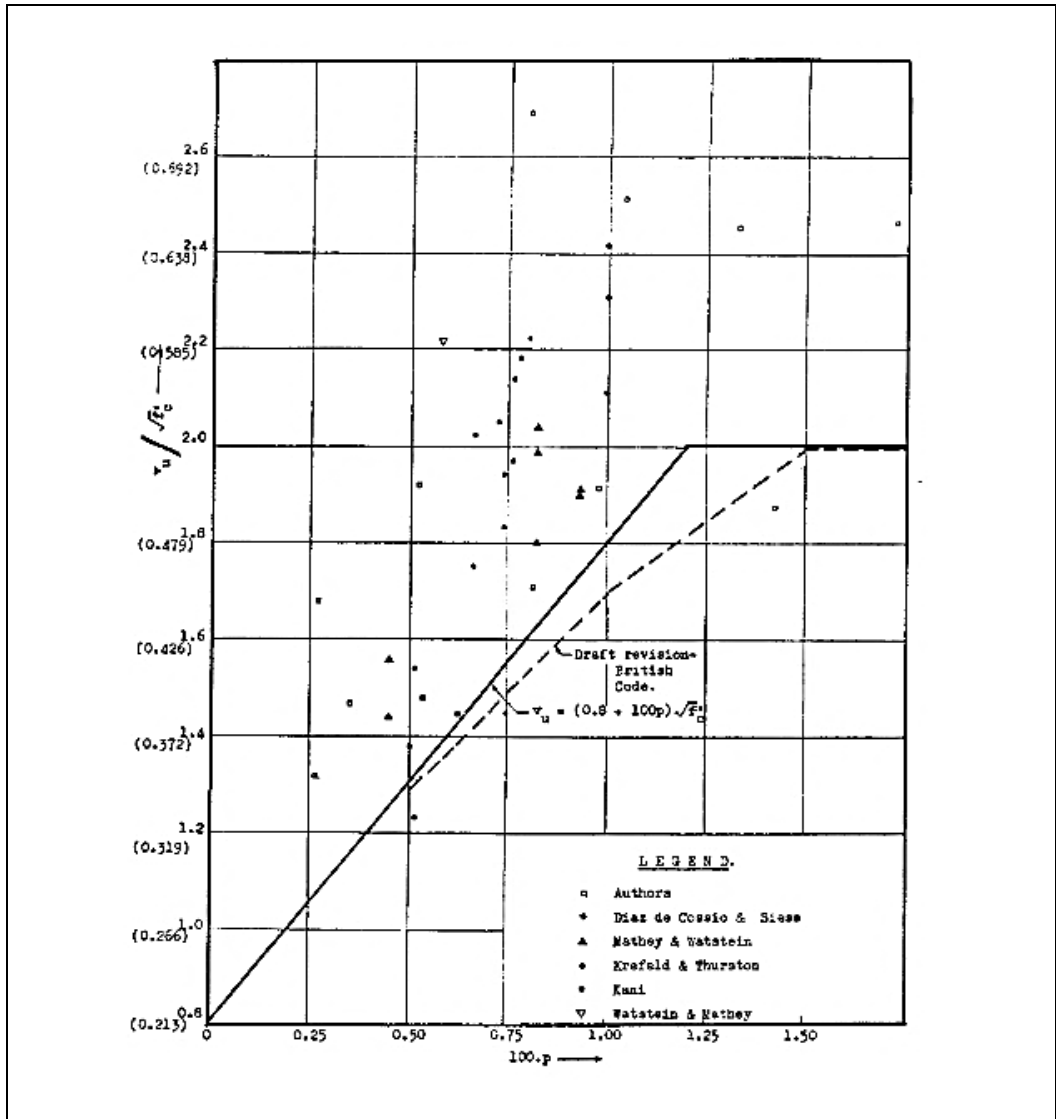


Figure 2.9 Relation between ρ and v_u ³⁶.

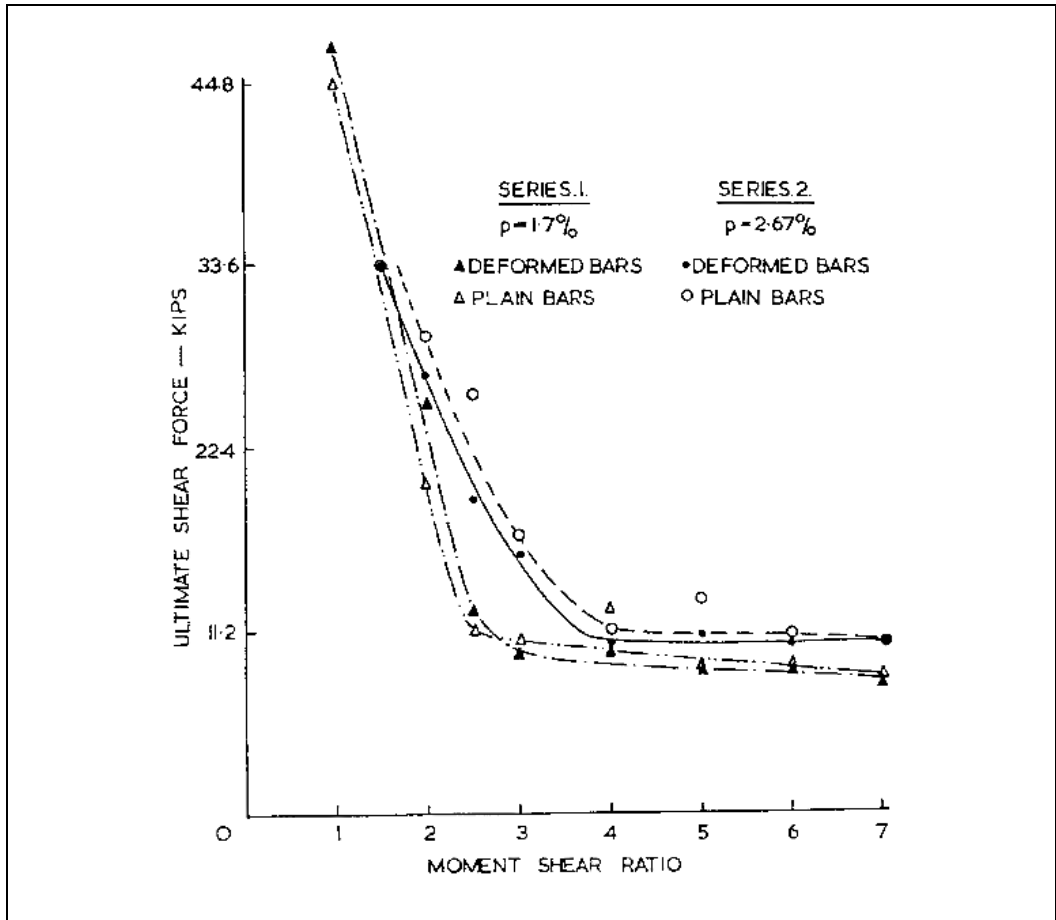


Figure 2.10 Ultimate shear force vs moment shear ratio for $\rho = 1.7\%$ and $\rho = 2.67\%$ for both deformed bars and plain bars³⁸.

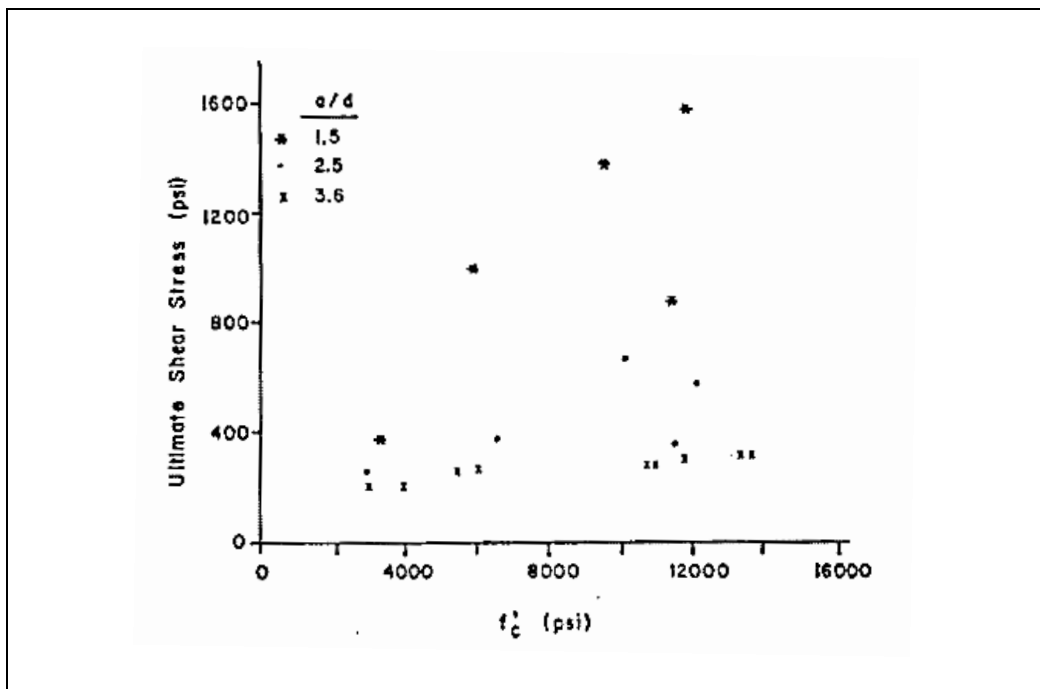
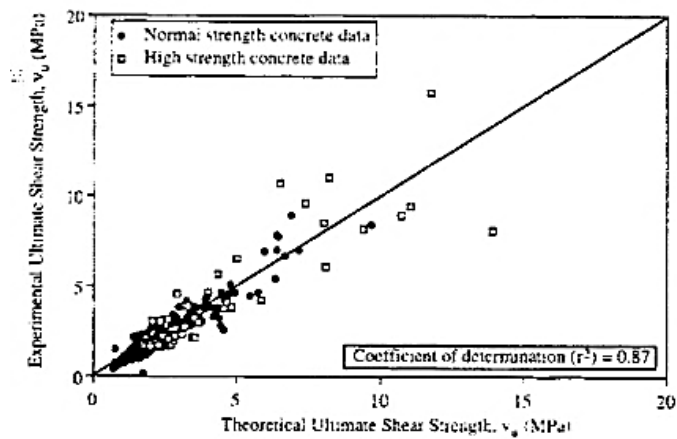
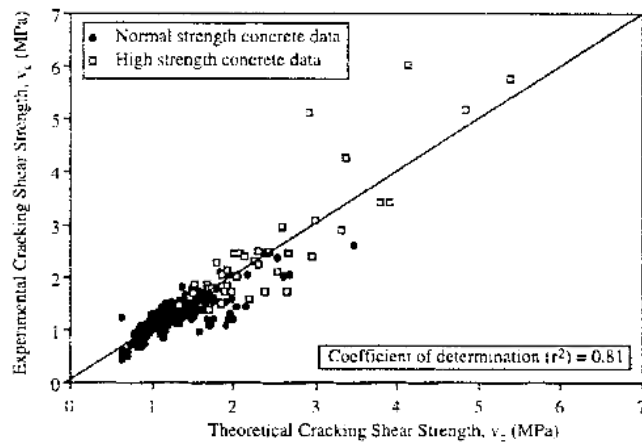


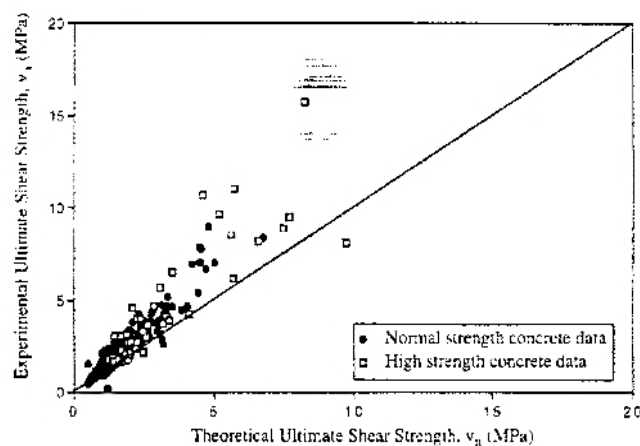
Figure 2.11 Test results of series a/d=1.5, 2.5 and 3.6 with respect to concrete strength³⁹.



(a) Theoretical Ultimate Shear Strength Values vs Experimental Ultimate Shear Strength Values



(b) Theoretical Cracking Shear Strength Values vs Experimental Cracking Shear Strength Values



(c) Theoretical Ultimate Design Shear Strength Values vs Experimental Ultimate Shear Strength Values for normal strength concrete and high strength concrete

Figure 2.12 Test results of theoretical vs experimental shear strength values⁴¹.

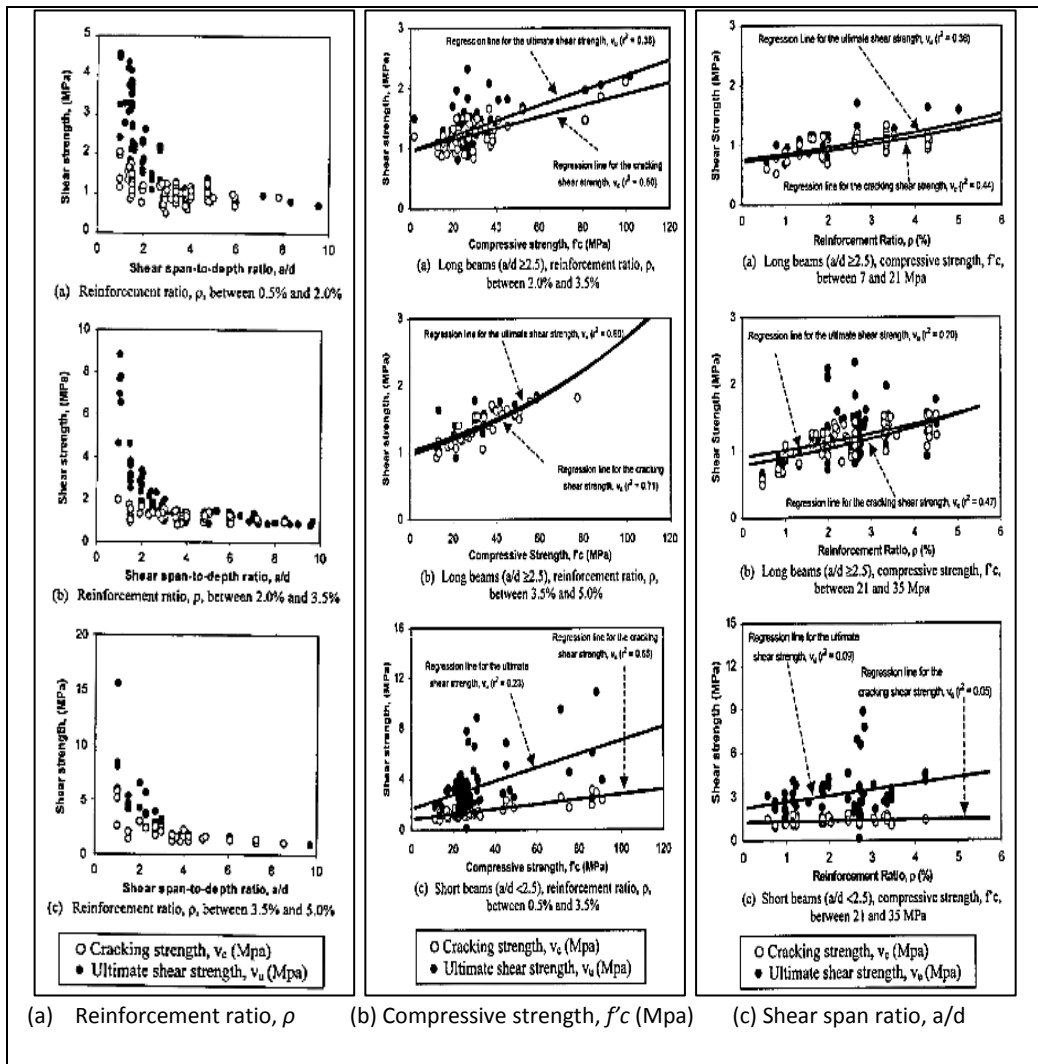


Figure 2.13 Effect of variables: reinforcement ratio, compressive strength and shear span on cracking and ultimate shear strength⁴².

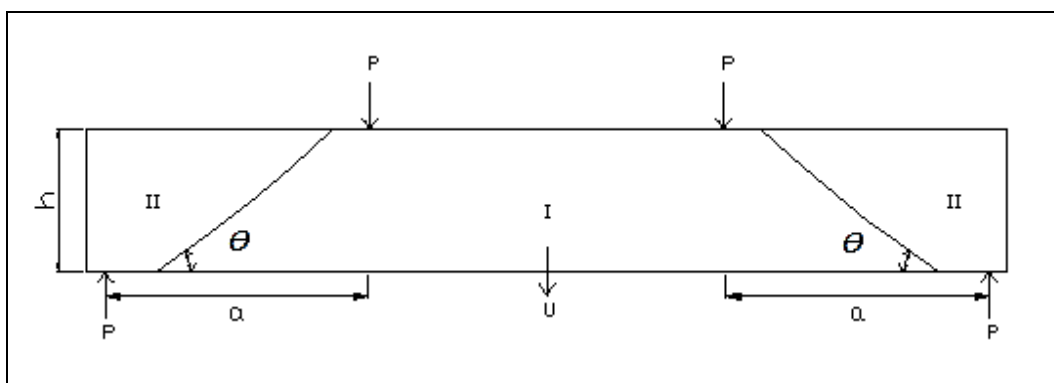


Figure 2.14 Plastic approach for reinforced concrete beams without shear reinforcement⁴⁶.

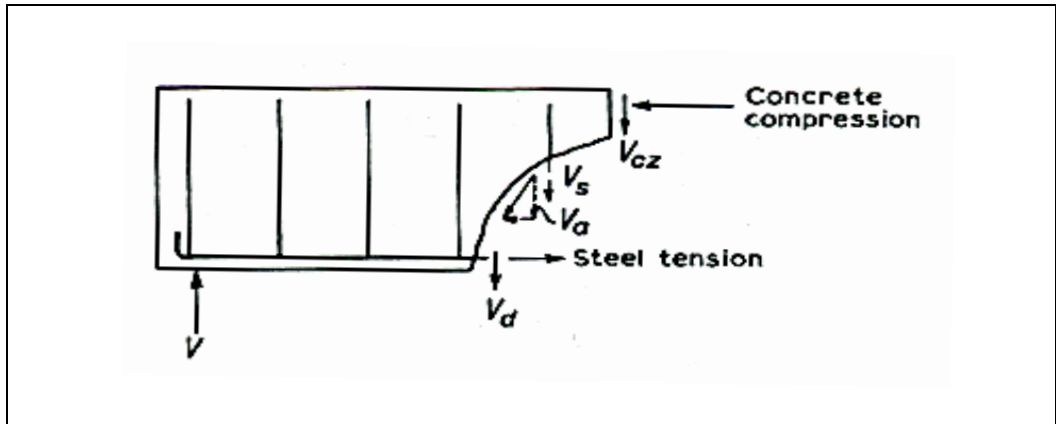


Figure 2.15 Four combined actions in reinforced concrete beams with shear reinforcement²⁷.

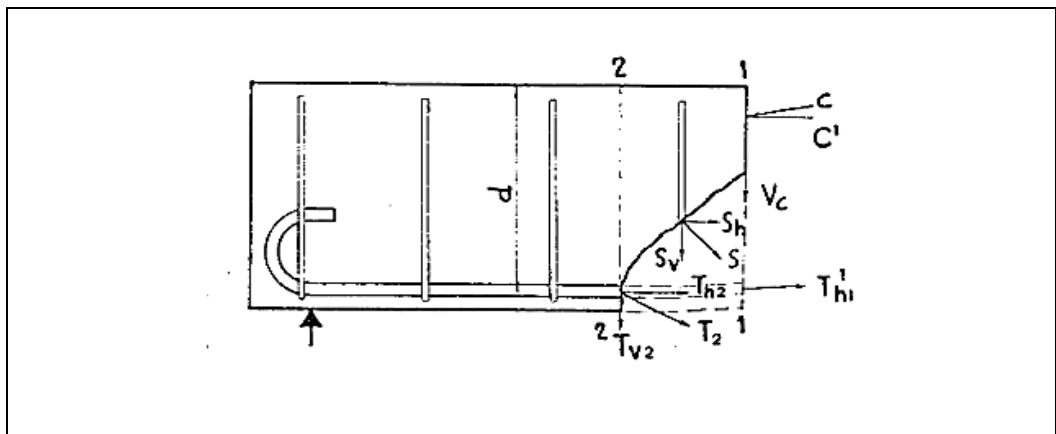


Figure 2.16 Diagonal tension cracks crossed one of the shear reinforcement⁵⁰.

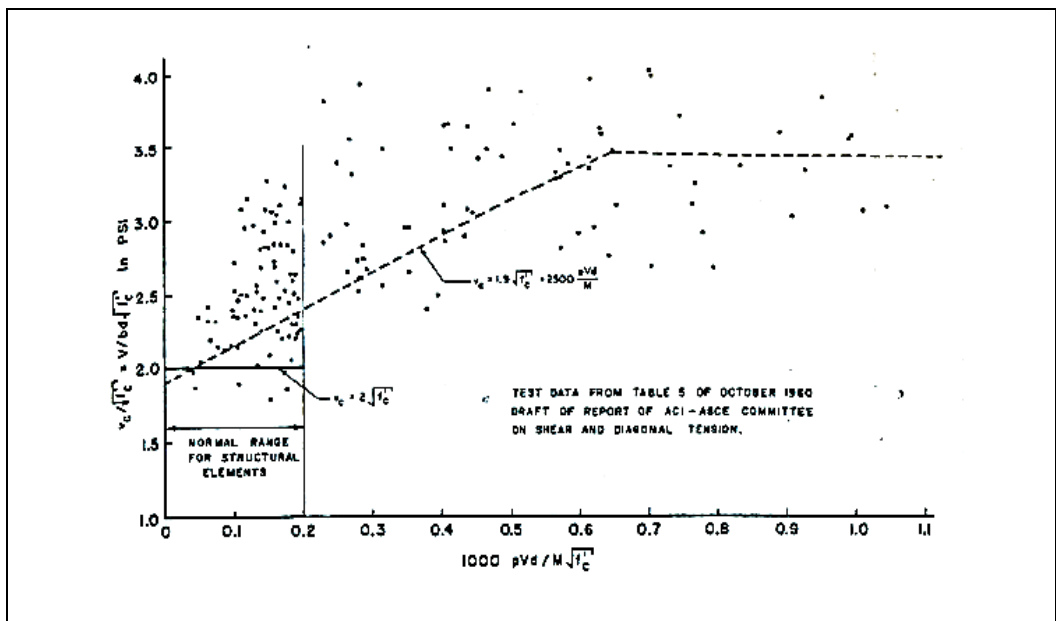


Figure 2.17 Comparison of test data with proposed formula⁵¹.

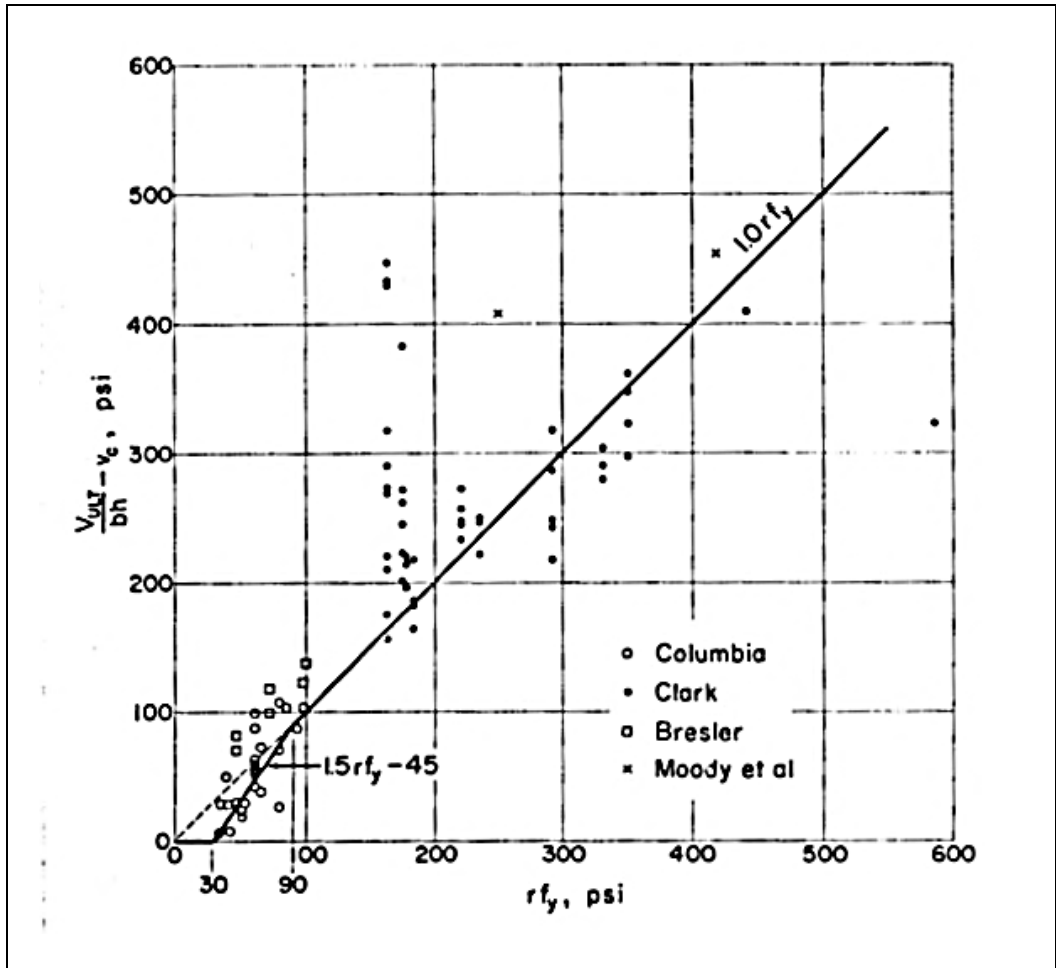


Figure 2.18 Shear contributions of shear reinforcement³⁴.

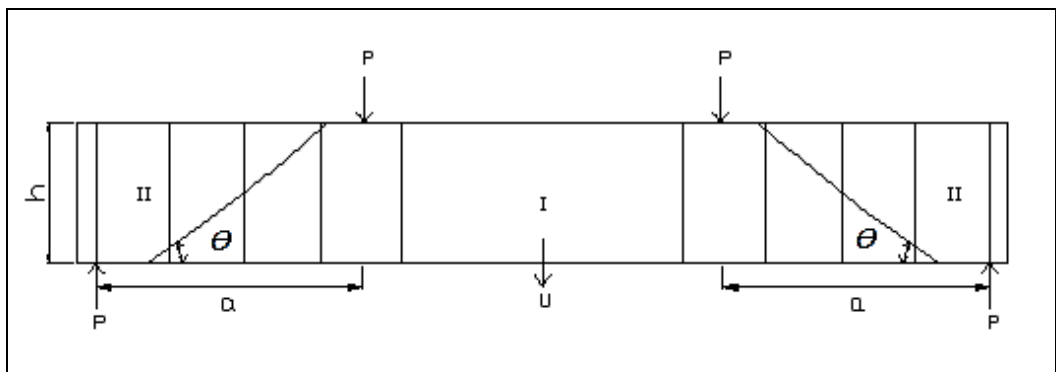


Figure 2.19 Plastic approach for reinforced concrete beams with shear reinforcement⁴⁶.

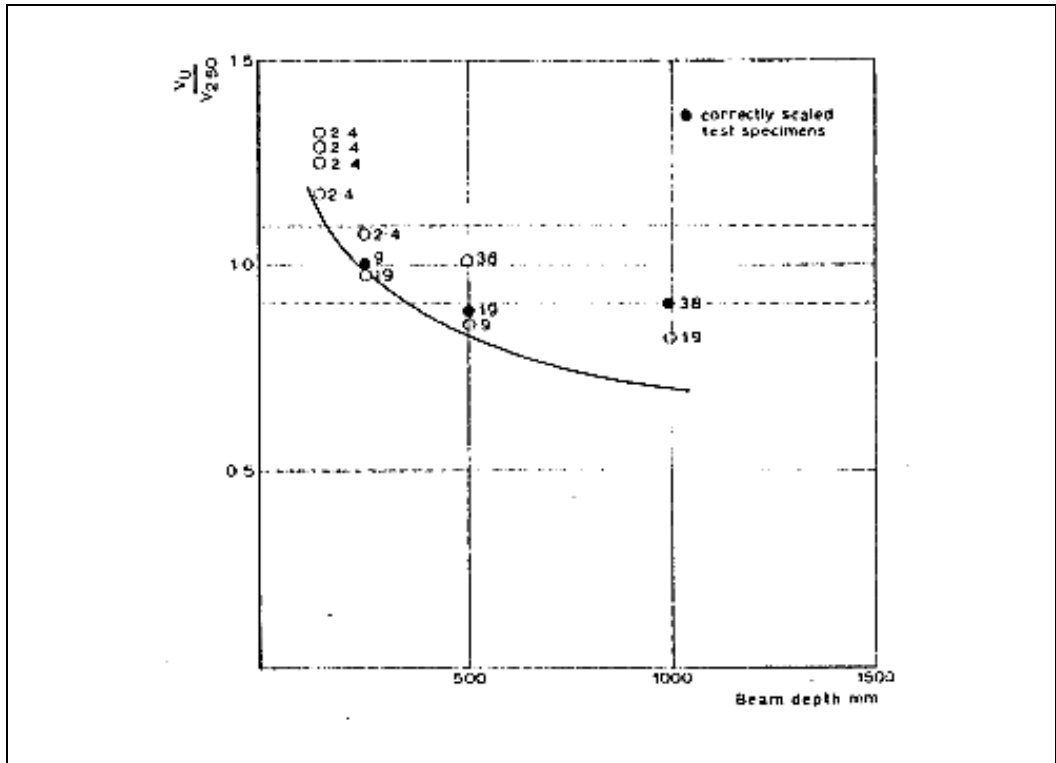


Figure 2.20 Test results of beams with varying depth⁵⁵.

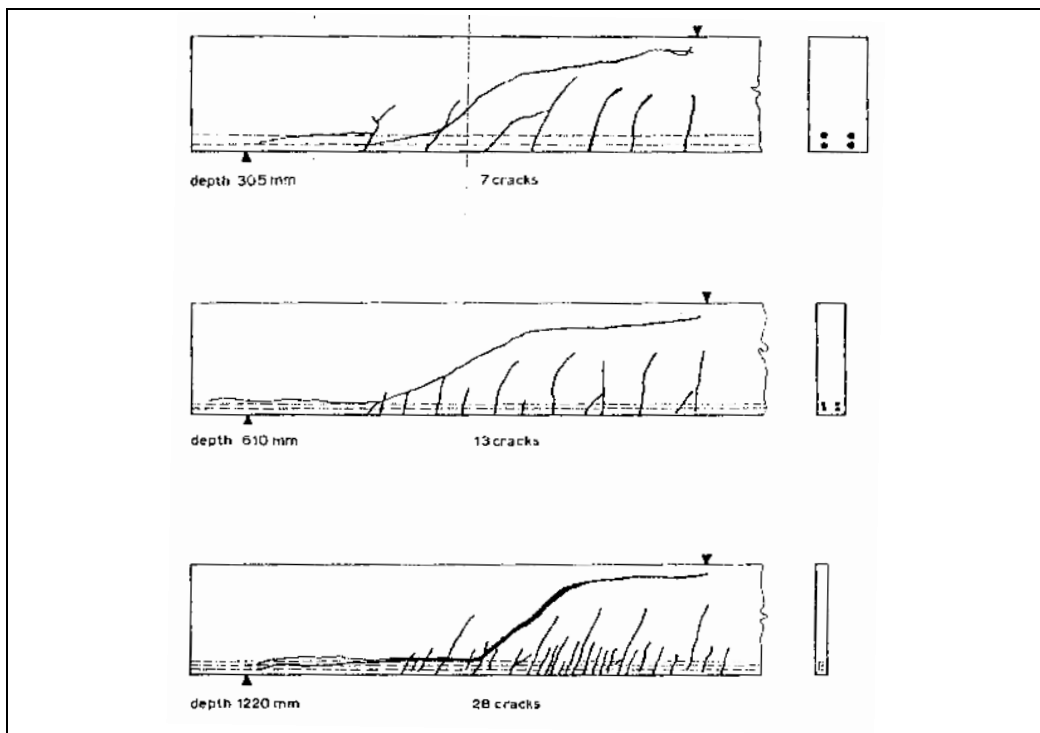


Figure 2.21 Test specimens casted by Kani⁵⁵.

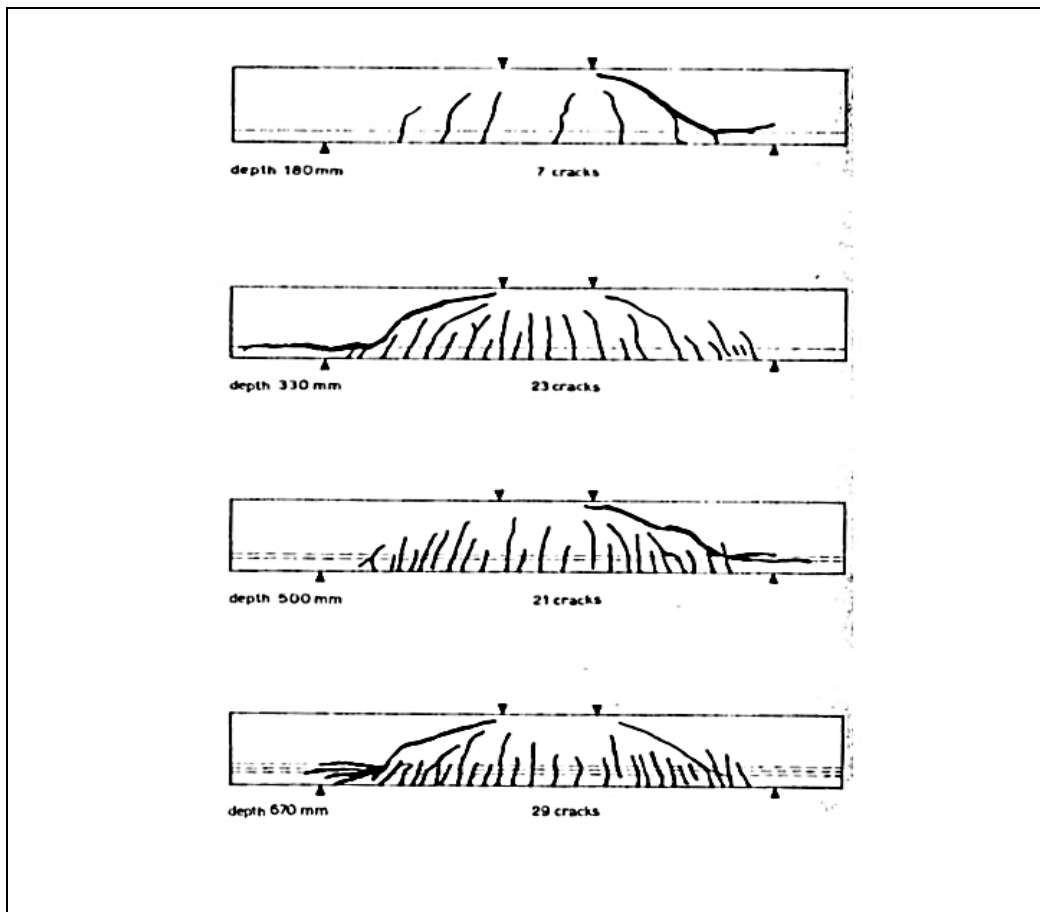


Figure 2.22 Test specimens series C casted by Leonhardt and Walther⁵⁵.

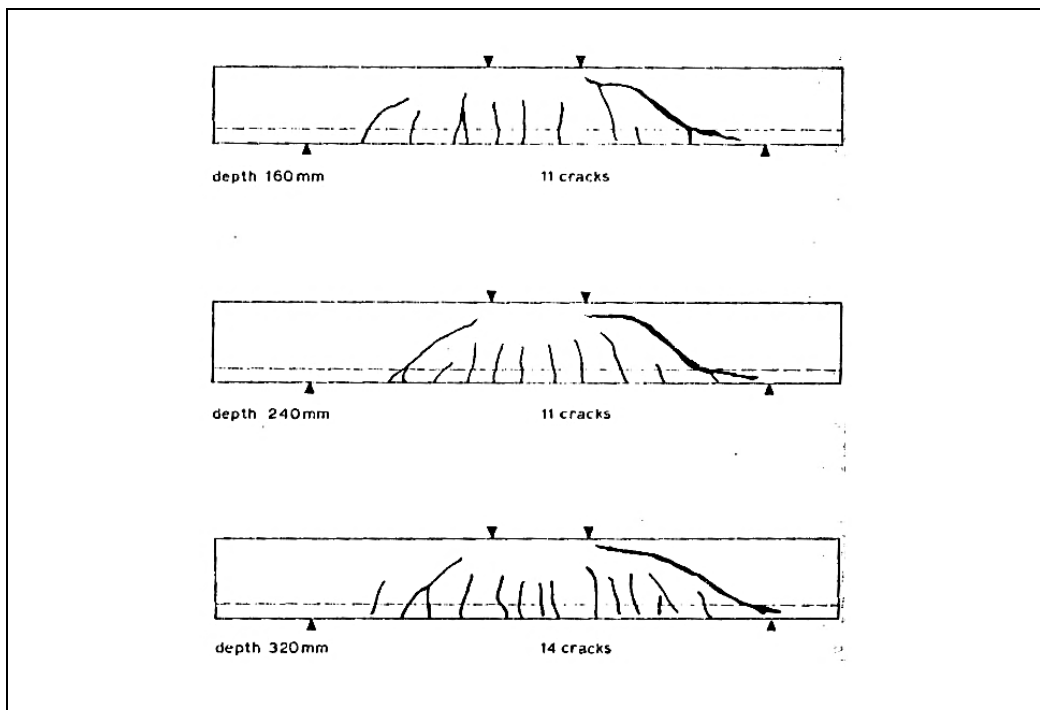


Figure 2.23 Test specimens series D casted by Leonhardt and Walther⁵⁵.

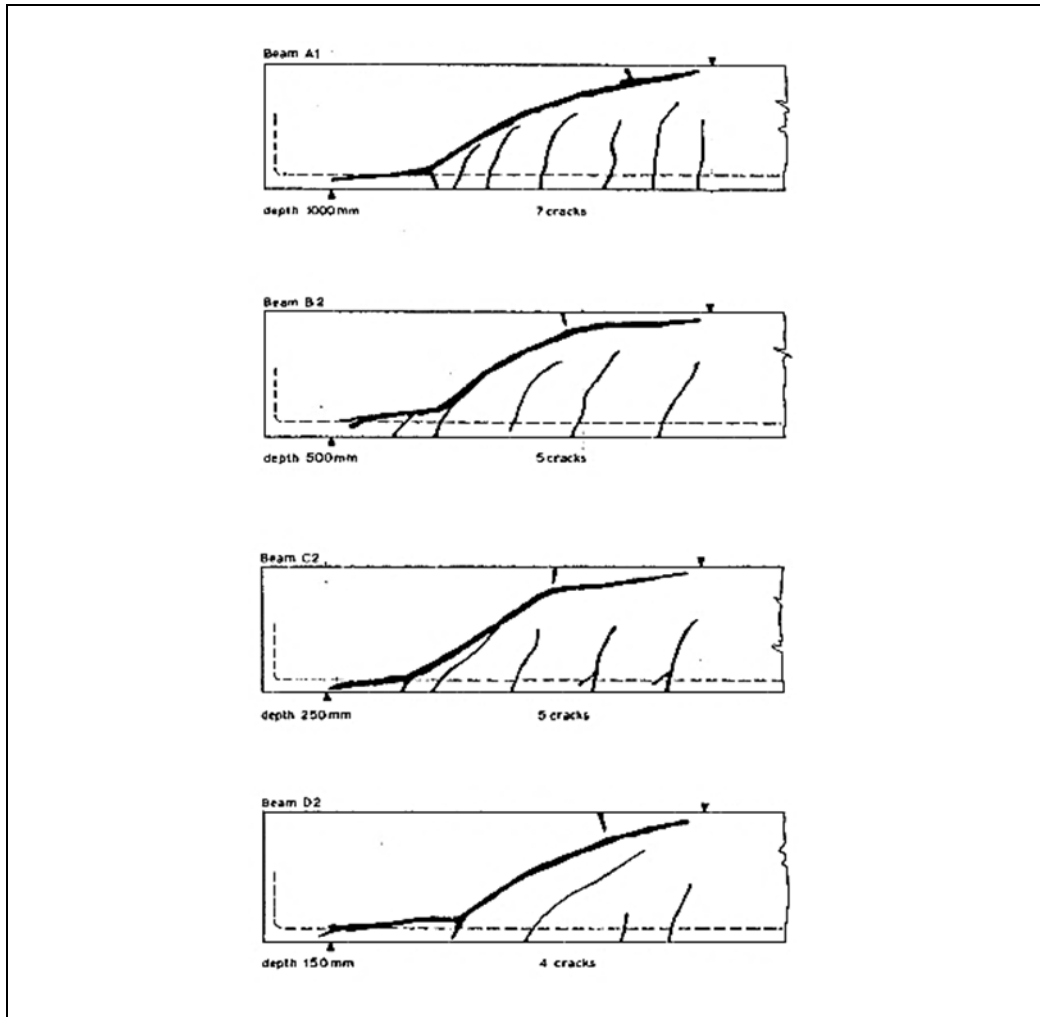


Figure 2.24 Test specimens casted by Taylor⁵⁵.

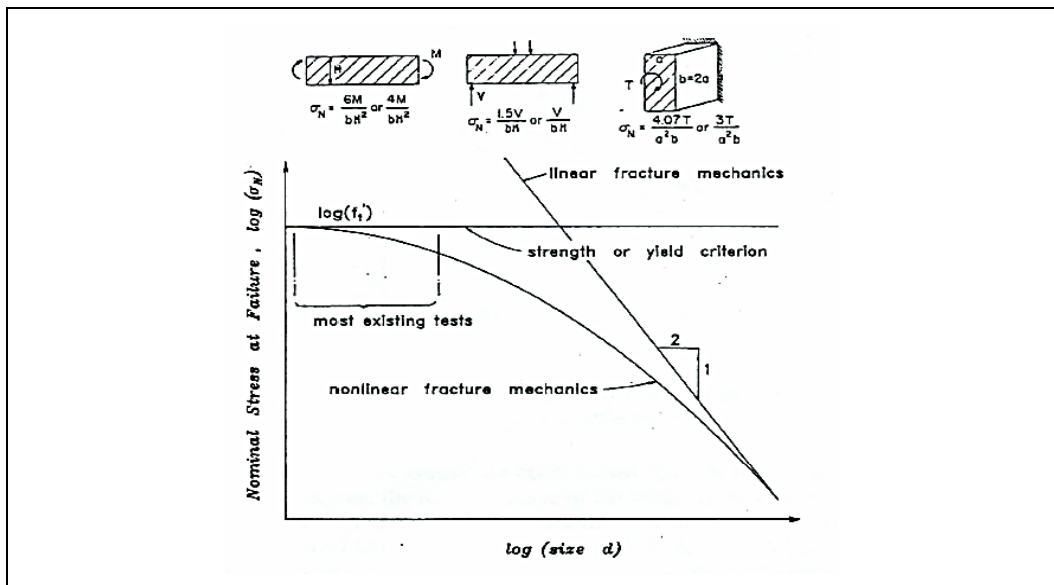


Figure 2.25 Illustration of size effect according to theory of linear fracture mechanics and nonlinear fracture mechanics⁵⁷.

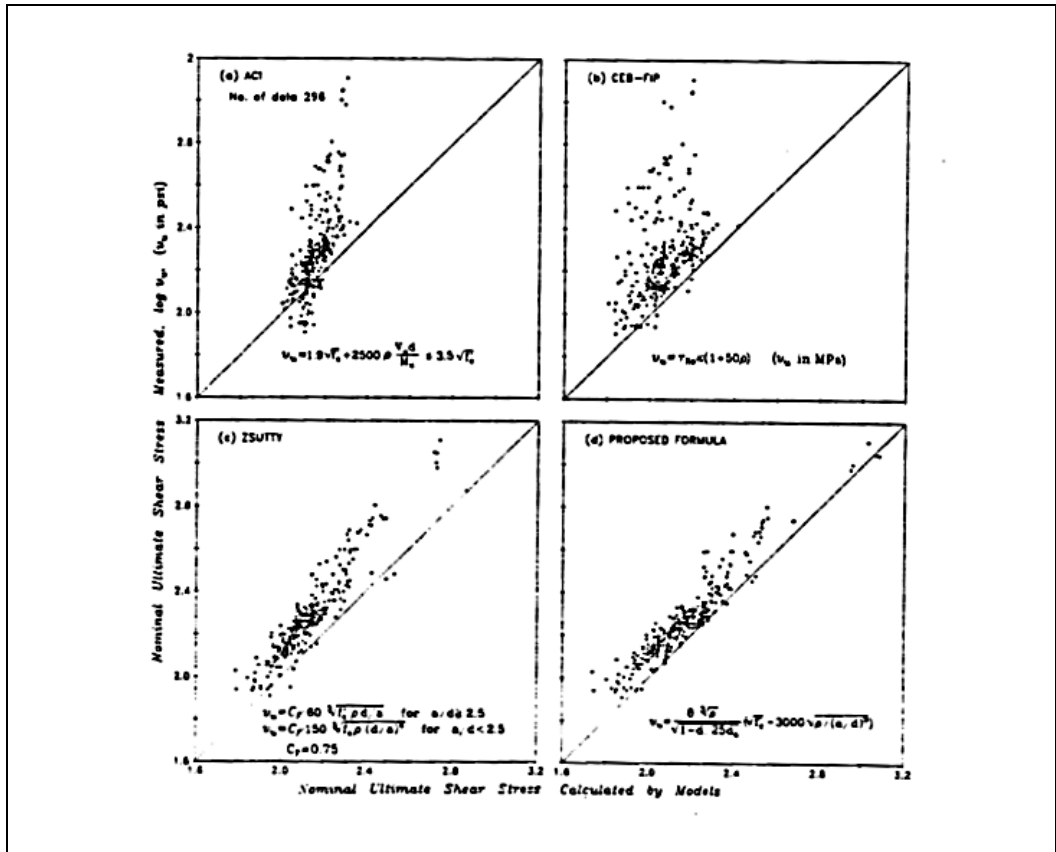


Figure 2.26 Comparisons of the design formula with literature data⁵⁷.

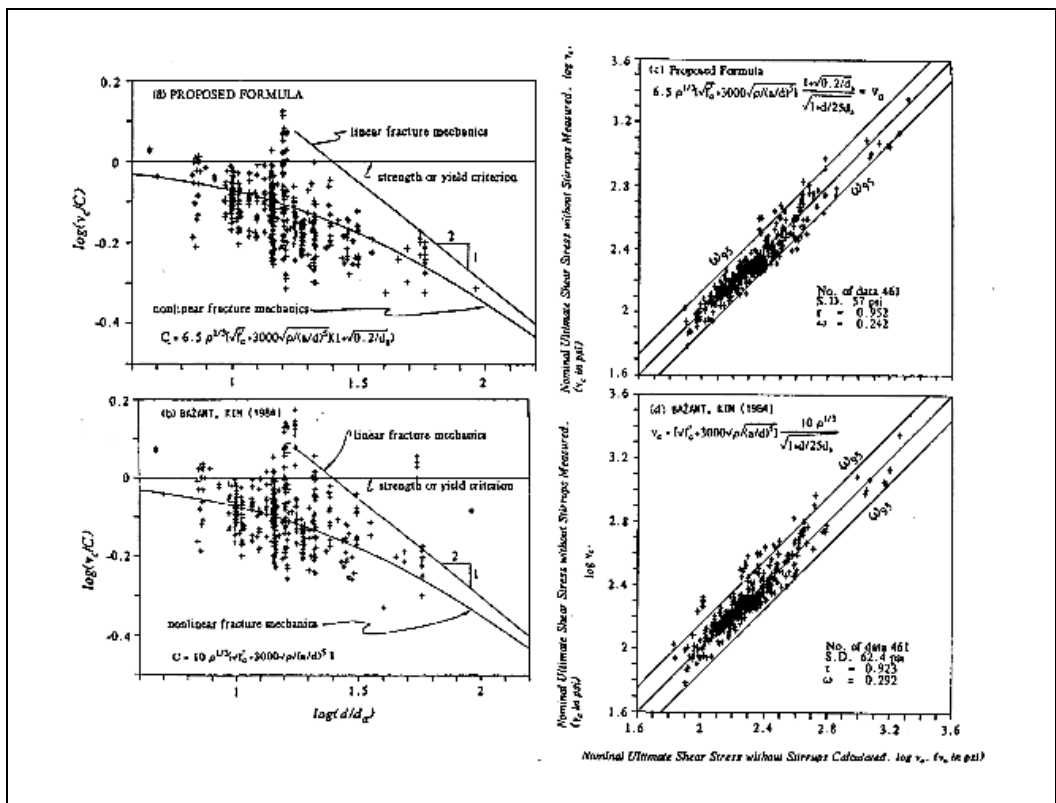


Figure 2.27 Experimental values vs. Calculated values of mean nominal shear strength for beams without shear reinforcement⁵⁸.

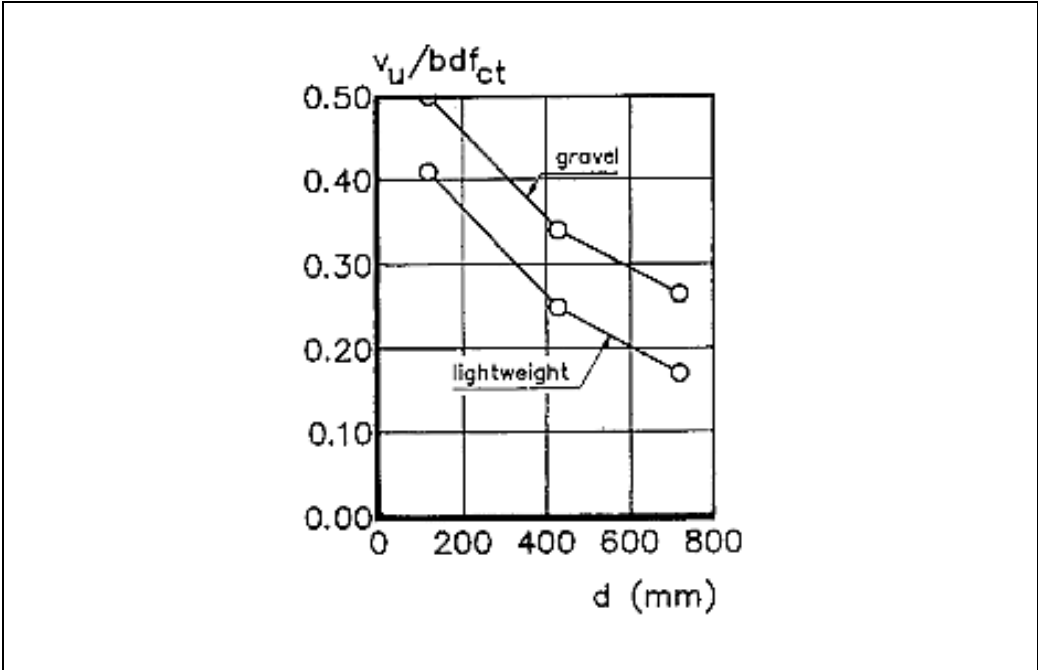


Figure 2.28 Relative nominal shear strength of gravel and lightweight concrete beams as function of the effective cross sectional depth ($a/d=3$)⁵⁹.

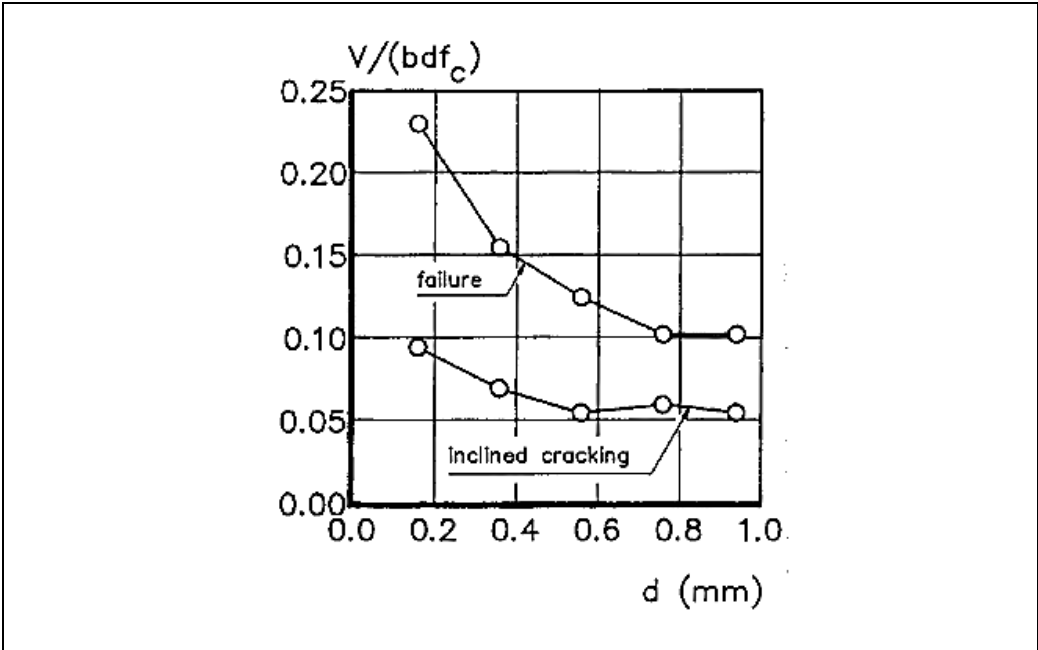


Figure 2.29 Shear stresses at inclined cracking and failure vs effective depth for short beams with $a/d = 1$ ⁵⁹.

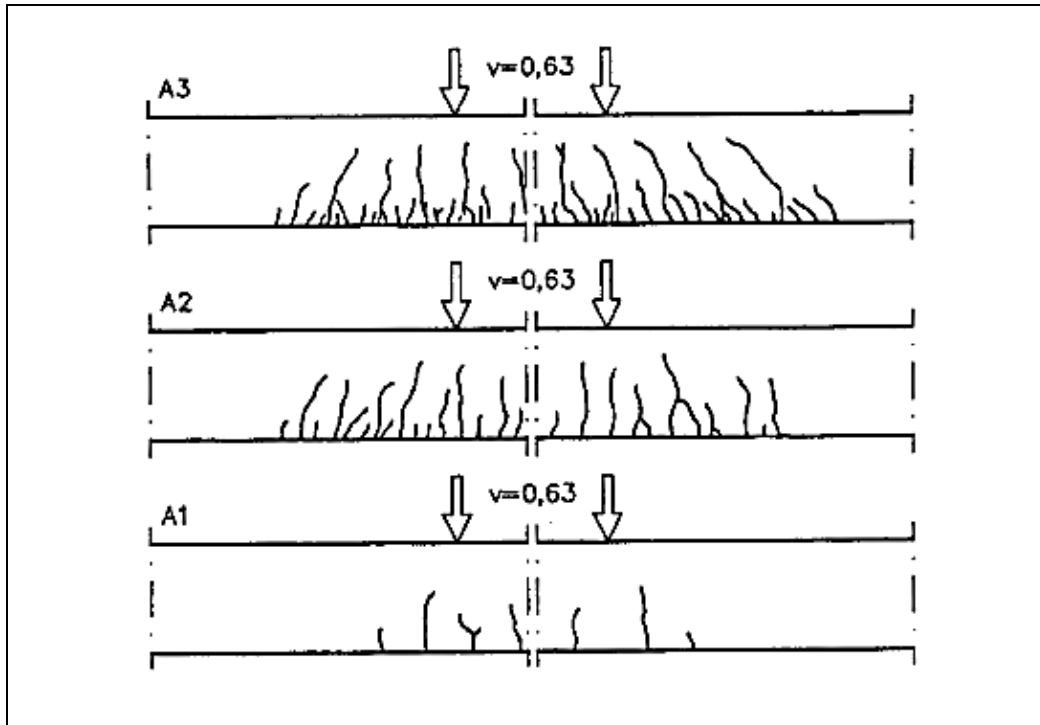


Figure 2.30 Crack patterns in slender beams ($a/d=3$) with various depths⁵⁹.

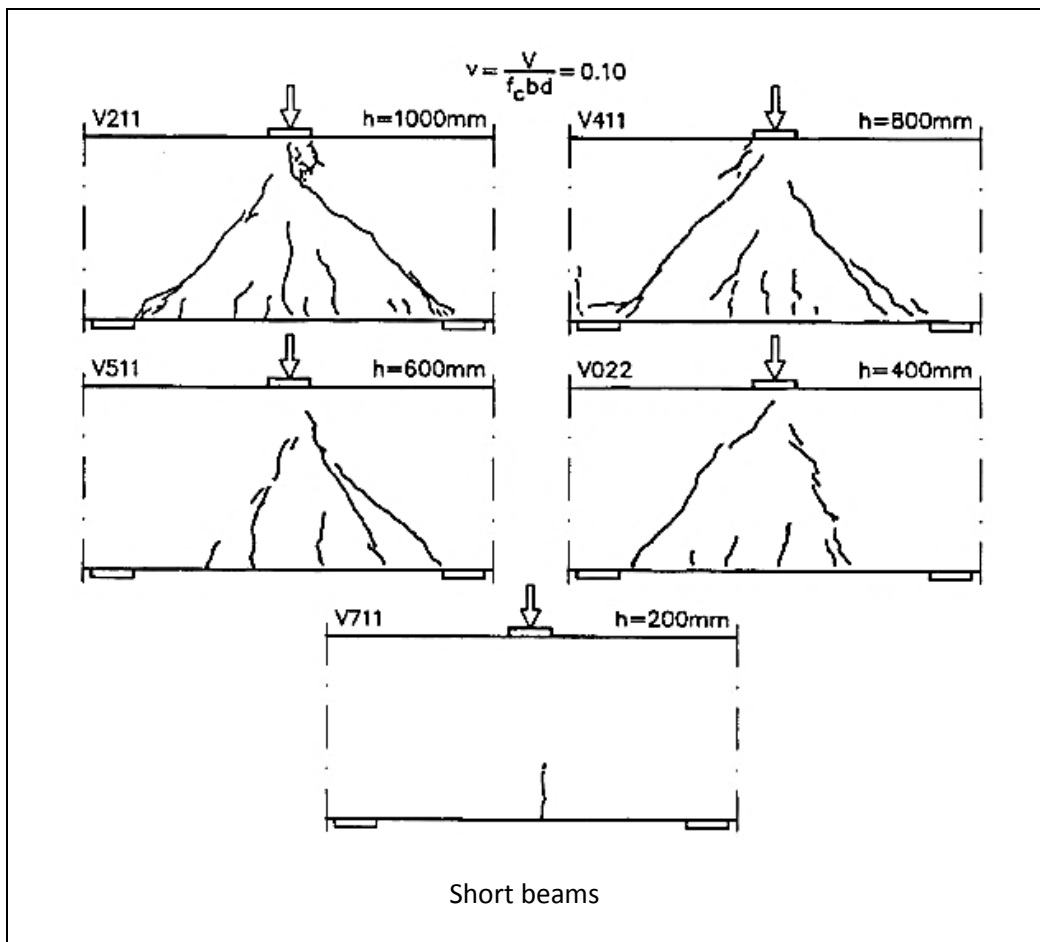


Figure 2.31 Crack patterns in short beams with various depths⁵⁹.

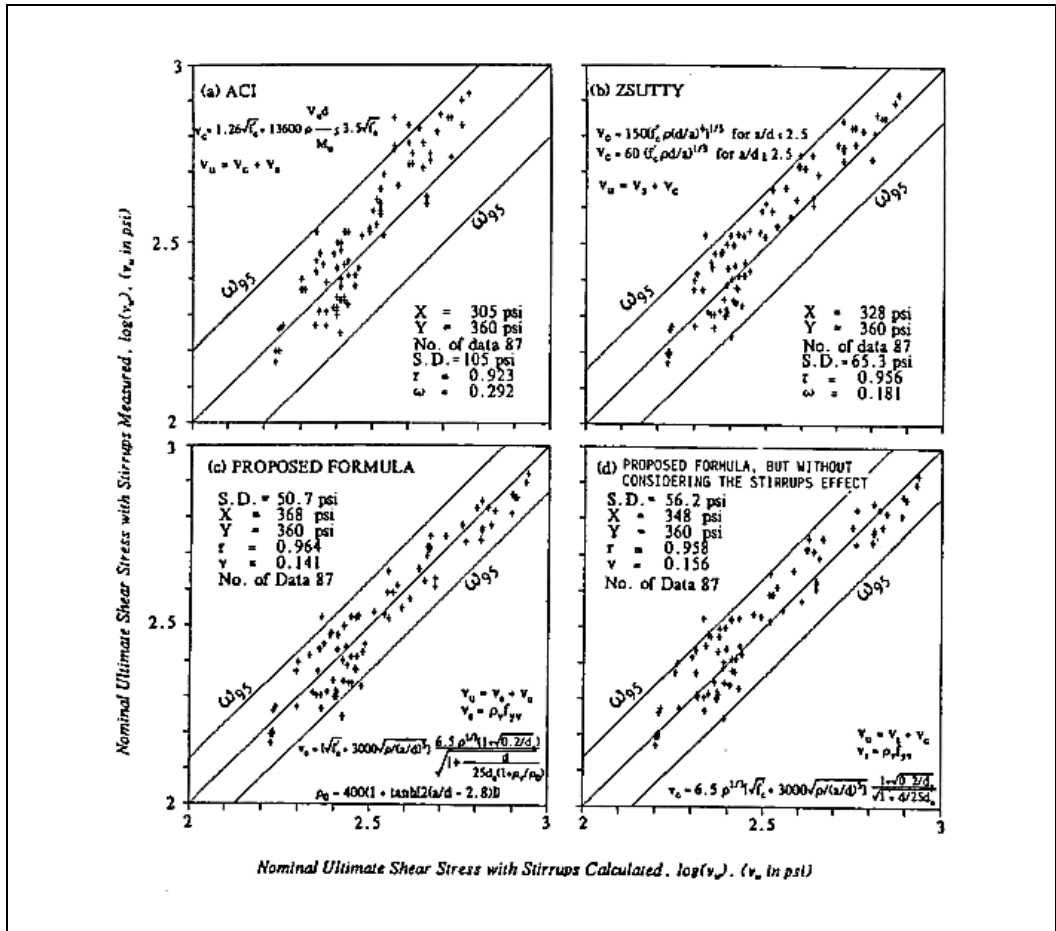


Figure 2.32 Experimental values vs Calculated values of mean nominal shear strength for beams with shear reinforcement⁶⁰.

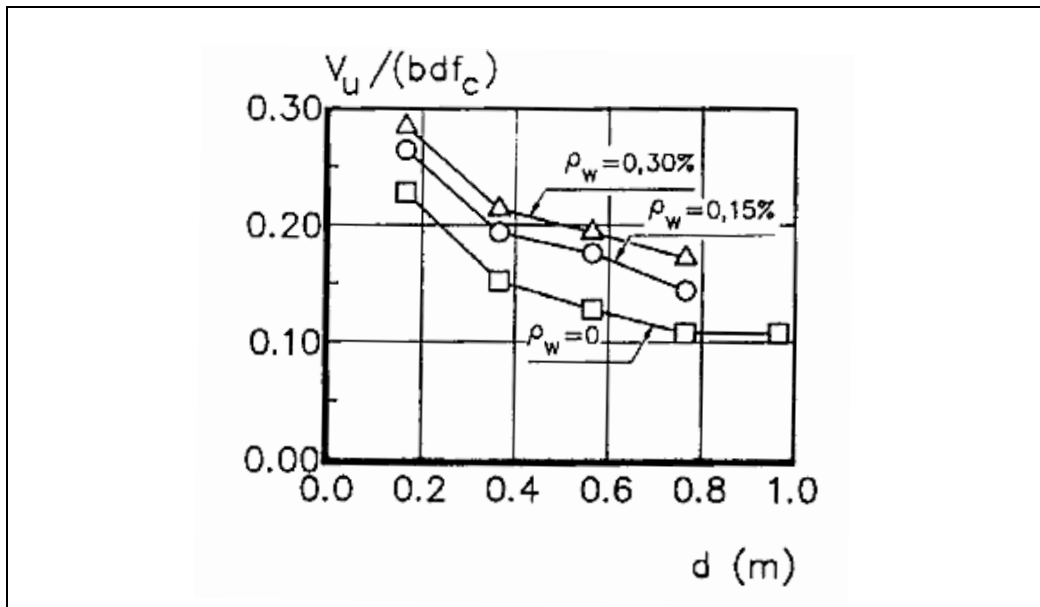


Figure 2.33 Shear stresses vs effective depth for short beams with shear reinforcement⁵⁹.

Chapter 3

Experimental Work

3.1 Introduction

As pointed out in Chapter 2, current research on Oil Palm kernel Shell Concrete (OPSC) have been concentrated on the development of understanding with regards to its material properties, and to author's knowledge, only limited amount of works have been conducted to study its bending and shear capacities. As a result, it is felt that more experimental studies are required to develop the current understanding with regards to the shear failure mechanisms of OPSC beams.

The experimental studies carried out in this research consisted of destructive shear tests on Oil Palm kernel Shell Concrete (OPSC) beams and normal weight concrete (NWC) beams. NWC beams were tested to form the basis of the comparative studies in this research.

Two types of specimens were cast and tested: specimens cast without shear reinforcement and specimens cast with shear reinforcement for OPSC and NWC beams, respectively.

For beams cast without shear reinforcement, variables considered were: shear span (SP), section depth (HT), longitudinal reinforcement ratio (LR), and concrete strength (CS). Whilst for beams cast with shear reinforcement, variables considered were: concrete strength (CG), shear reinforcement ratio (SR) and Inclination angle of shear

cracks (PL). During tests, all specimens were centrally loaded with concentrated loads on top of the beam and simply supported by steel rods at both ends.

Details of beam specimens, steel moulds, materials used, fabrication method, experimental programme, experimental apparatus, arrangements and the method of measurement used in this research are presented in this chapter.

3.2 Concrete material properties

3.2.1 Oil Palm Shell Concrete (OPSC)

The oil palm kernel shell concrete (OPSC) cast in this research constituted of Ordinary Portland Cement (OPC), sand (as fine aggregate), and oil palm kernel shell (OPS) (as coarse aggregates). Portable water was added to the OPSC mixtures to stimulate the mixtures binding of OPSC. Several trial mixes were carried out in order to obtain the desired mixes designs (see Appendix A). The desired mix designs were found to be suitable as shown in Table 3.1.

All palm oil kernel shells (OPS) were de-oiled with detergent to remove any residual oil deposits to allow for quality concrete binding. Prior to sieving, all oil palm kernel shell aggregates were oven dried at 100°C for 24 hours. However, the sieved oil palm kernel shell aggregates were remixed using the same grading curve (see Figure 3.1), which was based on the natural distributions of OPS aggregate size on the same batch of palm oil fruits, in order to achieve uniform concrete in every batch for worthy comparisons. The aggregate impact value of OPS aggregate is 8.4% whilst the aggregate crushing value is 5.9% (see Appendix B).

The fine aggregates used were natural sand of maximum size passing through 1.18 mm sieve (see Figure 3.2).

3.2.2 Normal Weight Concrete (NWC)

The normal weight concrete (NWC) used for the casting of control beam specimens constituted of Ordinary Portland Cement (OPC), sand (as fine aggregate), and crushed granite (as coarse aggregates). The concrete mixes used are shown in Table 3.2. The fine aggregate was natural sand with grading curve as shown in Figure 3.2. The coarse aggregate was crushed granite having maximum aggregate size of 20 mm and grading curve as shown in Figure 3.3.

3.3 Reinforcement

In all cases, the flexural reinforcement was designed to avoid flexural failure and to ensure shear failure (see Appendix C for Beam Design).

3.3.1 Specimens cast without shear reinforcement

For OPSC beam specimens, the sizes of flexural reinforcement include: 10 mm, 12 mm, 16 mm and 20 mm deformed bars. For NWC beam specimens, the flexural reinforcement used: 12 mm, 16 mm and 20 mm deformed bars. In all cases, these bars were bent up at both ends in accordance to the anchorage requirements of Eurocode 2: 2004 [48].

The general arrangement of the flexural reinforcement for OPSC and NWC beam specimens is presented in Figure 3.4.

3.3.2 Specimens cast with shear reinforcement

Tension reinforcement used in this research include: 16 mm, and 20 mm deformed bars while compression reinforcement were 14 mm deformed bars. Shear reinforcement used were fabricated from 6 mm plain bars.

In all cases, 14 mm bars were bent down and 16 mm bars were bent up at both ends in accordance to the anchorage requirements of EC2. The 20 mm bars however remained as straight bars and 1300 mm and 1350 mm in length when used as tension reinforcement and compression reinforcement, respectively.

OPSC specimens (3A, 3B, 3C, 4A, 4B, 4C, 4D, 4E) and NWC specimens (NWCA, NWCB, NWCD, NWCE) were reinforced with 2T14 as compression reinforcement and 2T16 as tension reinforcement (See Figure 3.5 and Figure 3.6). OPSC beam specimens (5A, 5B, 5C) and NWC specimens (NWCC) were reinforced with 2T14 and 2T20 as compression reinforcement and 2T16 and 2T20 as tension reinforcement (See Figure 3.7).

All shear reinforcement were 6mm plain bars with yield strength of 410 N/mm^2 . Link spacing used in this research include: 60 mm, 80 mm, and 120 mm. (See Figure 3.5 to Figure 3.7).

3.4 Beam specimens cast without shear reinforcement

3.4.1 OPSC Beam Specimens

A total of twenty-four OPSC beam specimens cast without shear reinforcement, as indicated in Table 3.3, were tested to investigate the variables considered in this

research; shear span to effective depth ratio (Series SP), concrete strength (Series CS), longitudinal steel reinforcement ratio (Series LR) and section depth (Series HT).

In general, all beam specimens were identical in their overall dimensions; 200 mm in height, 105 mm in width, and 1500 mm in length; except for specimens 12F and H2, where, the overall section depths were 113 mm and 313 mm, respectively.

The effect of Span to depth ratio, longitudinal reinforcement, concrete strength and overall section depth variations on the ultimate shear capacity of OPSC beams without shear reinforcement were investigated through destructive tests carried out on fifteen, eighteen, ten and three beams, respectively (see Table 3.3).

3.4.2 NWC Beam specimens

A total of five NWC beam specimens cast without shear reinforcement, as indicated in Table 3.4, were tested to form the basis for comparisons with the OPSC beam specimens with respects to the variables considered: span to depth (SP), concrete compressive strength (CS), longitudinal reinforcement ratio (LR) and overall section depth (HT).

Specimens (NWC2, NWC3, NWC4 and NWC5) were tested at $a/d = 2.5$, while specimen (NWC1) was tested at $a/d = 1$. The concrete strength for specimens (NWC1, NWC2, and NWC5) was 33N/mm^2 , while specimens (NWC3 and NWC4) were 29N/mm^2 . The overall section depth of specimens (NWC1, NWC2, NWC3 and NWC4) was 200 mm, while for specimen (NWC5) was 113 mm.

3.5 Beam specimens cast with shear reinforcement

3.5.1 OPSC beam specimens

A total of eleven OPSC beam specimens cast with shear reinforcement, as indicated in Table 3.5 were tested to investigate the variables considered in this research: concrete strength (CG), shear reinforcement spacing (SR) and shear span (PL). In general, all beam specimens were identical in their overall dimensions; 200 mm in height, 105 mm in width, and 1500 mm in length.

The effect of concrete compressive strength, shear reinforcement spacing, and shear span variations on the ultimate shear capacity of OPSC beams with shear reinforcement were investigated through destructive tests carried out on nine, nine and three beams, respectively (see Table 3.5).

3.5.2 NWC beam specimens

A total of five NWC beam specimens cast with shear reinforcement, as indicated in Table 3.6, were tested to form the basis for comparisons with the OPSC beam specimens with respects to variables: span to depth ratio (PL), concrete compressive strength (CG), and shear reinforcement spacing (SR).

Specimens (NWCA, NWCB, NWCC and NWCE) were tested at $a/d = 1.69$, while specimen (NWCD) was tested at $a/d = 1.06$. The concrete strength for specimens (NWC A, NWC B, NWCC and NWCD) was 30.61 N/mm^2 , while for specimen (NWCE) was 35 N/mm^2 . The shear reinforcement spacing for specimens (NWCB, NWCD and NWCE) was 80 mm, while for specimen NWCC and NWCA was 60 mm and 120 mm, respectively.

3.6 Fabrication of specimens

3.6.1 Mould

All beam specimens with overall section depth of 200 mm were cast using steel moulds. Each of these steel moulds consisted of a rectangular steel plate and four channel sections (see Figure 3.8 and Figure 3.9). The rectangular steel plates, forming the base plates, were predrilled with holes to receive the channel section, forming the sides of the mould.

Beam specimens having overall section depth less than 200 mm were cast using the abovementioned steel moulds. Depth control markings were made available within the moulds to allow for casting of specimens with lower section depth.

Beam specimens having overall section depth more than 200 mm were cast using plywood mould. The plywood moulds consisted of five rectangular plywood sections of various sizes (see Figure 3.10 and Figure 3.11).

In all cases, silicone was used to fill the gaps between the sides and the bases before every cast of beam specimens. This was done to avoid leakage of concrete.

In this research, standard steel cube moulds were used for the casting of concrete cubes (100 mm X 100 mm X 100 mm) for compression tests.

3.6.2 Casting and curing

All beam specimens were cast in an upright position so as to simulate the casting of the prototype structures. Five cubes and three beam specimens were cast in every

single batch. Prior to concreting, all moulds and cubes were cleaned and applied with de-moulding oil.

For every cast, concrete was poured into the moulds in three equal layers. Every layers of concrete were poured simultaneously among all cubes and beam specimens to ensure uniform distribution of concrete. After every layer of pouring, all beam specimens were compacted using handheld vibrating poker for equal number of times and until the bubbling subsided. All the cubes were compacted on vibrating table for three equal layers, and for each layer, compaction were carried out until bubbling subsided. These were done to ensure for similar compaction between the cubes and the beam specimens.

All the specimens were de-moulded approximately 24 hours after casting. All specimens were water cured, together in the same water tank, to ensure for identical curing conditions. The curing durations and the compressive strengths for all specimens are summarized and presented in Table 3.7 to Table 3.10.

3.7 Test setup

All beam specimens were tested in an upright manner so as to stimulate the prototype structures. During tests, all specimens were simply supported at both ends, as shown in Figure 3.18. The loads were applied at the centre, via spreader beams with mean of 30 ton hand operated hydraulic jack. (See Figure 3.12 and Figure 3.13)

In general, the loads were applied with increment(s) of 4.21 kN until failure occurred. Central deflections were measured and recorded after each load increment(s).

3.7.1 Beam specimens cast without shear reinforcement

Both OPSC and NWC specimens were loaded at designated positions from the support to achieve the required span-depth ratio(s), a/d , as stipulated in Table 3.3 and 3.4 (See Figure 3.14).

3.7.2 Beam specimens cast with shear reinforcement

In general, the locations of the shear reinforcement were marked prior to tests to ensure for correct positioning of supports and applying loads. (See Figure 3.15)

For OPSC specimens; beam specimens tested to investigate concrete strength (CG) and links spacing (SR), were loaded at distance(s) of 240 mm from the support(s) as shown from Figure 3.16 to Figure 3.18. Whilst for specimens tested to investigate shear span (PL) were loaded at distance(s) of 240 mm, 200 mm, and 160 mm from the support(s), as shown in Figure 3.17, Figure 3.19 and Figure 3.20, respectively.

For NWC control specimens; In general, beam specimens were loaded at distance(s) of 240 mm from the support(s) (See Figure 3.17). Except for specimen NWCD, it was loaded at distance(s) 160 mm from the support(s), as shown in Figure 3.19.

3.8 Central deflection

Mechanical dial gauge with a 100 mm strut, reading accuracy to 0.01 mm were used to measure the central deflection of the beam specimens. The dial gauge was positioned below the mid span of the beam specimens, as shown in Figure 3.21.

3.9 Testing procedures

Prior to testing, all beam specimens were positioned into the correct testing positioning and dial gauge installed. In all cases, compressive tests on cubes specimens were performed prior to any beam tests to ensure for the required concrete compressive strength. The beam tests would be carried out after the required compressive strength has been achieved.

After all the testing equipment had been accurately installed, the initial readings from the deflection gauge were recorded.

For all beam specimens, the loads were applied with an increment of 4.21 kN until failure occurred. Deflection was recorded and the cracks were marked at every load increments. A series of load vs central deflection curves are presented in Chapter 4.

After testing, some of the specimens were cut open for ease of examine on the shear crack interface. Details of these investigations are presented in Chapter 4.

Table 3.1 Mix design of Oil Palm Shell Concrete (OPSC)

Constitutions	Proportions in Volume		
	A	B	C
Ordinary Portland Cement	3	4	5
Sand as fine aggregate	1	1	1
Oil Palm Shell as coarse aggregate	3	3	3
Water/Cement ratio	0.44	0.37	0.34

Note:

1 volume Cement = 0.537 kg

1 volume Sand = 0.56 kg

1 volume OPS aggregates = 0.22 kg

Table 3.2 Mix design of Normal Weight Concrete Beam (NWC)

Constitutions	Proportion in Volume N
Ordinary Portland Cement	1
Sand as fine aggregate	0.58
Crushed gravel aggregate as coarse aggregate	0.79
Water/Cement ratio	0.43

Note:

1 volume Cement = 0.537 kg

1 volume Sand = 0.56 kg

1 volume gravel aggregates = 0.594 kg

Table 3.3 Details of OPSC beam specimens cast without shear reinforcement

Specimen No.	Section width, b (mm)	Overall section depth, h (mm)	Longitudinal steel ratio, ρ (%) $\frac{100 A_s}{b h}$	Shear span to effective depth, a/d	Shear span, a (mm)	Variable considered
10A	105	200	0.75	2.50	425	LR, CS
S1	105	200	0.75	2.50	425	LR, CS
12A	105	200	1.08	1.00	169	SP, LR
12B	105	200	1.08	1.50	254	SP
12C	105	200	1.08	2.50	423	SP, LR, CS
12D	105	200	1.08	3.00	507	SP, LR
12E	105	200	1.08	2.50	423	CS
12F	105	113	1.91	2.89	237	HT
16A	105	200	1.92	1.00	167	SP, LR
16B	105	200	1.92	1.50	251	SP, LR
16C	105	200	1.92	2.50	418	SP, LR, CS
16D	105	200	1.92	3.00	501	SP, LR
16E	105	200	1.92	2.50	418	LR, HT
20A	105	200	2.99	1.00	165	SP,LR
20B	105	200	2.99	1.50	248	SP, LR
20C	105	200	2.99	2.50	413	SP, LR, CS
20D	105	200	2.99	3.00	495	SP, LR
20E	105	200	2.99	2.50	413	LR, CS
AD1	105	200	1.92	1.00	167	SP, LR
AD2	105	200	1.92	2.50	418	SP, LR
F1	105	200	1.92	2.50	418	SP, LR, CS
F2	105	200	1.92	2.50	418	CS
H2	105	313	1.92	2.36	656	HT
S2	105	200	1.92	2.50	418	CS

Table 3.4 Details of NWC beam specimens cast without shear reinforcement

Specimen No.	Section width, b (mm)	Overall section depth, h (mm)	Longitudinal steel ratio, ρ (%) $\frac{100 A_s}{b h}$	Shear span to effective depth, a/d	Shear span, a (mm)	To be compared with OPSC specimen
NWC1	105	200	1.91	1	167	AD1
NWC2	105	200	1.91	2.5	418	F1
NWC3	105	200	1.91	2.5	418	16C
NWC4	105	200	2.99	2.5	413	20E
NWC5	105	113	1.90	2.5	237	12F

Table 3.5 Details of OPSC beam specimens cast with shear reinforcement

Specimen no.	Section width, b (mm)	Overall section depth, h (mm)	No. of shear reinforcement within shear span	Shear reinforcement spacing, s (mm)	Shear span, a (mm)	Variable considered
3A	105	200	3	120	240	CG, SR
3B	105	200	3	120	240	CG, SR
3C	105	200	3	120	240	CG, SR
4A	105	200	4	80	240	CG, SR
4B	105	200	4	80	240	CG, SR, PL
4C	105	200	4	80	240	CG, SR
5A	105	200	5	60	240	CG, SR
5B	105	200	5	60	240	CG, SR
5C	105	200	5	60	240	CG, SR
4D	105	200	6	80	200	PL
4E	105	200	6	80	160	PL

Table 3.6 Details of NWC beam specimens cast with shear reinforcement

Specimen no.	Overall section width (mm)	Overall section depth, h (mm)	No. of shear reinforcement within shear span	Shear reinforcement spacing, s (mm)	Shear span, a (mm)	To be compared with OPSC specimen
NWCA	150	200	3	120	240	3B
NWCB	150	200	4	80	240	4B
NWCC	150	200	5	60	240	5B
NWCD	150	200	4	80	160	4E
NWCE	150	200	4	80	240	4C

Table 3.7 Curing and concrete strength for OPSC beam specimens cast without shear reinforcement

OPSC beam Specimen No.	Mix design	w/c ratio	Curing duration (days)	Average cube compressive strength, f_{cu} (N/mm ²)
10A	B	0.37	28	30.05
S1	C	0.34	28	34.82
12A	B	0.37	32	31.03
12B	B	0.37	32	31.03
12C	B	0.37	32	31.03
12D	B	0.37	32	31.03
12E	C	0.34	55	39.20
12F	B	0.37	38	32.46
16A	A	0.44	30	26.14
16B	A	0.44	30	26.14
16C	A	0.44	30	26.14
16D	A	0.44	30	26.14
16E	B	0.37	32	32.46
20A	A	0.44	28	24.23
20B	A	0.44	28	24.23
20C	A	0.44	28	24.23
20D	A	0.44	28	24.23
20E	A	0.44	40	28.00
AD1	B	0.37	32	32.00
AD2	B	0.37	32	32.00
F1	B	0.37	32	32.00
F2	C	0.34	60	40.10
H2	B	0.37	37	32.46
S2	C	0.34	30	35.70

Table 3.8 Curing and concrete strength for NWC beam specimens cast without shear reinforcement

NWC beam Specimen no.	Mix design	w/c ratio	Curing duration (days)	Average cube compressive strength, f_{cu} (N/mm ²)
NWC1	N	0.43	11	33.00
NWC2	N	0.43	11	33.00
NWC3	N	0.43	7	29.00
NWC4	N	0.43	7	29.00
NWC5	N	0.43	11	33.00

Table 3.9 Curing and concrete strength for OPSC beam specimens cast with shear reinforcement

OPSC beam Specimen No.	Mix design	w/c ratio	Curing duration (days)	Average cube compressive strength, f_{cu} (N/mm ²)
3A	A	0.44	28	25.79
3B	B	0.37	30	31.93
3C	C	0.34	28	34.60
4A	A	0.44	28	25.79
4B	B	0.37	30	31.93
4C	C	0.34	28	34.60
5A	A	0.44	28	25.79
5B	B	0.37	30	31.93
5C	C	0.34	28	34.60
4D	B	0.37	28	30.15
4E	B	0.37	28	30.15

Table 3.10 Curing and concrete strength for NWC beam specimens cast with shear reinforcement

NWC beam Specimen no.	Mix design	w/c ratio	Curing duration (days)	Average cube compressive strength, f_{cu} (N/mm ²)
NWCA	N	0.43	7	30.61
NWCD	N	0.43	7	30.61
NWCC	N	0.43	7	30.61
NWCD	N	0.43	7	30.61
NWCE	N	0.43	13	35.00

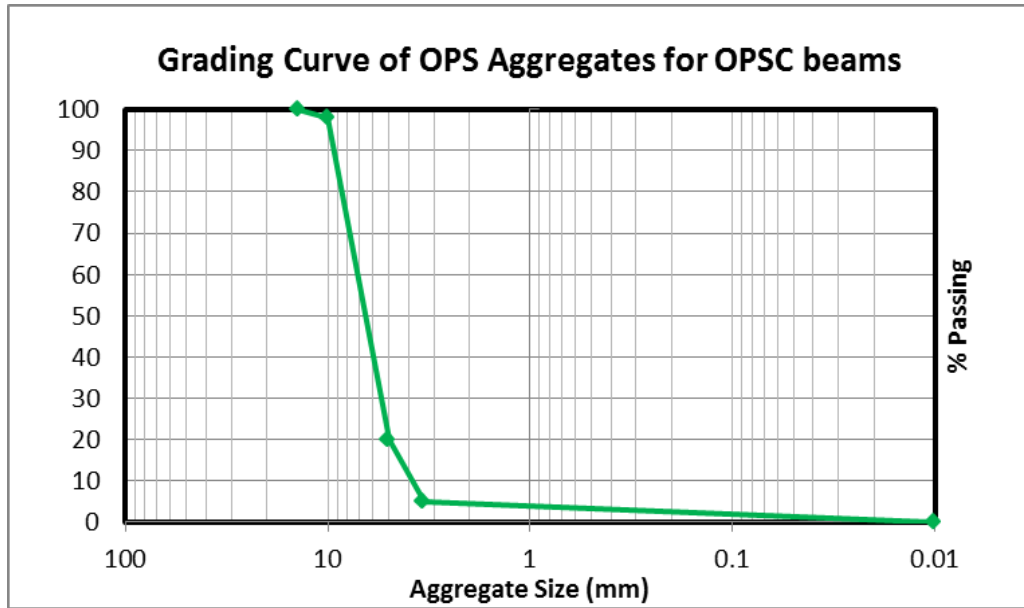


Figure 3.1 Grading curve of OPS Aggregate for OPSC beam specimens.

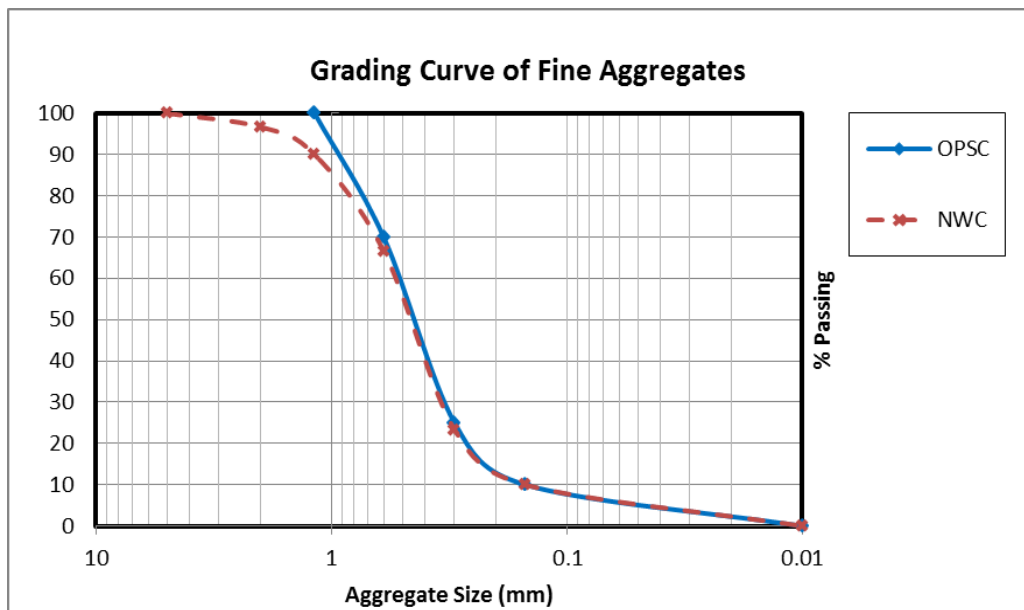


Figure 3.2 Grading curves of Fine Aggregate for OPSC and NWC beam specimens.

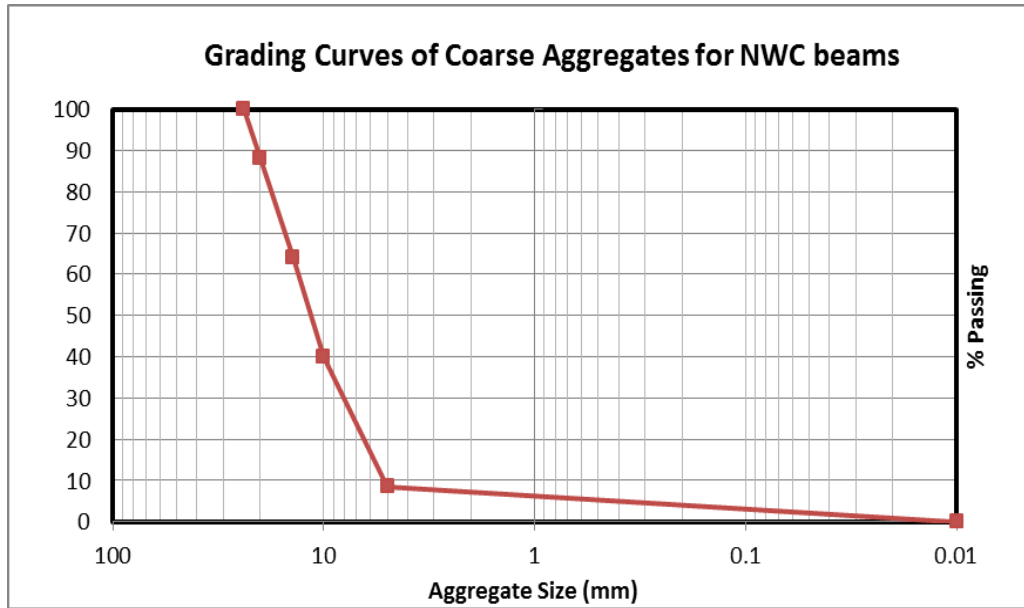


Figure 3.3 Grading curve of gravel Aggregate for NWC beam specimens.

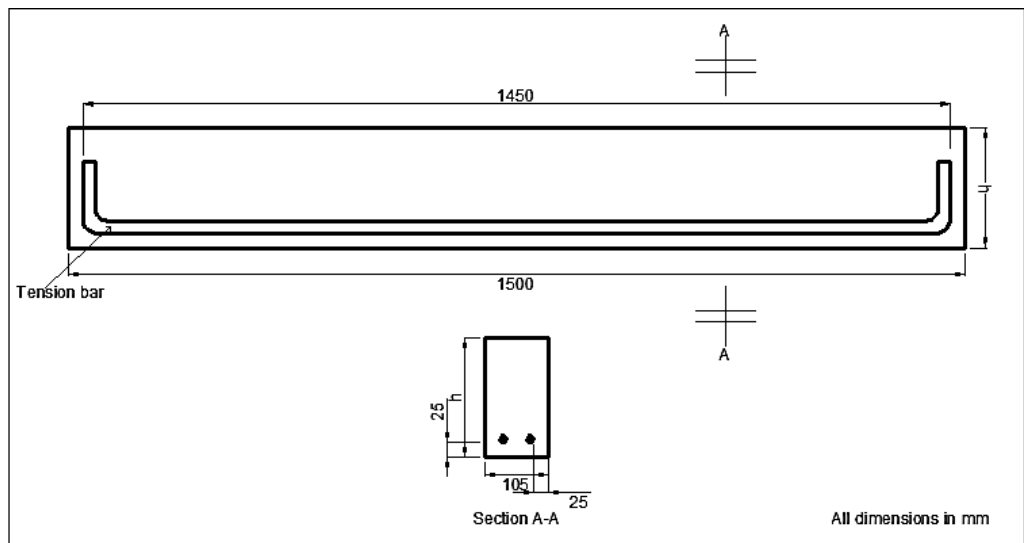


Figure 3.4 General arrangements of beams without shear reinforcement.

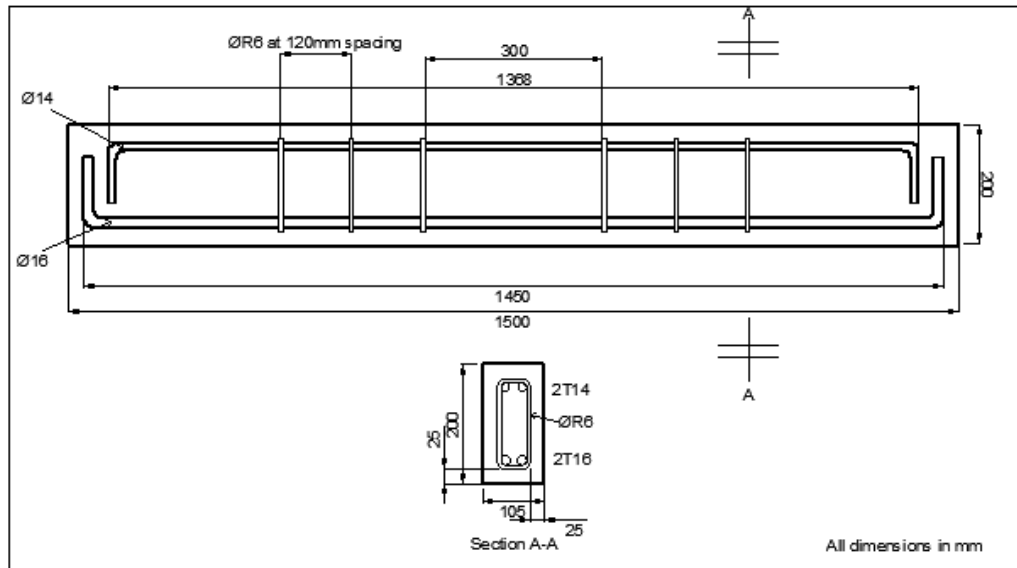


Figure 3.5 General arrangements of OPSC (3A, 3B, 3C) and NWC (NWCA) beams reinforced with 2T14 (compression), 2T16 (tension), and R6@120 mm (shear reinforcement).

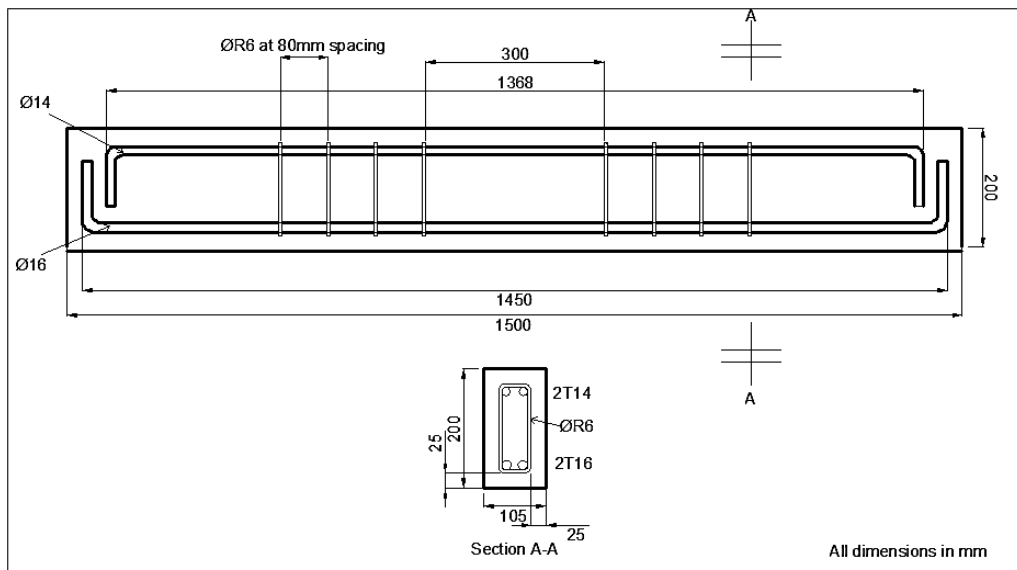


Figure 3.6 General arrangements of OPSC (4A, 4B, 4C, 4D, 4E) and NWC (NWCB, NWCD, NWCE) beams reinforced with 2T14 (compression), 2T16 (tension), and R6@80 mm (shear reinforcement).

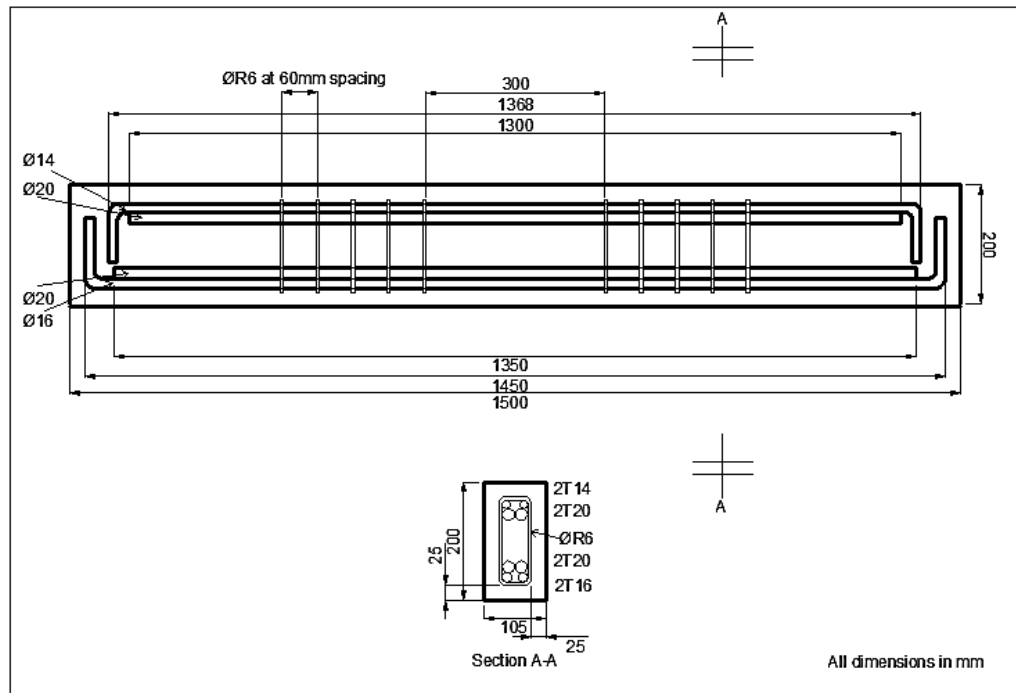


Figure 3.7 General arrangements of OPSC (5A, 5B, 5C) and NWC (NWCC) beams reinforced with 2T(14+20) (compression), 2T(16+20) (tension), and R6@60 mm (shear reinforcement).

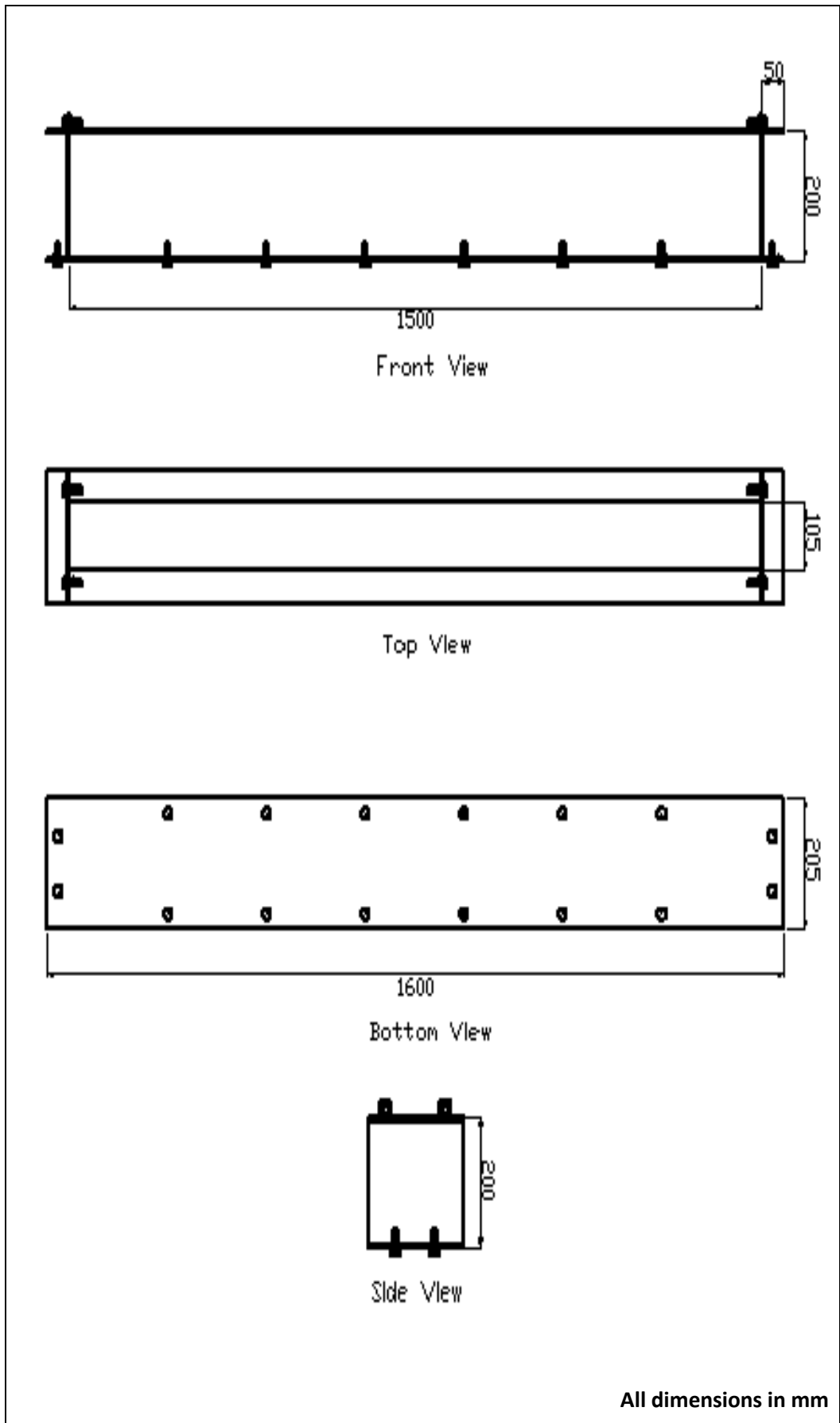


Figure 3.8 General arrangements of steel mould for casting of specimens having overall section depth ≤ 200 mm.

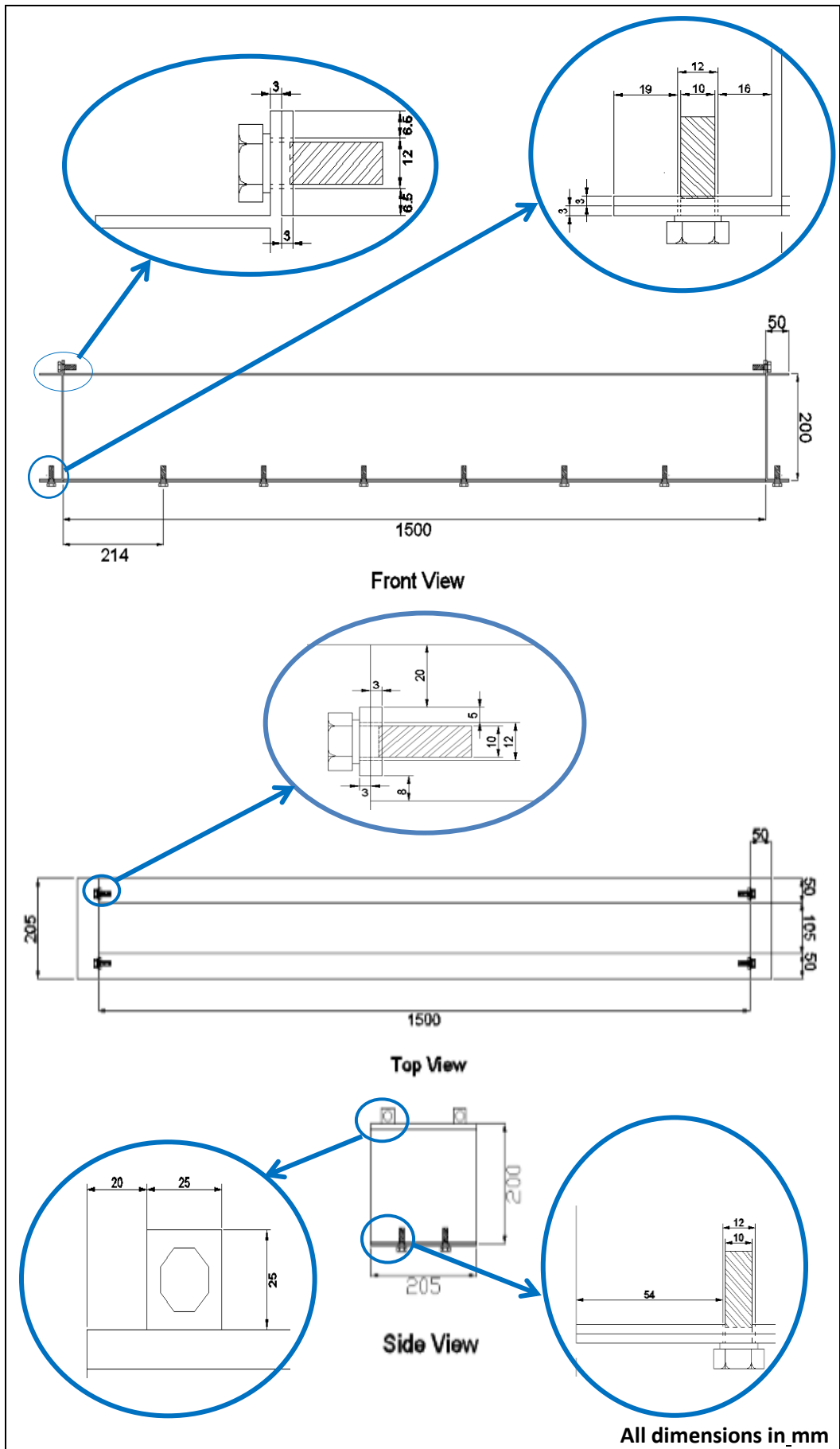


Figure 3.9 Bolting details of steel moulds shown in Figure 3.8.

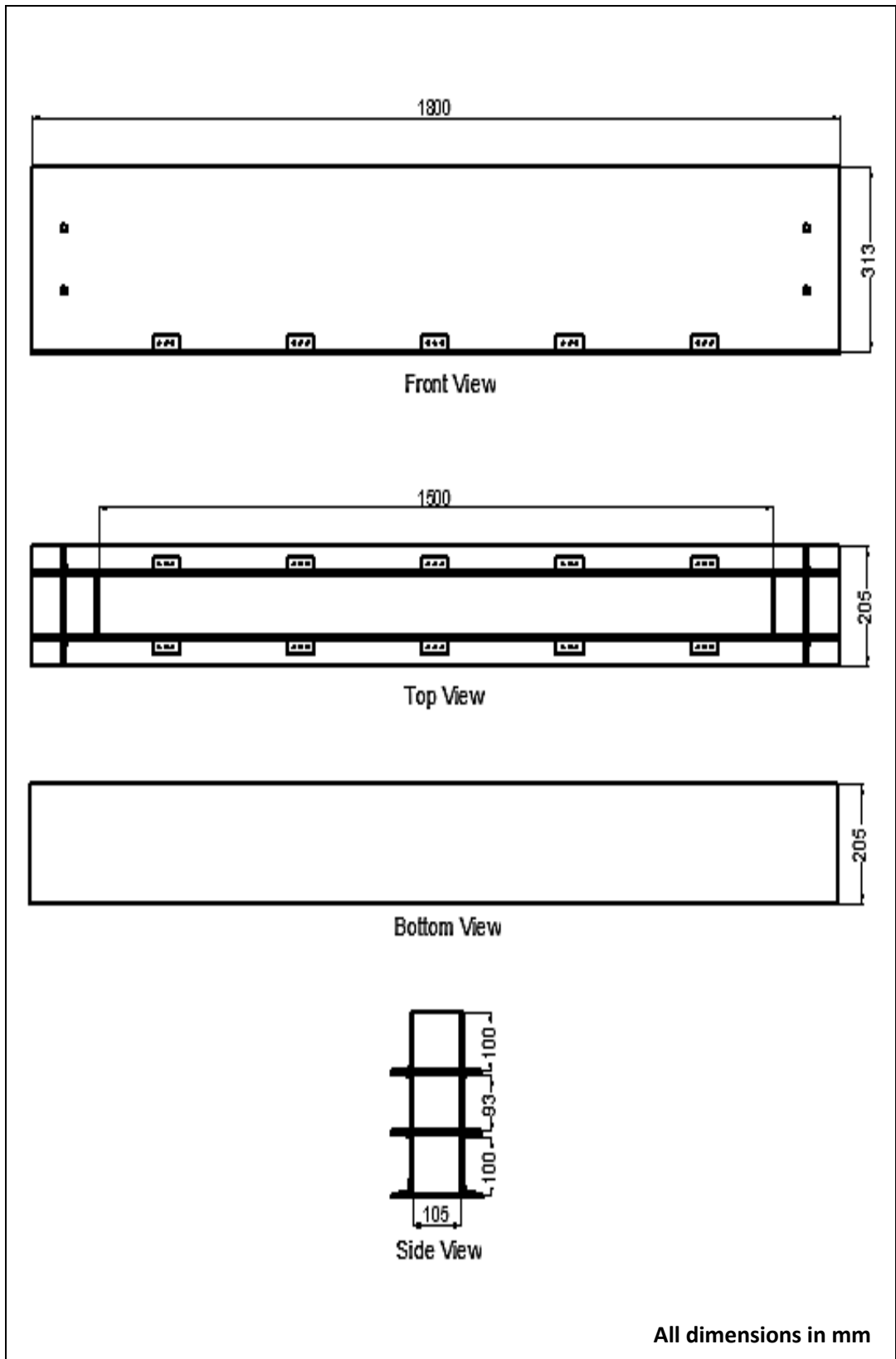


Figure 3.10 General arrangements of wooden mould for casting of specimens having overall section depth > 200 mm.

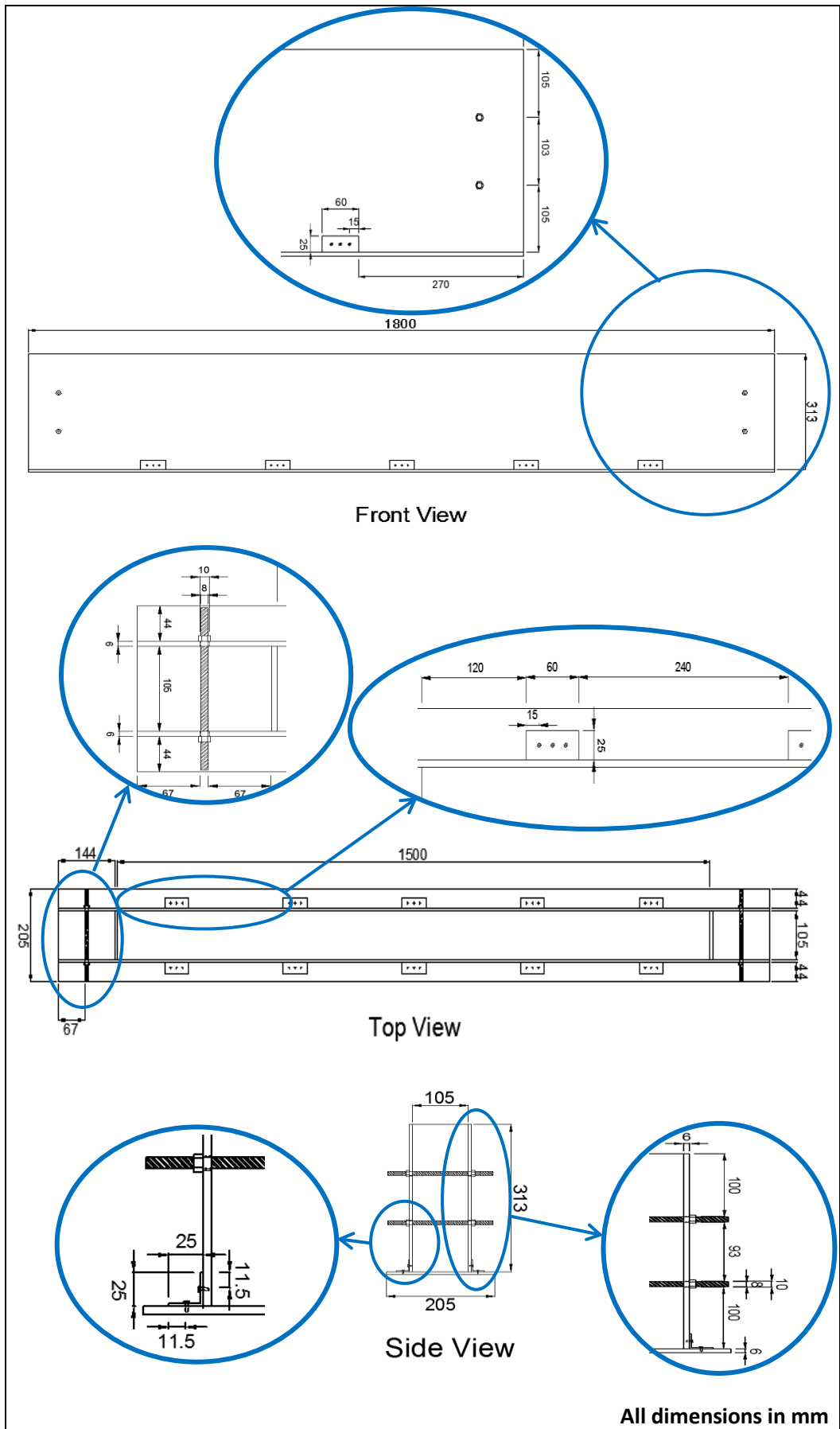


Figure 3.11 Bolting details of wooden moulds shown in Figure 3.10.

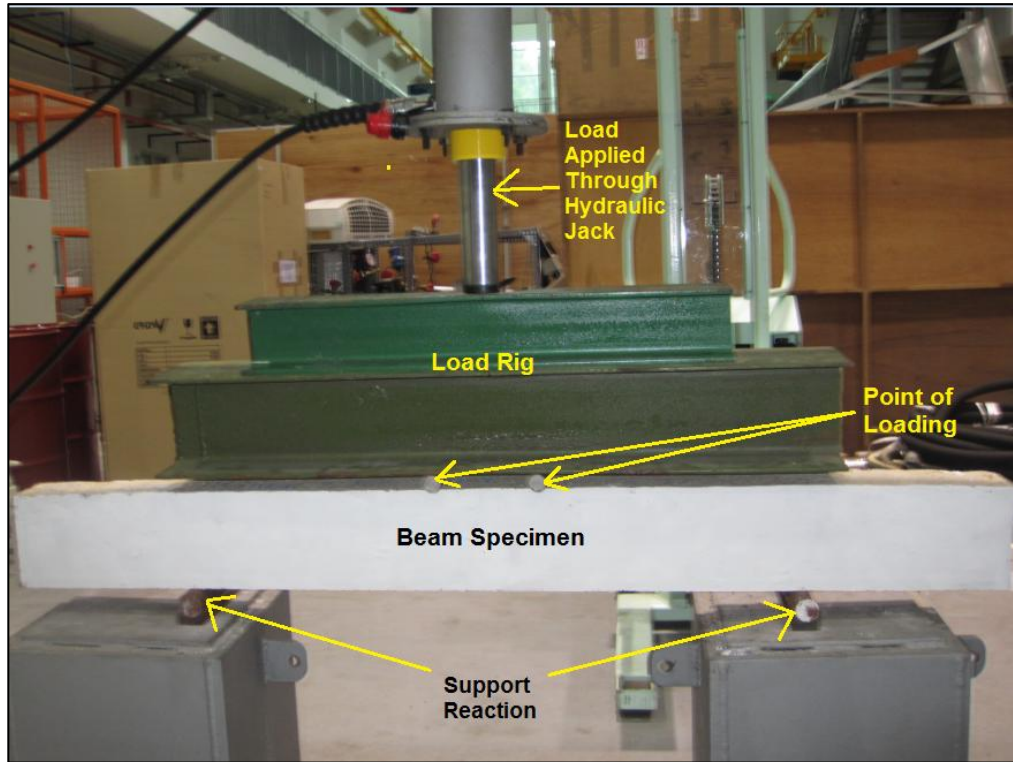


Figure 3.12 Test setup for OPSC and NWC beam specimens.

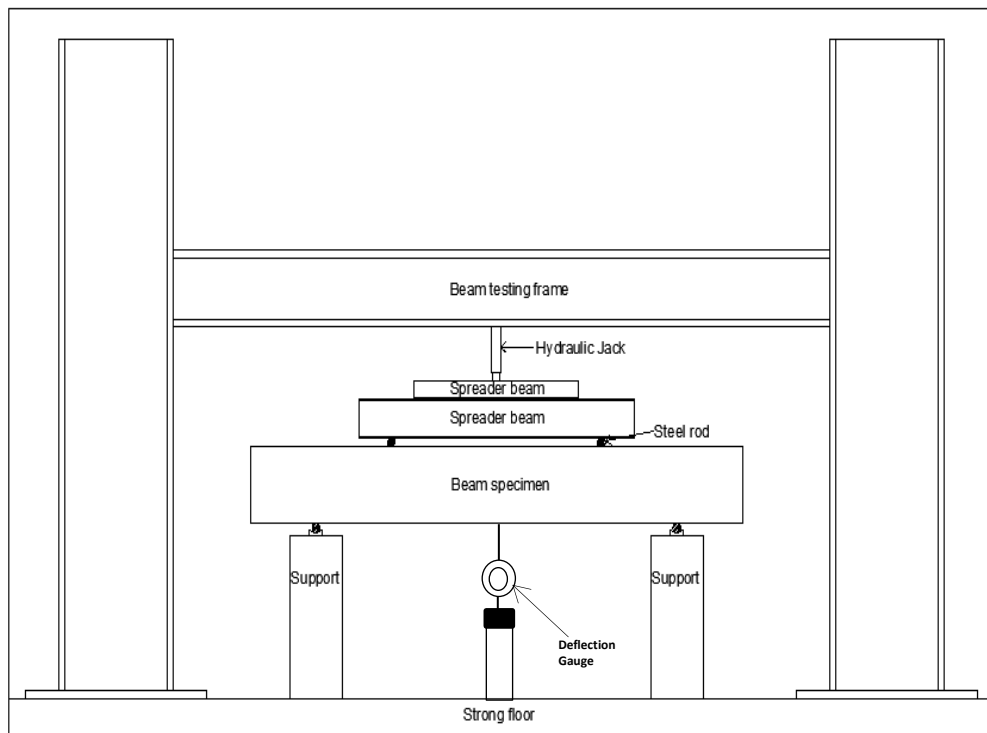


Figure 3.13 Loading rig for OPSC and NWC beam specimens.

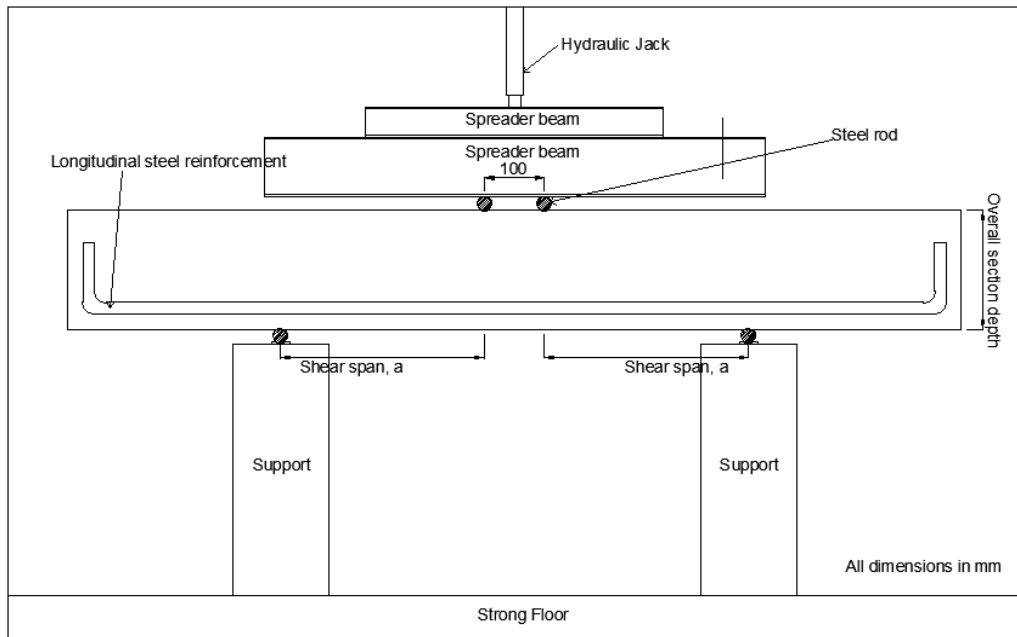


Figure 3.14 Loading arrangement for all beam specimens cast without shear reinforcement.

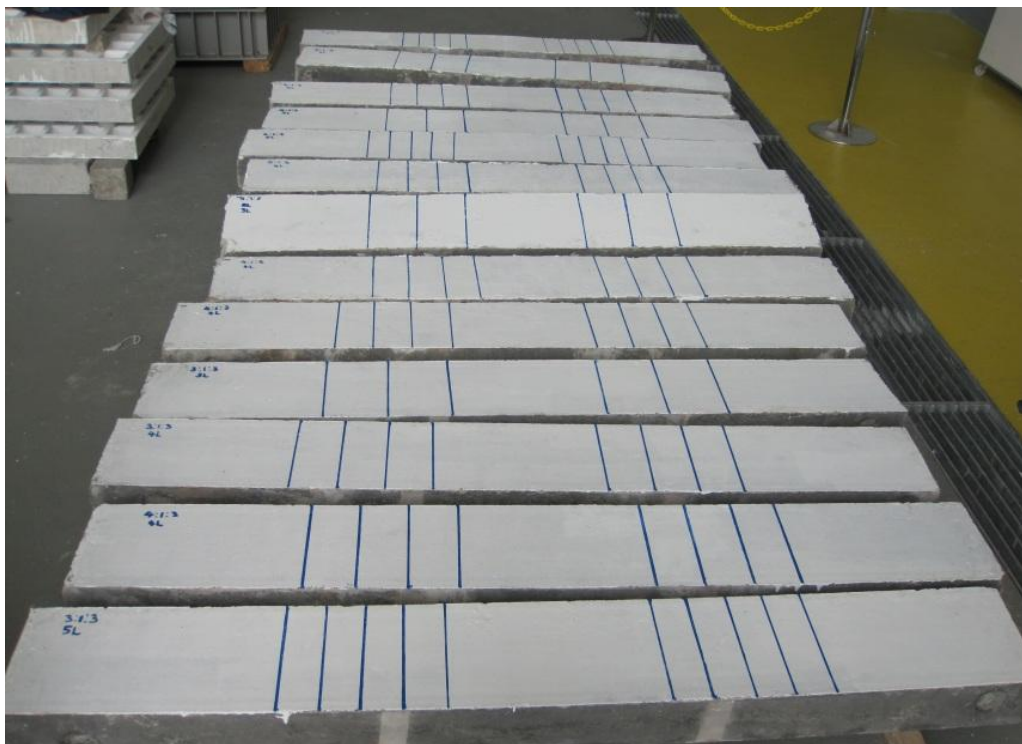


Figure 3.15 Location of shear reinforcement were marked to ensure for correct positioning of loads and supports.

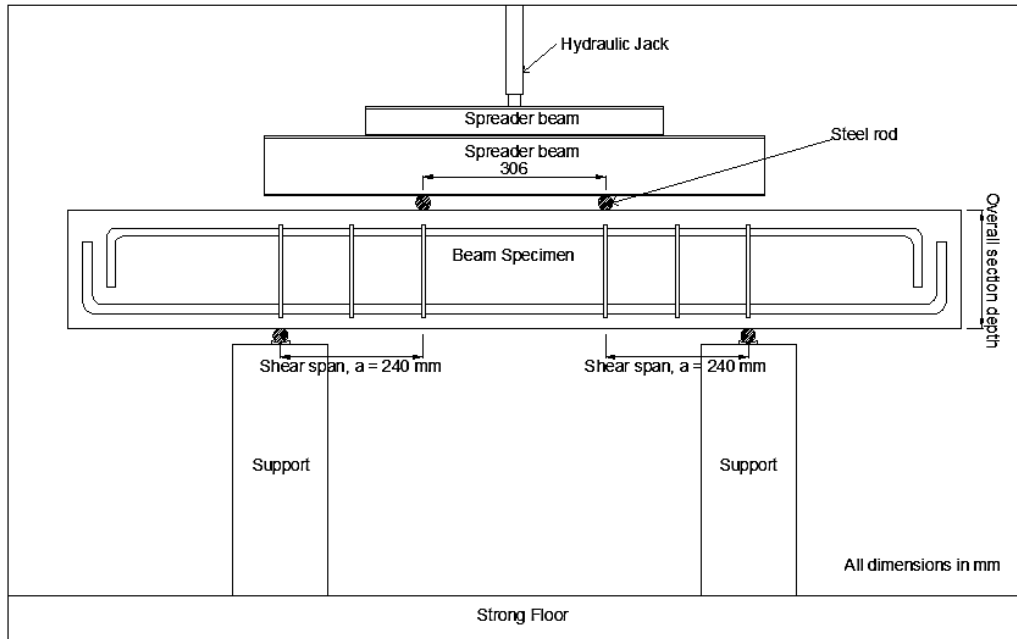


Figure 3.16 Loading arrangements for OPSC and NWC beam specimens cast with shear reinforcement spaced at 120 mm intervals and loaded with 240 mm shear span.

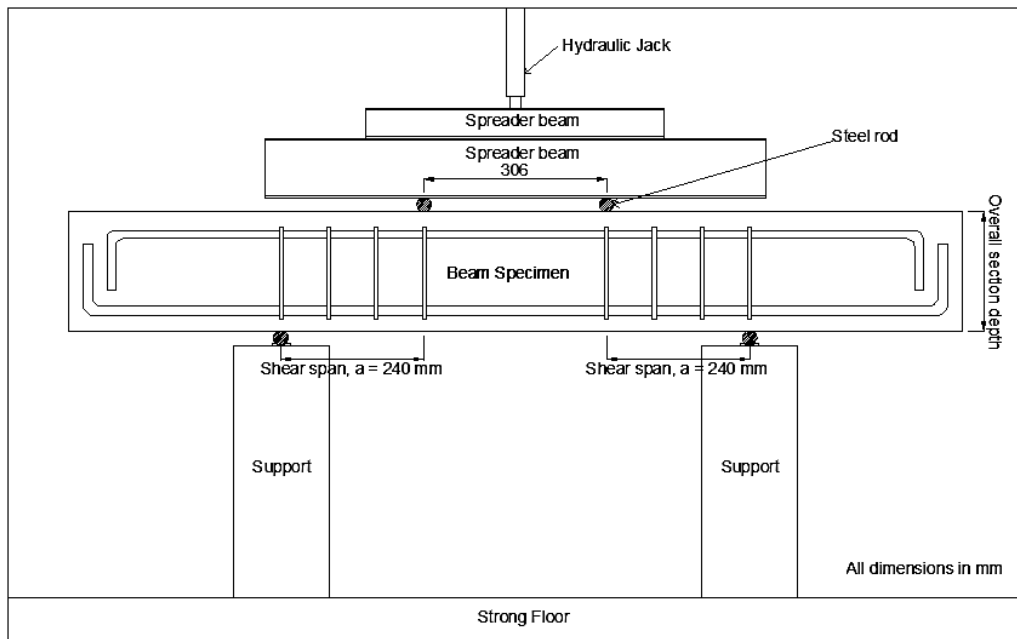


Figure 3.17 Loading arrangements for OPSC and NWC beam specimens cast with shear reinforcement spaced at 80 mm intervals and loaded with 240 mm shear span.

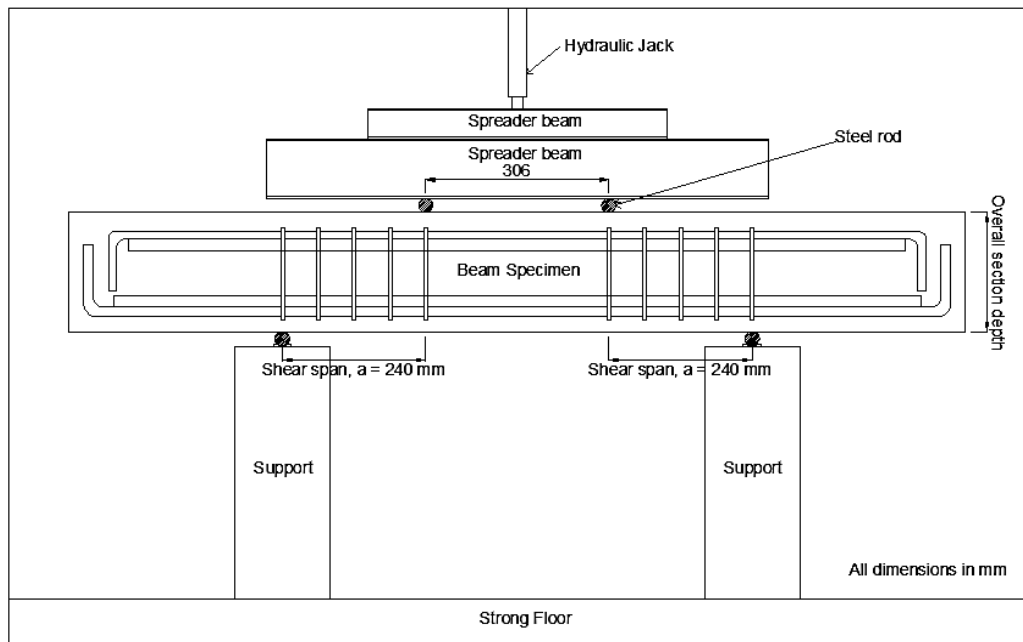


Figure 3.18 Loading arrangements for OPSC and NWC beam specimens cast with shear reinforcement spaced at 60 mm intervals and loaded with 240 mm shear span.

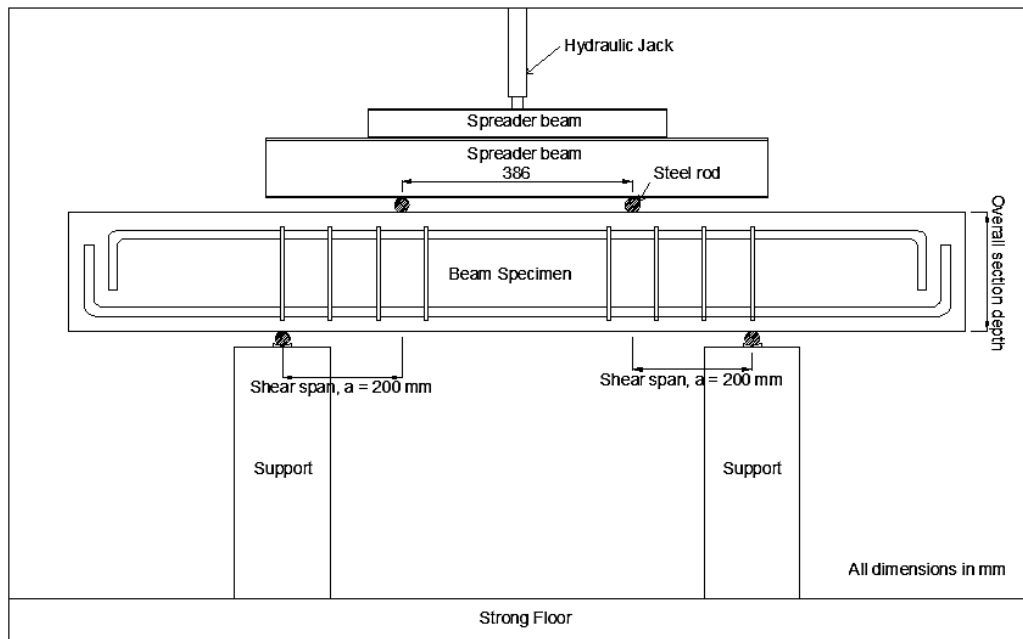


Figure 3.19 Loading arrangements for OPSC beam specimen cast with shear reinforcement spaced at 80 mm and loaded with 200 mm shear span.

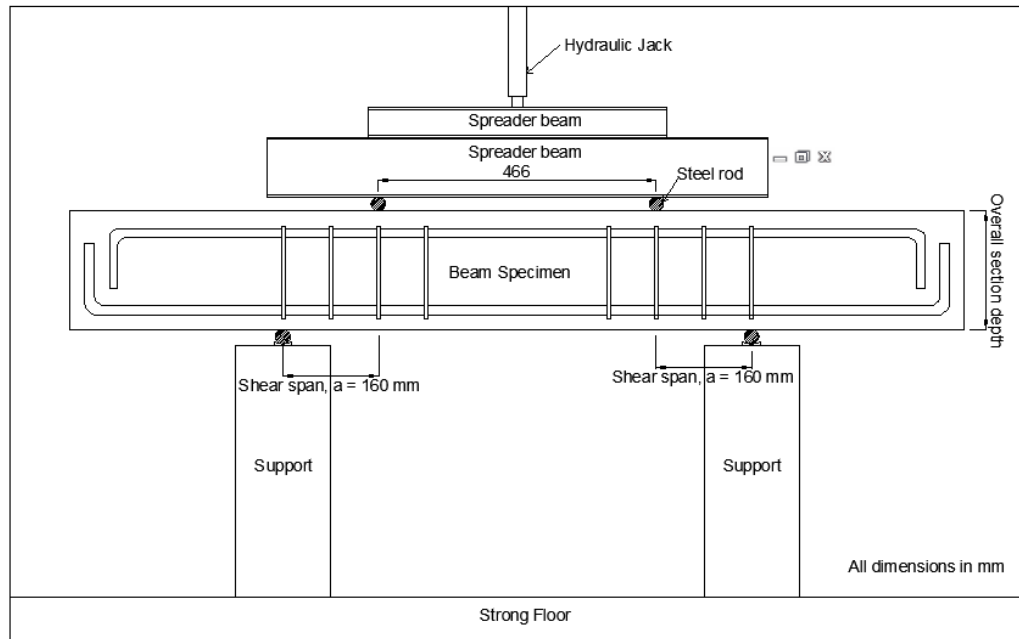


Figure 3.20 Loading arrangements for OPSC and NWC beam specimens cast with shear reinforcement spaced at 80 mm intervals and loaded with 160 mm shear span.

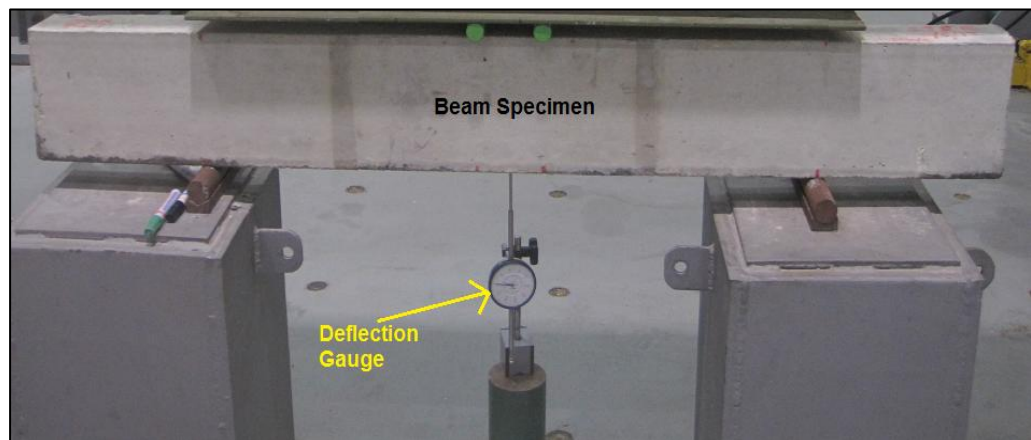


Figure 3.21 Position of mechanical dial gauge for measurements of mid span deflection.

Chapter 4

Failure Mechanisms and Test Results

4.1 Introduction

Full details of beam specimens cast in this research and their test setup have been described in Chapter 3. In this chapter, the observations made during tests, the measured deflections, the failure mechanisms, and the ultimate failure loads of all specimens are reported and discussed. In addition, the outcomes of comparative studies carried out to investigate the observed variations between the Oil Palm kernel Shell Concrete (OPSC) specimens and the Normal Weight Concrete (NWC) specimens with regards to variables considered are also presented in this chapter.

In this research, a total of forty five beam specimens were tested, of which, thirty five were cast from Oil Palm kernel Shell Concrete (OPSC) and ten were cast from Normal Weight Concrete (NWC). Among the OPSC beams, twenty four were cast without shear reinforcement, while the remaining eleven were cast with shear reinforcement. For NWC beams, five were cast without shear reinforcement, while the remaining five were cast with shear reinforcement.

In general, two distinct failure mechanisms were observed from tests on specimens cast without shear reinforcement, that is, for specimens loaded with span to depth ratio, $a/d < 2.5$, it is observed to fail in shear compression failure mechanism. Whilst for specimens loaded with span to depth ratio, $a/d \geq 2.5$, it is observed to fail in diagonal tension failure mechanism. However, for specimens cast with shear

reinforcement, all specimens were observed to fail in diagonal tension failure mechanism.

4.2 Specimens cast without shear reinforcement

A total number of twenty four OPSC beam specimens and five NWC beam specimens cast without shear reinforcement were tested. These specimens were loaded with a pair of concentrated loads on top of the beam at designated distances, a , away from the supports, as shown in Figure 3.14.

The observations made during tests, in regard to failure mechanisms and crack patterns, are presented from Figure 4.1 to Figure 4.24 and Figure 4.25 to Figure 4.29, for OPSC beam specimens and NWC beam specimens, respectively. The failure loads of OPSC and NWC beam specimens are presented in Table 4.1 and 4.2, respectively. Detailed discussions on these observations are presented in Section 4.2.1 to 4.2.3, as follows.

4.2.1 Overall behaviour of OPSC beams and NWC beams specimens

It is observed from tests that the entire twenty-nine beam specimens cast without shear reinforcement failed in shear mode of failure at the vicinity of shear span with the mid span of the beam displaced vertically by the loads applied. Three types of shear failure were observed: shear compression failure for $a/d < 2.5$, diagonal tension failure and shear failure, respectively, for $a/d \geq 2.5$. The systematically details observations from the flexural cracks initiation until the occurrence of the shear failure for the beams without shear reinforcement are explained herein.

Except for specimens 20A and 20B (see Table 4.3), it is observed that the formations of flexural cracks occurred prior to the shear cracks. The flexural cracks initiated from the mid-span bottom fibre, coinciding with the maximum tensile stress, and propagate through the section of the specimens as the applied load increases. The flexural cracks were noted to occur at 18% to 78% of the ultimate failure loads for OPSC beam specimens (see Table 4.3), and at 20% to 62% for NWC beam specimens (see Table 4.4). However, inferred from load deflection curves, the cracking load are noted to occur at 10% to 56% of the ultimate loads for OPSC beam specimens (see Table 4.3) and at 12% to 59% of the ultimate loads for NWC beam specimens (see Table 4.4). The load-deflection curves are presented from Figure 4.30 to Figure 4.34 and Figure 4.35 for OPSC beams and NWC beams, respectively. It is believed that the discrepancies noted between the observed and the inferred cracking loads were due to the formation of flexural micro-cracks that could not have been detected by the naked eye but can be clearly observed via the change of inclination angle on the load deflection curves.

Further analysis on the test results revealed that the formations of flexural cracks did not take place under loads having similar percentages to their ultimate failure loads. These inconsistencies derived from the fact that the percentages for formation of flexural cracks were determined with respect to the ultimate shear failure loads (V_{ult}) instead of their flexural failure loads. That is, specimens failed in shear at higher ultimate failure loads may in fact have been casted with high flexural resistance (such as specimens 20A, 20B, 20C), thus, appeared to have their flexural cracks formed at loads that are closer to their ultimate shear failure loads, hence, resulting the high percentages. In contrast, specimens failed in shear at lower ultimate failure loads were in fact casted with lower flexural resistance (such as Specimens 12A, 12B and

12C), thus, appeared to have their flexural cracks formed at loads that are further away from the ultimate shear failure loads, hence, resulting the low percentages. The implication is that the formations of flexural cracks are in fact independent to the formation of shear failure mechanism.

Upon further loading, the formations of shear cracks were observed to have initiated at the supports at 48% to 97% of the ultimate failure loads for OPSC beam specimens (see Table 4.3), and at 60% to 75% of the ultimate failure loads for NWC beam specimens (see Table 4.4). These inconsistencies deduced from the fact that specimens failed in shear at higher percentages of the ultimate failure loads were, in fact, loaded with high shear span to depth, a/d , ratio (such as Specimens 12C, 12D, 16C and 16D), thus, appeared to have their shear cracks formed at loads that are closer to their ultimate shear failure loads. In contrast, specimens that failed in shear at lower ultimate failure loads were loaded with low shear span to depth, a/d , ratio (such as specimens 12A, 12B, 16A and 16B), thus, appeared to have their shear cracks formed at loads that are far from the ultimate shear failure loads. The implication is that the formation of shear cracks are dependent on the loading position, that is beams loaded with high shear span to depth, a/d , ratio would have their shear cracks formed at loads further from their ultimate as compared to those loaded with a lower span to depth ratio. After formation of the initial shear cracks at the supports, these inclining shear cracks were observed to propagate towards the loading positions through the specimen's section depth as the applied load increases, upon further increases in the applied load, the formation of shear failure were observed with a sudden increase in the width of the shear cracks.

Further comparisons of flexural and shear cracks between OPSC and NWC beam specimens with similar variables (span to depth ratio (a/d), longitudinal steel ratio

(ρ), concrete strength (f_{cu}) and overall section depth (h), such as OPSC specimen AD1 and NWC specimen NWC1 (see Figure 4.19 and Figure 4.25, respectively), and OPSC specimen F1 and NWC specimen NWC2 (see Figure 4.21 and Figure 4.26, respectively) shown that the amount of flexural and shear cracks formed in OPSC specimens were greater than NWC specimens, which it is observed during testing that the visibility of flexural and shear cracks for OPSC beam specimens were more evident, hence the shear failure indications in OPSC beam specimens are more apparent with ample warning to be given before failure occurred.

In general, for specimens loaded with span to depth ratio, $a/d < 2.5$, it was noted that shear compression failure occurred by crushing of the concrete at the compression zone and the ultimate shear failure loads are higher than those specimens loaded with span to depth ratio, $a/d \geq 2.5$. This have been expected that the ultimate loads are higher for $a/d < 2.5$ due to the fact that the loads from the loading position were able to be transferred to the support reaction through the shorter shear span distance, where diagonal shear cracks were observed to propagate towards the loading position, prior to the ultimate occurrence of shear compression failure. It is observed that the crushing of concrete at the compression zone were less evident for specimens casted with lower percentage of longitudinal steel ratio (ρ) of less than 2.99% (such as Specimen 12A, 12B, 16A, 16B and NWC1) compared to specimens casted with longitudinal steel ratio, $\rho = 2.99\%$ (Specimen 20A and 20B). For beams casted with lower longitudinal steel ratio, the crushing of concrete at the compression zone were less pronounced as the mid span of the longitudinal steel reinforcement would have bent alongside with the vertical displacement of the specimen as the load was increased, resulting in a limited concrete crushing at the beam compression zone. In contrast, for specimens casted with higher longitudinal

steel ratio, $\rho = 2.99\%$, specifically Specimen 20A and 20B (see Figure 4.14 and Figure 4.15, respectively) concrete crushing at the beam compression zone was more apparent as the longitudinal steel reinforcement in each specimen would have remained rigid due to the higher beam stiffness provided, hence, the bending of longitudinal steel reinforcement were limited with the increment of applied loads.

For beam specimens loaded with span to depth ratio, $a/d \geq 2.5$, it is observed that shear failure took place at the shear span except for OPSC beam specimens cast with $\rho = 0.75\%$ (Specimen 10A and S1 in Figure 4.1 and Figure 4.2, respectively), which failed in diagonal tension mode. During testing, it is observed that for beams, which failed in diagonal tension mode (Specimen 10A and S1), the diagonal cracks were originated from the flexural cracks formed at the mid-span closest to the shear span, and subsequently, developed into diagonal shear cracks, which propagated to the loading position prior to diagonal tension failure. Whilst for beams that failed in shear failure mode, it is observed during testing that the diagonal shear cracks were initiated from the support reaction and propagated towards the loading position prior to the shear failure.

The difference of failure mode observed for beams loaded with span to depth ratios, $a/d > 2.5$ was due to the longitudinal steel ratio provided. For specimens casted with lower longitudinal steel ratio, flexural cracks observed were more evident, hence lower resistance against bending were provided by the lower beam stiffness of the longitudinal steel reinforcement as bending of the beams were more significant compared to specimens casted with higher longitudinal steel ratio. As the results, the beams casted with lower longitudinal steel ratio were observed to fail in diagonal tension failure mode instead of shear failure mode. The implication is that for beams loaded with span to depth ratio, $a/d > 2.5$, the higher longitudinal steel ratio

provided increases the beam stiffness, which subsequently increased the resistance against bending and hence, shear failure occurred.

Further, it is observed that for all beams loaded with span to depth ratio, $a/d \geq 2.5$, both the shear failure: diagonal tension failure and shear failure were abrupt and explosive. In addition, it is observed that both types of failures also consist of beam splitting, which horizontal splitting of concrete occurred due to dowel action between the concrete and surface of longitudinal steel bar from the support reaction to the shear span. Subsequently, the beam splitting propagated from the shear span diagonally via the diagonal shear cracks to the loading position, where the concrete beam were separated into two regions, which is observed in all specimens loaded with $a/d \geq 2.5$ (see Example Figure 4.1 for Specimen 10A, which failed in diagonal tension failure and Figure 4.5 for Specimen 4.5, which failed in shear failure). After shear failure, although splitting of the beam occurred, it is observed from all specimens that the two regions of the beam remained intact as a beam due to the presence of anchorage at bottom of both end of the beam, which would have prevented the whole beam from splitting into two sections.

For OPSC specimens, two types of crack mechanisms were observed (see Figure 4.36 and 4.37) at the diagonal shear cracks: (1) crack sheared through the OPS aggregates and (2) bond failure between cement paste and OPS aggregates in concrete (see Figure 4.37 for illustrations). However, the occurrence of either one of these two observed mechanisms depend on the natural alignment of OPS aggregates along shear crack. The natural alignment of OPS aggregates was found to incline either towards perpendicular or parallel axis of the diagonal shear crack. It was observed that the OPS aggregates were sheared through by the crack when the alignment of OPS aggregates inclined towards the perpendicular axis of the crack. Whilst the bond

failure between cement paste and OPS aggregates was observed when the OPS aggregates inclined towards parallel axis of the diagonal shear cracks. Whilst for NWC specimens, the crack mechanism was observed to shear through the cement paste (See Figure 4.38) and in between the normal aggregates (see also Figure 4.60 for illustration).

4.2.2 Central deflection

The central deflection of all beam specimens were recorded after every increment of applied load. For every beam specimens cast without shear reinforcement, a graph of load versus central deflection curve has been plotted and presented in Figure 4.31 to Figure 4.34, and Figure 4.35, for OPSC beam specimens and NWC beam specimens, respectively.

In general, these curves exhibit similar load deflection behaviour among the specimens, that is, a linear elastic behaviour can be inferred up to approximately half of the ultimate failure loads, and subsequently, the rate of increment in the applied loads decreased until failure occurred. The increases in the rate of deflection were due to the formation of flexural cracks at the mid-span bottom tension surface of the beam specimens.

A comparison between the actual cracking loads inferred from the load-deflection curves and the observed cracking loads are presented in Table 4.3 and Table 4.4 for OPSC beam specimens and NWC beam specimens, respectively. From these comparisons, it is observed that the inferred cracking loads were 4% to 25% and 3% to 11% lower than the observed flexural cracking loads for OPSC beam specimens and NWC beam specimens, respectively. It is believed that these discrepancies derive

from the fact that the early formation of the micro-cracks could not be detected by the naked eye.

4.2.3 Ultimate Failure Loads

The ultimate failure loads of beam specimens were derived from the last recorded loads applied to the specimens prior to failure. For beam specimens cast without shear reinforcement, the ultimate shear failure loads of specimens cast from OPSC and NWC are summarized and presented in Table 4.1 and 4.2, respectively. Among the twenty-nine beam specimens, twenty four were casted from OPSC while the remaining five were casted from NWC.

Among the twenty-four OPSC beam specimens, four variables were considered in the tests (See Table 4.1): span to depth ratio (SP), longitudinal steel reinforcement ratio (LR), concrete strength (CS) and overall section depth (HT). Of which, eighteen out of the twenty four specimens derived with results that addresses for more than one variables considered (see Table 4.1).

Whilst, among the five NWC beam specimens, four identical variables were considered (See Table 4.2): span to depth ratio (SP), concrete strength (CS), longitudinal steel reinforcement ratio (LR) and overall section depth (HT). These NWC specimens were designed and tested to form the basis (control samples) from the current research investigation.

In general, it is apparent that the load carrying capacities of both the OPSC beams and NWC beams (cast without shear reinforcement) are influenced by the variables considered. Details of the effects of variables and the comparisons of OPSC

specimens with control sample are described fully from Section 4.2.3.1 to Section 4.2.3.4.

4.2.3.1 Span to depth ratio

Among the twenty four OPSC beams casted without shear reinforcement, fifteen beam specimens (see Table 4.1) were cast and tested to evaluate the effect of shear span-depth ratio, a/d , with respect to the ultimate shear resistance. These fifteen OPSC beam specimens have been further sub-categorised into: SP-LR12B, SP-LR16A, SP-LR16B, and SP-LR20A; to take account for three longitudinal steel reinforcement ratios and two range of concrete cube compressive strength (see Table 4.5). The three longitudinal steel reinforcement ratios were: 1.08% (Category SP-LR12B), 1.92% (Category SP-LR16A and SP-LR16B) and 2.99% (Category SP-LR20A). Whilst the two range of concrete cube compressive strength were: 24 N/mm² to 26 N/mm² (Category SP-LR16A and SP-LR20A) and 31 N/mm² to 32 N/mm² (Category SP-LR12B and SP-LR16B).

In general, the observations made from tests indicate that the ultimate shear resistance increases as the span to depth ratio (a/d) decreases (see Figure 4.38). Such observations are to be expected, because as the shear span, a , reduces, the shear inclination angle increases, which in turn, enhance the contribution of aggregate interlocking towards the ultimate shear capacity, and as a result, a higher shear resistance could be mobilised.

Comparisons with the NWC beam specimens reveal that the rate of increase in the ultimate shear resistance of OPSC beam specimens as a result of the decreasing shear span depth ratio, a/d , are observed to be less significant, as shown in Figure

4.39. That is, the shear resistance of NWC specimens (NWC2 to NWC1) increased by 100% as the span to depth ratio, a/d , reduces from 2.5 to 1.0, while the shear resistance of OPSC specimens (F1 to AD1) increased only by 78% for the same reduction in span depth ratio. Such discrepancy is believed to be attributed to the smoother shear surface observed from the OPSC specimen (AD1) (see Figure 4.40 and 4.41), where a lower aggregate interlocking resistance could be mobilised.

However, observations made on specimens loaded with $a/d = 2.5$ revealed that specimen cast with OPSC (F1) exhibited rougher shear surface than those cast with NWC (NWC2) (see Figure 4.40 and 4.42). Although a rougher surface has been observed in beams cast with OPSC, a lower shear resistance was observed (90% of that observed in specimen cast with NWC-NWC2) (see Figure 4.39). It is believed that the lower shear resistance found in OPSC beams is in fact attributed to the lower aggregate strength found in Oil Palm Kernel Shell (OPSC), which in turn, provide a lower aggregate interlocking capacity.

On the other hand, it was observed that for the same shear to depth ratio, a/d , the ultimate failure load obtained by OPSC specimens casted with higher longitudinal steel reinforcement ratio exhibited higher shear capacity (see Figure 4.39). This result is as expected, because as the longitudinal steel reinforcement ratio increases, the contribution of dowel shear capacity on the ultimate shear capacity of the OPSC beams would have increases, and as a result, higher ultimate failure loads is obtained.

4.2.3.2 Longitudinal steel ratio

Eighteen OPSC beam specimens (see Table 4.6) were selected from the twenty four OPSC beam specimens without shear reinforcement and are categorized under Category LR to evaluate the effect of longitudinal steel ratio to the ultimate shear resistance. These eighteen OPSC beam specimens have been further subcategorised into: LR-SP1A, LR-SP1B, LR-SP1.5A, LR-SP2.5A, LR-SP2.5B, LR-SP3A and LR-SP3B; to account for four span to depth ratios and two range of cube compressive strength. The four shear span – depth ratios consist of $a/d = 1$ (Category LR-SP1A and LR-SP1B), $a/d = 1.5$ (Category LR-SP1.5A), $a/d = 2.5$ (Category LR-SP2.5A and LR-SP2.5B) and $a/d = 3$ (Category LR-SP3A and LR-SP3B). Whilst the two range of cube compressive strength consists of 24 N/mm^2 to 26 N/mm^2 (Category LR-SP1A, LR-SP1.5A, LR-SP2.5A and LR-SP3A) and 31 N/mm^2 to 32 N/mm^2 (Category LR-SP1B, LR-SP2.5B and LR-SP3B).

Comparing the test results of ultimate failure load with respect to the variable of longitudinal steel reinforcement ratio shown in Table 4.6, it is evident that the ultimate shear resistance increases with the increment of longitudinal steel reinforcement ratios (see also Figure 4.43). It is generally believed that when the longitudinal steel reinforcement ratios provided for the beams decreases, the shear force carried by the dowel action of longitudinal steel reinforcement decreases [27]. Hence, wider shear crack widths is observed on the beams casted with lower longitudinal steel reinforcement ratio, which is shown on the OPSC specimen 12C shown in Figure 4.6, compared with the beam casted with higher longitudinal steel reinforcement ratio (OPSC specimen 20C shown in Figure 4.16). Subsequently, the wider shear crack widths would reduce the aggregate interlock capacity [27], and, as a result, the ultimate failure loads obtained are lower. In contrast, OPSC beams

casted with higher longitudinal steel reinforcement ratio would lead to increment of dowel shear capacity, thus, higher aggregate interlock capacity and results in higher ultimate load obtained.

In comparison to the NWC beam specimens, it was observed from tests that the ultimate failure load obtained for OPSC beams are lower (See Figure 4.44), which the ultimate failure load obtained for Specimen F1 and 20E is 10% and 47% lower with respect to the NWC beam specimen NWC3 and NWC4 for longitudinal steel ratio of 1.92% and 2.99%. For NWC beam specimens casted with lower and higher longitudinal steel reinforcement (NWC3 and NWC4), it is believed that higher aggregate impact strength is provided by the gravel aggregates (see Table 2.1), which observations from the sheared plane of diagonal shear cracks show that the gravel aggregates remain rigid. This would allow sufficient dowel action of longitudinal steel reinforcement to be mobilised and subsequently, leads to the increment of aggregate interlock capacity in NWC beams. As a result, higher ultimate failure load is obtained by NWC beams compared to OPSC beams. In contrast, lower OPS aggregates impact strength are provided for OPSC beam specimens, which the OPS aggregates are observed to be easily fractured in concrete. Therefore, this would lead to lack of dowel action of the longitudinal steel reinforcement to be mobilised and also leads to lower aggregate interlocking and as a result, lower ultimate failure load is obtained by OPSC beams than NWC beams.

Further comparisons with the NWC beam specimens indicate that the increment in the ultimate shear resistance of OPSC beam specimens as a result of the reduction of longitudinal steel reinforcement, ρ , are less significant (see Figure 4.44). That is, a comparisons of OPSC beam specimens (Specimen 16C and 20E) with NWC beam specimens (Specimen NWC3 and NWC4), show that the shear resistance of NWC

specimens increased by 56% as longitudinal steel ratio increased from 1.92% to 2.99%, while the shear resistance of OPSC specimens increased only by 21%. It is believed that for NWC beams, higher increment rate of dowel action capacity and aggregate interlock capacity are provided by the contribution of rigid behaviour of gravel aggregates compared to easily fractured behaviour of OPS aggregates in OPSC beams. As a result, the rate of ultimate shear strength increment obtained from the tests for NWC beams is higher than OPSC beams.

4.2.3.3 Concrete strength

From the twenty four OPSC beam specimens without shear reinforcement, ten beam specimens (see Table 4.7) were selected and are categorized under Category CS to evaluate the effect of concrete strength to the ultimate shear resistance of OPSC beams. These ten OPSC beam specimens have been further subcategorized into: CS-LR10, CS-LR12, CS-LR16 and CS-LR20; to account for four longitudinal reinforcement ratios. The four longitudinal reinforcement ratios are 0.75% (Category CS-LR10), 1.08% (CS-LR12), 1.92% (CS-LR16) and 2.99% (CS-LR20).

In general, from test results of the selected ten OPSC beam specimens with parameter of concrete strength (see last column in Table 4.7), it is apparent that as the concrete strength, f_{cu} , increases, the ultimate shear resistance increases (see Figure 4.45). For increment of concrete strength in a beam, it is generally believed that the tensile strength of concrete would increase, in which, bond within the cement paste and interlocking between the cement paste and aggregates would grow stronger. Hence, this would delay the rupture of concrete and as a result, the ultimate failure load increases with the concrete strength.

In addition, in view of shear transfer mechanism, the concrete strength affects shear strength because as concrete strength increases, the dowel action capacity would increase [27]. Subsequently, this would lead to the smaller shear crack widths as observed in OPSC beam specimens (for example specimen 12E shown in Figure 4.7) compared with OPSC beams tested at lower concrete strength (for example OPSC specimen 12C shown in Figure 4.5). Consequently, the smaller shear crack widths would have increased the aggregate interlock capacity and compression zone capacity. As a result, higher ultimate failure load is required to fail the OPSC beam, which was tested at higher concrete strength.

Further comparisons with the NWC beam specimens reveal that for NWC beam specimens, the ultimate shear strength obtained with respect to concrete strength was higher than the OPSC beams with only a slightly lower rate of shear strength increment observed compared to the OPSC beam specimens (see Figure 4.46). That is, from comparing the OPSC beams (Specimens F1 and 16C) to NWC beams (Specimens NWC2 and NWC3), it was revealed that the shear resistance of NWC specimen increased 6% as the concrete strength increased from 29 N/mm² to 33 N/mm², while the shear resistance of OPSC specimen increased 10% as the concrete strength increased from 26.14 N/mm² to 32 N/mm².

For OPSC specimens (Specimen 16C and F1), the lower shear strength achieved is believed due to the lower aggregate strength provided by the OPS aggregates (see Table 2.1) compared to gravel aggregates in NWC specimens. Hence, this led to lower aggregate interlocking capacity and resulted in lower shear resistance. Whilst for NWC beams, the rigid behaviour of gravel aggregates would have provided higher aggregate interlocking capacity and thus, higher shear resistance was mobilised.

4.2.3.4 Section depth

Among the twenty four OPSC beam specimens, three beam specimens (see Table 4.8) were cast and tested (Category HT) to evaluate the effect of overall section depth, h , with respect to the ultimate shear resistance of OPSC beams.

In general, the observations made from tests demonstrate that the ultimate shear resistance increases as the section depth increases (see Figure 4.47). Such observations are to be expected because the area of shear interface would be increases as the section depth increases, higher shear stress would be transferred by the aggregates across the shear cracks, and as a result, a higher ultimate shear strength could be mobilised against shear failure.

However, when the ultimate shear stress is to be considered, it is observed that the ultimate shear stress of OPSC beams decreases as the section depth increases (see Figure 4.48). Such observations would be expected due to the fact that size effects occur in shear mechanism of OPSC specimens (See also Section 2.3).

Comparison with test results of NWC beams indicates less significant increase in the attainment of the ultimate shear resistance of OPSC beam specimens as the section depth increases (see Figure 4.49). That is, the ultimate shear resistance of NWC specimens (NWC5 to NWC2) increased by 42% as the overall section depth increases from 113 mm to 200 mm, while the shear resistance of OPSC specimens (12F to F1) increased only by 24% for the same increment of overall section depth. Such discrepancy is believed to be attributed to the lower aggregate strength found in Oil Palm kernel Shell (OPS) with respect to that in the normal aggregates. As a result, a

lower aggregate interlocking capacity could be mobilised, hence, resulting in a lower ultimate shear resistance.

4.3 Specimens cast with shear reinforcement

A total of eleven OPSC beam specimens and five NWC beam specimens cast with shear reinforcement were tested. These specimens were loaded with a pair of concentrated loads on top of the beam at designated distance(s), a , away from the supports, as shown in Figure 3.16 to 3.20 .

The observations made from tests, failure mechanisms and crack patterns, are presented from Figure 4.50 to Figure 4.60 and Figure 4.61 to Figure 4.65, for OPSC beam specimens and NWC beam specimens respectively. The failure loads of OPSC and NWC beam specimens are presented in Table 4.9 and Table 4.10 respectively. Detailed discussions on these observations are presented in the Sections 4.3.1 to 4.3.3 as follow.

4.3.1 Overall failure behaviour of OPSC and NWC beam specimens

It is observed from tests that, all the sixteen beam specimens cast with shear reinforcement failed in mode of shear compression failure, which is evident and foreseeable during failure. The systematically details of observations for the beams with shear reinforcement from the flexural cracks initiation until the occurrence of the shear failure are explained herein.

For all beam specimens, the formation of flexural cracks occurred prior to formation of shear cracks during testing, which is observed to initiate from mid-span bottom

fibre of the specimens, this has been as expected, to coincide with the maximum tensile stress. These appearances of flexural cracks were first noted from 28% to 37% of the ultimate failure loads for OPSC beam specimens (see Table 4.11), and from 36% to 46% for NWC beam specimens (see Table 4.12). The load-deflection curves are presented from Figure 4.66 to Figure 4.68 for OPSC beams and Figure 4.69 for NWC beams. However, it was observed that the inferred cracking load deflection curves occurred from 17% to 30% of the ultimate loads for OPSC beam specimens (see Table 4.11) and from 28% to 38% of the ultimate loads for NWC beam specimens (see Table 4.12). It is believed that the discrepancies noted between the observed and the inferred cracking loads were due to the formation of micro-cracks, which could not have been detected by the naked eye but can be visibly observed through the change of inclination angle on the load deflection curves.

Further analysis on the test results revealed that the formations of flexural cracks did not occur under loads having similar percentages to their ultimate failure loads. These discrepancies derived from the fact that the percentages for formation of flexural cracks were determined with respect to the ultimate shear failure loads (V_{ult}) instead of their flexural failure loads. That is, specimens failed in shear at higher ultimate failure loads have been casted with high flexural resistances (such as Specimens 5A, 5B, 5C), thus, appeared to have their flexural cracks formed at loads that are close to their ultimate shear failure loads, hence resulted in the high percentages. On the other hand, specimens failed in shear at lower ultimate failure loads have been casted with lower flexural resistance (such as specimens 3A, 3B and 3C), hence, appeared to have their flexural cracks formed at loads that are further away from the ultimate shear failure loads, hence resulting in the low percentages.

The implication is that the formations of flexural cracks are in fact independent to the formation of shear failure mechanism.

As the applied loads were further increased, the formation of shear cracks were observed to have appeared at the neutral axis of shear span vicinity, where shear reinforcement are provided. The shear cracks were observed to occur from 53% to 68% of the ultimate failure loads for OPSC beam specimens (see Table 4.11), and from 49% to 54% of the ultimate failure loads for NWC beam specimens (see Table 4.12). These inconsistencies deduced from the fact that, specimens which failed in shear at higher ultimate failure loads were loaded with span distance closer to the supports (such as specimens 4D, 4E, and NWCD), thus, the formation of shear cracks were observed to appear at loads that are close to their ultimate shear failure loads. On the other hand, specimens failed in shear at lower ultimate failure loads were loaded with span distances further from the supports (such as Specimens 4A, 4B, 4C, 3A, 3B, 3C, 5A, 5B, 5C, NWCA, NWCB, NWCC, and NWCE), therefore, the formation of shear cracks were observed to appear at loads that are far from their ultimate shear failure loads. The inference is that the formations of shear cracks are in fact subjected to the loading position, where higher percentage of shear cracks formation were observed in beams tested with low a/d ratio compared to high a/d ratio. After the formation of initial shear cracks at neutral axis section of the shear span vicinity, it was observed that the diagonal shear cracks propagated diagonally towards the loading positions and supports, respectively, which was as expected, to coincide with the maximum shear stresses where shear compression finally took place. It was observed that concrete crushes at the compression region of the beam where loading was applied. All specimens were observed to remain intact even after failure as the inclusion of shear reinforcement in the specimens would have formed a cage

with the presence of anchorage at both end of the beam, hence, keeping the specimens to be intact (see Figure 4.50 to Figure 4.65).

In view of crack mechanism, beams with shear reinforcements exhibit similar observations to those of beams without shear reinforcement (See Section 4.2.1). For OPSC specimens with shear reinforcement, two types of crack mechanisms were observed (see Figure 4.70 and 4.71) at the diagonal shear cracks: (1) cracks sheared through the OPS aggregates and (2) bond failure between cement paste and OPS aggregates in concrete (see Figure 4.37 for illustrations). Either one of these two cracking mechanisms observed from OPSC specimens depend on the natural alignment of OPS aggregates along shear cracks: (1) crack sheared through the OPS aggregates when OPS is inclined perpendicular to the diagonal shear crack and (2) bond failure between cement paste and OPS aggregates in concrete when OPS is inclined parallel to the diagonal shear cracks, as mentioned in Section 4.2.1 (See also Figure 4.37 for illustrations). Whilst for NWC specimens, the crack mechanism occurred through the cement paste (See Figure 4.70 and 4.71), which the shear cracks was observed to occur in between the normal aggregates (see also Figure 4.70 and 4.71).

4.3.2 Central deflection

The central deflection of all beam specimens were recorded after every increment of applied load. For every beam specimen cast with shear reinforcement, the load-deflection curves are plotted and presented in Figure 4.66 to Figure 4.68, and Figure 4.69, for OPSC beam specimens and NWC beam specimens, respectively.

In general, the curves exhibit similar load deflection behaviour among the specimens, that is, a linear elastic behaviour up to approximately half of the ultimate failure loads, and subsequently, the rate of increment in the applied loads decreases until failure occurs. The increases in the rate of deflection were due to the formation of flexural cracks at the mid-span bottom tension surface of the beam specimens.

A comparison between the actual cracking loads inferred from the load-deflection curves and the observed cracking loads are presented in Table 4.11 and Table 4.12 for OPSC beam specimens and NWC beam specimens, respectively. From these comparisons, it is observed that the inferred cracking loads were 2% to 12% and 3% to 18% lower than the observed flexural cracking loads for OPSC beam specimens and NWC beam specimens, respectively. It is believed that these discrepancies between the observed and the inferred cracking loads were due to the formation of flexural micro-cracks that could not have been detected by the naked eye but can be clearly observed via the change of inclination angle on the load deflection curves.

4.3.3 Ultimate Failure Loads

The ultimate failure loads of beam specimens were derived from the last recorded loads prior to failure. For beam specimens cast with shear reinforcement, the ultimate failure loads of specimens cast from OPSC and NWC are summarized and presented in Table 4.9 and Table 4.10, respectively. Among the sixteen beam specimens, eleven were casted from Oil Palm kernel Shell (OPSC) while the remaining five were casted from Normal aggregate Concrete (NWC).

Among the eleven OPSC beam specimens, three variables were considered in the tests (see Table 4.9); shear reinforcement spacing (SR), inclination angle of shear

cracks (PL) and concrete strength (CG). Of which, nine of the eleven OPSC beam specimens derived with results that addresses for more than one variables considered (see Table 4.9).

On the other hand, three identical variables were also considered among the five NWC beam specimens (see Table 4.10; shear reinforcement spacing (SR), inclination angle of shear cracks (PL), and concrete strength (CG). These NWC beams were designed and tested to form the basis (control samples) for the current research investigation.

In general, it is apparent that the load carrying capacities of both the OPSC and NWC beam specimens (cast with shear reinforcement) are influenced by the variables considered. Effects of the variables considered and their comparisons with control specimens are described in detail from Section 4.3.3.1 to 4.3.3.3.

4.3.3.1 Shear reinforcement spacing

Among the eleven OPSC beam specimens casted with shear reinforcement, nine beam specimens (see Table 4.13) were cast and tested to assess the effect of shear reinforcement spacing, s to the ultimate shear resistance. These nine OPSC beam specimens have been further subcategorized into: SR-CG26, SR-CG32 and SR-CG35; to take account for three concrete cube compressive strengths. The three concrete cube compressive strengths were: 25.8 N/mm² (category SR-CG26), 31.9 N/mm² (category SR-CG32) and 34.6 N/mm² (category SR-CG35).

From the test results shown in Figure 4.72, it is apparent that the ultimate shear resistance increases with the reduction of shear reinforcement spacing, s . Such

observations are to be expected, because when the shear reinforcement spacing reduces, the shear reinforcement ratio increases, and, hence, the shear force carried by the dowel action of shear reinforcement increases. That is, comparison to Specimen 3A from Figure 4.50, Specimen 5A from Figures 4.56 exhibited lower crack width which allowed for a better aggregate interlocking to be mobilised between the crack interfaces, and as a result, higher ultimate shear resistance was mobilised.

Comparisons with NWC beam specimens indicate that the ultimate shear resistance of OPSC beams are higher than the NWC beams for all the shear reinforcement spacing: 120 mm, 80 mm and 60 mm (see Figure 4.73). That is, the shear resistance of OPSC beam specimens (3B, 4B and 5B) are 3%, 10% and 7% higher compared to the NWC beam specimens (NWCC, NWCB and NWCA) for shear reinforcement spacing of 120 mm, 80 mm and 60 mm, respectively. Such discrepancy is believed to be attributed to the rougher shear surface observed from the OPSC beam specimen compared to NWC beam specimen(see Figure 4.70 and 4.71), where, a higher aggregate interlocking could be provided and resulted in higher shear resistance.

4.3.3.2 Inclination angle of shear cracks

Among the eleven OPSC beams casted with shear reinforcement, three specimens (see Table 4.9) were cast and tested to evaluate the effect of inclination angle of shear cracks θ (deg) to the ultimate shear resistance. These specimens have been categorized as PL (see Table 4.14). In general, it is apparent that from the observations made from tests indicate the ultimate shear resistance increases as the inclination angle of shear cracks (θ) increases (see Figure 4.74). Such observations are to be expected due to the fact that the shear span would have decreased as the

inclination angle of shear cracks increases, which in turn, allowed for a better aggregate interlocking to be mobilised, and hence, resulting in a higher shear resistance.

In comparison to NWC beam specimens, the test observations reveal that the rate of increase in the ultimate shear resistance of OPSC beam specimens as a result of the increases in the inclination angle of shear cracks, θ , are less pronounced (see Figure 4.75). That is, the shear resistance of NWC specimen (NWCB to NWCD) increased by 14% as the inclination angle of shear cracks, θ , increased from 39.8 degree to 51.8 degree, while the shear resistance of OPSC specimen (4B to 4E) increased only by 11% for the same increase in the inclination angle in shear cracks. However, in all cases, the OPSC beam specimens exhibited higher ultimate shear resistance compared to NWC specimens, that is, at inclination angle, $\theta = 39.8$ degree, the shear strength achieved by OPSC specimen (4B) is 11% higher than NWC specimen (NWCB) whilst at $\theta = 51$ degree, the shear strength achieved by OPSC specimen (4E) is 4% higher than NWC specimen (NWCD). Such discrepancy is believed to be attributed to the rougher shear surface observed from the OPSC specimen (see Figure 4.70 and 4.71), which in turn, provided with a higher aggregate interlocking, and as a result, a higher shear resistance were achieved.

4.3.3.3 Concrete strength

Among the eleven OPSC beam specimens casted with shear reinforcements, nine specimens (see Table 4.15) were casted and tested to evaluate the effect of concrete cube compressive strength (f_{cu}) to the ultimate shear resistance. These specimens

have been further subcategorised into: CG-S60, CG-S80 and CG-S120 to account for three shear reinforcement spacing: 60 mm, 80 mm and 120 mm, respectively.

In general, observations from test indicate that the ultimate shear resistance increases with the concrete cube compressive strength (see Figure 4.76). Such observations are to be expected due to the fact that as the concrete compressive strength increases, the concrete tensile strength would also be increased, which in turn, the bond between the cement paste and OPS aggregate increases and hence, delayed the rupture of concrete and resulting in higher shear resistance. In addition, in view of shear transfer mechanism, the increment of concrete strength would enhance the dowel capacity of the beams and thus, smaller shear cracks were observed in OPSC beams (see Specimen 4A in figure 4.53 in comparison to Specimen 3A in Figure 3.50). Hence, this leads to higher shear resistance from the aggregate interlock capacity and compression zone capacity and resulting in a higher shear resistance of OPSC beams.

Comparisons with the NWC beam specimens (NWCB and NWCE) reveal that the increase in ultimate shear resistance of OPSC beam specimens (from 4B and 4C) as the concrete compressive strength increased from 31 N/mm² to 35 N/mm² are more pronounced (see Figure 4.77). That is, the ultimate shear resistance of OPSC beam specimens (4B and 4C) increased by 15.19% as the concrete strength increases, while the shear resistance of NWC beam specimens (NWCB and NWCC) increased only by 13.33%. Such discrepancies are believed to be attributed to the rougher shear surface observed from the OPSC specimen (see Figure 4.70 and 4.71), which in turn, provide with higher lower aggregate interlocking ability, thus, a higher ultimate shear resistance would be mobilised.

4.4 Summary

For OPSC beam specimens without shear reinforcement, three distinct shear failure mechanisms have been observed from the tests, which are the shear compression mechanism, the diagonal tension mechanism and the shear mechanism. Whilst for NWC beam specimens without shear reinforcement, two distinct shear failure mechanisms have been observed from the tests, which are the shear compression mechanism and the shear mechanism.

The shear compression mechanism is observed for both OPSC and NWC beam specimens tested at shear span to effective depth ratio, $a/d < 2.5$, which the formation of shear cracks was initiated from the support and propagated through the shear span towards the loading position before ultimate failure occurred by crushing of concrete at the compression zone.

The diagonal tension mechanism is observed for OPSC beam specimens as there are two specimens casted with longitudinal steel ratio, $\rho = 0.75\%$ and tested at shear span to effective depth ratio, $a/d \geq 2.5$. The formation of shear cracks was initiated from the flexural cracks at the bottom of the beam and propagated towards the loading position prior to failure by splitting of the beam occurred along the longitudinal tensile steel reinforcement towards the support.

The shear mechanism is observed for both OPSC and NWC beam specimens casted with longitudinal steel ratio, $\rho \geq 1.08\%$ and tested at shear span to effective depth ratio, $a/d < 2.5$. The formation of shear cracks is observed to initiate from the support and propagated through the shear span to the loading position before ultimate failure occurred by splitting of the beam occurred along the longitudinal tensile steel reinforcement towards the support.

Whilst for OPSC and NWC beam specimens with shear reinforcement, shear compression failure mechanism have been observed from the tests, which shear cracks appeared at the Neutral Axis of the beam and subsequently, propagated towards the support and loading position, respectively, before shear failure occurred by crushing of concrete at the compression zone at the loading position. However, it is observed that the beam remained intact due to the presence of shear reinforcements in the beams, which formed a cage to prevent the beam from separated.

Comparisons were carried out on the ultimate shear failure capacities and the shear failure mechanisms between OPSC beams and NWC beams cast with and without shear reinforcement, respectively. It was found that the ultimate shear strength of OPSC beams and NWC beams is comparable for the parameters: effective depth (for beams without shear reinforcement), and shear reinforcement spacing and inclination angle of shear cracks (for beams with shear reinforcements). However, discrepancies were observed in ultimate shear strength between the OPSC beams and NWC beams for the parameters: span to depth ratio, longitudinal steel ratio and concrete strength (for beams without shear reinforcement) and concrete strength (for beams with shear reinforcement).

In view on the theoretical models and the design models for OPSC beams cast with and without shear reinforcement, it was undefined whether the current theoretical models based upon plastic approach and the design models: BS8110 Code and Eurocode 2 based upon upper bound approach are applicable for the ultimate shear strength predictions of OPSC beams. Hence, detailed studies were carried out on OPSC beam with and without shear reinforcement, respectively in Chapter 5 for theoretical plastic models, Chapter 6 for BS8110 design models and Chapter 7 for

Eurocode 2 (EC2) design model. Subsequently, this results in other contributions in this research, where a model has been proposed each for OPSC beam with and without shear reinforcement in Chapter 5, 6, and 7, respectively.

Table 4.1 Test results of OPSC beam specimens cast without shear reinforcement.

Specimen No.	Section width, b (mm)	Section effective depth, d (mm)	Shear span to effective depth ratio, a/d	Cube strength, f_{cu} (N/mm ²)	Steel ratio, ρ (%) $= \frac{A_s}{b h}$	Ultimate Failure Load V_{OPSC} (kN)	Variables considered
10A	105	170	2.50	30.05	0.75	18.95	LR, CS
S1	105	170	2.50	34.82	0.75	21.05	LR, CS
12A	105	169	1.00	31.03	1.08	54.73	SP, LR
12B	105	169	1.50	31.03	1.08	40.00	SP
12C	105	169	2.50	31.03	1.08	27.37	SP, LR, CS
12D	105	169	3.00	31.03	1.08	25.26	SP, LR
12E	105	169	2.50	39.20	1.08	31.58	CS
12F	105	82	2.89	32.46	1.91	26.31	HT
16A	105	167	1.00	26.14	1.92	56.80	SP, LR
16B	105	167	1.50	26.14	1.92	42.10	SP, LR
16C	105	167	2.50	26.14	1.92	29.50	SP, LR, CS
16D	105	167	3.00	26.14	1.92	26.32	SP, LR
16E	105	167	2.50	32.46	1.92	35.79	LR, HT
20A	105	165	1.00	24.23	2.99	73.68	SP, LR
20B	105	165	1.50	24.23	2.99	52.63	SP, LR
20C	105	165	2.50	24.23	2.99	33.68	SP, LR, CS
20D	105	165	3.00	24.23	2.99	27.37	SP, LR
20E	105	165	2.50	28.00	2.99	35.79	LR, CS
AD1	105	167	1.00	32.00	1.92	58.19	SP, LR
AD2	105	167	3.00	32.00	1.92	32.33	SP, LR
F1	105	167	2.50	32.00	1.92	32.67	SP, LR, CS
F2	105	167	2.50	40.10	1.92	47.41	CS
H2	105	278	2.36	32.46	1.91	52.53	HT
S2	105	167	2.50	35.70	1.92	36.64	CS

Table 4.2 Test results of NWC beams cast without shear reinforcement.

Specimen No.	Section width b (mm)	Overall section depth h (mm)	Shear span to effective depth Ratio a/d	Cube compressive strength f_{cu} (N/mm ²)	Steel ratio ρ (%) $= \frac{A_s}{b h}$	NWC Ultimate Failure Load V_{NWC} (kN)	Compared with OPSC specimen	Variable considered
NWC1	105	200	1	33.00	1.92	71.57	AD1	SP
NWC2	105	200	2.5	33.00	1.92	35.79	F1	SP, CS, HT
NWC3	105	200	2.5	29.00	1.92	33.69	16C	LR, CS
NWC4	105	200	2.5	29.00	2.99	52.63	20E	LR
NWC5	105	113	2.5	33.00	1.91	25.26	12F	HT

Table 4.3 Cracking load of OPSC beam specimens cast without shear reinforcement.

Specimen No.	$V_{ultimate}$ (kN)	V_{crack} (kN) Inferred	$V_{flexural\ crack}$ (kN) Observed	$V_{shear\ crack}$ (kN) Observed
10A	18.95	2.11 11%	6.32 33%	10.53 56%
S1	21.05	2.11 10%	4.21 20%	12.63 60%
12A	54.73	10.53 19%	16.84 31%	33.68 62%
12B	40.00	6.32 16%	12.63 32%	31.58 79%
12C	27.37	4.21 15%	8.42 31%	5.26 92%
12D	25.26	10.53 42%	16.84 67%	23.16 92%
12E	31.58	8.42 27%	10.53 33%	25.26 80%
12F	26.31	10.53 40%	11.58 44%	12.63 48%
16A	56.80	10.53 19%	14.74 26%	35.77 63%
16B	42.10	18.95 45%	25.25 60%	33.68 80%
16C	29.50	6.32 21%	8.42 29%	21.05 71%
16D	26.32	6.32 24%	8.42 32%	25.26 97%
16E	35.79	8.42 24%	10.53 29%	31.58 88%
20A	61.05	21.05 35%	-	48.15 79%
20B	52.63	27.37 52%	40.00 76%	31.58 60%
20C	33.68	4.21 13%	12.63 38%	27.37 81%
20D	27.37	6.32 23%	12.63 46%	25.26 92%
20E	35.79	17.74 50%	-	31.58 88%
AD1	58.19	10.53 18%	14.74 25%	37.89 65%
AD2	32.33	21.05 65%	25.24 78%	27.37 85%
F1	32.67	8.42 26%	12.63 39%	25.26 77%
F2	47.41	8.42 18%	12.63 27%	27.37 58%
H2	52.53	25.26 48%	27.37 52%	29.47 56%
S2	36.64	6.32 17%	12.63 34%	33.68 92%

Table 4.4 Cracking load of NWC beam specimens cast without shear reinforcement.

Specimen No.	$V_{ultimate}$ (kN)	V_{rack} (kN) Inferred	$V_{flexural\ crack}$ (kN) Observed	$V_{shear\ crack}$ (kN) Observed
NWC1	71.57	42.1 59%	44.21 62%	48.42 68%
NWC2	35.79	8.42 24%	12.63 35%	25.26 71%
NWC3	33.69	14.74 44%	16.84 50%	23.16 69%
NWC4	52.63	6.32 12%	10.53 20%	31.58 60%
NWC5	25.26	6.32 25%	8.42 33%	16.84 66%

Table 4.5 Span to effective depth ratio, a/d for OPSC beam specimens cast without shear reinforcement.

Category SP	Specimen no.	Shear span to effective depth ratio, a/d	Concrete strength f_{cu} (N/mm ²)	Steel ratio ρ (%) $= \frac{A_s}{b h}$	Ultimate Failure Load V_{OPSC} (kN)	$\frac{V_{OPSC}}{b d}$ (N/mm ²)
SP-LR12B	12A	1.0	31.03	1.08	73.68	4.15
	12B	1.5	31.03	1.08	40.00	2.25
	12C	2.5	31.03	1.08	27.37	1.54
	12D	3.0	31.03	1.08	25.26	1.42
SP-LR16A	AD1 ⁸	1.0	32.00	1.92	58.19	3.32
	F1	2.5	32.38	1.92	32.67	1.86
	AD2 ⁸	3.0	32.00	1.92	32.33	1.84
SP-LR16B	16A	1.0	26.14	1.92	56.80	3.24
	16B	1.5	26.14	1.92	42.10	2.40
	16C	2.5	26.14	1.92	29.50	1.68
	16D	3.0	26.14	1.92	26.32	1.50
SP-LR20A	20A	1.0	24.23	2.99	73.68	4.25
	20B	1.5	24.23	2.99	52.63	3.04
	20C	2.5	24.23	2.99	33.68	1.94
	20D	3.0	24.23	2.99	27.37	1.58

Table 4.6 Longitudinal steel reinforcement, ρ for OPSC beam specimens cast without shear reinforcement.

Category LR	Specimen no.	Shear span to effective depth ratio, a/d	Concrete strength f_{cu} (N/mm ²)	Steel ratio ρ (%) $= \frac{A_s}{b h}$	Ultimate Failure Load V_{OPSC} (kN)	$\frac{V_{OPSC}}{b d}$ (N/mm ²)
LR-SP1A	20A	1.0	24.23	2.99	73.68	4.25
	16A	1.0	26.14	1.92	56.80	3.24
LR-SP1B	12A	1.0	31.03	1.08	54.73	3.08
	AD1	1.0	32.00	1.92	58.19	3.32
LR-SP1.5A	20B	1.5	24.23	2.99	52.63	3.04
	16B	1.5	26.14	1.92	42.10	2.40
LR-SP2.5A	20C	2.5	24.23	2.99	33.68	1.94
	16C	2.5	26.14	1.92	29.50	1.68
LR-SP2.5B	10A	2.5	30.05	0.75	18.95	1.06
	S1	2.5	34.82	1.08	21.05	1.19
	12C	2.5	31.03	1.08	27.37	1.54
	16E	2.5	35.70	1.92	35.79	2.04
	F1	2.5	32.38	1.92	32.67	1.86
	20E	2.5	24.23	2.99	35.79	2.07
LR-SP3A	20D	3.0	26.14	2.99	27.37	1.58
	16D	3.0	31.03	1.92	26.32	1.50
LR-SP3B	12D	3.0	32.00	1.08	25.26	1.42
	AD2	3.0	24.23	1.92	32.33	1.84

Table 4.7 Cube concrete strength, f_{cu} for OPSC beam specimens cast without shear reinforcement.

Category CS	Specimen no.	Shear span to effective depth ratio, a/d	Concrete strength f_{cu} (N/mm ²)	Steel ratio ρ (%) $= \frac{A_s}{b h}$	Ultimate Failure Load V_{OPSC} (kN)	$\frac{V_{OPSC}}{b d}$ (N/mm ²)
CS-LR10	10A	2.5	30.05	0.75	18.95	1.06
	S1	2.5	34.83	0.75	21.05	1.18
CS-LR12	12C	2.5	31.03	1.08	27.37	1.54
	12E	2.5	39.20	1.08	31.58	1.78
CS-LR16	16C	2.5	26.14	1.92	29.50	1.68
	F1 ⁸	2.5	32.38	1.92	32.67	1.86
	S2	2.5	35.70	1.92	36.64	2.09
	F2 ⁸	2.5	40.10	1.92	47.41	2.70
CS-LR20	20C	2.5	24.23	2.99	33.68	1.94
	20E	2.5	28.00	2.99	35.79	2.07

Table 4.8 Overall sectional depth, h for OPSC beam specimens cast without shear reinforcement.

Category HT	Specimen no.	Overall section depth, h (mm)	Shear span to overall height ratio, a/h	Concrete strength f_{cu} (N/mm ²)	Reinforcement ratio ρ (%) $= \frac{A_s}{b h}$	Ultimate Failure Load V_{OPSC} (kN)	$\frac{V_{OPSC}}{b d}$ (N/mm ²)
HT	12F	113	2.10	32.46	1.91	26.31	3.06
	16E	200	2.10	32.46	1.92	35.79	2.04
	H2	313	2.09	32.46	1.92	52.53	1.80

Table 4.9 Test results of OPSC beam specimens cast with shear reinforcement.

Specimen no.	Cube concrete strength, f_{cu} (N/mm ²)	Shear reinforcement spacing, s (mm)	Angle, θ (degree)	Ultimate Failure Load V_{OPSC} (kN)	Assigned to variable
3A	25.79	120	39.8	75.78	CG, SR
3B	31.93	120	39.8	88.41	CG, SR
3C	34.60	120	39.8	92.62	CG, SR
4A	25.79	80	39.8	79.99	CG, SR
4B	31.93	80	39.8	94.73	CG, SR, PL
4C	34.60	80	39.8	107.36	CG, SR
5A	25.79	60	39.8	88.41	CG, SR
5B	31.93	60	39.8	107.36	CG, SR
5C	34.60	60	39.8	119.99	CG, SR
4D	30.15	80	45.0	101.04	PL
4E	30.15	80	51.3	105.25	PL

Table 4.10 Tests results of NWC beam specimens cast with shear reinforcement.

Specimen no.	Cube Concrete strength, f_{cu} (N/mm ²)	Shear reinforcement spacing, s (mm)	Angle, θ (degree)	Ultimate Failure Load V_{NWC} (kN)	Compared with OPSC specimen	Variable considered
NWCA	30.61	120	39.8	82.10	3B	SR
NWCB	30.61	80	39.8	88.41	4B	CG, SR, PL
NWCC	30.61	60	39.8	99.99	5B	SR
NWCD	30.61	80	51.3	101.04	4E	PL
NWCE	35.00	80	39.8	98.94	4C	CG

Table 4.11 Cracking load of OPSC beam specimens cast with shear reinforcement.

Specimen no.	$V_{ultimate}$ (kN)	V_{crack} (kN) Inferred	$V_{flexural\ crack}$ (kN) Observed	$V_{shear\ crack}$ (kN) Observed
3A	75.78	12.63 17%	21.05 28%	42.10 56%
3B	88.41	18.95 21%	27.37 31%	54.73 62%
3C	92.62	16.84 18%	25.26 27%	48.42 52%
4A	79.99	24.21 30%	25.26 32%	46.31 58%
4B	94.73	25.26 27%	29.47 31%	54.73 58%
4C	107.36	29.47 27%	31.58 29%	56.84 53%
5A	88.41	25.26 28%	29.47 33%	56.63 64%
5B	107.36	27.37 25%	33.68 31%	56.84 53%
5C	119.99	23.16 20%	37.89 32%	63.15 53%
4D	101.04	27.37 27%	31.58 31%	67.36 67%
4E	105.25	31.58 30%	37.89 37%	71.57 68%

Table 4.12 Cracking load of NWC beam specimens cast with shear reinforcement.

Specimen no.	$V_{ultimate}$ (kN)	V_{crack} (kN) Inferred	$V_{flexural\ crack}$ (kN) Observed	$V_{shear\ crack}$ (kN) Observed
NWCA	82.10	23.16 28%	37.89 46%	40.00 49%
NWCB	88.41	29.47 33%	31.58 36%	46.31 52%
NWCC	99.99	37.89 38%	44.21 44%	50.52 51%
NWCD	101.04	35.79 35%	-	54.72 54%
NWCE	98.94	37.89 38%	44.21 45%	50.52 51%

Table 4.13 Shear reinforcement spacing, s for OPSC beam specimens cast with shear reinforcement.

Category SR	Specimen no.	Spacing of shear reinforcement, s (mm)	Cube concrete strength, f_{cu} (N/mm ²)	Angle, θ (deg)	Ultimate Failure Load V_{OPSC} (kN)	$\frac{V_{OPSC}}{b d}$ (N/mm ²)
SR-CG26	5A	60	25.79	39.8	88.41	5.36
	4A	80	25.79	39.8	79.99	4.48
	3A	120	25.79	39.8	75.78	4.25
SR-CG32	5B	60	31.93	39.8	107.36	6.51
	4B	80	31.93	39.8	94.73	5.31
	3B	120	31.93	39.8	88.41	4.95
SR-CG35	5C	60	34.60	39.8	119.99	7.28
	4C	80	34.60	39.8	107.36	6.01
	3C	120	34.60	39.8	92.62	5.19

Table 4.14 Inclination angle of shear cracks, θ for OPSC beam specimens cast with shear reinforcement.

Category PL	Specimen no.	Cube concrete strength, f_{cu} (N/mm ²)	Shear span, a (mm)	Angle, θ (deg)	Ultimate Failure Load V_{OPSC-s} (kN)	$\frac{V_{OPSC-s}}{b d}$ (N/mm ²)
PL	4B	31.93	240	39.8	94.73	5.31
	4D	30.15	200	45.0	101.04	5.66
	4E	30.15	160	51.3	105.25	5.90

Table 4.15 **Cube concrete strength, f_{cu} (N/mm²) for OPSC beam specimens cast with shear reinforcement.**

Category CG	Specimen no.	Spacing of shear reinforcement, s (mm)	Concrete strength, f_{cu} (N/mm ²)	Angle, θ (deg)	Ultimate Failure Load V_{OPSC} (kN)	$\frac{V_{OPSC}}{b d}$ (N/mm ²)
CG-S60	5A	60	25.79	39.8	88.41	5.36
	5B	60	31.93	39.8	107.36	6.51
	5C	60	34.60	39.8	119.99	7.28
CG-S80	4A	80	25.79	39.8	79.99	4.48
	4B	80	31.93	39.8	94.73	5.31
	4C	80	34.60	39.8	107.36	6.01
CG-S120	3A	120	25.79	39.8	75.78	4.25
	3B	120	31.93	39.8	88.41	4.95
	3C	120	34.60	39.8	92.62	5.19

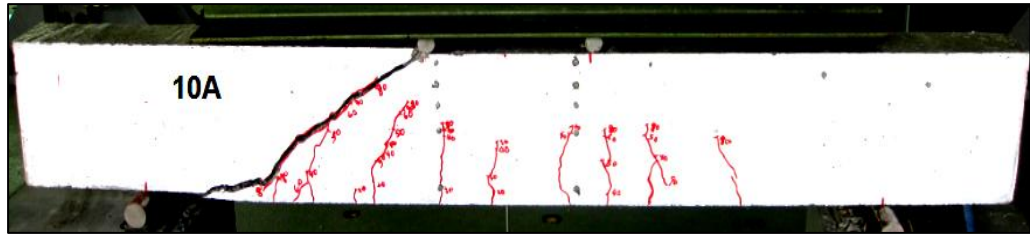


Figure 4.1 Failure mechanism of OPSC beam cast without shear reinforcement, 10A.

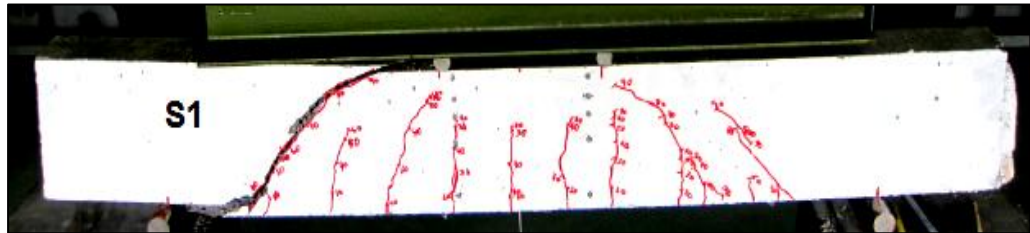


Figure 4.2 Failure mechanism of OPSC beam cast without shear reinforcement, S1.

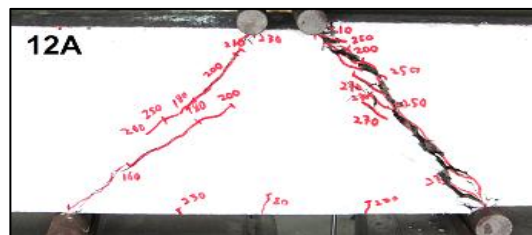


Figure 4.3 Failure mechanism of OPSC beam cast without shear reinforcement, 12A.



Figure 4.4 Failure mechanism of OPSC beam cast without shear reinforcement, 12B.

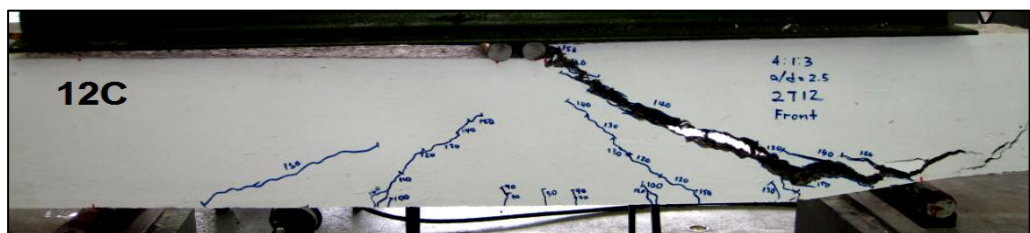


Figure 4.5 Failure mechanism of OPSC beam cast without shear reinforcement, 12C.



Figure 4.6 Failure mechanism of OPSC beam cast without shear reinforcement, 12D.

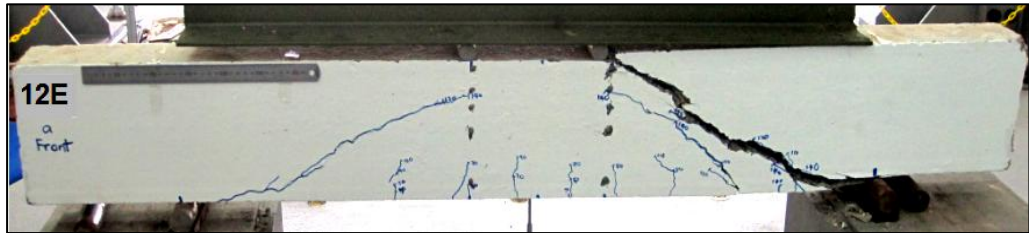


Figure 4.7 Failure mechanism of OPSC beam cast without shear reinforcement, 12E.



Figure 4.8 Failure mechanism of OPSC beam cast without shear reinforcement, 12F.

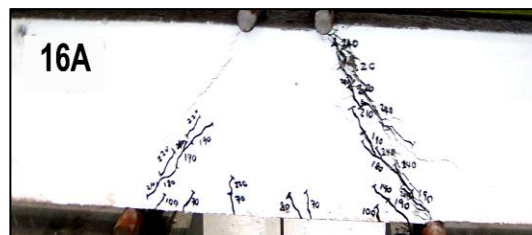


Figure 4.9 Failure mechanism of OPSC beam cast without shear reinforcement, 16A.

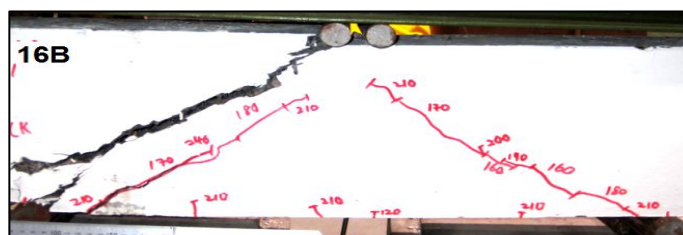


Figure 4.10 Failure mechanism of OPSC beam cast without shear reinforcement, 16B.

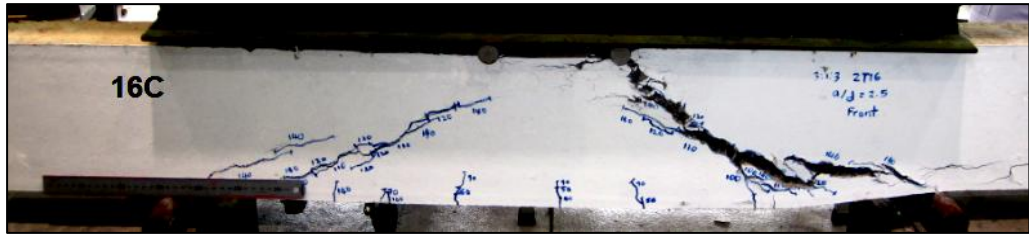


Figure 4.11 Failure mechanism of OPSC beam cast without shear reinforcement, 16C.



Figure 4.12 Failure mechanism of OPSC beam cast without shear reinforcement, 16D.

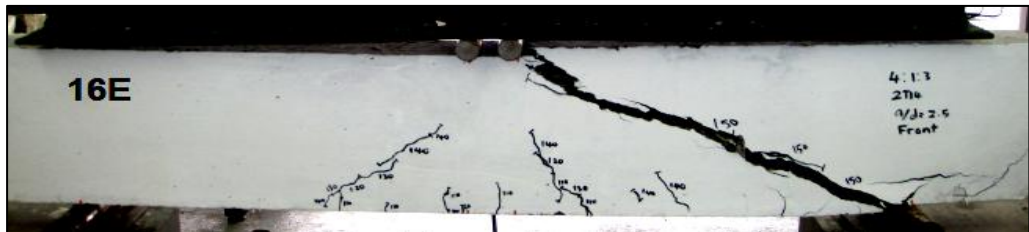


Figure 4.13 Failure mechanism of OPSC beam cast without shear reinforcement, 16E.

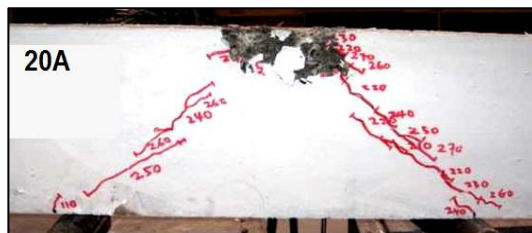


Figure 4.14 Failure mechanism of OPSC beam cast without shear reinforcement, 20A.

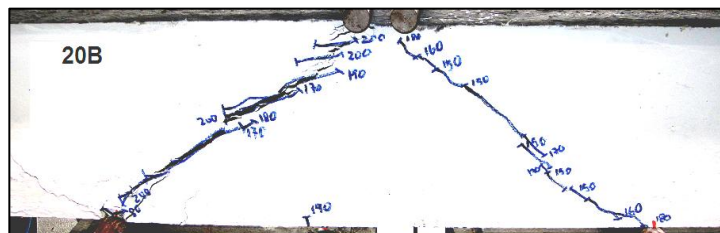


Figure 4.15 Failure mechanism of OPSC beam cast without shear reinforcement, 20B.

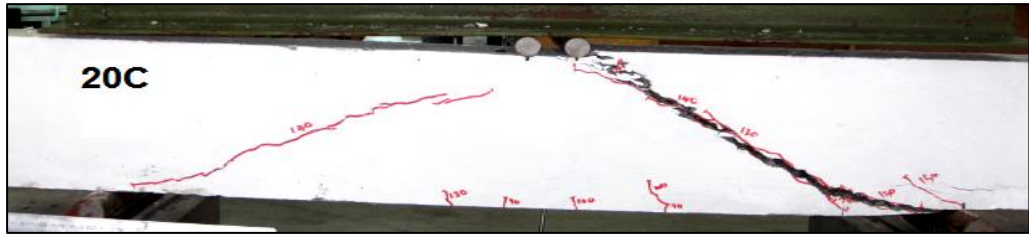


Figure 4.16 Failure mechanism of OPSC beam cast without shear reinforcement, 20C.



Figure 4.17 Failure mechanism of OPSC beam cast without shear reinforcement, 20D.

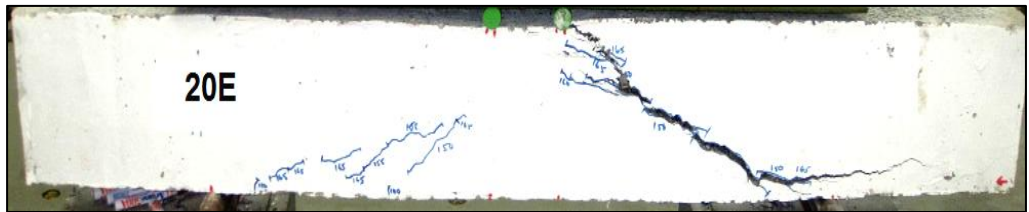


Figure 4.18 Failure mechanism of OPSC beam cast without shear reinforcement, 20E.



Figure 4.19 Failure mechanism of OPSC beam cast without shear reinforcement, AD1.



Figure 4.20 Failure mechanism of OPSC beam cast without shear reinforcement, AD2.

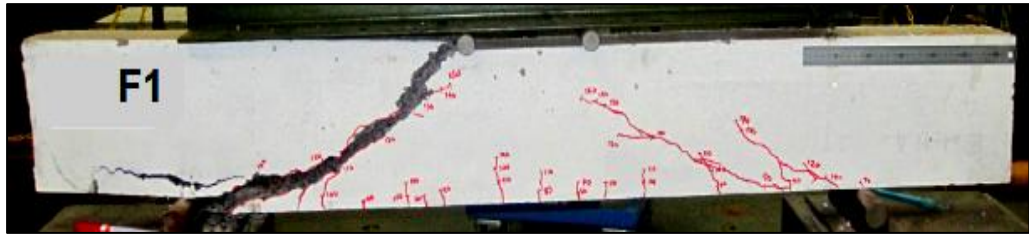


Figure 4.21 Failure mechanism of OPSC beam cast without shear reinforcement, F1.



Figure 4.22 Failure mechanism of OPSC beam cast without shear reinforcement, F2.

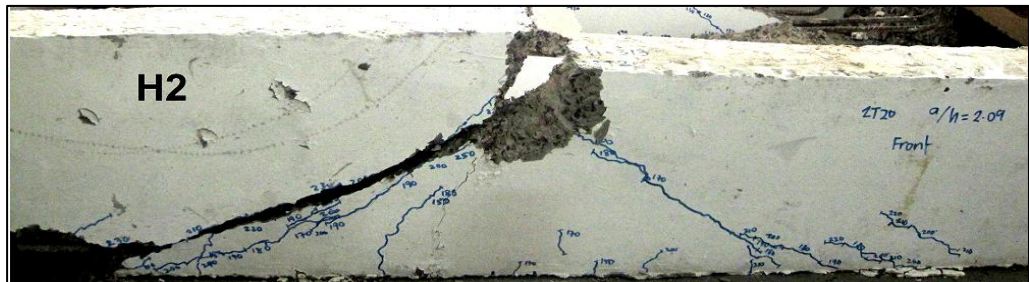


Figure 4.23 Failure mechanism of OPSC beam cast without shear reinforcement, H2.



Figure 4.24 Failure mechanism of OPSC beam cast without shear reinforcement, S2.

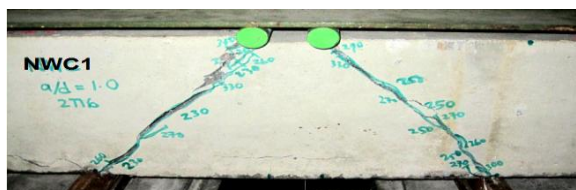


Figure 4.25 Failure mechanism of NWC beam cast without shear reinforcement, NWC1.

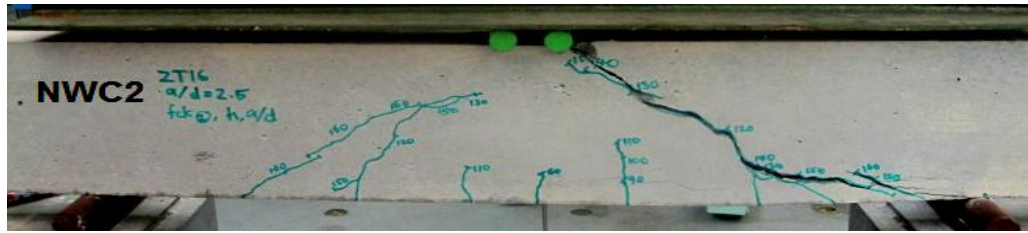


Figure 4.26 Failure mechanism of NWC beam cast without shear reinforcement, NWC2.

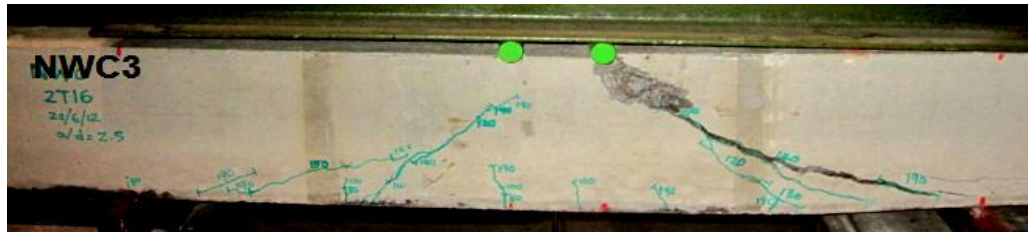


Figure 4.27 Failure mechanism of NWC beam cast without shear reinforcement, NWC3.

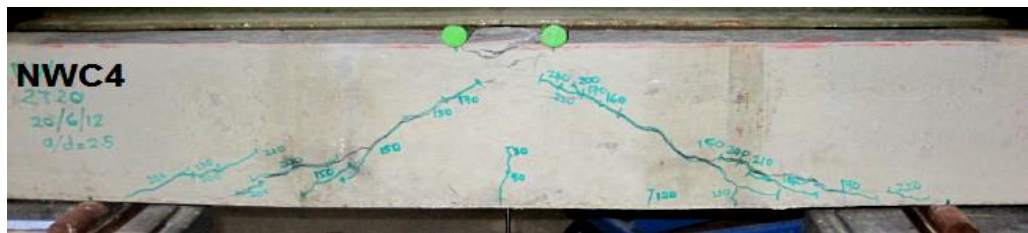


Figure 4.28 Failure mechanism of NWC beam cast without shear reinforcement, NWC4.

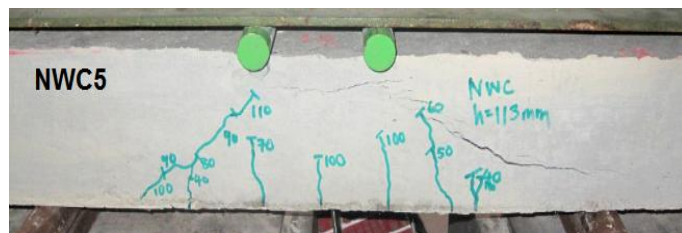


Figure 4.29 Failure mechanism of NWC beam cast without shear reinforcement, NWC5.

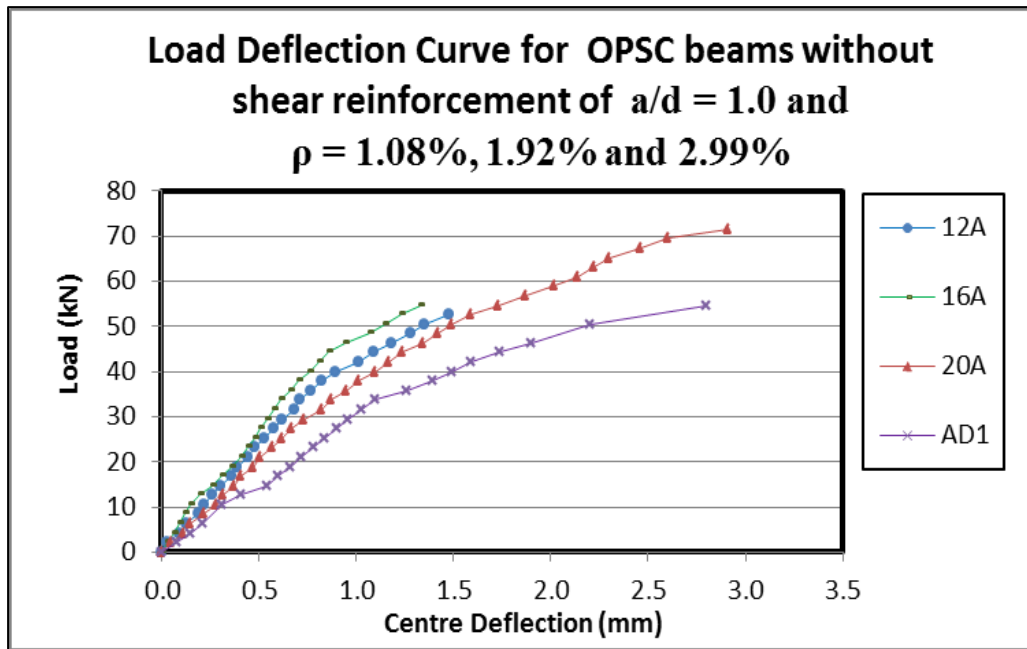


Figure 4.30 Load (kN) vs Central deflection (mm) for OPSC beam specimens cast without shear reinforcement of $a/d = 1$ and $\rho = 1.08\%$, 1.92% and 2.99% .

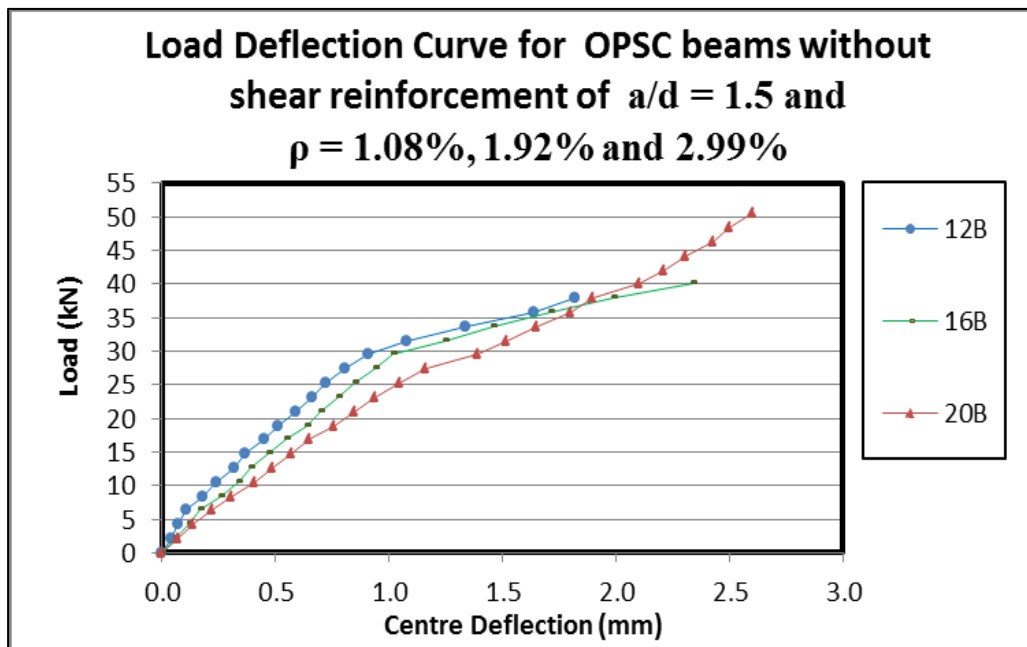


Figure 4.31 Load (kN) vs Central deflection (mm) for OPSC beam specimens cast without shear reinforcement of $a/d = 1.5$ and $\rho = 1.08\%$, 1.92% and 2.99% .

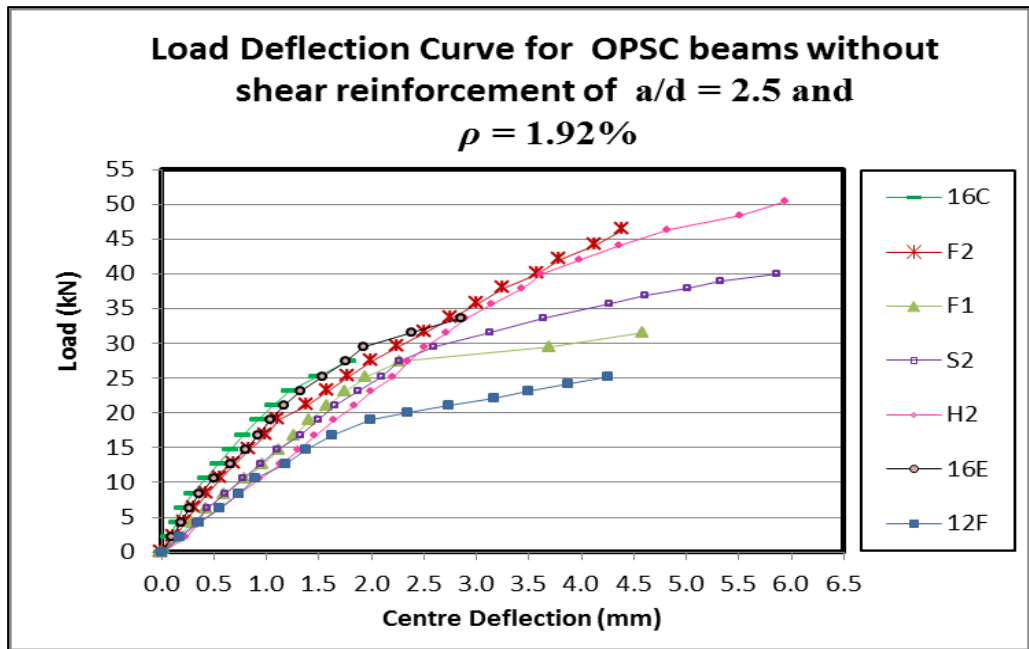


Figure 4.32 Load (kN) vs Central deflection (mm) for OPSC beam specimens cast without shear reinforcement of $a/d = 2.5$ and $\rho = 1.92\%$.

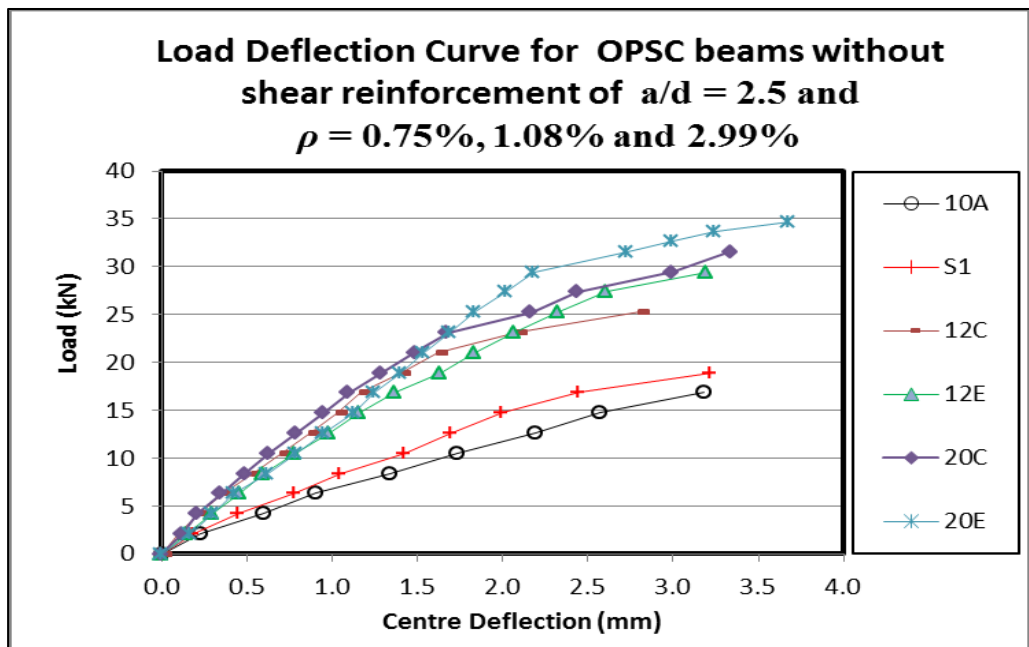


Figure 4.33 Load (kN) vs Central deflection (mm) for OPSC beam specimens cast without shear reinforcement of $a/d = 2.5$ and $\rho = 0.75\%$, 1.08% , and 2.99% .

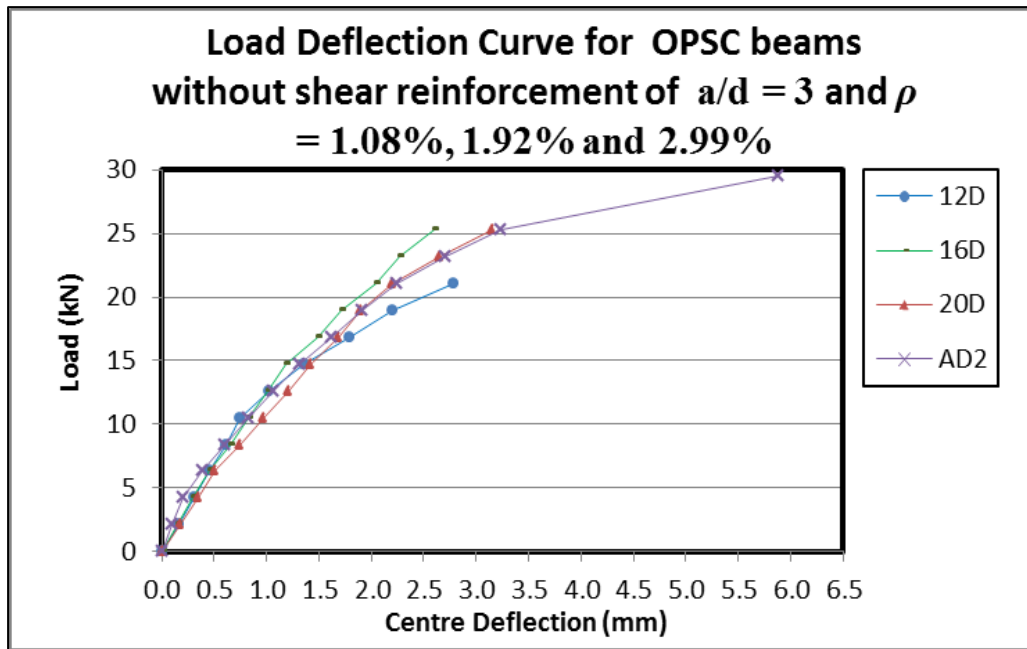


Figure 4.34 Load (kN) vs Central deflection (mm) for OPSC beam specimens cast without shear reinforcement of $a/d = 3$ and $\rho = 1.08\%$, 1.92% and 2.99% .

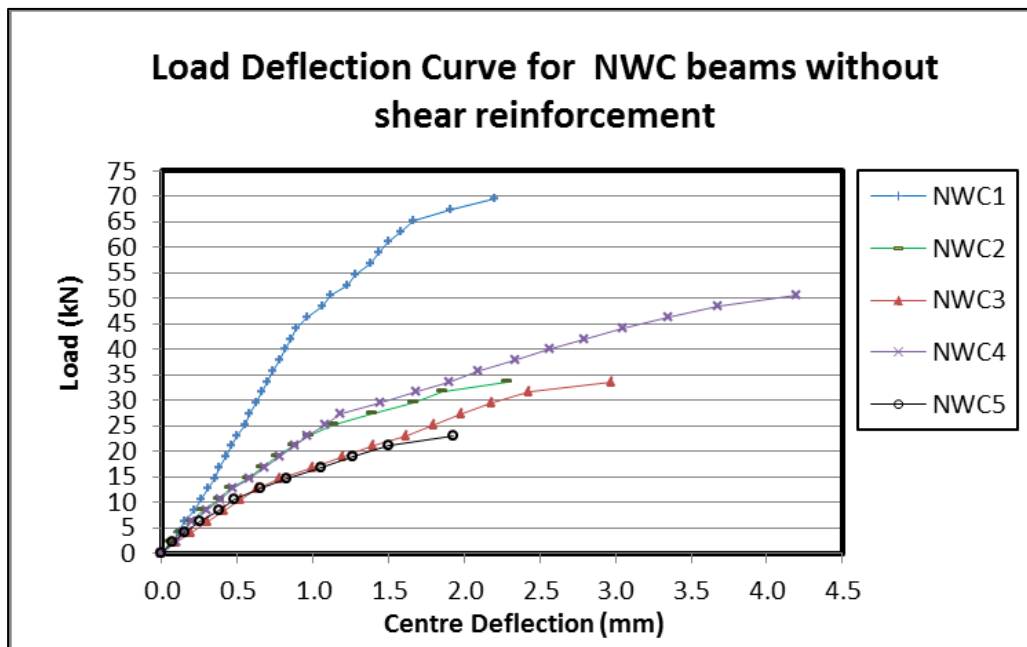


Figure 4.35 Load (kN) vs Central deflection (mm) for NWC beam specimens cast without shear reinforcement.

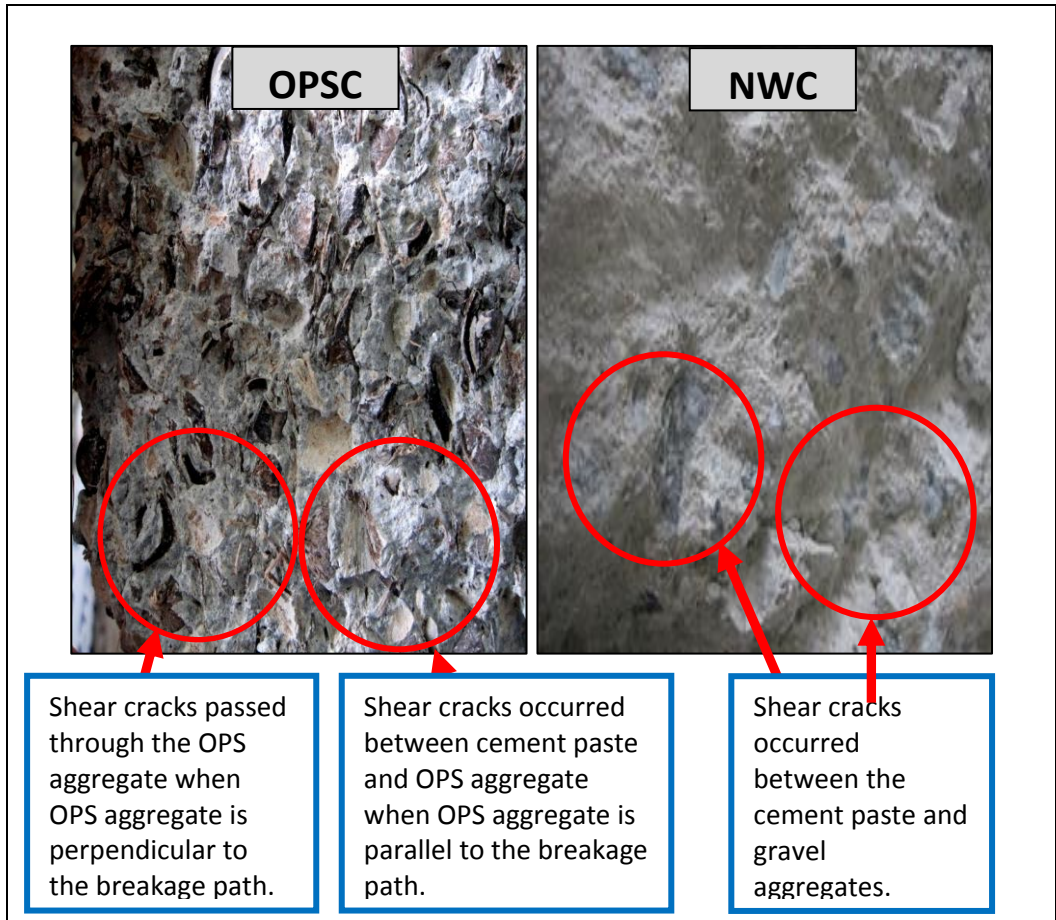


Figure 4.36 Surface texture of diagonal shear cracks interface of OPSC and NWC beams cast without shear reinforcement (Sectional View).

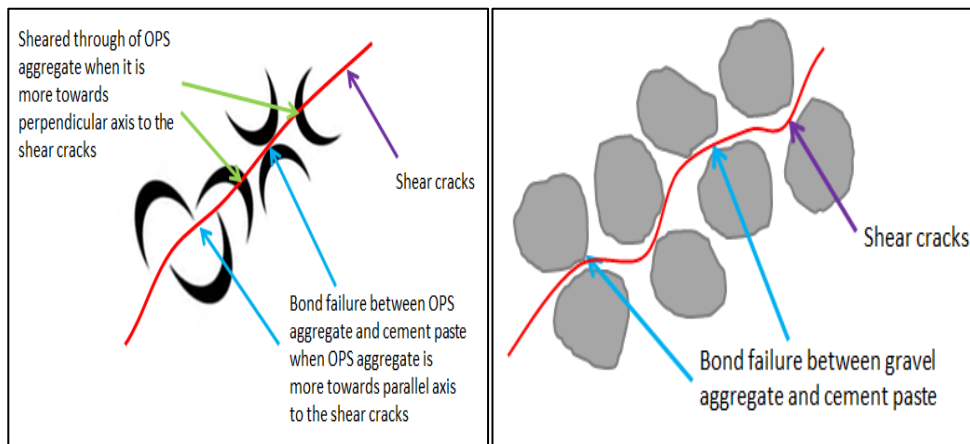


Figure 4.37 Diagonal shear cracks of OPSC and NWC beams cast without shear reinforcement (Side view).

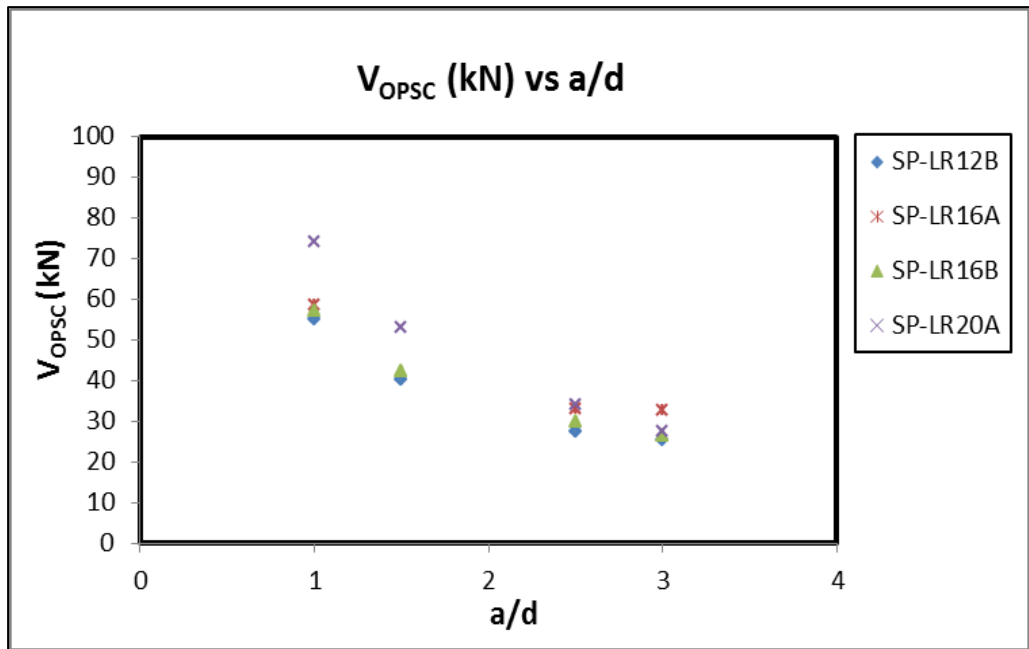


Figure 4.38 V_{OPSC} (kN) vs Shear span to effective depth ratio, a/d for OPSC beam specimens cast without shear reinforcement.

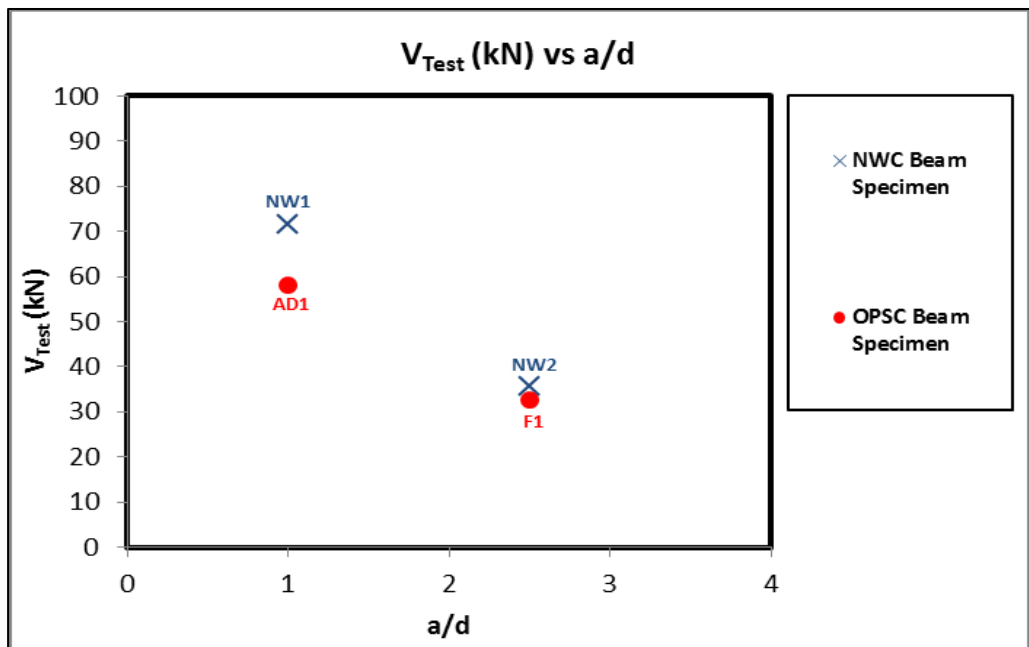


Figure 4.39 V_{Test} (kN) vs Shear span to effective depth ratio, a/d for OPSC and NWC beam specimens cast without shear reinforcement.

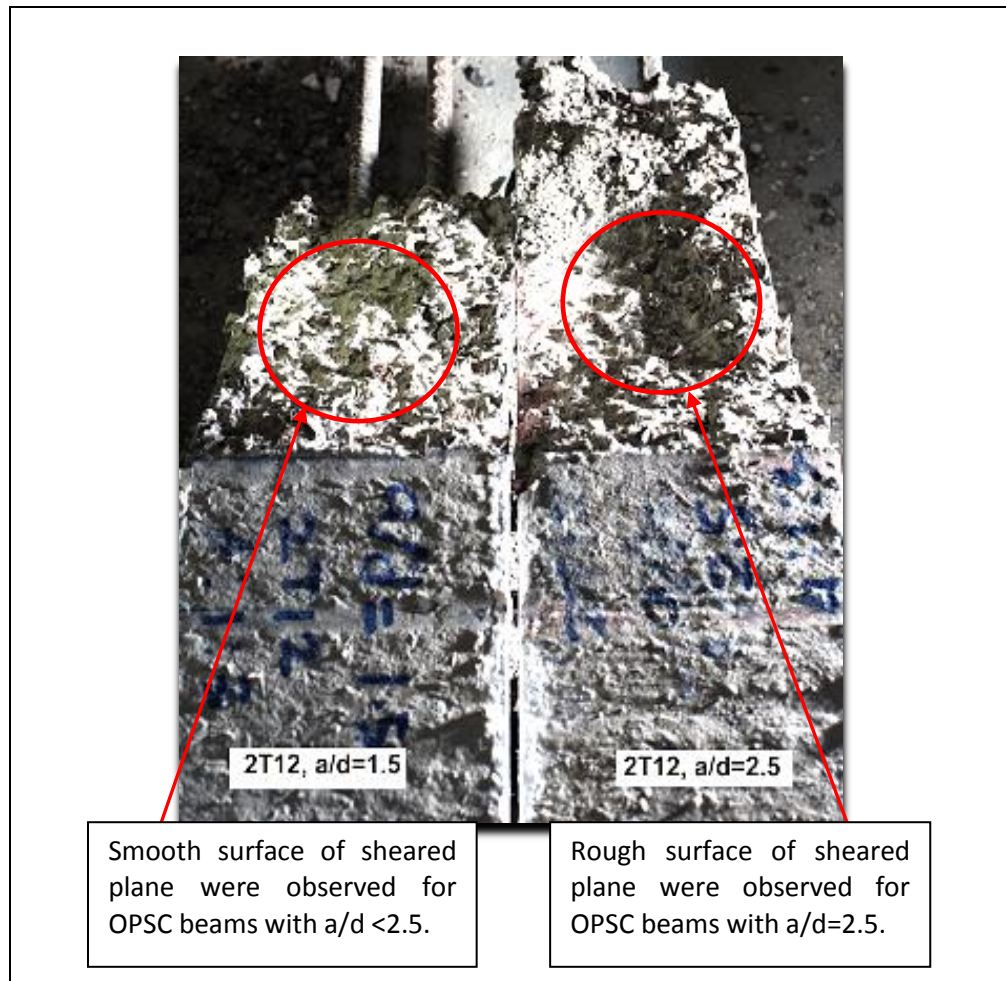


Figure 4.40 Surface texture of diagonal shear interface of OPSC beams cast without shear reinforcement tested at $a/d=1.5$ and $a/d=2.5$ (Sectional view).

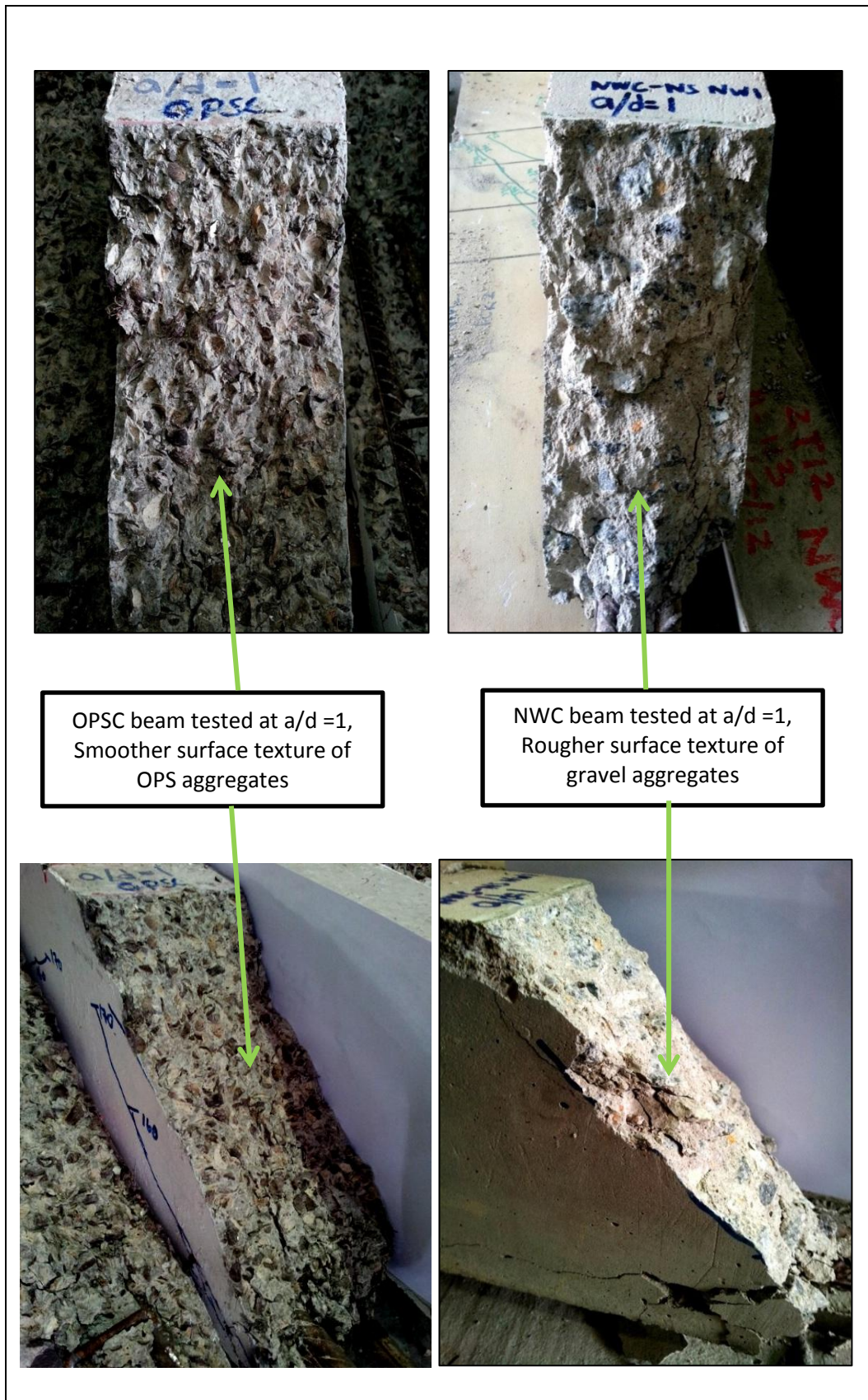


Figure 4.41 Surface texture of diagonal shear interface of OPSC and NWC beams cast without shear reinforcement tested at a/d ratio = 1 (Sectional view and Isometric view).

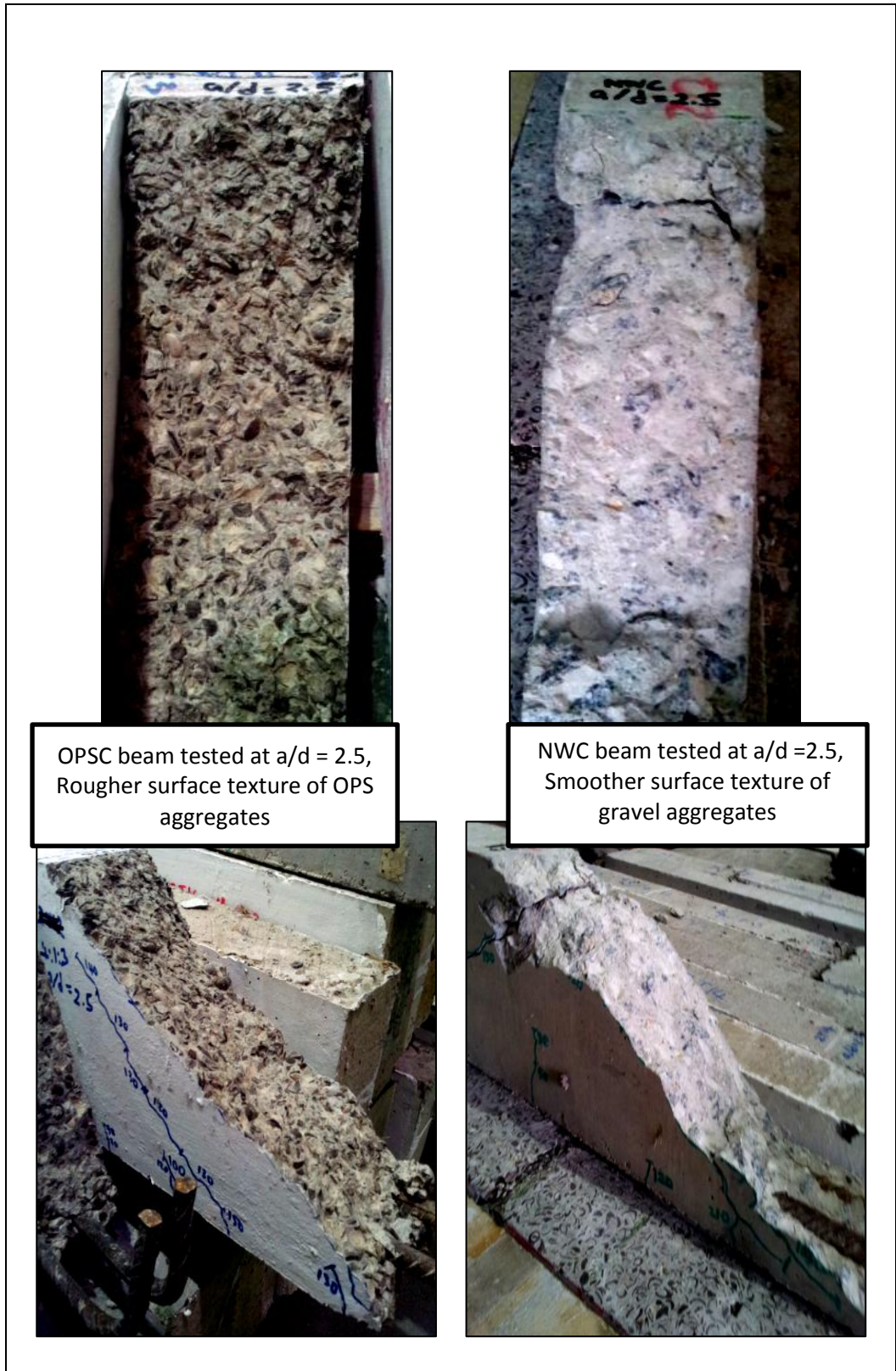


Figure 4.42 Surface texture of diagonal shear interface of OPSC and NWC beams cast without shear reinforcement tested at a/d ratio = 2.5 (Sectional view and Isometric view).

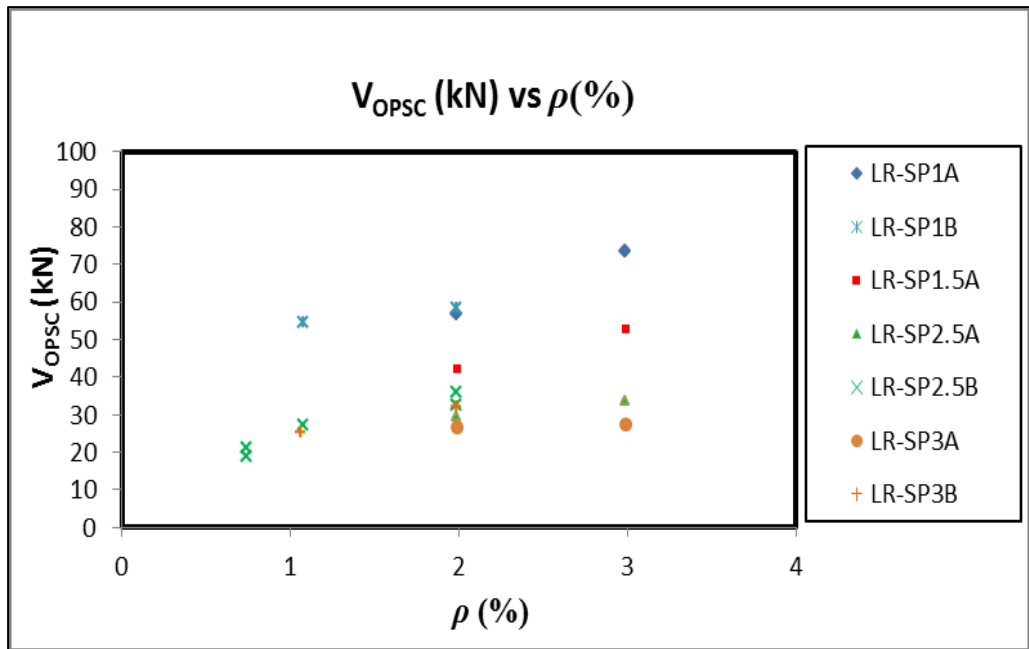


Figure 4.43 V_{OPSC} (kN) vs Longitudinal steel ratio, ρ (%) for OPSC beam specimens cast without shear reinforcement.

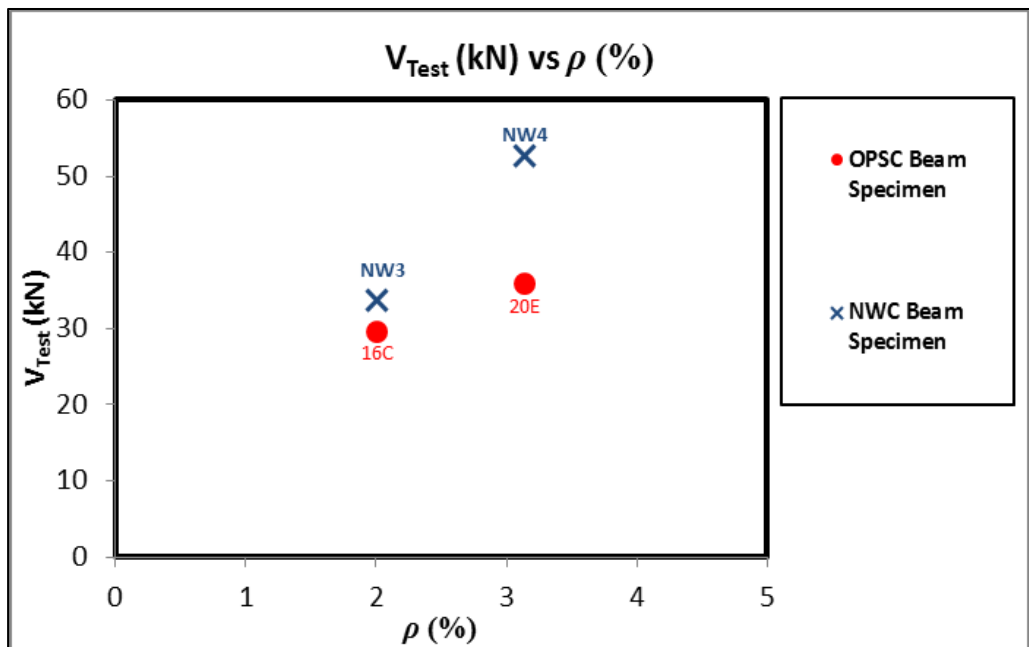


Figure 4.44 V_{Test} (kN) vs Longitudinal steel ratio, ρ (%) for OPSC and NWC beam specimens cast without shear reinforcement.

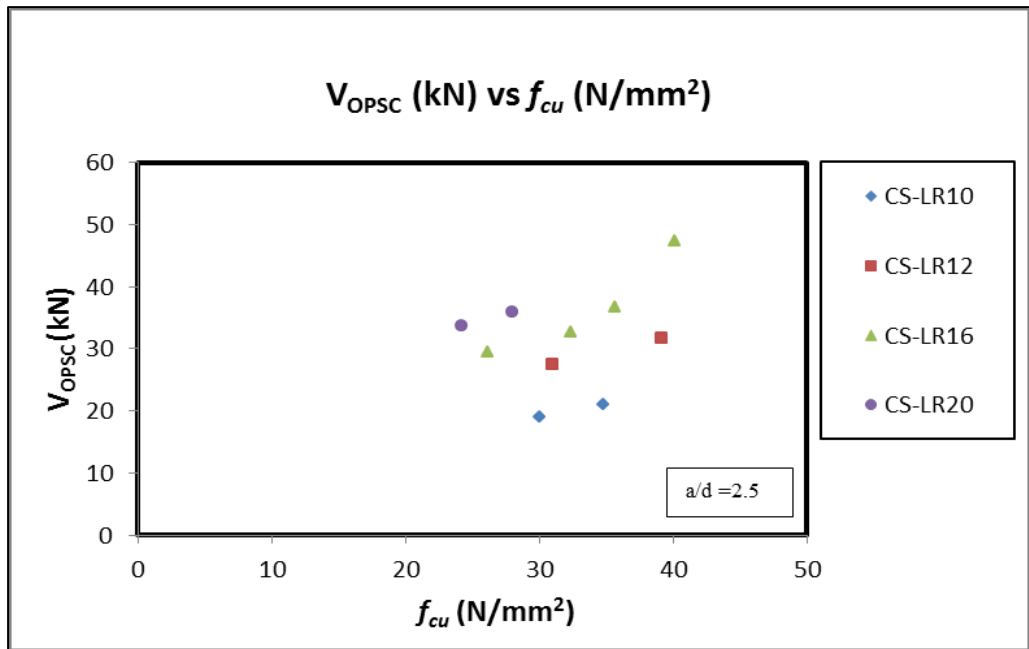


Figure 4.45 V_{OPSC} (N/mm²) vs Concrete strength, f_{cu} (N/mm²) for OPSC beam specimens cast without shear reinforcement.

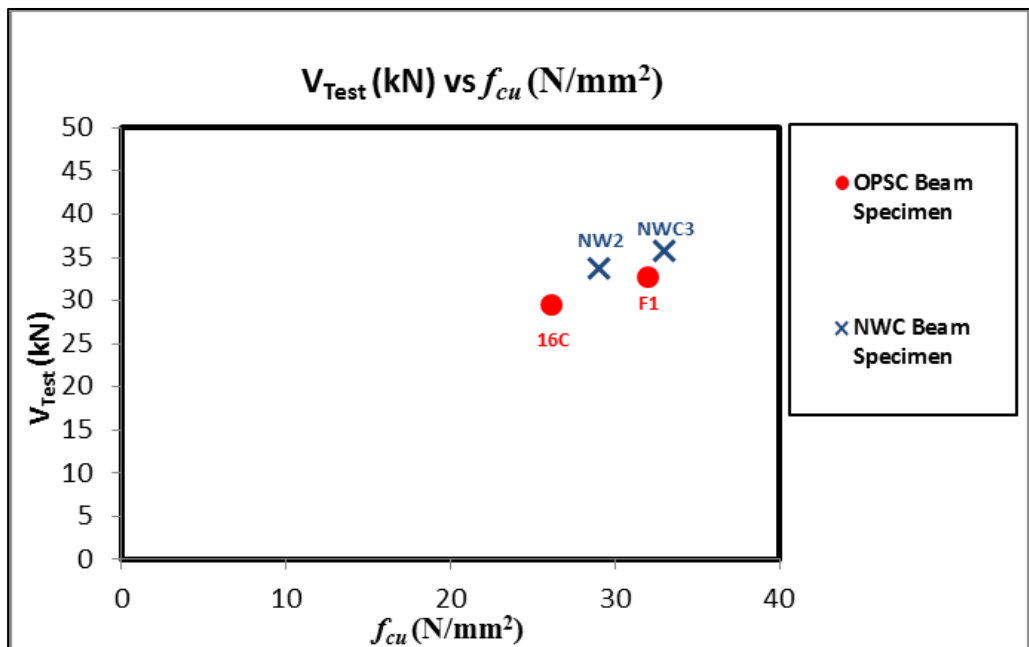


Figure 4.46 V_{Test} (kN) vs Concrete strength, f_{cu} (N/mm²) for OPSC and NWC beam specimens cast without shear reinforcement.

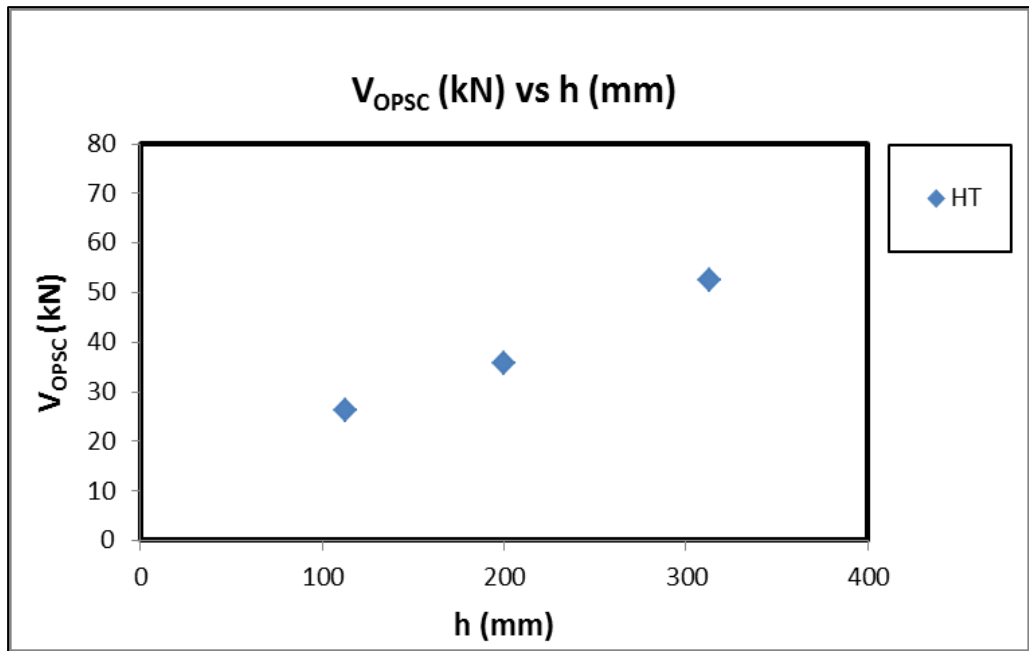


Figure 4.47 V_{OPSC} (kN) vs Overall section depth, h (mm) of OPSC beam specimens without shear reinforcement.

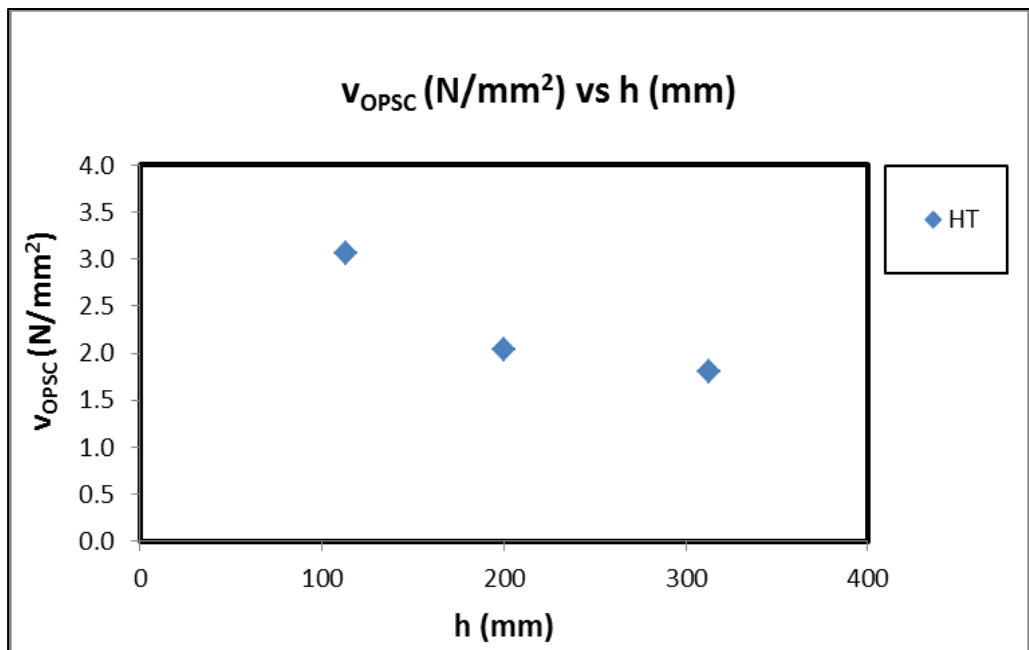


Figure 4.48 v_{OPSC} (N/mm²) vs Overall section depth, h (mm) of OPSC beam specimens without shear reinforcements.

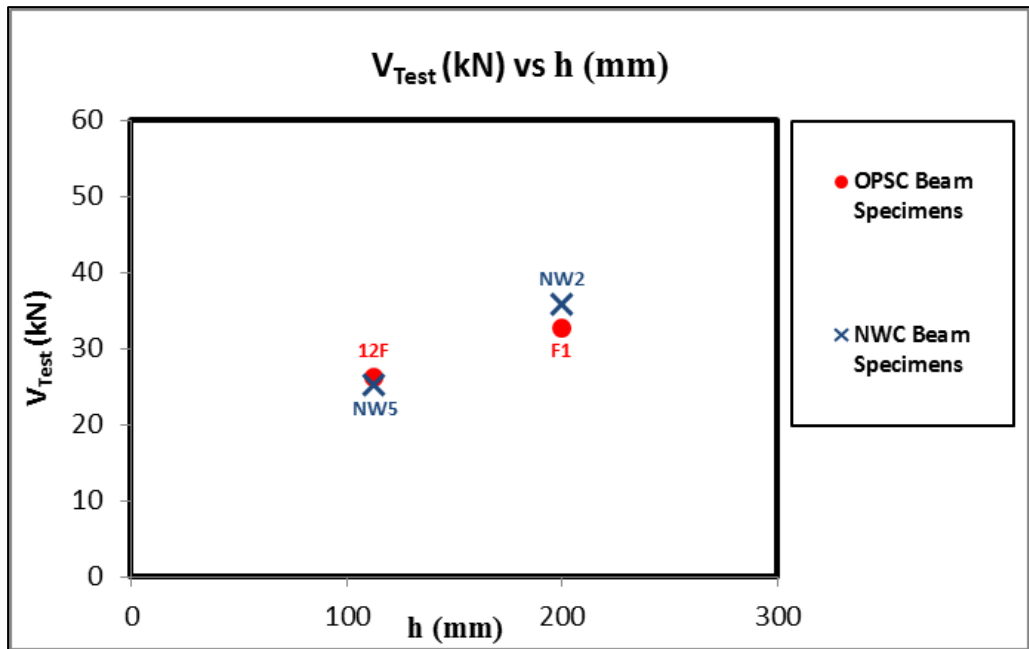


Figure 4.49 V_{Test} (kN) vs Overall section depth, h (mm) for OPSC and NWC beam specimens cast without shear reinforcement.

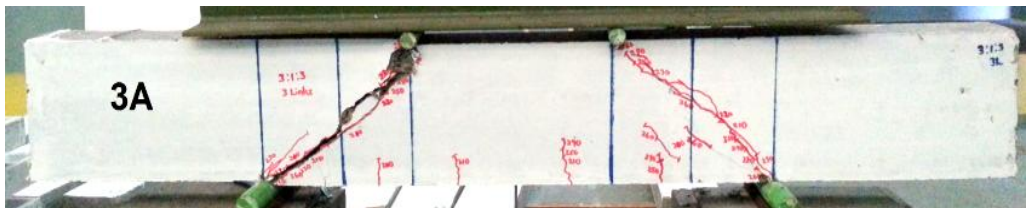


Figure 4.50 Failure mechanisms of OPSC beam cast with shear reinforcements, 3A.

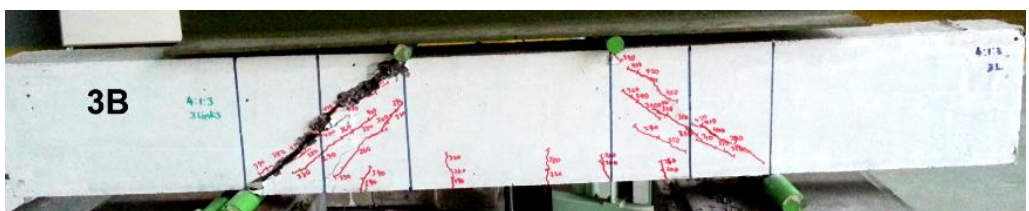


Figure 4.51 Failure mechanisms of OPSC beam cast with shear reinforcements, 3B.

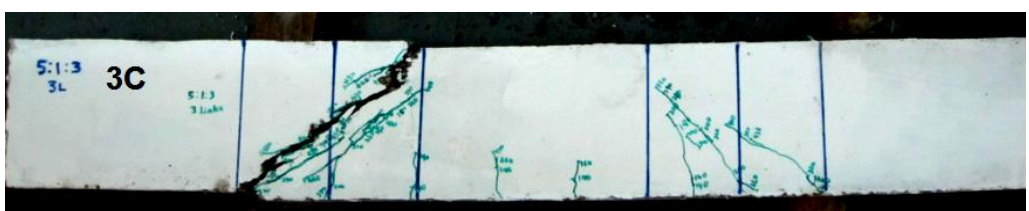


Figure 4.52 Failure mechanisms of OPSC beam cast with shear reinforcements, 3C.



Figure 4.53 Failure mechanisms of OPSC beam cast with shear reinforcement, 4A.



Figure 4.54 Failure mechanisms of OPSC beam cast with shear reinforcement, 4B.

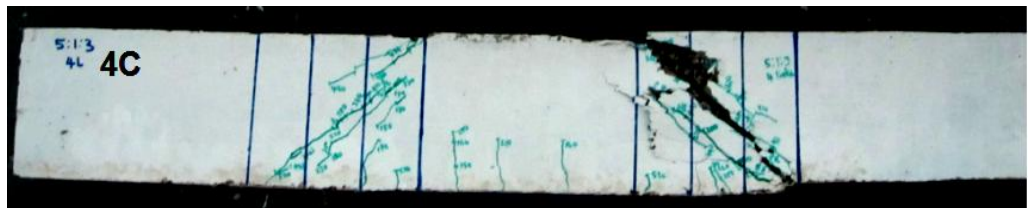


Figure 4.55 Failure mechanisms of OPSC beam cast with shear reinforcement, 4C.



Figure 4.56 Failure mechanisms of OPSC beam cast with shear reinforcement, 5A.

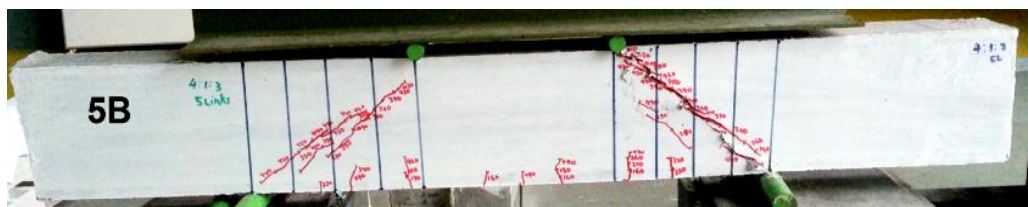


Figure 4.57 Failure mechanisms of OPSC beam cast with shear reinforcement, 5B.

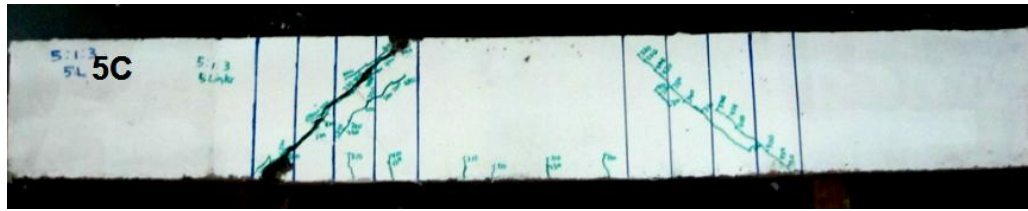


Figure 4.58 Failure mechanisms of OPSC beam cast with shear reinforcement, 5C.

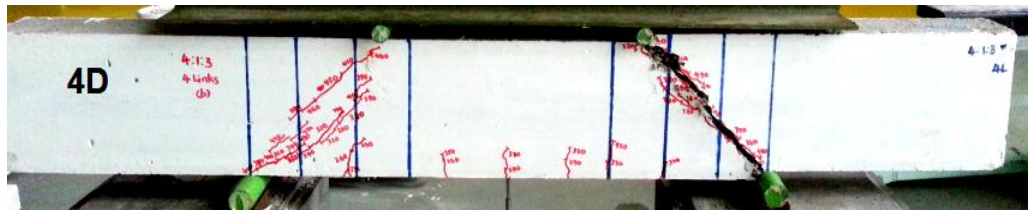


Figure 4.59 Failure mechanisms of OPSC beam cast with shear reinforcement, 4D.

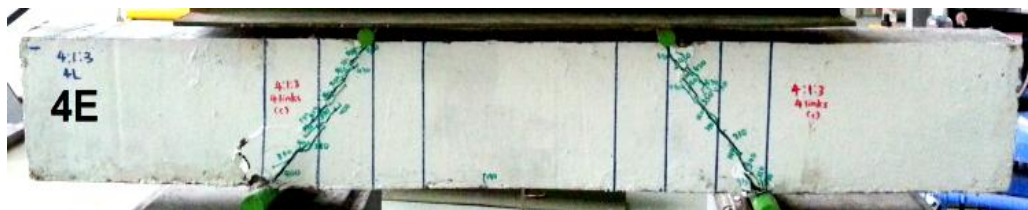


Figure 4.60 Failure mechanisms of OPSC beam cast with shear reinforcement, 4E.

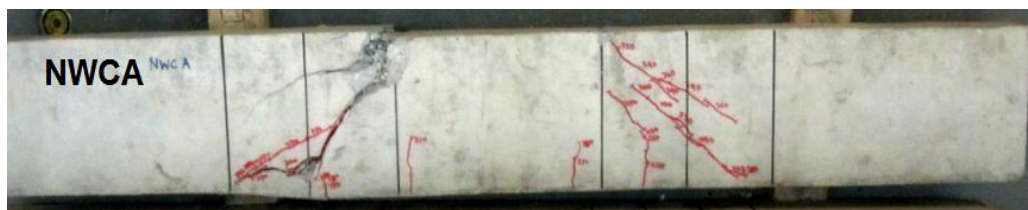


Figure 4.61 Failure mechanisms of NWC beam cast with shear reinforcement, NWCA.



Figure 4.62 Failure mechanisms of NWC beam cast with shear reinforcement, NWCB.

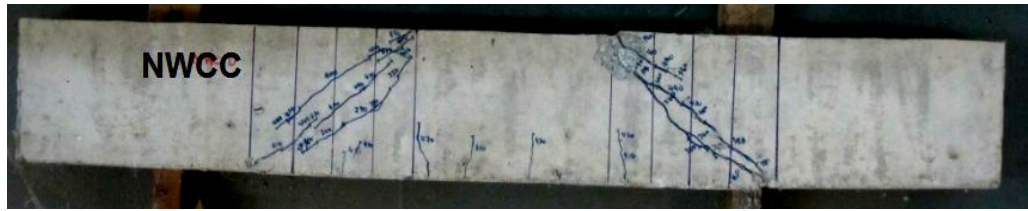


Figure 4.63 Failure mechanisms of NWC beam cast with shear reinforcement, NWCC.



Figure 4.64 Failure mechanisms of NWC beam cast with shear reinforcement, NWCD.

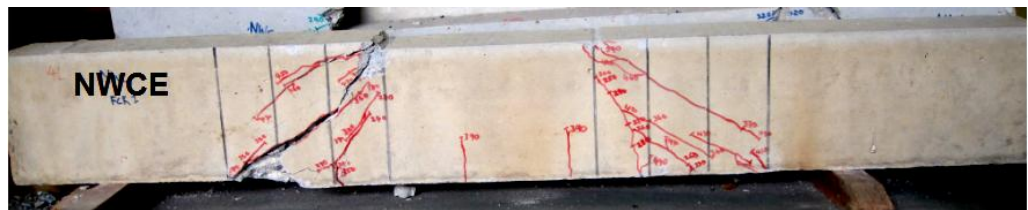


Figure 4.65 Failure mechanisms of NWC beam cast with shear reinforcement, NWCE.

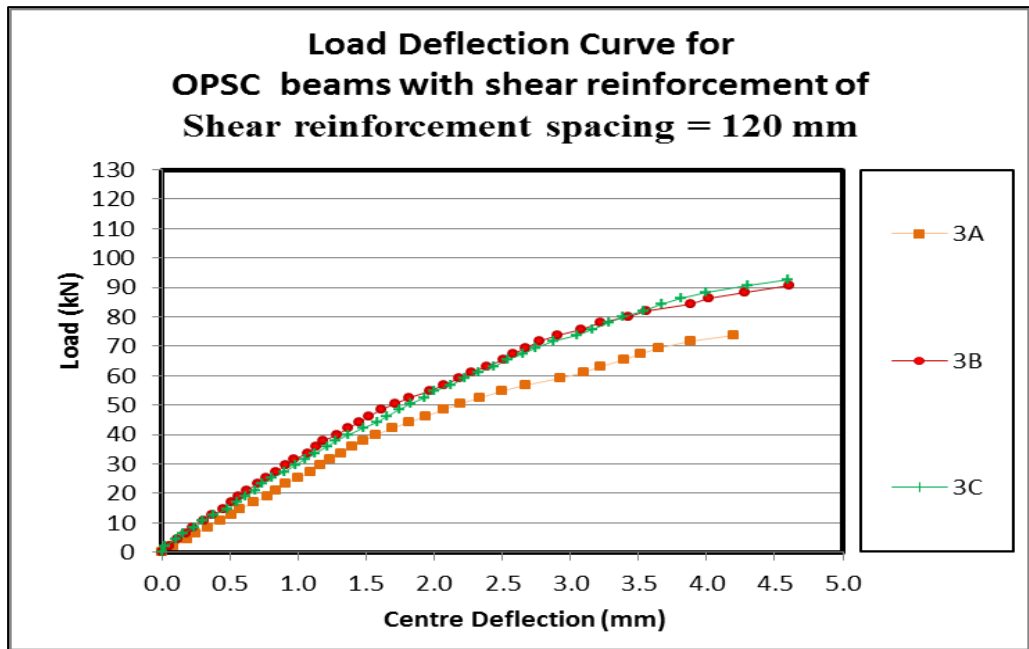


Figure 4.66 Load (kN) vs Central deflection (mm) for OPSC beam specimens with shear reinforcement of shear reinforcement spacing = 120 mm.

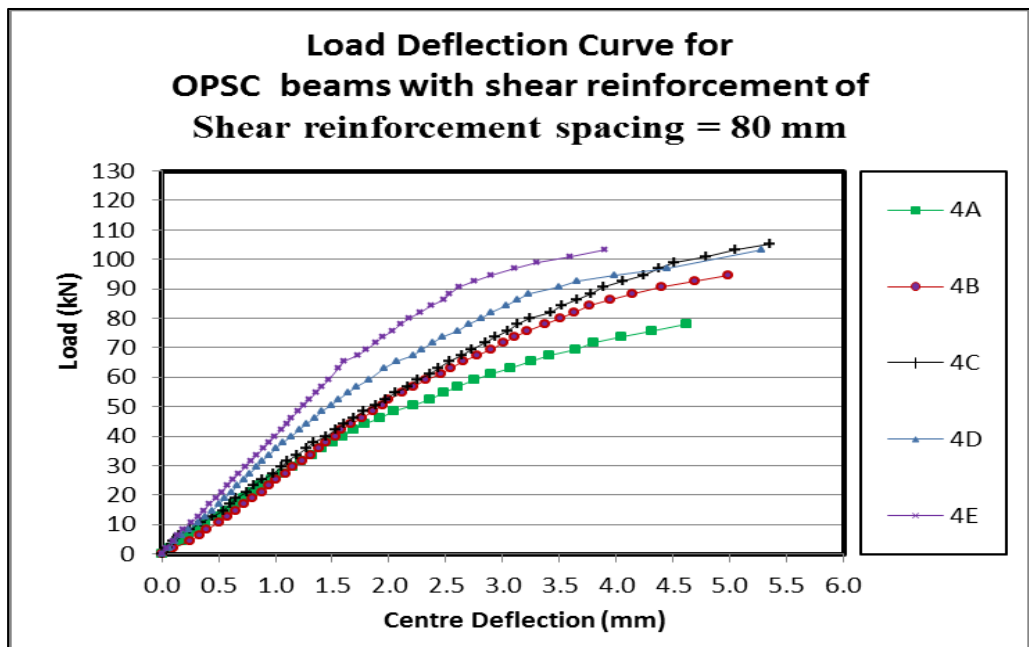


Figure 4.67 Load (kN) vs Central deflection (mm) for OPSC beam specimens with shear reinforcement of shear reinforcement spacing = 80 mm.

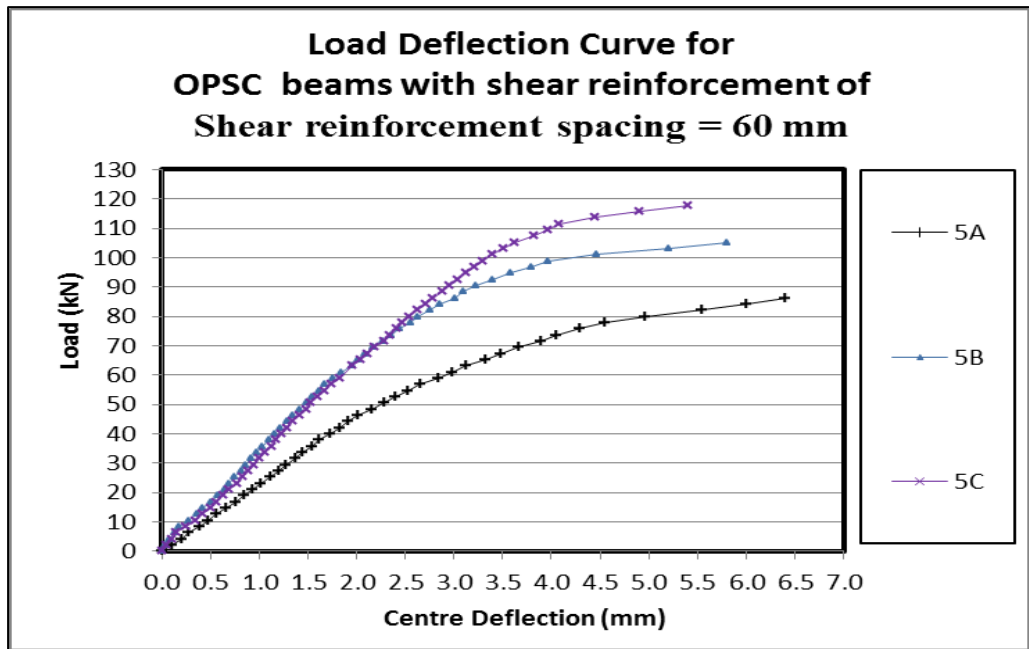


Figure 4.68 Load (kN) vs Central deflection (mm) for OPSC beam specimens with shear reinforcement of shear reinforcement spacing = 60 mm.

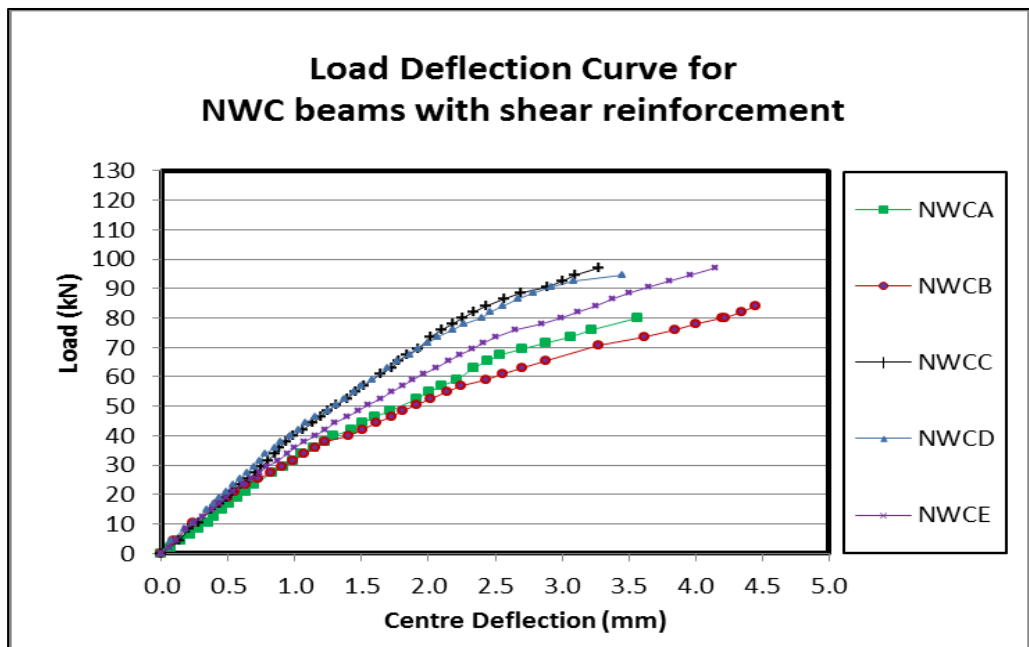


Figure 4.69 Load (kN) vs Central deflection (mm) for NWC beam specimens with shear reinforcement.

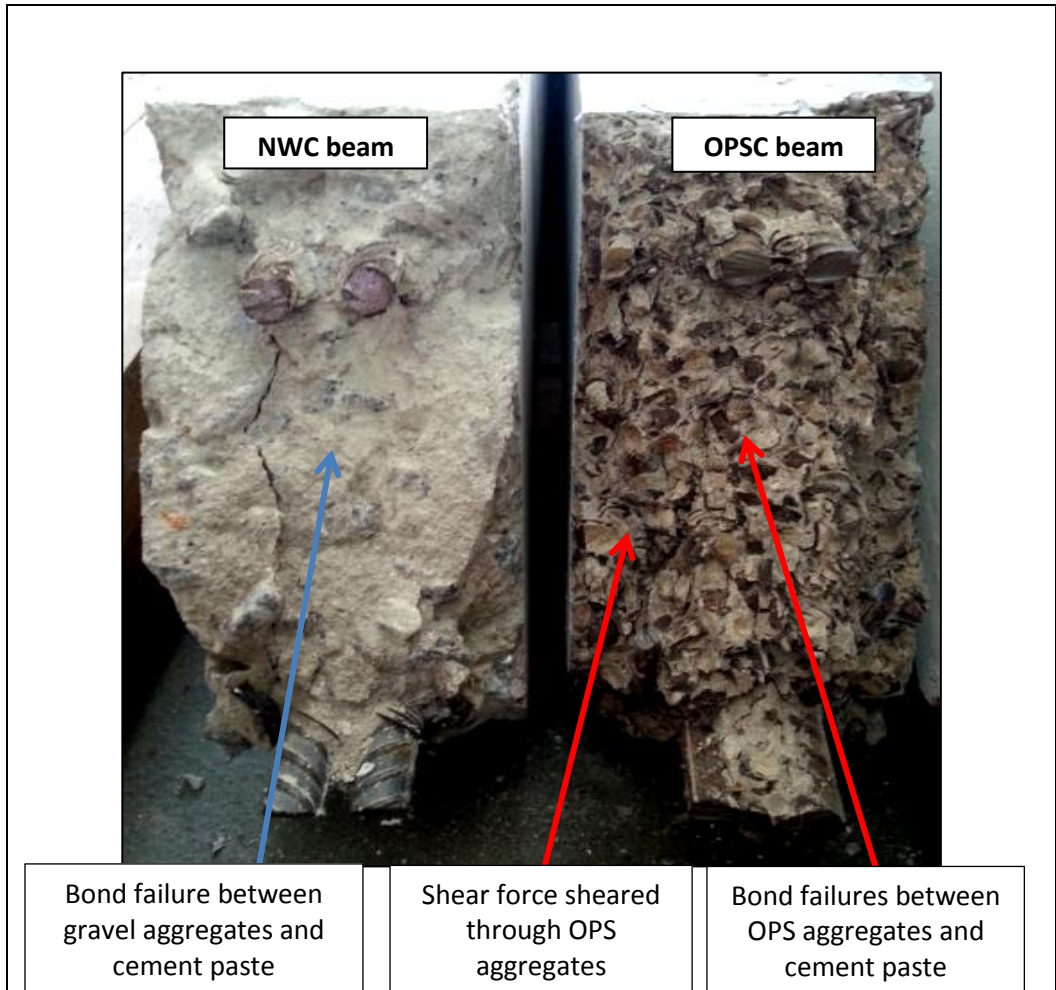


Figure 4.70 Surface texture of diagonal shear interface of OPSC and NWC beam specimens cast with shear reinforcement (Sectional view).



Figure 4.71 Surface texture of diagonal shear interface of OPSC and NWC beam specimens cast with shear reinforcement (Isometric View).

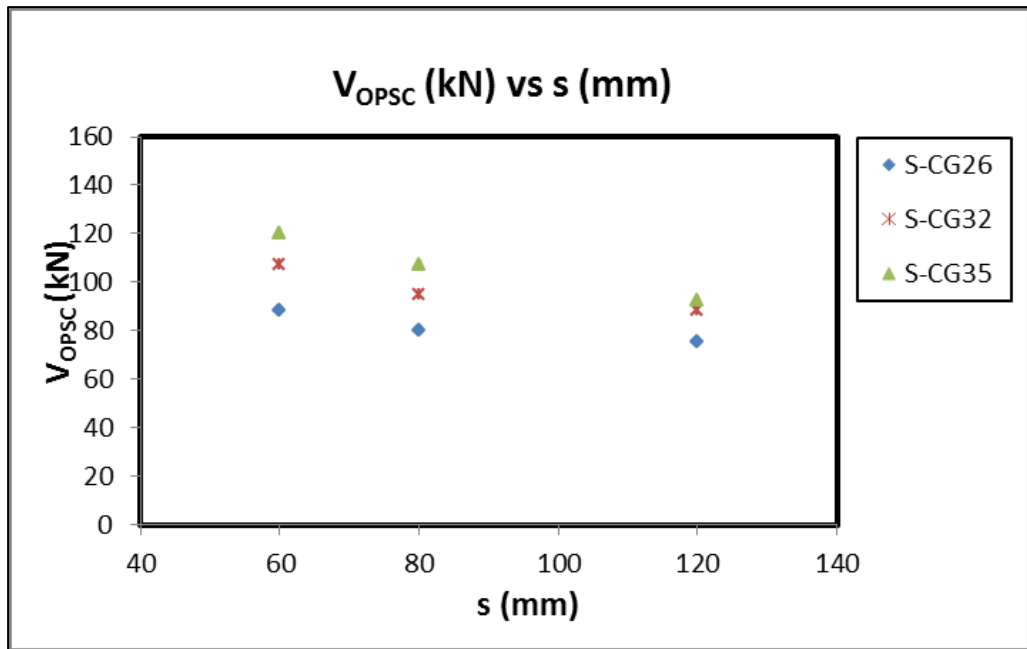


Figure 4.72 V_{OPSC} (kN) vs Shear reinforcement spacing, s (mm) for OPSC beam specimens cast with shear reinforcement.

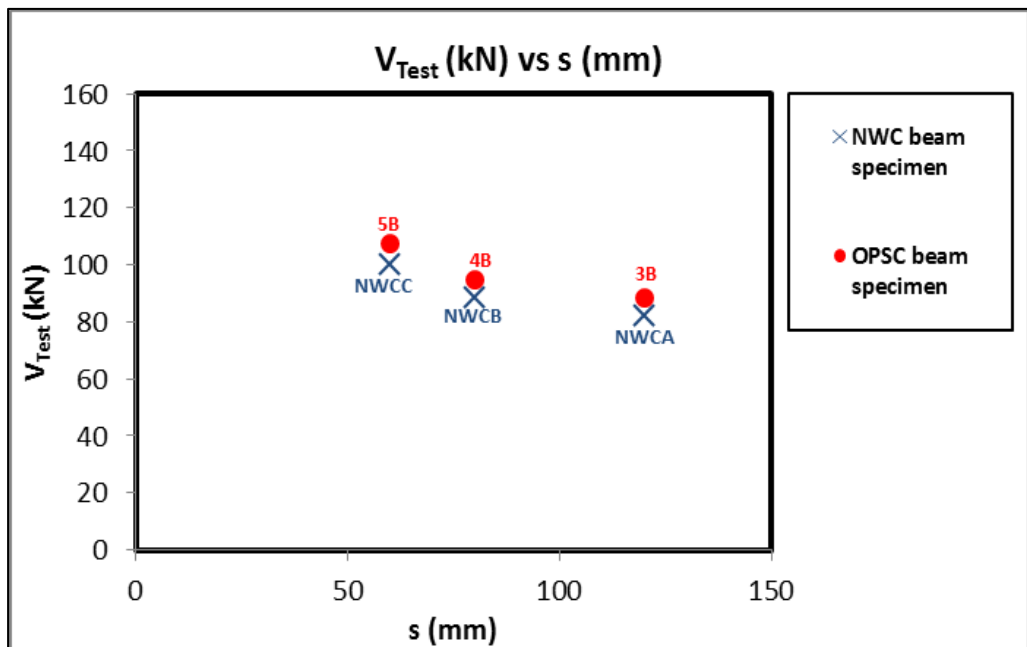


Figure 4.73 V_{Test} (kN) vs Shear reinforcement spacing, s for OPSC and NWC beam specimens cast with shear reinforcement.

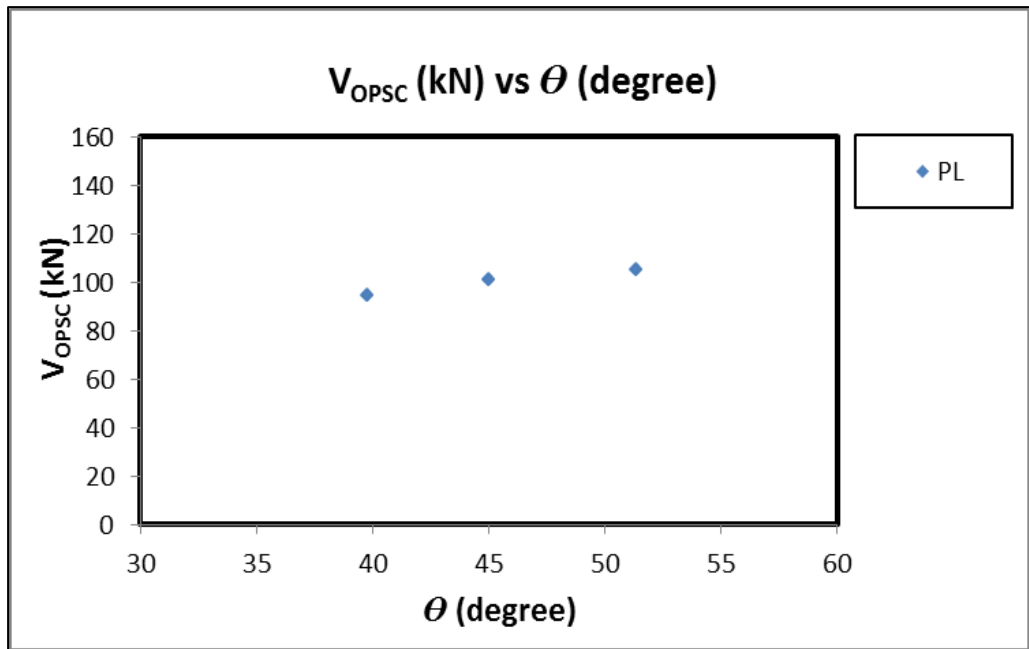


Figure 4.74 V_{OPSC} (kN) vs Inclination angle of shear cracks, θ (degree) for OPSC beam specimens cast with shear reinforcement.

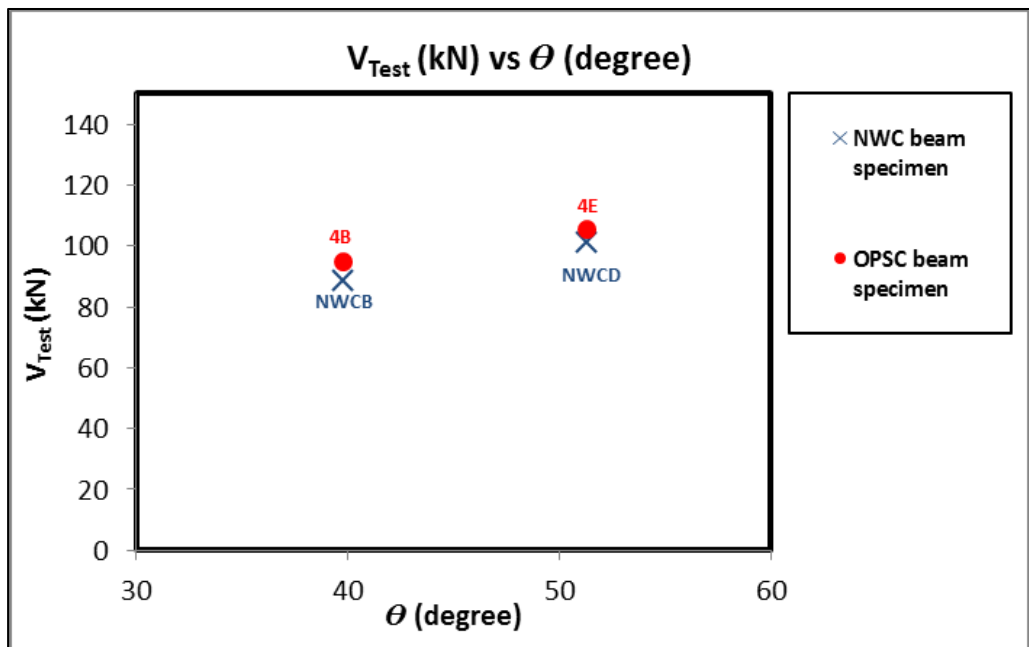


Figure 4.75 V_{Test} (kN) vs Inclination angle of shear cracks, θ (degree) for OPSC and NWC beam specimens cast with shear reinforcement.

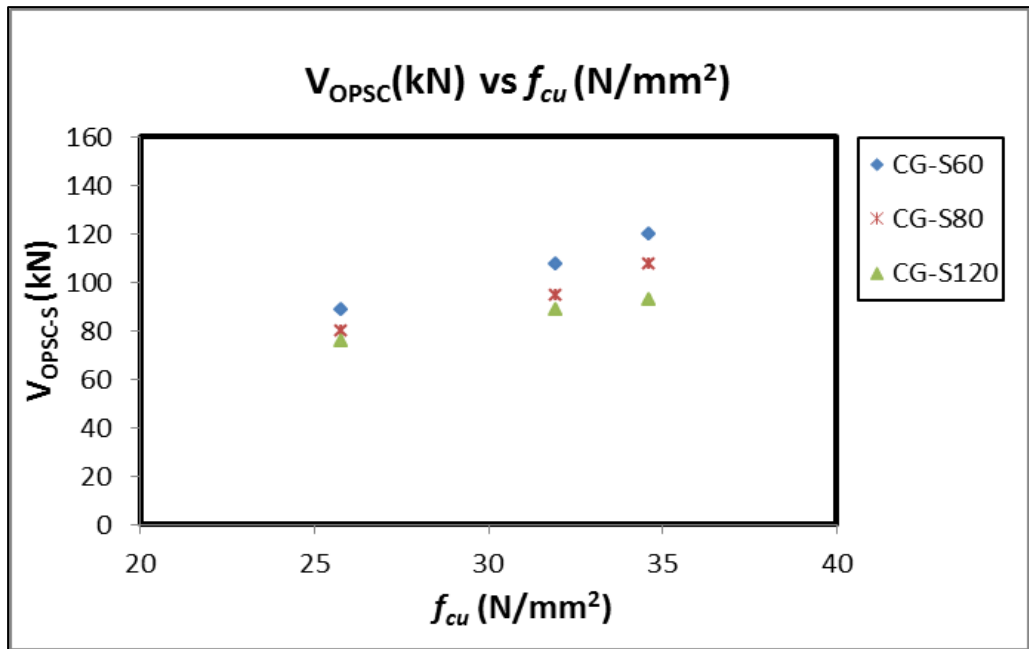


Figure 4.76 V_{OPSC} (kN) vs Concrete strength, f_{cu} (N/mm²) for OPSC beam specimens cast with shear reinforcement.

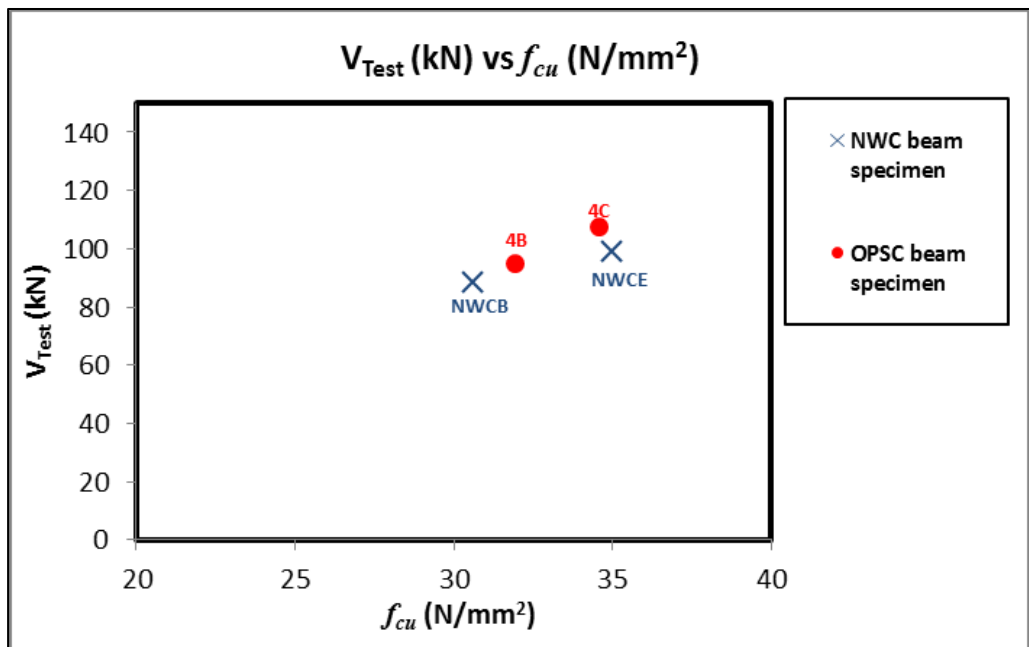


Figure 4.77 V_{Test} (kN) vs Concrete strength, f_{cu} (N/mm²) for OPSC and NWC beam specimens cast with shear reinforcement.

Chapter 5

Theoretical Plastic Models

5.1 Introduction

In Chapter 4, the test observations, the test results, the failure mechanisms and the effect of parameters were fully described. It was noted that variations on the ultimate shear strength do occurred between the Oil Palm kernel Shell Concrete (OPSC) beams and Normal Weight Concrete (NWC) beams, both cast with and without shear reinforcement. Since the existing upper bound plastic models have been proposed for the predictions of shear resistance of NWC beams, both with and without shear reinforcement, it is therefore sensible to adopt these models as the basis of the theoretical models proposed in this chapter.

As mentioned in Section 2.2, although the upper bound plastic approach for predicting concrete shear resistance of reinforced concrete structural beam elements was first introduced in 1975 by Braestrup [45], agreement with the test results were only found with the inclusion of effectiveness factor, v , in 197 for beams without shear reinforcement) 8 by Neilsen et.al [46]. For concrete beam specimens cast without shear reinforcement, better agreement with tests were found when the effectiveness factor, v , was considered to be a function of concrete cylindrical compressive strength (σ_c), overall section depth (h), longitudinal steel ratio (ρ), and span to overall depth ratio (a/h). Whilst for concrete beam specimens cast with shear reinforcement, the effectiveness factor, v , was considered to be limited to the function of concrete cylindrical compressive strength (σ_c), as the effects of other parameters were considered to be nominal [46]. However, as described in Chapter 4,

it was found that the shear reinforcement's ratio, ρ_s , and the inclination angle of shear cracks, θ , influenced the shear resistance of the OPSC beam cast with shear reinforcement. Hence, further investigations were carried out in the current research to determine the need for modification to the existing prediction model.

In this chapter, investigations on the requirements for modification on shear strength parameters' are reported for both cases of casting with and without shear reinforcement. From the current research, two theoretical concrete plastic model: CP-I Model and CP-II Model, which adopt the upper bound plastic approach as their fundamental basis, are proposed for OPSC cast without and with shear reinforcement, respectively.

For OPSC beam without shear reinforcement, CP- I Model modified the parameters' equations of concrete compressive strength (σ_c), overall section depth (h), longitudinal steel ratio (ρ), and span to overall depth ratio (a/h). Whilst for OPSC beam with shear reinforcement, CP-II modified the parameter's equation: concrete compressive strength (σ_c). Full detail of the prediction models, CP-I Model and CP-II Model,, are presented in Section 5.2 and 5.3, respectively.

5.2 Beams cast without shear reinforcement

5.2.1 Theoretical plastic model for concrete beam without shear reinforcement, (CP-I Model)

The proposing (CP-I Model) is developed to predict for the ultimate shear resistance of a reinforced concrete beam element cast using Oil Palm kernel Shell (OPSC) as coarse aggregate. The model is essentially the existing upper bound plastic approach

(Eqn 2.15) with some modifications to its effectiveness parameters. That is, both the concrete and the reinforcement are assumed to be rigid plastic materials with plastic strains and yield condition assumed to follow the associated flow law (normality condition) and modified Coulomb failure criterion, respectively. At failure, a concrete beam is assumed to be separated into rigid regions by the shear failure surfaces (as shown in Figure 2.14). These regions are considered to remain rigid and to move relative to each other. The discontinuities are assumed to be narrow rigid-plastic region of concrete as shown in Figure (2.14).

Since a significant similarity has been adopted in the failure mechanism, the test results were then compared with the predictions of the existing model (Eqn 2.16.1 to 2.16.4) to evaluate whether the existing model is relevant (see Column 2 and 3 in Table 5.1). The comparisons have been summarised and presented in Table 5.1 (see Column 5). It can be noted that the existing model overestimate the test results by 11%. The test results were then further evaluated with respect to the associating parameters of the effectiveness factor (as shown in Figure 5.1 to Figure 5.4). The outcomes of these evaluations review that the existing model, as it is, does not give good agreement with the ultimate shear resistance of OPSC beam specimens. As a result, it is decided to carry out modifications to the effectiveness parameters to reflect the observation derive from tests. The parameters modified are; span to overall depth ratio (a/h), longitudinal steel ratio (ρ), concrete compressive strength (σ_c), and overall section depth (h). Such modifications are required to accommodate for the variations observed from tests, such as overestimations of the parameters shear span to depth ratio ($a/h \leq 2$), longitudinal steel ratio, concrete strength and underestimation of overall section depth ($h < 150$ mm).

5.2.2 Modification on parameters

5.2.2.1 Span to overall depth ratio, a/h

It can be noted from Figure 5.1 that, the shear failure loads of OPSC specimens loaded with span to overall depth ratio, $a/h \leq 2$, are observed to be lower than those casted with NWC. As such, the prediction values derived from the existing theoretical plastic model (CP-NS Model) (Eqn 2.16.1) are therefore observed to overestimate the failure loads of OPSC specimens. It is believed that such phenomenon was attributed to the lower aggregate interlock ability resulting from the smoother shear crack interface observed in OPSC specimen AD1 with respect to NWC specimen NWC1 (see Figure 4.41).

Whilst for OPSC specimens loaded with $a/h > 2$ ($a/d \geq 2.5$), the shear failure loads were noted to be similar to that of NWC specimens. As such, the prediction values derived from the existing theoretical plastic model (CP-NS Model) (Eqn 2.16.1) agree with the failure loads of OPSC specimens. Such phenomenon is believed to be attributed to the higher aggregate interlock ability resulting from the rougher shear interface observed in OPSC specimen F1 with respect to NWC specimen NWC2 (See Figure 4.42), as highlighted in Section 4.2.3.1.

In view of the discrepancy noted in shear behaviour of OPSC specimens as the shear span reduces, modification to the existing parameter, a/h , is required. The existing expression was therefore revised to be Eqn 5.1.1 to accommodate for the smoother shear crack interface observed in the OPSC specimens. With the revised expression for span ratio (Eqn 5.1.1), good agreement with test results are achieved, as shown in Figure 5.1.

$$f\left(\frac{a}{h}\right) = 1 + 0.05 \left(\frac{a}{h} - 2.6\right)^2 \quad \left(0.82 \leq \frac{a}{h} \leq 2.54\right) \quad (\text{Eqn 5.1.1})$$

5.2.2.2 Longitudinal steel ratio, ρ

In general, it can be noted from Figure 5.2 that the test results with respect to the longitudinal steel ratio, $f(\rho)$, of OPSC beam specimens cast without shear reinforcement are observed to be lower than the predictions derived from the existing theoretical plastic model (CP-NS Model) (Eqn 2.16.2). Furthermore, it is observed that the rate of increases in shear strength of OPSC specimens with respect to the longitudinal steel ratio (ρ) were observed to be less significant for beam specimens casted with $\rho = 2.99\%$, while the control samples (NWC) were observed to be consistent with the theoretical prediction (see figure 4.44).

Such discrepancies are believed to be attributed to the differences found in the fracture strength of coarse aggregates (See Section 2.1). That is, a lower fracture strength found in Oil Palm kernel Shell (OPS) (see Table 2.1) would have led to a lower shear stress being transferred across the shear crack interface, which in turn, resulted in a lower shear resistance been mobilised.

In view of the discrepancies noted in OPSC, a modification has been proposed to the existing plastic model (CP-NS Model) (Eqn 2.16.2) to account for the losses observed in shear strength, which would resulted from the increase in reinforcement ratio. With the revised expression for longitudinal steel ratio (Eqn 5.1.2), good agreement with test results are achieved, as shown in Figure 5.2.

$$f(\rho) = 0.13 \rho + 0.53 \quad (\rho < 3.14 \%) \quad (\text{Eqn 5.1.2})$$

5.2.2.3 Cylindrical concrete strength, σ_c

In general, it can be noted from Figure 5.3 that the shear strength of OPSC with respect of the cylindrical concrete strength, $f(\sigma_c)$, of specimens cast without shear reinforcement are observed to be lower than the predictions of the existing theoretical plastic model (CP-NS Model) (Eqn 2.16.3). As such, the prediction values derived from the existing theoretical plastic model (CP-NS Model) (Eqn 2.16.3) are therefore observed to overestimate the failure loads of OPSC specimens. It is believed that such phenomenon was attributed to the lower fracture strength of OPS aggregates (see Section 2.1). That is, a lower fracture strength found in Oil Palm kernel Shell (OPS) (see Table 2.1) would have led to a lower shear stress being transferred across the shear cracks interface, and hence, resulted in a lower shear resistance been mobilised.

In view of the discrepancies noted in OPSC, a modification has been proposed to the existing plastic model (CP-NS Model) with respect to the influence of cylindrical concrete strength in shear strength, to accommodate for the shear strength provided. With the revised expression for concrete strength (Eqn 5.1.3), good agreement with test results are achieved, as shown in Figure 5.3.

$$f(\sigma_c) = \frac{3.3}{\sqrt{\sigma_c}} \quad (19 < \sigma_c < 33 \text{ MPa}) \quad (\text{Eqn 5.1.3})$$

5.2.2.4 Overall section depth, h

It can be noted from Figure 5.4 that, the shear failure loads of OPSC specimens loaded with overall section depth, $h < 160$ mm, are observed to be higher than those casted with NWC. As for OPSC specimens with increase of overall section depth, it is

observed that the rate of reduction in shear strength of OPSC specimens with respect to the overall section depth are more significant, while the control samples (NWC) were observed to be consistent with the theoretical prediction of existing plastic model (CP-NS Model) (Eqn 2.16.4).

Such discrepancies are believed to be attributed to the differences found in the fracture strength of coarse aggregates (See Section 2.1). That is, a lower fracture strength found in Oil Palm kernel Shell (OPS) (see Table 2.1) would have led to a lower aggregate interlock capacity accumulated as the overall section depth increases, which in turn, resulted in a lower ultimate shear resistance.

In view of the discrepancies noted in OPSC, a modification has been proposed to the existing plastic model (CP-NS Model) to account for the losses observed in shear strength, which would resulted from the increase in overall section depth. With the revised expression for overall section depth (Eqn 5.1.4), good agreement with test results are achieved, as shown in Figure 5.4.

$$f(h) = 0.25 \left(1.1 + \frac{1}{h^{0.6}} \right) \quad (0.113\text{m} \leq h \leq 0.313\text{m}) \quad (\text{Eqn 5.1.4})$$

5.2.3 Comparisons with test results

It can be observed from the Figure 5.5 to Figure 5.8 that with the proposing theoretical plastic model (CP-I Model) with respect to the parameters: span to overall depth ratio (a/h), longitudinal steel ratio (ρ), concrete strength (σ_c), and overall section depth (h) (Eqn 5.1.1 to 5.1.4) exhibits good agreement (mean value of 1.07 and standard deviation of 0.15) with the test results (see also Table 5.1 Column 6).

5.3 Beams cast with shear reinforcement

5.3.1 Theoretical plastic model for concrete beam with shear reinforcement, (CP-II Model)

The proposing (CP-II Model) is developed to predict for the ultimate shear resistance of a reinforced concrete element with shear reinforcement cast using Oil Palm kernel Shell (OPSC) as coarse aggregate. The model is essentially the existing upper bound plastic approach (Eqn 2.41) with some modifications to its effectiveness parameter. That is, both the concrete and the reinforcement are assumed to be rigid plastic materials with plastic strains and yield condition assumed to follow the associated flow law (normality condition) and modified Coulomb failure criterion, respectively. A concrete beam is assumed to be separated into rigid regions by the shear failure surfaces at failure (as shown in Figure 2.19). These regions are considered to remain rigid and to move relative to each other and the discontinuities are assumed to be narrow rigid-plastic region of concrete as shown in Figure 2.19.

Since similarity has been observed in the failure mechanism of OPSC and NWC beams, the test results of OPSC beams were compared with the predictions of the existing model (Eqn 2.42) to evaluate whether the existing model is relevant (see Column 2 and 3 in Table 5.2). It can be noted that the existing model overestimate the test results by 8%. The test results were then further evaluated with respect to the associating parameter of the effectiveness factor (as shown in Figure 5.9). In addition to the effectiveness parameter, additional parameters of shear reinforcement ratio and inclination angle of shear cracks were investigated (see Figure 5.10 and 5.11). The outcomes of these evaluations review that the existing model, as it is, does not give good agreement with the ultimate shear resistance of OPSC beam specimens. The model is essentially the existing upper bound plastic

model (Eqn 2.41) with a modification to its effectiveness parameter: concrete strength.

Hence, detailed investigations were carried out on the shear strength predictions given by the existing theoretical plastic model (CP-S Model) with respect to the OPSC beam's test results to investigate the requirement for modifications on the shear strength parameters. The results of these investigations are shown in Table 5.2 (Column 5), which it is found that the existing theoretical plastic model (CP-S Model) overestimated the shear strength capacity of OPSC beam specimens cast with shear reinforcement with a mean value of 0.92 and standard deviation of 0.05.

5.3.2 Modification on parameter

From Section 5.3.1, it was found that the existing theoretical plastic model (CP-S Model) overestimated the shear strength of the OPSC beam cast with shear reinforcement. Hence, detailed investigations were carried out on the parameter of cylindrical concrete strength (σ_c), which governed the effectiveness factor, ν to investigate the requirement for modification on parameter. Apart from the concrete strength parameter suggested by Nielsen et.al [46], it is observed from the test results in Section 4.3.3 that two other parameters: (1) shear reinforcement ratio (ρ_s) and (2) inclination angle of shear cracks (θ), also influence the ultimate shear strength obtained for the OPSC beam with shear reinforcement.

Hence, further investigations on the two parameters: (1) cylindrical concrete strength (σ_c) (see Figure 5.21) (2) inclination angle of shear cracks (θ) (see Figure 5.22), and (3) shear reinforcement ratio (ρ_s) (see Figure 5.23) were carried out to observe the comparisons between the shear failure loads of the OPSC beams without shear

reinforcement and the shear strength predictions derived from the existing theoretical plastic model (CP-S Model), to examine the requirement for the modification.

5.3.2.1 Cylindrical concrete strength, σ_c

It can be noted from Figure 5.9 that the shear failure loads of OPSC beams with shear reinforcement with respect to the parameter: cylindrical concrete strength are lower than the predictions derived from the existing CP Model (CP-S Model) (Eqn 2.42). However, it is observed from tests that the ultimate shear strength achieved by the OPSC beam specimens (Specimen 4B and 4C) are slightly higher compared to the ultimate shear strength by NWC beam specimens (Specimen NWCB and NWCE) (see Figure 4.77). It is believed that the higher shear strength achieved by OPSC beams is due to the rougher shear cracks interface of OPSC beams (See Figure 4.70 and 4.71) compared to those of NWC beams. Therefore, this would lead to higher aggregate interlocking capacity and resulted in higher shear resistance in OPSC beams. Hence, it can be noted that the existing plastic model (CP-S Model) overestimated the shear failure loads of the OPSC beams.

A modification has therefore been proposed to the existing plastic model (CP-S Model) to account for the variations observed between the shear strength of the OPSC specimens and the predictions by CP-S Model. With the revised expression for concrete strength (Eqn 5.2), good agreement with test results are achieved, as shown in Figure 5.9.

$$f(f_{ck}) = 0.7 - \frac{f_{ck}}{300} \quad (20.5 \text{ MPa} \leq f_{ck} \leq 27.7 \text{ MPa}) \quad (\text{Eqn 5.2})$$

5.3.2.2 Shear reinforcement ratio, ρ_s

It can be noted from Figure 5.10 that the shear failure loads of OPSC beams with respect to shear reinforcement ratio are higher than those of NWC control specimens (See also Figure 4.73). It is believed that such discrepancy is due to the rougher surface interface observed at the surface texture of diagonal shear cracks of the OPSC beams compared to NWC beams (see Figure 4.70 and 4.71), which in turn, would have enhanced the aggregate interlocking capacity, and resulted in higher shear resistance of OPSC beams.

However, it can be noted from Figure 5.10 that the shear failure loads of the OPSC beams are in good agreement with the predictions derived from the existing plastic model (CP-S Model) (Eqn 2.42). Therefore, there is no requirement for the parameter shear reinforcement modification. The predictions of the CP-S Model with respect to the parameter: shear reinforcement ratio are reasonable to be included to the proposed modified plastic model (CP-II Model) without any requirement of modification to the parameter.

5.3.2.3 Inclination angle of shear cracks, θ

It can be noted from Figure 5.11 that the shear failure loads of OPSC beams with respect to shear reinforcement ratio are higher than those of NWC control specimens (See also Figure 4.75). Such discrepancy is believed attributed to the rougher surface interface observed at the surface texture of diagonal shear cracks of the OPSC beams compared to NWC beams (see Figure 4.70 and 4.71), which in turn, would have enhanced the aggregate interlocking capacity, and resulted in higher shear resistance of OPSC beams.

However, it can be noted from Figure 5.11 that the shear failure loads of OPSC beams with respect to inclination angle of shear cracks, $f(\theta)$ are in good agreement with the predictions derived from the existing plastic model (CP-S Model) (Eqn 2.41). Hence, no requirement of modification on the parameter: inclination angle of shear cracks is recommended. The existing parameter formula is therefore acceptable to be included to the proposed modified plastic model (CP-II Model).

5.3.3 Comparisons with test results

It can be observed from Figure 5.12 to Figure 5.14 that good agreement between the test results and the prediction derived from the proposed modified theoretical plastic model with respect to parameters: cylindrical concrete strength (σ_c), inclination angle of shear cracks (θ) and shear reinforcement ratio (ρ_s) are achieved (mean value of 1.03 and standard deviation of 0.05, as shown Table 5.2 Column 6).

5.4 Summary

Two theoretical models based upon the modification of the existing theoretical concrete plastic models via the parameters equations were proposed in this chapter for the shear strength predictions of the OPSC beams cast with and without shear reinforcement, respectively.

For OPSC beams cast without shear reinforcement, the proposed CP-I Model took into account the variables: concrete cylindrical compressive strength (σ_c), overall section depth (h), longitudinal steel ratio (ρ), and span to overall depth ratio (a/h), which governed the effectiveness factor, u , from the existing plastic model (CP-NS

Model), which each shear strength parameters were modified for the ultimate shear strength predictions of the OPSC beams without shear reinforcement.

Whilst for OPSC beams cast with shear reinforcement, the proposed CP-II Model are the results of the modified parameter equations of cylindrical compressive strength (σ_c) for the ultimate shear strength predictions of the OPSC beams with shear reinforcement. In general, all the modified theoretical concrete plastic models (CP-I Model and CP-II Model) achieved good agreement with the OPSC beam test results.

Table 5.1 Comparisons of shear strength predictions with respect to the test results of OPSC beams cast without shear reinforcement

1	2	3	4	5	6
Specimen No	V_{OPSC} (kN)	V_{CP-NS} (kN)	V_{CP-I} (kN)	$\frac{V_{OPSC}}{V_{CP-NS}}$	$\frac{V_{OPSC}}{V_{CP-I}}$
10A	18.95	25.30	22.44	0.75	0.84
S1	21.05	27.23	24.16	0.77	0.87
12A	54.73	83.91	57.73	0.65	0.95
12B	40.00	53.59	40.71	0.75	0.98
12C	27.37	27.74	24.51	0.99	1.12
12D	25.26	22.57	20.49	1.12	1.23
12E	31.58	31.18	27.54	1.01	1.15
12F	26.31	23.16	21.30	1.14	1.24
16A	56.80	91.12	62.17	0.62	0.91
16B	42.10	58.37	43.93	0.72	0.96
16C	29.50	30.22	26.46	0.98	1.11
16D	26.32	24.52	22.11	1.07	1.19
16E	35.79	33.68	29.49	1.06	1.21
20A	73.68	105.29	71.27	0.70	1.03
20B	52.63	67.65	50.46	0.78	1.04
20C	33.68	35.04	30.43	0.96	1.11
20D	27.37	28.35	25.41	0.97	1.08
20E	35.79	37.67	32.71	0.95	1.09
AD1	58.19	100.81	68.78	0.58	0.85
AD2	32.33	27.13	24.47	1.19	1.32
F1	32.67	33.63	29.45	0.97	1.11
F2	47.41	37.43	32.78	1.27	1.45
H2	52.53	52.43	23.69	1.00	0.80
S2	36.64	35.32	30.93	1.04	1.18
			Mean	0.89	1.07
			S.D.	0.19	0.15

V_{OPSC} (kN) = Ultimate shear failure load of OPSC beam specimens cast without shear reinforcement

V_{CP-NS} (kN) = Shear resistance of Existing Concrete Plastic Model (CP-NS Model)

$$V_{CP-NS} = \frac{\sigma_c}{2} (1 - \cos \theta) \left(\frac{b h}{\sin \theta} \right)$$

Which, $u = f_1(\sigma_c) f_2(h) f_3(\rho) f_4\left(\frac{a}{h}\right)$

$$\text{Where, } f_1(\sigma_c) = \frac{3.5}{\sqrt{\sigma_c}} \quad (\sigma_c \text{ in N/mm}^2)$$

$$f_2(h) = 0.27 \left(1 + \frac{1}{\sqrt{h}} \right) \quad (h \text{ in m})$$

$$f_3(\rho) = 0.15\rho + 0.58 \quad (\rho < 4.5\%)$$

$$f_4\left(\frac{a}{h}\right) = 1 + 0.17 \left(\frac{a}{h} - 2.6 \right)^2 \quad \left(\frac{a}{h} < 5.5 \right)$$

V_{CP-I} (kN) = Shear resistance of proposing Modified Concrete Plastic Model (CP-I Model)

$$V_{CP-I} = \frac{\sigma_c}{2} (1 - \cos \theta) \left(\frac{b h}{\sin \theta} \right)$$

Which, $u = f_1(\sigma_c) f_2(h) f_3(\rho) f_4\left(\frac{a}{h}\right)$

$$\text{Where, } f_1(\sigma_c) = \frac{3.3}{\sqrt{\sigma_c}} \quad (19 \text{ MPa} \leq \sigma_c \leq 33 \text{ MPa})$$

$$f_2(h) = 0.25 \left(1.1 + \frac{1}{h^{0.6}} \right) \quad (0.113 \text{ m} \leq h \leq 0.313 \text{ m})$$

$$f_3(\rho) = 0.13\rho + 0.53 \quad (\rho < 3.14\%)$$

$$f_4\left(\frac{a}{h}\right) = 1 + 0.17 \left(\frac{a}{h} - 2.6 \right)^2 \quad (0.82 \leq \frac{a}{h} \leq 2.54)$$

Table 5.2 Comparisons of shear strength predictions with respect to the test results of OPSC beams cast with shear reinforcement

1	2	3	4	5	6
Specimen No	V_{OPSC} (kN)	V_{CP-S} (kN)	V_{CP-II} (kN)	$\frac{V_{OPSC}}{V_{CP-S}}$	$\frac{V_{OPSC}}{V_{CP-II}}$
3A	75.78	78.04	72.70	0.97	1.04
3B	88.41	88.67	82.89	0.95	1.07
3C	92.62	93.01	87.14	0.95	1.06
4A	79.99	89.73	84.29	0.87	0.95
4B	94.73	100.36	94.49	0.91	1.00
4C	107.36	104.70	98.73	0.98	1.09
5A	88.41	101.42	95.88	0.81	0.92
5B	107.36	112.05	106.08	0.89	1.01
5C	119.99	116.39	110.33	0.95	1.09
4D	101.04	98.94	93.98	0.95	1.08
4E	105.25	103.15	98.61	0.93	1.07
			Mean	0.92	1.03
			S.D.	0.05	0.05

V_{OPSC} (kN) = Ultimate shear failure loads of OPSC beam specimens cast with shear reinforcement

V_{CP-S} (kN) = Shear resistance of Existing Concrete Plastic Model (CP-S Model)

$$V_{CP-S} = \rho_s \sigma_f b h \cot \theta + \frac{\sigma_c}{2} (1 - \cos \theta) \left(\frac{b h}{\sin \theta} \right)$$

$$\text{Where, } u = 0.8 - \frac{\sigma_c}{200}$$

V_{CP-II} (kN) = Shear resistance of proposing Modified Concrete Plastic Model (CP-II Model)

$$V_{CP-II} = \rho_s \sigma_f b h \cot \theta + \frac{\sigma_c}{2} (1 - \cos \theta) \left(\frac{b h}{\sin \theta} \right)$$

$$\text{Where, } u = 0.7 - \frac{\sigma_c}{300}$$

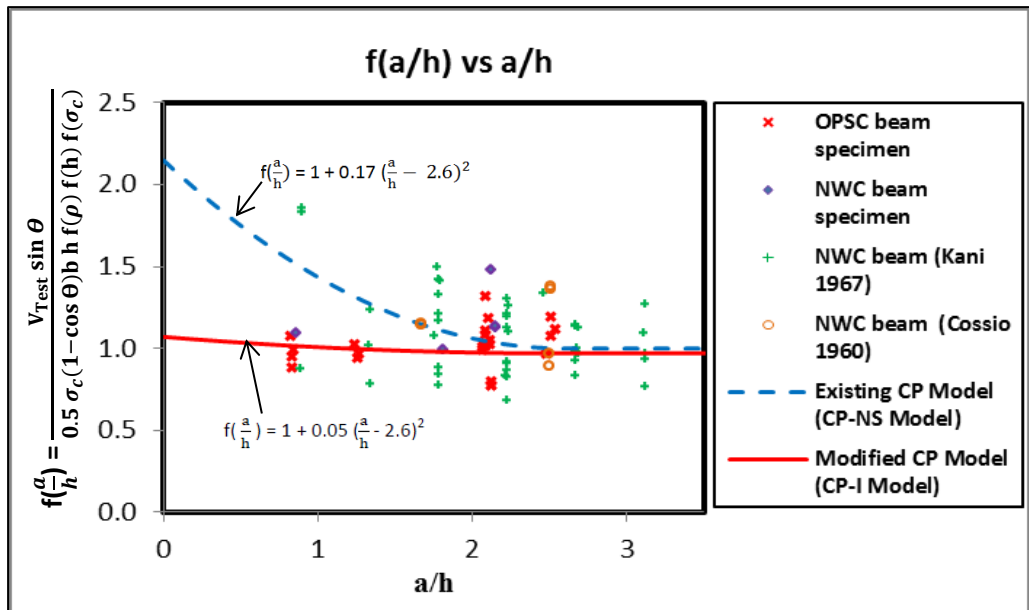


Figure 5.1 $f(a/h)$ vs a/h for Existing plastic model (CP-NS Model) and Modified plastic model (CP-I Model).

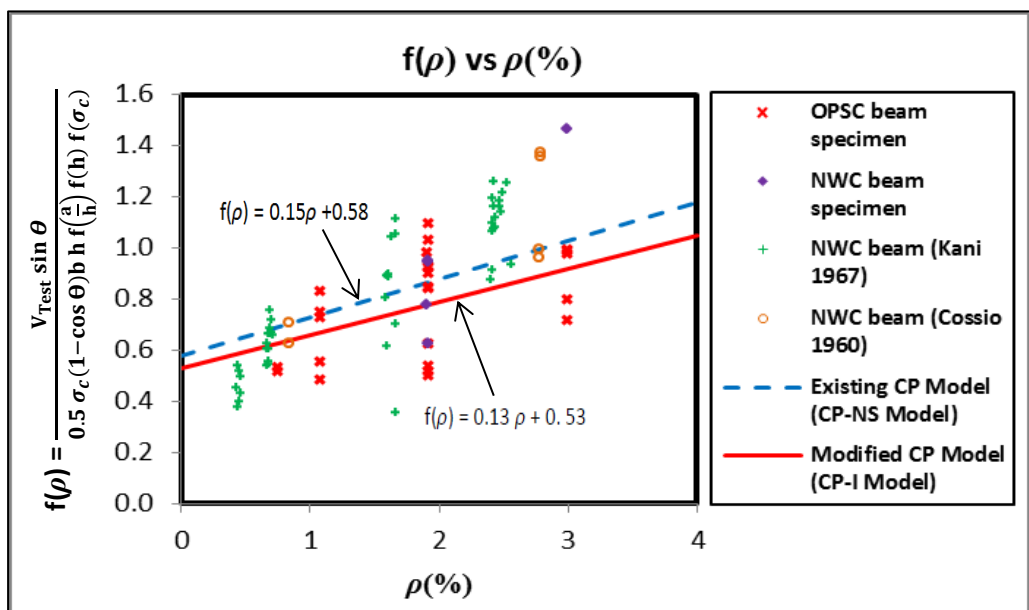


Figure 5.2 $f(\rho)$ vs $\rho(\%)$ for Existing plastic model (CP-NS Model) and Modified plastic model (CP-I Model).

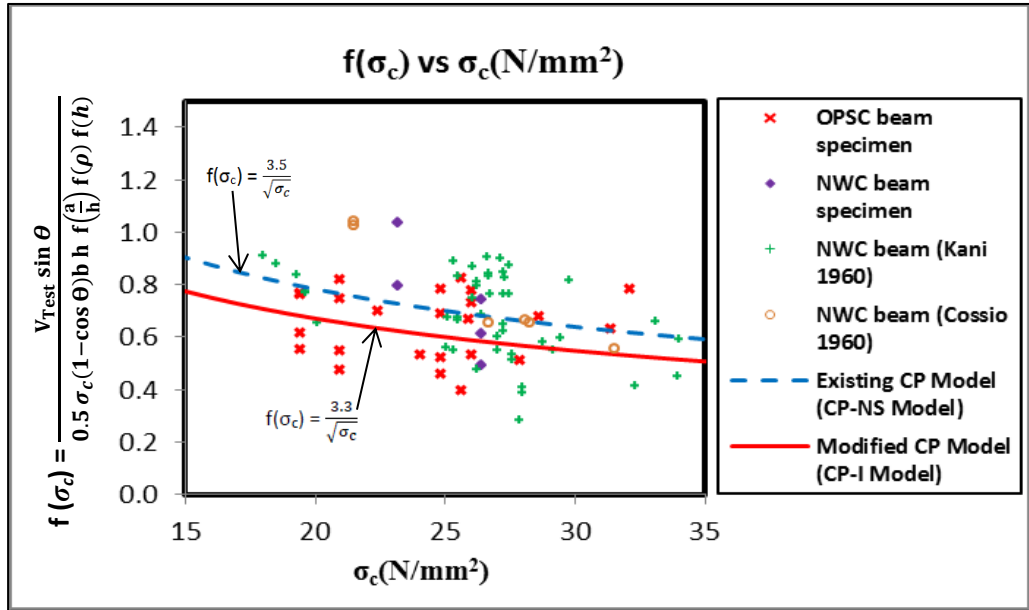


Figure 5.3 $f(\sigma_c)$ vs σ_c (N/mm²) for Existing plastic model (CP-NS Model) and Modified plastic model (CP-I Model).

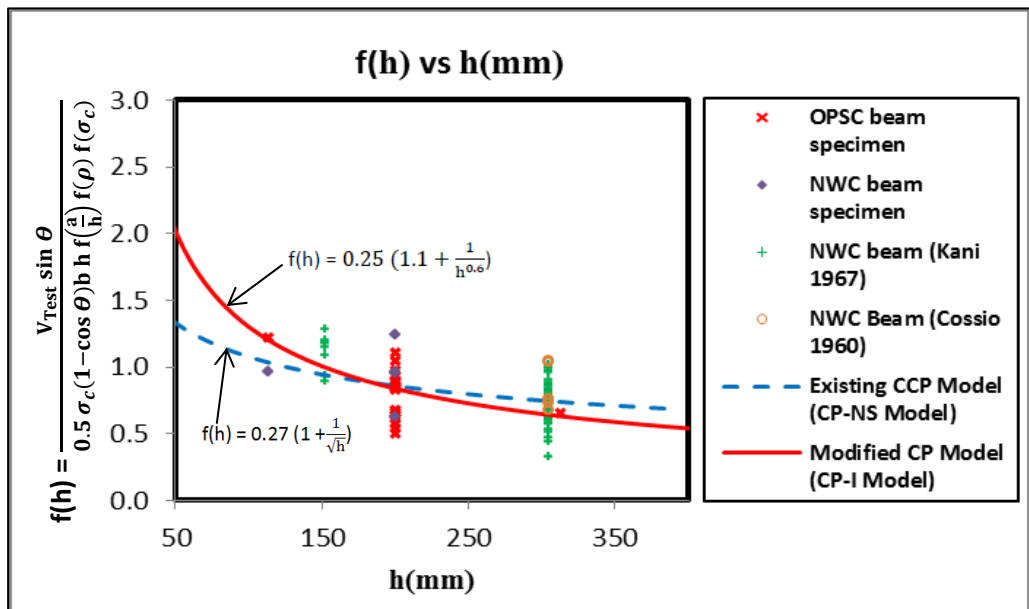


Figure 5.4 $f(h)$ vs h (mm) for Existing plastic model (CP-NS Model) and Modified plastic model (CP-I Model).

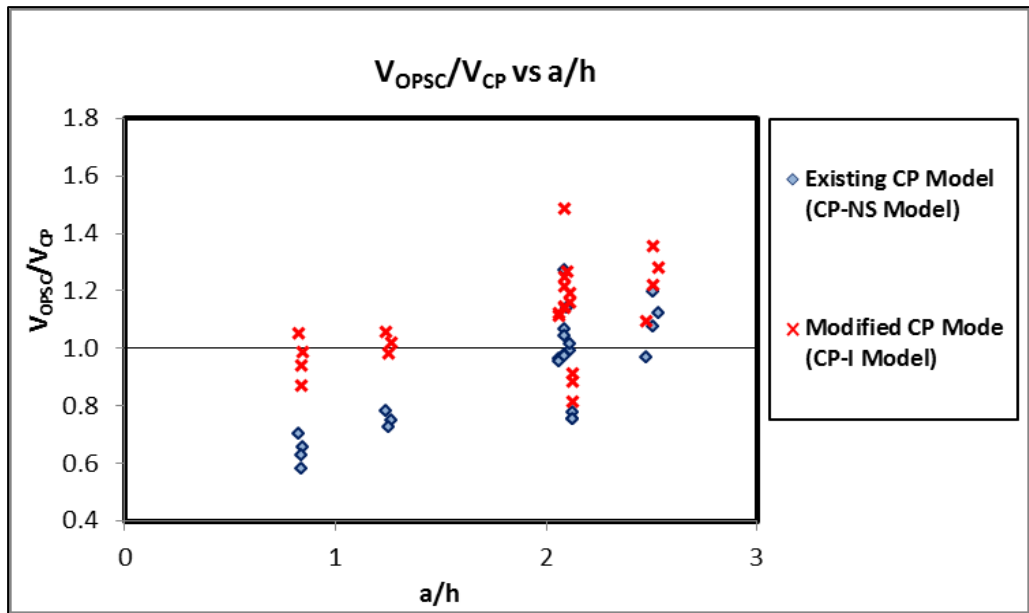


Figure 5.5 V_{OPSC}/V_{CP} vs Span to overall depth ratio, a/h .

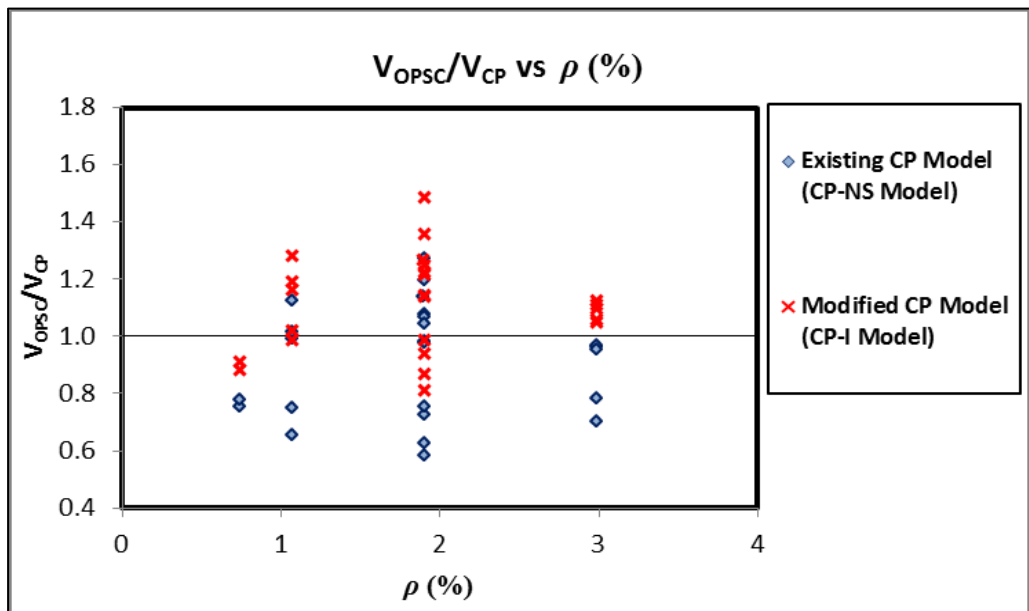


Figure 5.6 V_{OPSC}/V_{CP} vs Longitudinal steel ratio, ρ (%).

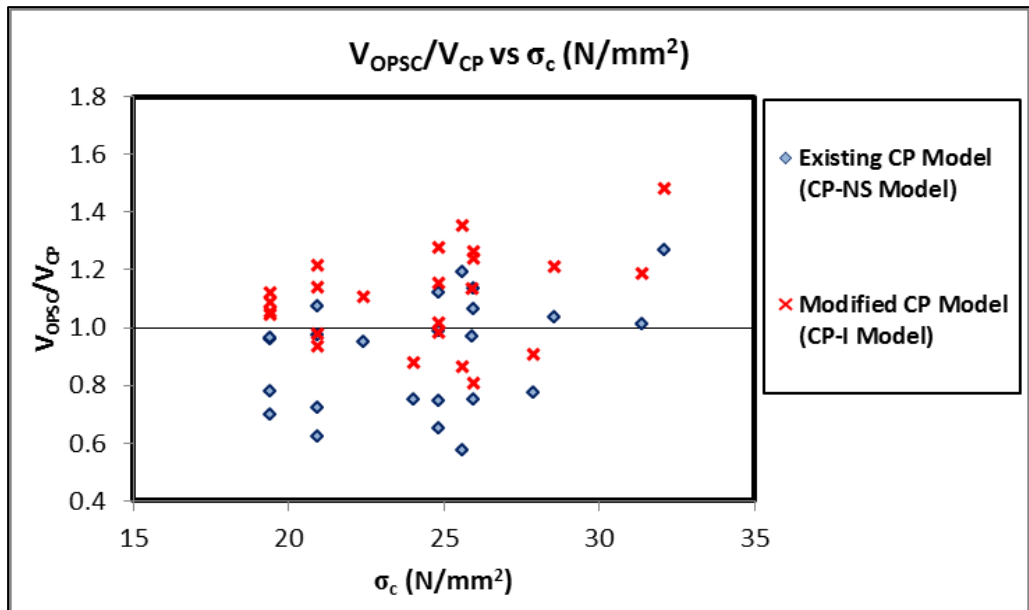


Figure 5.7 V_{OPSC}/V_{CP} vs Cylindrical concrete strength, σ_c (N/mm^2).

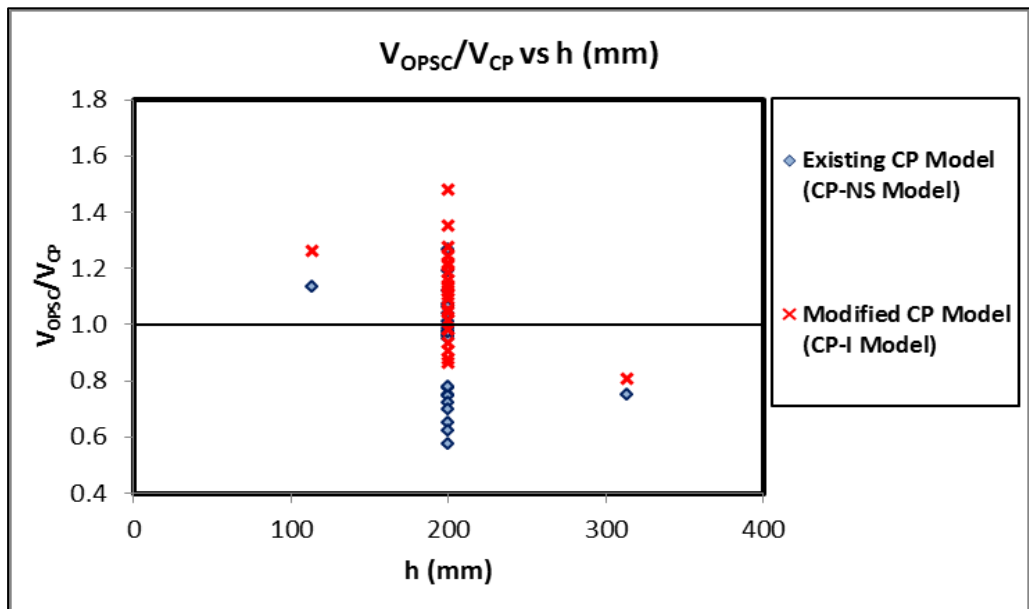


Figure 5.8 V_{OPSC}/V_{CP} vs Overall sectional depth, h (mm).

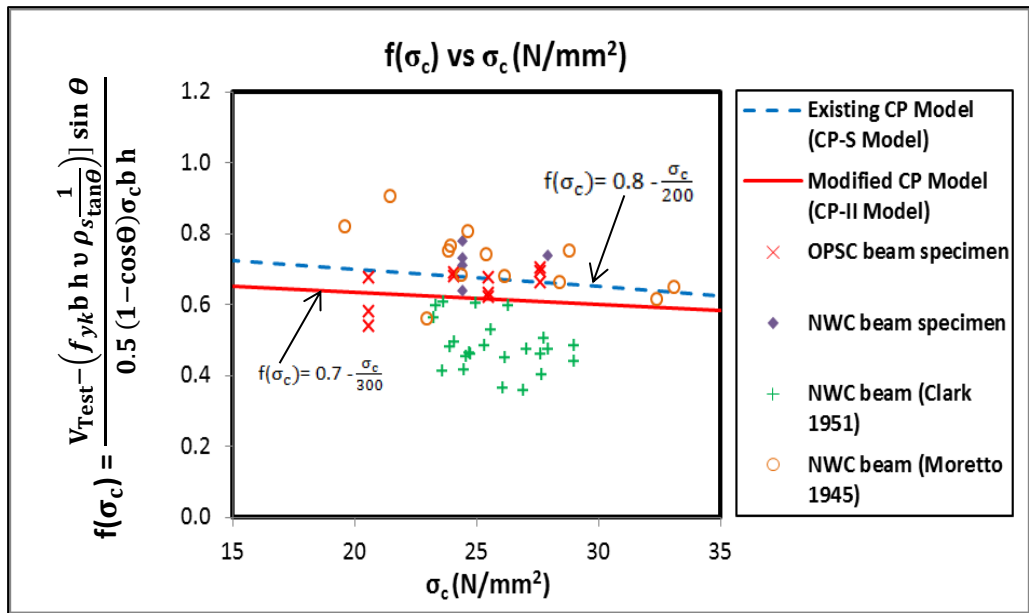


Figure 5.9 $f(\sigma_c)$ vs σ_c (N/mm²) for Existing CP Model (CP-S Model) and Modified CP Model (CP-II Model).

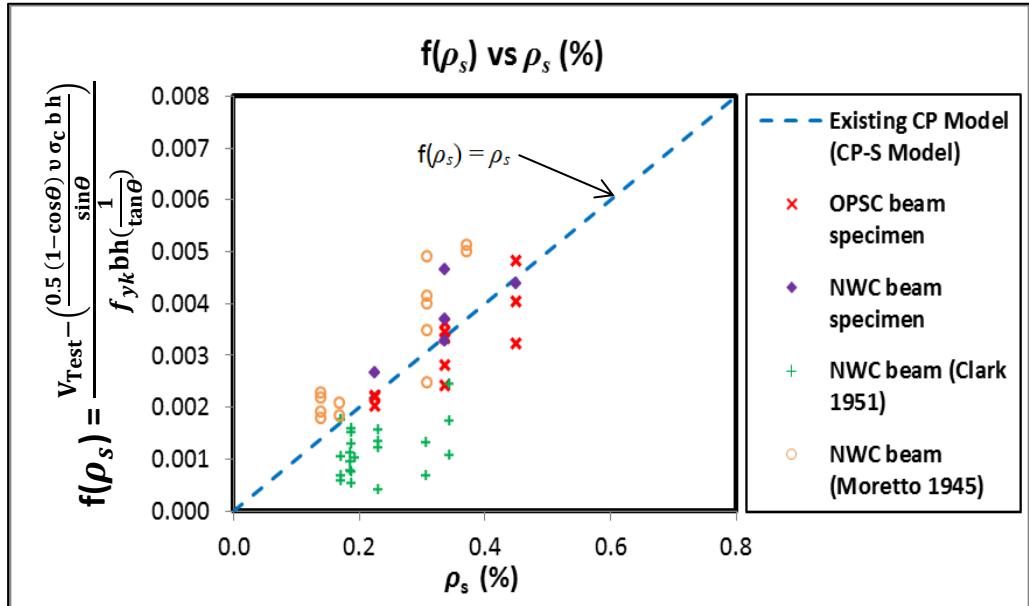


Figure 5.10 $f(\rho_s)$ vs ρ_s (%) for Existing CP Model (CP-S Model).

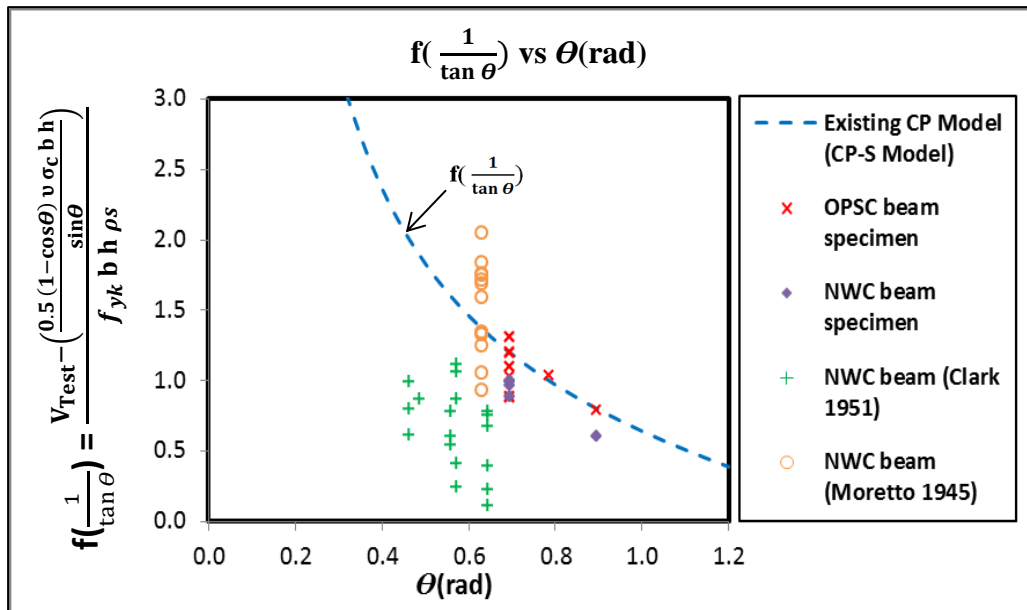


Figure 5.11 $f(\frac{1}{\tan \theta})$ vs $\theta(\text{rad})$ for Existing CP Model (CP-S Model).

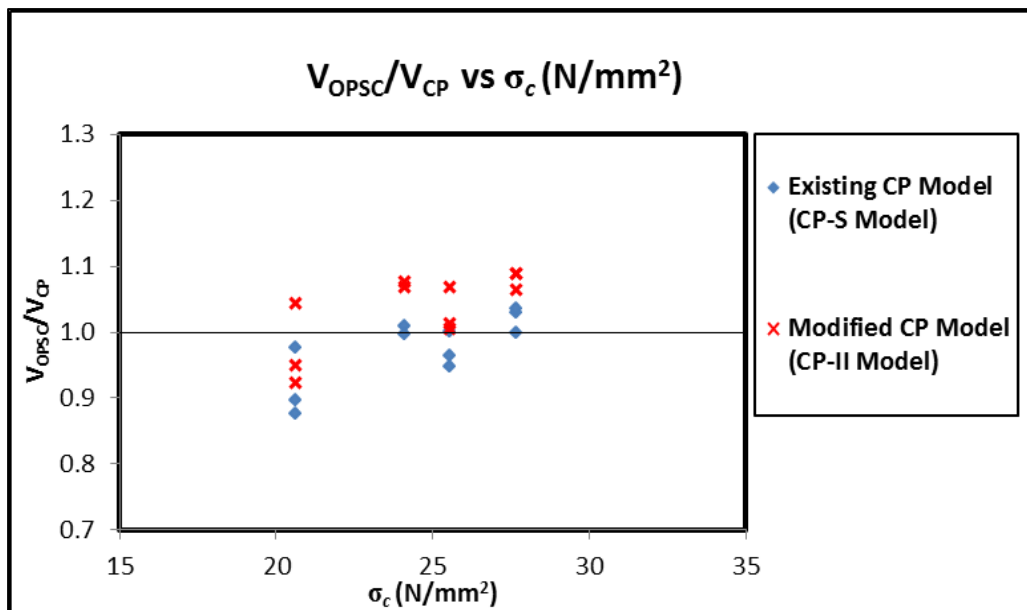


Figure 5.12 V_{OPSC}/V_{CP} vs Cylindrical concrete compressive strength, σ_c (N/mm^2).

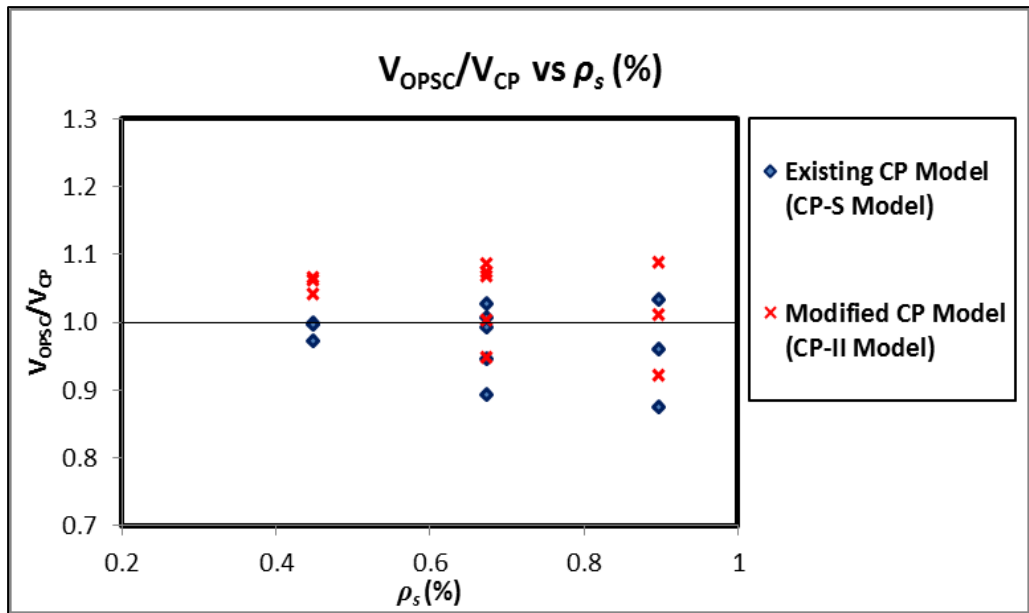


Figure 5.13 V_{OPSC}/V_{CP} vs Shear reinforcement ratio, ρ_s (%).

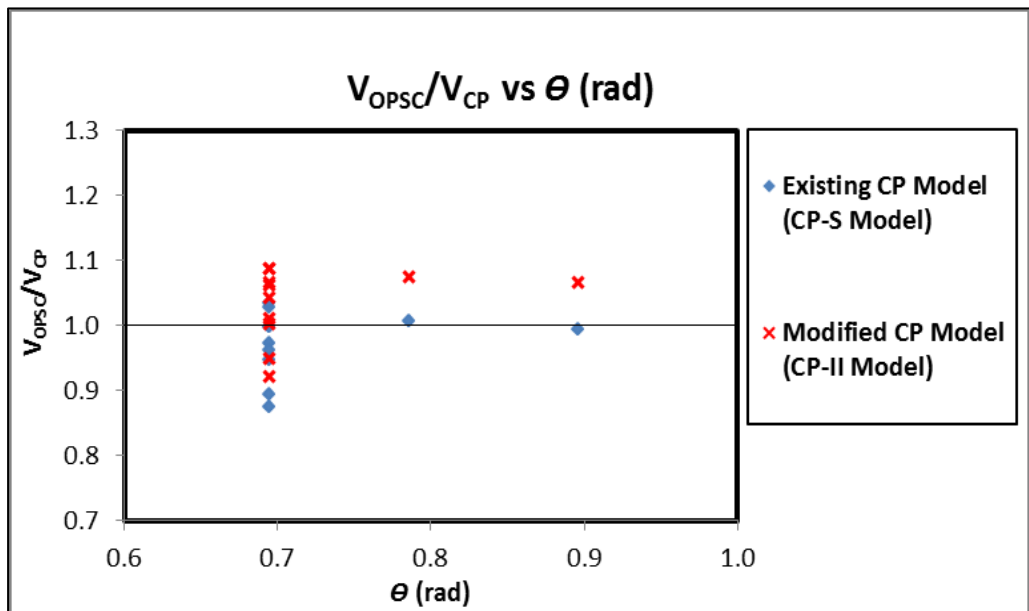


Figure 5.14 V_{OPSC}/V_{CP} vs Inclination angle of shear cracks, θ (rad).

Chapter 6

BS8110 Design Models

6.1 Introduction

In Chapter 4, the test observations, the test results, the failure mechanism and the effect of parameters were fully described. It was noted that variations on the ultimate shear strength was observed between the Oil Palm kernel Shell Concrete (OPSC) beams and Normal Weight Concrete (NWC) beams, both cast with and without shear reinforcement. Hence, in Chapter 5, two modified theoretical models based on upper bound plastic approach were proposed for predicting the ultimate shear capacity of Oil Palm kernel Shell Concrete (OPSC) beams cast with and without shear reinforcement, respectively, which good agreement with test results have been achieved

The existing BS8110 design model (BS8110-NS Model) [46] took into account the parameter of span to effective depth ratio (a/d), longitudinal steel ratio (ρ), cube concrete compressive strength (f_{cu}), and effective section depth (d), for the ultimate shear strength predictions of NWC beam cast without shear reinforcement (see Section 2.2.1.4.1). Whilst for NWC beam cast with shear reinforcement, the existing BS8110 model (BS8110-S Model) considered the parameter of concrete cylinder compressive strength (f_{ck}), span to effective depth ratio (a/d) and shear reinforcement ratio (ρ_s) to be the function of the ultimate shear strength predictions (see Section 2.2.2.4.1).

In this chapter, investigations on the requirements for modification on shear strength parameters are reported for both cases of beams cast with and without shear reinforcement. From the current investigations, two BS8110 design model: BS8110-I Model and BS8110-II Model are proposed for OPSC beam cast without and with shear reinforcement, respectively.

For OPSC beam without shear reinforcement, BS8110-I Model modified the parameters' equations of span to effective depth ratio (a/d), and effective section depth (d). Whilst for OPSC beam with shear reinforcement, BS8110-II Model modified the parameter: span to effective depth ratio (a/d). Full detail of the predictions models: BS8110-I Model and BS8110-II Model are presented in Section 6.2 and 6.3, respectively.

A point to note in this chapter is that the partial safety factor, γ_m , for both concrete and steel reinforcement is equal to 1 in the ultimate shear strength equation. Furthermore, it is to be noted that the concrete strength, f_{cu} in both the existing and modified BS8110 design models is based on the cube compressive strength of concrete, which were obtained from the tested 100 mm cubes specimens. The tested 100 mm cube specimens were casted from the same concrete batch with the concrete beam specimens.

6.2 Beams cast without shear reinforcement

6.2.1 BS8110 design model for concrete beam without shear reinforcement, (BS8110-I Model)

The proposing “BS8110-I” Model is developed to predict the ultimate shear resistance of a reinforced concrete beam element cast using Oil Palm kernel Shell (OPS) as coarse aggregate. Since a significant similarity has been observed in Section 4.2.1 for both failure mechanisms of OPSC and NWC beams cast without shear reinforcement, the test results of OPSC beams were then compared with the predictions of the existing BS8110 design model (BS8110-NS Model) to evaluate whether the model is relevant (see Column 2 and 3 in Table 6.1).

Summary of the comparisons are presented in Table 6.1 (Column 5). It can be noted that the existing model underestimated the ultimate shear strength capacity of OPSC beam specimens cast without shear reinforcement with a mean value of 1.35 and standard deviation of 0.16. The test results were then further evaluated with respect to the associating parameters: span to effective depth ratio (a/d), longitudinal steel ratio (ρ), cube concrete compressive strength (f_{cu}), and effective section depth (d).

The results of these evaluations review that the existing BS8110 model (BS8110-NS Model) does not give good agreement with the ultimate shear resistance of OPSC beam specimens. Therefore, it is decided to carry out modifications to the parameters to reflect the observations made from the test. The modifications of parameters consist of span to effective depth ratio (a/d), and effective section depth (d). The parameters modified are; span to effective depth ratio (a/d), and effective section depth (d). Such modifications are required to accommodate for the variations

observed from tests, such as underestimations of the parameters span to effective depth ratio, $a/d \leq 2.5$, and effective section depth, $d = 82$ mm.

6.2.2 Modification on parameters

It was noted from Section 6.2.1 that the existing BS8110 design model (BS8110-NS Model) underestimated the ultimate shear strength of OPSC beams cast without shear reinforcement. Hence, further analyses were carried out to assess the relevancy of the parameters: (1) span to effective depth ratio (a/d), (2) cube concrete strength (f_{cu}), (3) longitudinal steel ratio (ρ) and (4) effective section depth (d), governing the existing BS8110 design model and to provide with appropriate modifications, which full details are elaborated in Section 6.2.2.1 to 6.2.2.4.

6.2.2.1 Span to effective depth ratio, a/d

It can be noted from Figure 6.1 that the existing BS8110 design model (BS8110-NS Model) underestimated the rate of increase in the ultimate shear strength of OPSC beams as span to effective depth, a/d , decreases. Such discrepancy is believed to be attributed to expression (Eqn 2.19.1) given by the existing BS8110 model (BS8110-NS Model), which took into account the increment of ultimate shear strength with the reduction of span to effective depth ratio for beams loaded with $a/d \leq 2$.

In general, from the current research (Section 4.2.3.1), it is noted that the failure modes varied for OPSC beams loaded with $a/d < 2.5$ and $a/d \geq 2.5$, respectively. That is, shear compression failure occurred for beams loaded with $a/d < 2.5$ whilst shear failure or diagonal tension failure occurred for beams loaded with $a/d \geq 2.5$. Therefore, the existing expression was revised to be Eqn 6.1.1 to accommodate for

both the rate of increase in shear capacity as span to effective depth (a/d) reduces and the two distinct failure modes observed for beams loaded with $a/d < 2.5$ and $a/d \geq 2.5$. With the revised expression for span ratio (Eqn 6.1.1), good agreement with test results are achieved (see Figure 6.1).

$$f\left(\frac{a}{d}\right) = 2.5 \frac{d}{a} \quad \left(\frac{a}{d} < 2.5\right) \quad (\text{Eqn 6.1.1})$$

6.2.2.2 Longitudinal steel ratio, ρ

It can be noted in Figure 6.2 that the shear failure loads of OPSC specimens are lower than the NWC control specimens. Test observations also indicate that the ultimate shear strength obtained by OPSC specimens (Specimen 16C and 20E) were lower than those of NWC beam specimens (Specimen NWC1 and NWC4) (see Figure 4.44). It is believed such discrepancy observed in the shear strength between NWC and OPSC beams is due to the variations found in the fracture strength of coarse aggregates. That is, lower fracture strength found in the OPS aggregates (see Table 2.1) would have led to lower aggregate interlocking capacity, and resulted in lower shear resistance mobilised by OPSC beam.

However, it can be observed from Figure 6.2 that the shear failure loads of OPSC specimens are slightly higher than the predictions derived from the existing BS8110 design model (BS8110-NS Model) (Eqn 2.19.2). Thus, the existing expression (Eqn 2.19.2) are satisfactory since the $f(\rho)$ of the ultimate shear strength predictions derived from the existing BS8110 design model (BS8110-NS Model) slightly underestimated the shear failure loads of the OPSC beams. Hence, adequate predictions of shear strength increment would be provided for the OPSC beams as longitudinal steel ratio increases. The existing parameter longitudinal reinforcement

ratio's equation (Eqn 2.19.2) is therefore adopted into the modified BS8110 design model (BS8110-I Model) to accommodate for the increment of the ultimate shear strength of OPSC beam as longitudinal steel ratio increases.

6.2.2.3 Cube concrete strength, f_{cu}

It can be noted from Figure 6.3 that the shear failure loads of OPSC specimens with respect to cube concrete strength parameter, $f(f_{cu})$ were observed to be lower to those of NWC control specimens. Observations found from test indicate that the ultimate shear strength obtained by OPSC beam specimens (Specimen 16C and F1) were lower than those of NWC control specimens (Specimen NWC2 and NWC3) (see Figure 4.46). It is believed that the lower shear failure loads of OPSC beams is believed due to the lower fracture strength found in the OPS aggregates (see Table 2.1) would have led to shear stress to be transferred across the shear cracks, and resulted in lower shear resistance mobilised by OPSC beam.

However, it can be noted from Figure 6.3 that the shear failure loads of OPSC specimens with respect to the cube concrete strength $f(f_{cu})$ are slightly higher in comparison to the predictions derived from the existing BS8110 model (BS8110-NS Model) (Eqn 2.19.3). Since the predictions derived from the existing BS8110 design model (BS8110-NS Model) with respect to $f(f_{cu})$ slightly underestimated the shear failure loads of the OPSC beams, the existing expression are therefore acceptable. Hence, the existing parameter cube concrete strength's equation (Eqn 2.19.3) are adopted into the modified BS8110 design model (BS8110-I Model) to take into account for the increment in the ultimate shear strength of OPSC beam as the concrete compressive strength increase.

6.2.2.4 Beam effective depth, d

It can be noted from Figure 6.4 that the shear failure loads of both OPSC specimens and NWC control specimens with effective section depth, $d = 82 \text{ mm}$ ($h=113 \text{ mm}$) are higher compared to the existing BS8110 design model (BS8110-NS model) (Eqn 2.19.4). However, observations from test observations indicate that for beams with $d = 82\text{mm}$, the ultimate shear failure loads obtained by the OPSC and NWC beams (Specimen 12F and NWC5) are comparable with variances of 4% (see Figure 4.48).

Whilst for beams with effective depth, $165 \leq d \leq 167$, the shear failure loads of OPSC beam specimens were noted to be lower than those of NWC control specimens (See Figure 6.4). It is believed that such discrepancy is due to the lower aggregate strength found in Oil Palm kernel Shell (OPS) compared to that found in normal aggregates. Hence, this would have led to lower aggregate interlocking capacity, and as a result, lower ultimate shear resistance was mobilised.

Therefore, the existing equation was revised to be Eqn 6.1.2 to take into account for the rate of increase in shear capacity with respect to the reduction in effective section depth, d . With the revised expression for effective section depth (Eqn 6.1.2), good agreement with test results are achieved, as shown In Figure 6.4.

$$f(d) = \frac{380^{1/4}}{d} \quad (d \text{ in mm}) \quad (\text{Eqn 6.1.4})$$

6.2.3 Comparisons with test results

From the modifications of parameters proposed in Section 6.2.2 for the shear strength predictions of OPSC beams without shear reinforcement, the proposing modified BS8110 design model (BS8110-I Model) is given as:

For $a/d \leq 2$,

$$V_{Rdc} = \frac{0.79 \left(\frac{100 A_s}{b_v d}\right)^{1/3} \frac{380^{1/4}}{d} \left(\frac{f_{cu}}{25}\right)^{1/3} \frac{2.5 d}{a}}{\gamma_m} b d \quad (\text{Eqn 6.2})$$

For $a/d > 2$,

$$V_{Rdc} = \frac{0.79 \left(\frac{100 A_s}{b_v d}\right)^{1/3} \frac{380^{1/4}}{d} \left(\frac{f_{cu}}{25}\right)^{1/3}}{\gamma_m} b d \quad (\text{Eqn 6.3})$$

Where,

γ_m = partial factor of material

It can be noted from Figure 6.5 to 6.8 that the modified BS8110 design model (BS8110-I Model) (Eqn 6.2 and 6.3 for beams loaded with $a/d < 2.5$ and $a/d \geq 2.5$, respectively), with respect to parameters: shear span to height ratio (a/h), longitudinal steel ratio (ρ), concrete strength (σ_c), and overall section depth (h), exhibited good agreement with the test results (mean value of 1.03 and standard deviation of 0.15 as shown in see Table 6.1 Column 6).

6.3 Beams cast with shear reinforcement

6.3.1 BS8110 design model for concrete beam with shear reinforcement, (BS8110-II Model)

The proposing (BS8110-II Model) is developed to predict for the ultimate shear resistance of a reinforced concrete beam element with shear reinforcement cast using Oil Palm kernel Shell (OPS) as coarse aggregate. The BS8110-II model is basically the existing upper bound BS8110 design model (BS8110-S Model) (Eqn 2.44 and 2.45) with approximate modifications to its parameters.

Since both of the OPSC and NWC beams exhibited similar failure mechanism (see Chapter 4.3), hence, the test results were then compared with the predictions of the existing BS8110-S model (Eqn 2.44 and Eqn 4.45) to determine whether the relevancy of the existing model (see Column 2 and 3 in Table 6.2). The comparisons have been summarized and presented in Column 5 of Table 6.2. It can be noted that the existing model underestimated the ultimate shear strength capacity of OPSC beam specimens cast with shear reinforcement with a mean value of 1.25 and standard deviation of 0.18. The results of these evaluations indicate that the existing model does not give good agreement with the ultimate shear resistance of OPSC beam specimens. The test results were then further evaluated with respect to the parameters (see Section 6.3.2.1 to 6.3.2.4). As a result, a modification to the parameter was carried out on the parameters to reflect the observations derive from the analyses and test. The parameter modified is span to depth ratio (a/d). Such modification is required to allow better agreement to be achieved between the BS8110 design model and OPSC beams with shear reinforcement for the increased rate of shear failure when the specimens as the load was loaded near to the support, $a/d < 2.5$.

6.3.2 Modification on parameters

From Section 6.3.1, it was noted that the existing BS8110 design model (BS8110-S Model) for the ultimate shear strength predictions of OPSC beam with shear reinforcement underestimated the ultimate shear strength of the OPSC beams with shear reinforcement. Hence, further analyses were carried out to evaluate the relevancy of the parameters: (1) Shear reinforcement ratio ($\frac{A_{sw}}{s}$), (2) Cube concrete strength, (f_{cu}) and (3) span to effective depth ratio (a/d), and to provide appropriate modifications of the parameters as described in Section 6.3.2.1 to 6.3.2.3, respectively.

6.3.2.1 Shear reinforcement ratio, $\frac{A_{sw}}{s}$

In general, it can be noted from Figure 6.11 that the shear failure loads of OPSC beam specimens with respect to Shear reinforcement ratio, $f(\frac{A_{sw}}{s})$ were observed to be slightly higher to those of NWC control samples. It is believed that higher shear strength noted in OPSC beams is attributed to the rougher surface texture observed in OPSC beams compared to NWC beams (See figure 4.70 and 4.71). Therefore, this would have led to higher shear stress to be transferred across the shear cracks, and as a result, higher shear resistance was mobilised.

However, it can be noted from Figure 6.11 that the mean shear failure loads of OPSC beams is slightly higher than the predictions derived from the existing BS8110 design model (BS8110-S Model). Therefore, modification was not recommended for the parameter shear reinforcement ratio since the existing expression (Eqn 2.46.1) is satisfactory. The existing expression (Eqn 2.46.1) is therefore adopted into the

proposed modified BS8110 design model (BS8110-II Model) to take into account for the increment of ultimate shear strength of OPSC beam as the shear reinforcement ratio increases.

6.3.2.2 Cube concrete strength, f_{cu}

In general, it can be noted from Figure 6.12 that the shear failure loads of OPSC beam specimens with respect to cube concrete strength parameter, f_{cu} were observed to be slightly higher to those of NWC control samples. It is believed that such discrepancy in shear strength between NWC and OPSC beams is attributed to the rougher surface texture observed in OPSC beams compared to NWC beams, as shown in Figure 4.70 and 4.71. Hence, this would have led to higher shear stress to be transferred across the shear cracks, and as a result, higher shear resistance was mobilised.

However, from the Figure 6.12, observation exhibit that the mean shear failure loads of OPSC specimens with respect to the cube concrete strength f_{cu} , of specimens cast with shear reinforcement is slightly higher than the predictions derived from the existing BS8110 design model (BS8110-S Model) (Eqn 2.46.2). Since the predictions derived from the existing BS8110 design model (BS8110-S Model) with respect to f_{cu} marginally underestimated the mean of shear failure loads of OPSC beams, the existing expression are therefore acceptable. Hence, the existing parameter concrete compressive strength's equation (Eqn 2.46.2) are adopted into the proposed modified BS8110 design model (BS8110-II Model) to account for the increment in the ultimate shear strength of OPSC beam as concrete compressive strength increases.

6.3.2.3 Span to effective depth ratio, a/d

In general, it can be noted from Figure 6.13 that as the span to effective depth ratio (a/d) decreases, the rate of increase of ultimate shear strength for OPSC specimens are more pronounced than the prediction derived from the existing BS8110 design model (BS8110-S Model) (Eqn 2.46.3). That is, the existing BS8110 design model (BS8110-S Model) underestimated the increment of the ultimate shear strength of OPSC beams with respect to low a/d ratio of 2.5. Such discrepancies arose due to the existing expression given by the existing BS8110 model (BS8110-S Model), which took into account for the rate of increment in ultimate shear strength as the span to effective depth ratio reduces for beams loaded at $a/d \leq 2$.

Therefore, the existing expression (Eqn 2.46.3) was revised to be Eqn 6.4 to allow for better agreement with the test results for the rate of increase in shear capacity as span to effective depth ratio (a/d) decreases. With the revised expression for span ratio (Eqn 6.4), good agreement with test results are achieved (see Figure 6.14).

$$f\left(\frac{a}{d}\right) = 2.5 \frac{d}{a} \quad \left(\frac{a}{d} < 2.5\right) \quad (\text{Eqn 6.4})$$

6.3.3 Comparisons with test results

From the modifications of parameters proposed in Section 6.3.2 for the shear strength predictions of OPSC beams with shear reinforcement, the proposing modified BS8110 design model (BS8110-II Model) is given as:

$$\text{For } \frac{a}{d} < 2.5,$$

$$V_{\text{BS8110-II}} = \left[\frac{0.79 \rho^{1/3} \frac{f_{cu}^{1/3}}{25} \frac{400^{1/4}}{d} 2.5 \frac{d}{a}}{\gamma_m} + 0.87 \frac{f_{yw}}{b} \frac{A_{sw}}{s} \right] b d \quad (\text{Eqn 6.5})$$

For $\frac{a}{d} \geq 2.5$,

$$V_{BS8110-I} = \left[\frac{0.79 \rho^{1/3} \frac{f_{cu}^{1/3}}{25} \frac{400^{1/4}}{d}}{\gamma_m} + 0.87 \frac{f_{yw}}{b} \frac{A_{sw}}{s} \right] b d \quad (\text{Eqn 6.6})$$

From Figure 6.15 to Figure 6.17, it can be observed that the modified BS8110 design model based upon upper bound approach (BS8110-II Model) (Eqn 6.5 and 6.6), which adopted the modification via the parameter's equation of span to effective depth (a/d), exhibited good agreement with the test results, where a mean value of 1.11 and standard deviation of 0.16 is achieved (see also Table 6.2 Column 6).

6.4 Summary

Two empirical BS8110 design models based upon the modification of existing BS8110 design models have been proposed in this chapter: BS8110-I Model for OPSC cast without shear reinforcement and BS8110-II Model for OPSC cast with shear reinforcement.

The BS8110-I Model were proposed for OPSC beams cast without shear reinforcement, which resulted from the modification of parameters' equations of the existing BS8110 Model. The modified parameters' equations were the span to effective depth ratio (a/d), and the effective section depth (d), for the ultimate shear strength predictions.

Whilst for OPSC beams cast with shear reinforcement, modified BS8110-II Model were proposed, which were based upon the modified parameter's equation of span to effective depth (a/d) of the existing BS8110 Model, for the ultimate shear strength predictions. In general, all the modified BS8110 design models have achieved good agreement with Author's test results for OPSC beams.

Table 6.1: Comparisons of shear strength predictions with respect to the test results of OPSC beams cast without shear reinforcement

1	2	3	4	5	6
Specimen No	V_{OPSC} (kN)	$V_{BS8110-NS}$ (kN)	$V_{BS8110-I}$ (kN)	$\frac{V_{OPSC}}{V_{BS8110-NS}}$	$\frac{V_{OPSC}}{V_{BS8110-I}}$
10A	18.95	16.80	21.48	1.06	0.88
S1	21.05	18.69	22.56	1.13	0.93
12A	54.73	40.52	61.24	1.35	0.89
12B	40.00	26.02	40.83	1.48	0.98
12C	27.37	20.26	24.50	1.35	1.12
12D	25.26	20.26	24.50	1.25	1.03
12E	31.58	21.90	26.48	1.44	1.19
12F	26.31	15.22	22.04	1.73	1.19
16A	56.80	46.13	69.92	1.23	0.81
16B	42.10	30.76	46.62	1.37	0.90
16C	29.50	23.07	26.97	1.28	1.05
16D	26.32	23.07	26.97	1.14	0.94
16E	35.79	24.79	30.06	1.44	1.19
20A	73.68	52.48	78.96	1.40	0.93
20B	52.63	34.99	52.64	1.50	1.00
20C	33.68	26.24	31.58	1.28	1.07
20D	26.37	26.24	31.58	1.04	0.87
20E	35.79	26.25	33.14	1.31	1.08
AD1	58.19	49.35	74.80	1.18	0.78
AD2	32.33	24.68	29.92	1.31	1.08
F1	32.67	24.77	30.04	1.32	1.09
F2	47.41	26.60	32.26	1.78	1.47
H2	52.53	35.58	45.21	1.48	1.16
S2	36.64	25.05	31.03	1.43	1.18
			Mean	1.35	1.03
			S.D.	0.18	0.15

V_{OPSC} (kN) = Ultimate shear failure load of OPSC beam specimens cast without shear reinforcement

$V_{BS8110-NS}$ (kN) = Shear resistance of Existing BS8110 design Model (BS8110-NS Model)

$$\text{For } a/d \leq 2, V_{BS8110-NS} = \frac{0.79 \left(\frac{100 A_s}{b_v d}\right)^{1/3} \left(\frac{400}{d}\right)^{1/4} \left(\frac{f_{cu}}{25}\right)^{1/3} \frac{2d}{a}}{\gamma_m} b d$$

$$\text{For } a/d > 2, V_{BS8110-NS} = \frac{0.79 \left(\frac{100 A_s}{b_v d}\right)^{1/3} \left(\frac{400}{d}\right)^{1/4} \left(\frac{f_{cu}}{25}\right)^{1/3}}{\gamma_m} b d$$

$V_{BS8110-I}$ (kN) = Shear resistance of proposing Modified BS8110 design Model (BS8110-I Model)

$$\text{For } a/d < 2.5, V_{BS8110-I} = \frac{0.79 \left(\frac{100 A_s}{b_v d}\right)^{1/3} \left(\frac{380}{d}\right)^{1/4} \left(\frac{f_{cu}}{25}\right)^{1/3} \frac{2.5d}{a}}{\gamma_m} b d$$

$$\text{For } a/d \geq 2.5, V_{Rdc} = \frac{0.79 \left(\frac{100 A_s}{b_v d}\right)^{1/3} \left(\frac{380}{d}\right)^{1/4} \left(\frac{f_{cu}}{25}\right)^{1/3}}{\gamma_m} b d$$

Table 6.2: Comparisons of shear strength predictions with respect to the test results of OPSC beams cast with shear reinforcement

1	2	3	4	5	6
Specimen No	V_{OPSC} (kN)	$V_{BS8110-S}$ (kN)	$V_{BS8110-II}$ (kN)	$\frac{V_{OPSC}}{V_{BS8110-S}}$	$\frac{V_{OPSC}}{V_{BS8110-II}}$
3A	75.78	57.41	65.00	1.32	1.17
3B	88.41	59.65	67.79	1.48	1.30
3C	92.62	60.53	68.90	1.53	1.34
4A	79.99	70.94	78.53	1.13	1.02
4B	94.73	73.18	81.33	1.29	1.16
4C	107.36	74.07	82.43	1.45	1.30
5A	88.41	98.35	110.24	0.90	0.80
5B	107.36	101.86	114.63	1.05	0.94
5C	119.99	103.24	116.36	1.16	1.03
4D	101.04	78.96	88.55	1.28	1.14
4E	105.25	88.55	100.53	1.19	1.05
			Mean	1.25	1.11
			S.D.	0.18	0.16

V_{OPSC} (kN) = Ultimate shear failure load of OPSC beam specimens cast with shear reinforcement

$V_{BS8110-S}$ (kN) = Shear resistance of Existing BS8110 design Model (BS8110-S Model)

For $\frac{a}{d} \leq 2$,

$$V_{BS8110-S} = \left[\frac{0.79 \rho^{1/3} \frac{f_{cu}^{1/3}}{25} \frac{400^{1/4}}{d} 2 \frac{d}{a} + 0.87 \frac{f_{yw}}{b} \frac{A_{sw}}{s} \right] b d$$

For $\frac{a}{d} > 2$,

$$V_{BS8110-S} = \left[\frac{0.79 \rho^{1/3} \frac{f_{cu}^{1/3}}{25} \frac{400^{1/4}}{d} + 0.87 \frac{f_{yw}}{b} \frac{A_{sw}}{s} \right] b d$$

$V_{BS8110-II}$ (kN) = Shear resistance of proposing Modified BS8110 design Model (BS8110-II Model)

For $\frac{a}{d} < 2.5$,

$$V_{BS8110-II} = \left[\frac{0.79 \rho^{1/3} \frac{f_{cu}^{1/3}}{25} \frac{400^{1/4}}{d} 2.5 \frac{d}{a} + 0.87 \frac{f_{yw}}{b} \frac{A_{sw}}{s} \right] b d$$

For $\frac{a}{d} \geq 2.5$,

$$V_{BS8110-II} = \left[\frac{0.79 \rho^{1/3} \frac{f_{cu}^{1/3}}{25} \frac{400^{1/4}}{d} + 0.87 \frac{f_{yw}}{b} \frac{A_{sw}}{s} \right] b d$$

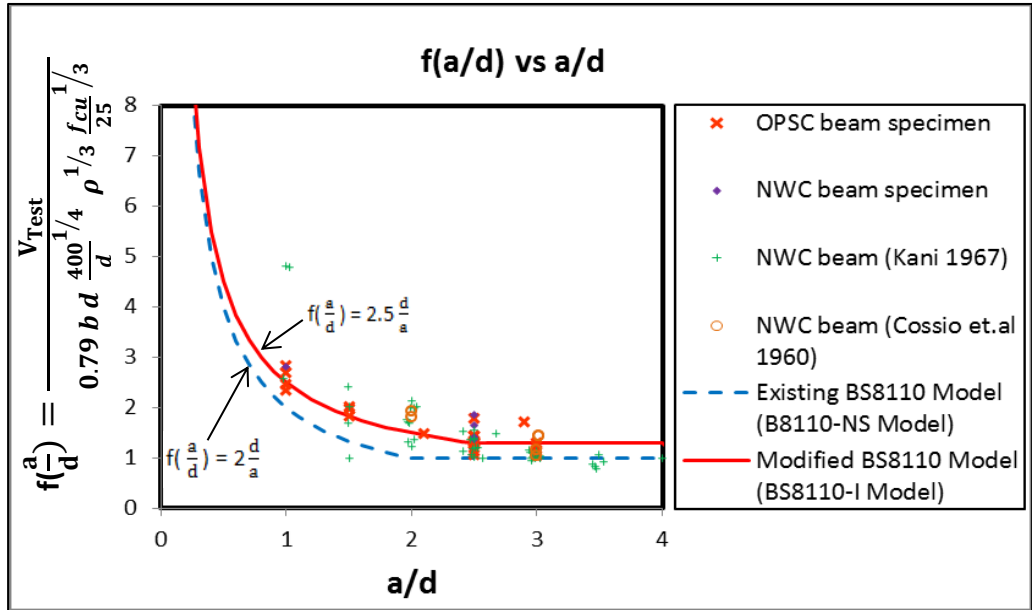


Figure 6.1 $f(a/d)$ vs a/d for Existing BS8110 design Model (BS8110-NS Model) and Modified BS8110 design Model (BS8110-I Model).

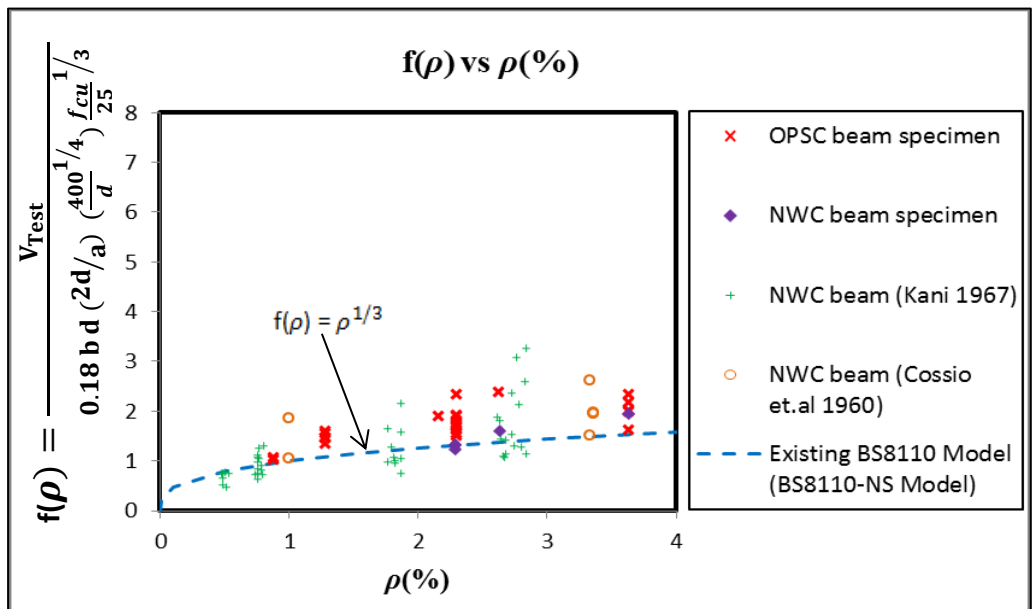


Figure 6.2 $f(\rho)$ vs $\rho(\%)$ for Existing BS8110 design Model (BS8110-NS Model).

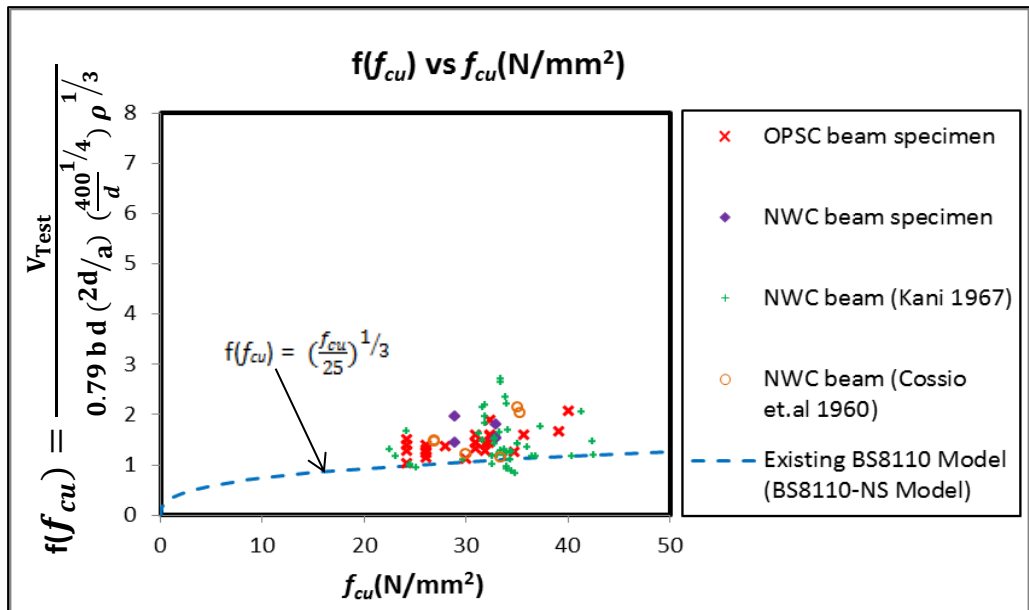


Figure 6.3 $f(f_{cu})$ vs f_{cu} (N/mm²) for Existing BS8110 design Model (BS8110-NS Model).

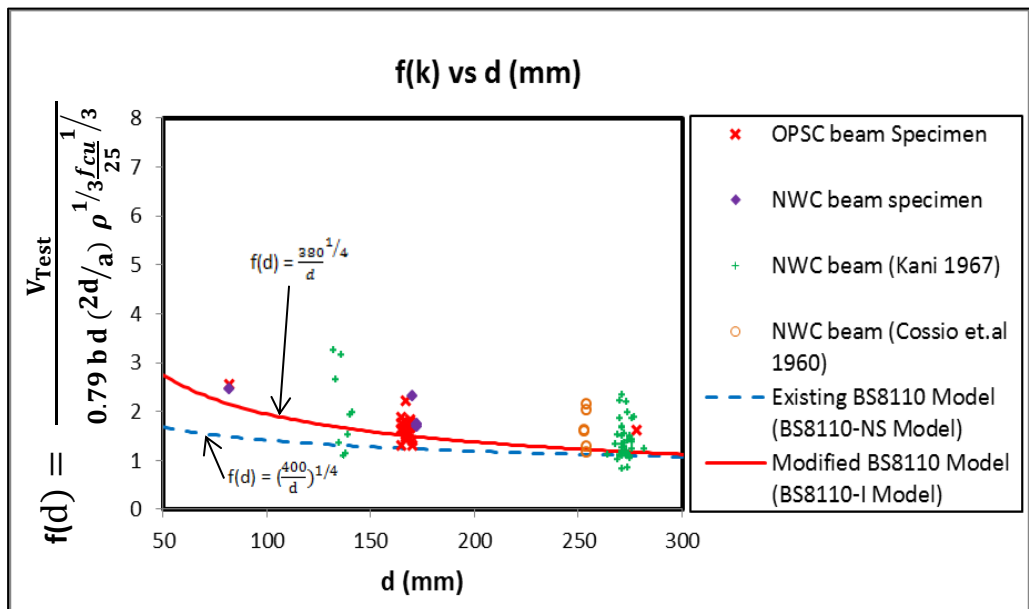


Figure 6.4 $f(d)$ vs d (mm) for Existing BS8110 design Model (BS8110-NS Model) and Modified BS8110 design Model (BS8110-I Model).

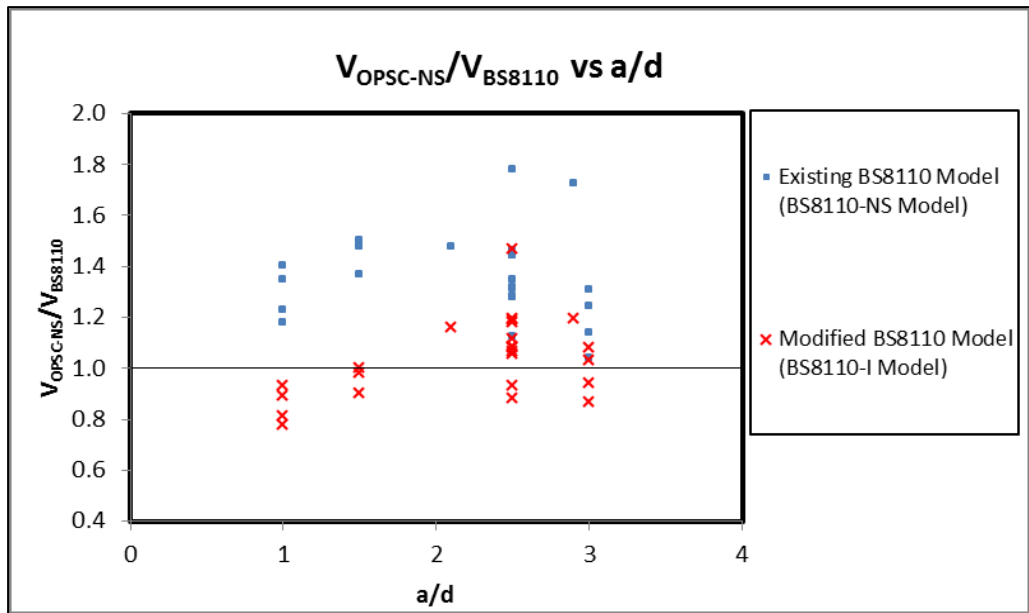


Figure 6.5 V_{OPSC}/V_{BS8110} vs Shear span to effective section depth, a/d .

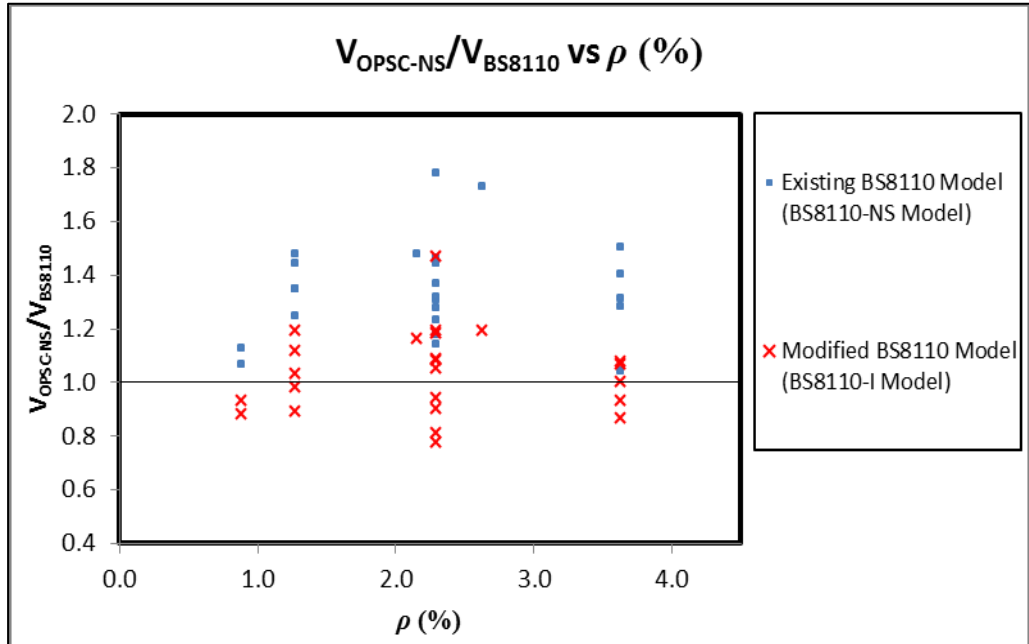


Figure 6.6 V_{OPSC}/V_{BS8110} vs Longitudinal steel ratio, ρ (%).

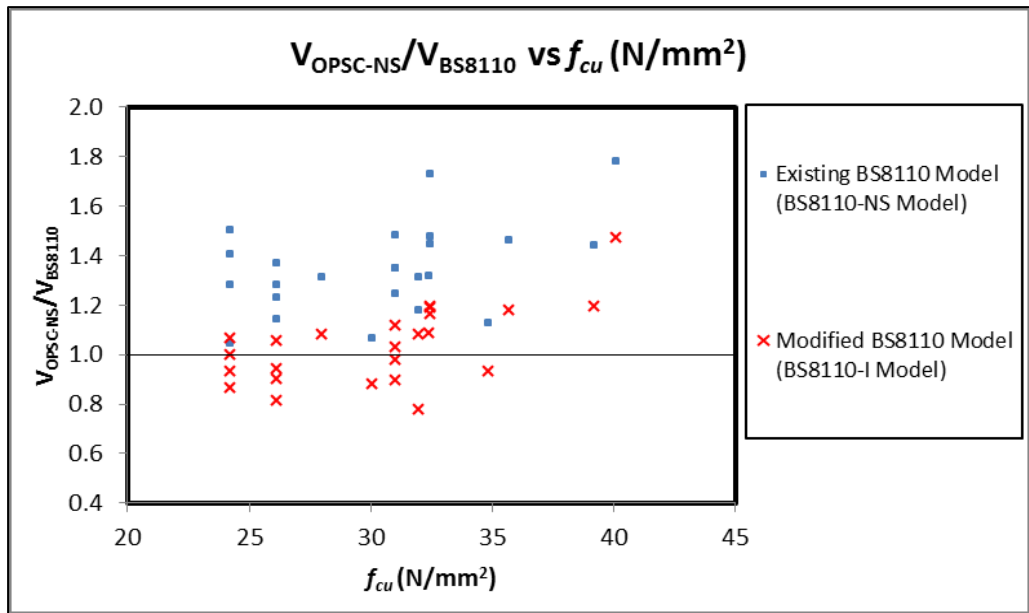


Figure 6.7 V_{OPSC}/V_{BS8110} vs Cube concrete strength, f_{cu} (N/mm²).

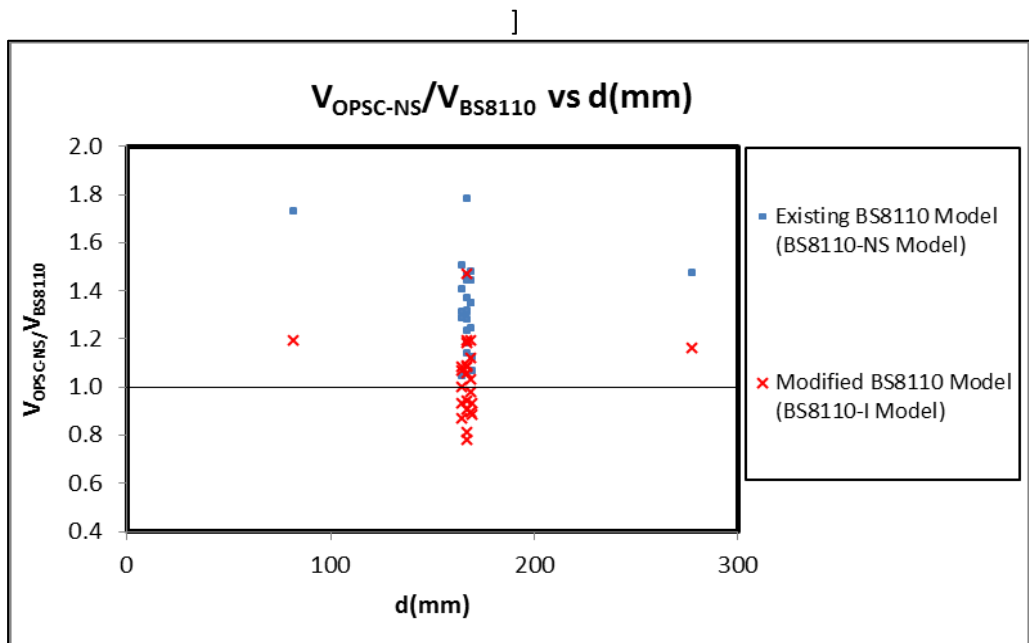


Figure 6.8 V_{OPSC}/V_{BS8110} vs Effective section depth, d (mm).

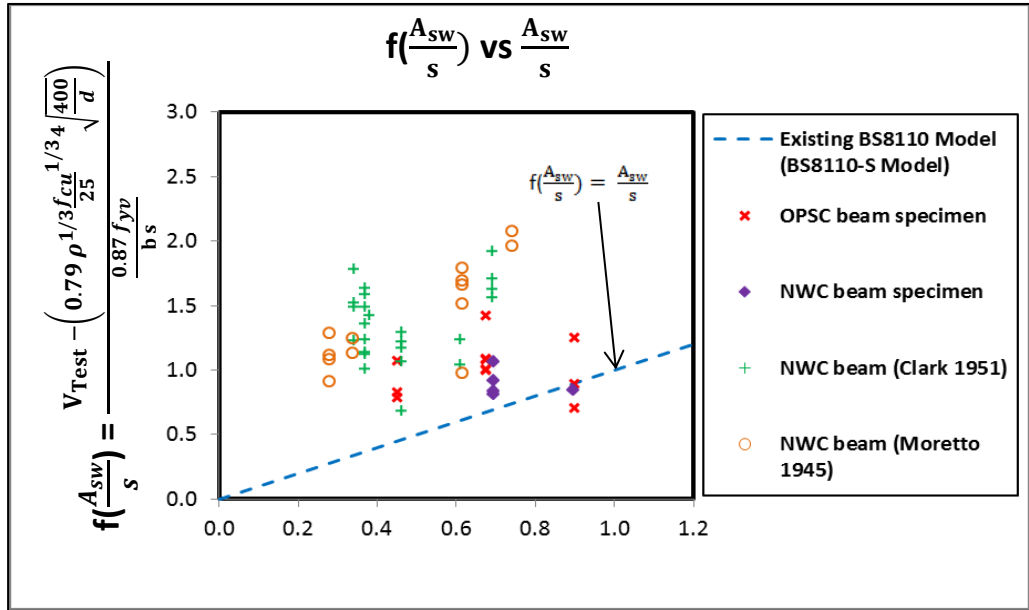


Figure 6.9 $f\left(\frac{A_{sw}}{s}\right)$ vs $\frac{A_{sw}}{s}$ for Existing BS8110 design Model (BS8110-S Model) and Modified BS8110 design Model (BS8110-II Model).

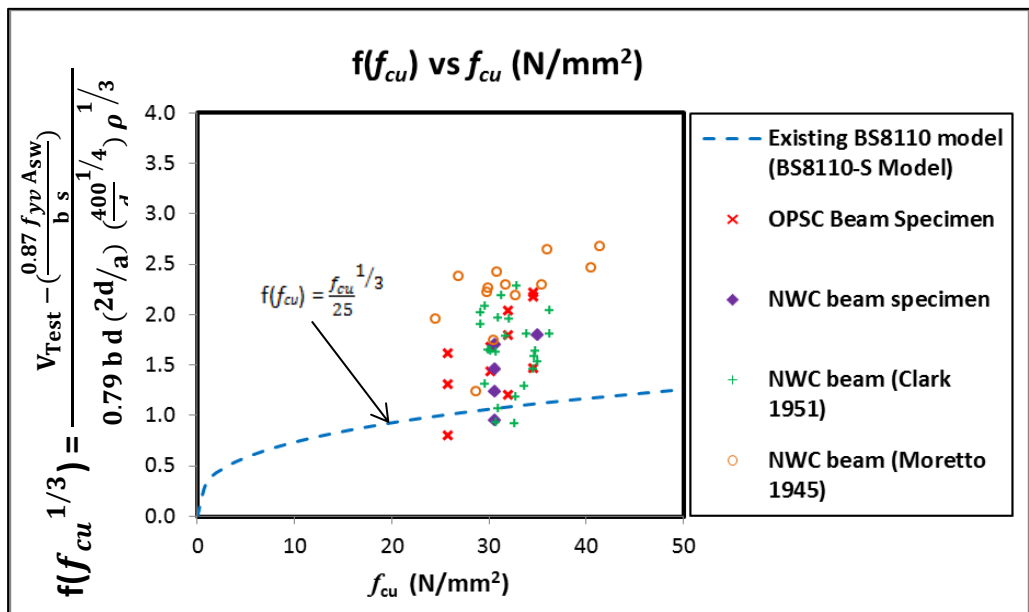


Figure 6.10 $f(f_{cu}^{1/3})$ vs f_{cu} (N/mm²) for Existing BS8110 design Model (BS8110-S Model).

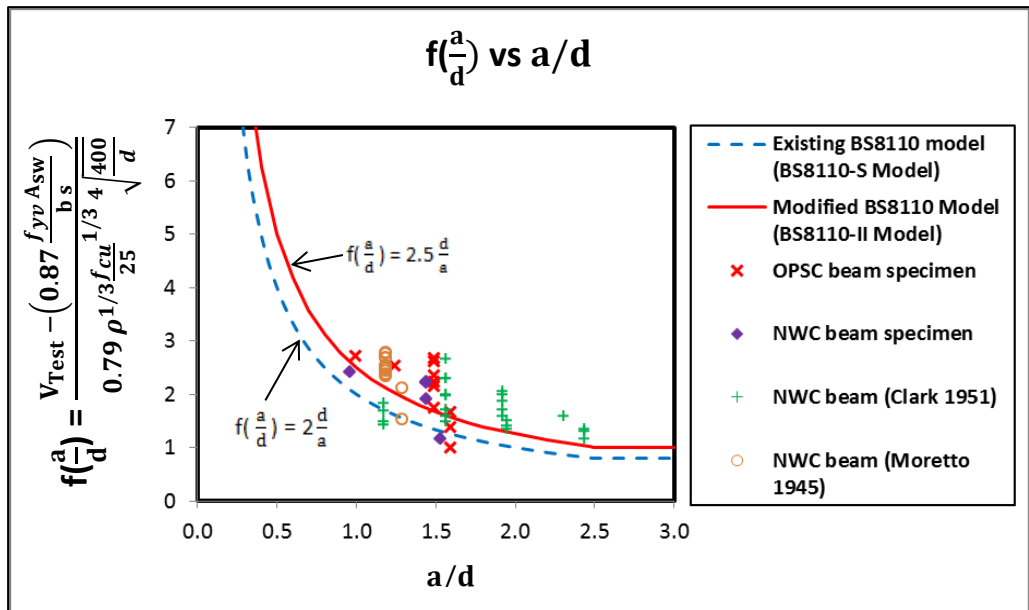


Figure 6.11 $f(a/d)$ vs a/d for Existing BS8110 design Model (BS8110-S Model) and Modified BS8110 design Model (BS8110-II Model).

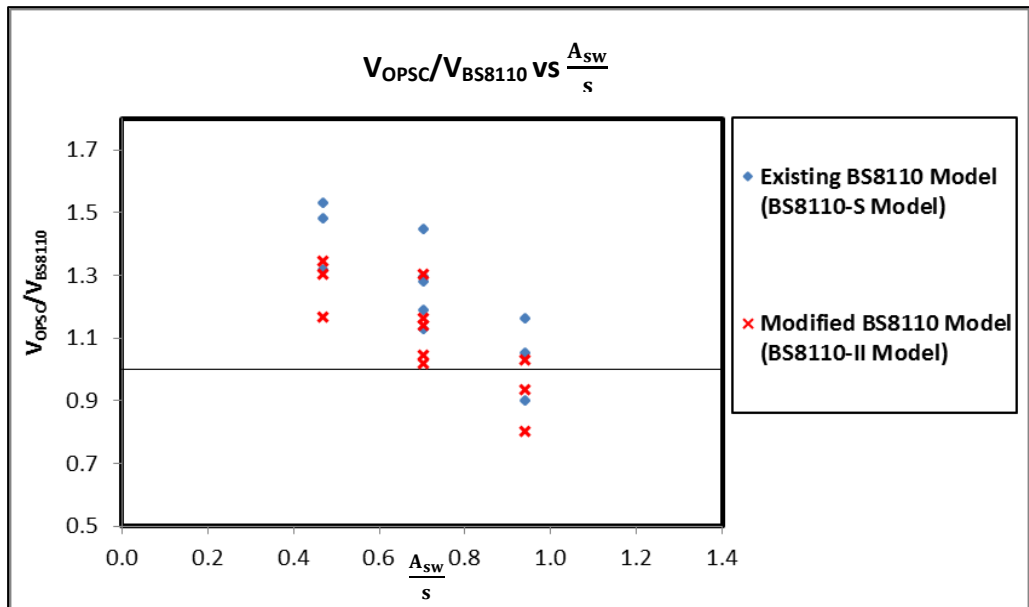


Figure 6.12 V_{OPSC}/V_{BS8110} vs Shear reinforcement ratio, $\frac{A_{sw}}{s}$.

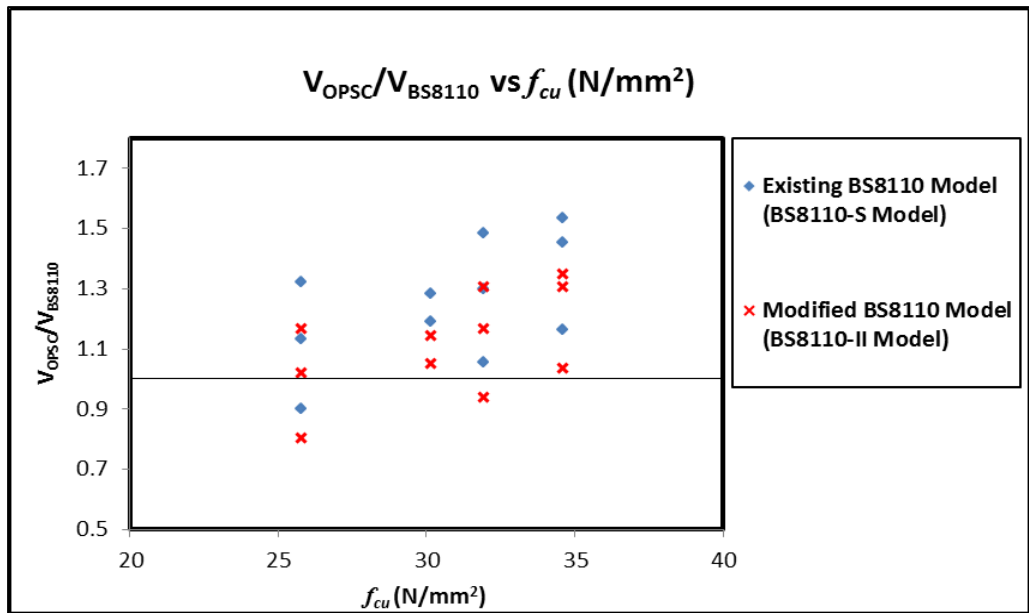


Figure 6.13 V_{OPSC}/V_{BS8110} vs Cube Concrete strength, f_{cu} (N/mm²).

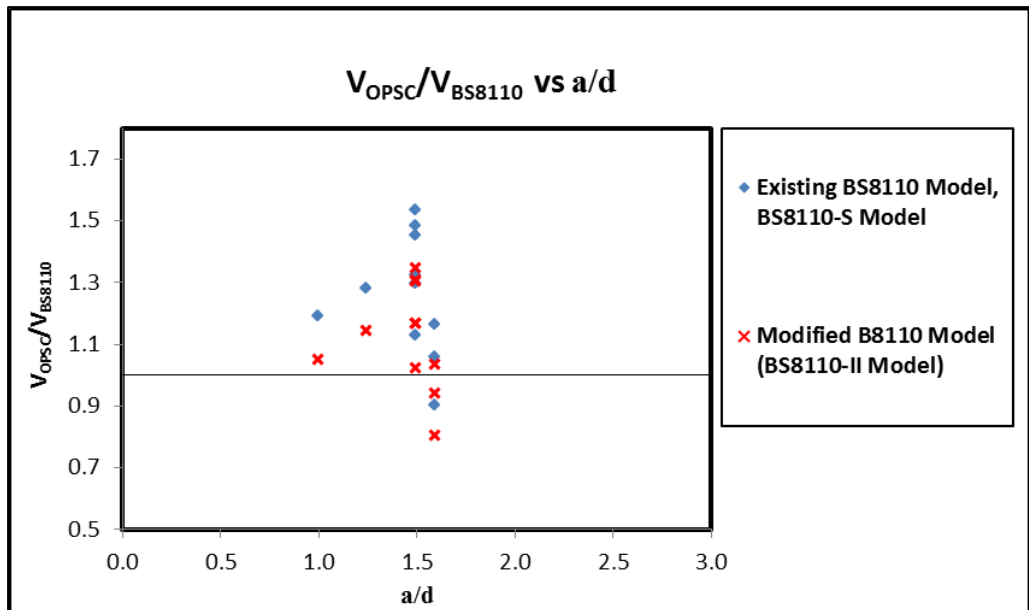


Figure 6.17 V_{OPSC}/V_{BS8110} vs Span to effective depth ratio, a/d .

Chapter 7

Eurocode 2 Design Models

7.1 Introduction

The test observations, the test results, the failure mechanisms and the effect of parameters were fully described in Chapter 4. It was noted that variations on the ultimate shear strength do occurred between the Oil Palm kernel Shell Concrete (OPSC) beams and Normal Weight Concrete (NWC) beams, both cast with and without shear reinforcement. In Chapter 5 and 6, two theoretical plastic models and two empirical BS8110 design models were presented, respectively. In Chapter 5 and 6, a model was proposed each for OPSC beams with and without shear reinforcement and it was noted that good agreement with the test results were achieved.

In this chapter, Eurocode 2 design model are considered for the shear strength predictions of the OPSC beam specimens. As mentioned in Section 2.2.1.4.2, the existing Eurocode 2 design model (EC2-NS Model) considered the shear strength predictions to be a function of parameters: (1) shear span to effective section depth ratio (a/d), (2) longitudinal steel ratio (ρ), (3) concrete cylindrical compressive strength (f_{ck}), and (4) effective section depth (d), to account for common variations that would occur in NWC beam cast without shear reinforcement. Whilst for NWC beam cast with shear reinforcement, the existing EC2 design model (EC2-S Model) considered the (1) concrete cylindrical compressive strength (f_{ck}), (2) inclination angle of shear cracks (θ), and (3) shear reinforcement ratio (ρ_s) as the parameters, which

influenced the ultimate shear resistance of NWC Beams with shear reinforcement (see Section 2.2.2.4.2).

In this chapter, investigations on the requirements for modification on shear strength parameters are reported for both cases of OPSC beams casting with and without shear reinforcement. From the investigations, two empirical design models (EC2-I Model and EC2-II Model), which are the results of modifications of the parameters, are proposed to predict for the ultimate shear capacity of Oil Palm kernel Shell Concrete (OPSC) beams cast without and with shear reinforcement, respectively.

For OPSC beam without shear reinforcement, EC2-I Model modified the parameters' equations of shear span to effective section depth ratio (a/d), longitudinal steel ratio (ρ), concrete compressive strength (f_{ck}), and effective section depth (d). Whilst for OPSC beam with shear reinforcement, EC2-II Model modified the parameter of shear reinforcement ratio (ρ_s) for the prediction of ultimate shear capacity of the beams. Full detail of the prediction models, EC2-I Model and EC2-II Model are presented in Section 7.2 and 7.3, respectively.

A point to note in this chapter is that the partial safety factor, γ_m , for both concrete and steel reinforcement is equal to 1 in the ultimate shear strength equation. In addition, it is to be noted that the concrete strength, f_{ck} in both the existing and modified Eurocode 2 design models is based on the cylindrical compressive strength of concrete, f_{ck} . Hence, a multiplication of 0.8 to the cube compressive strength, f_{cu} from the test data were adopted to convert the cube size of 100 mm wide and 100 mm height to cylindrical size of 150 mm diameter and 300 mm height to obtain the cylindrical compressive strength of concrete, f_{ck} , as suggested by Bill et. al [63] for concrete strength conversion of 100 mm cube to 150 diameter cylindrical.

7.2 Beams cast without shear reinforcement

7.2.1 Eurocode 2 design model for OPSC beam without shear reinforcement, "EC2- I model"

The proposing "EC2-I" Model is developed to predict for the ultimate shear resistance of a reinforced concrete beam element without shear reinforcement cast using Oil Palm kernel Shell Concrete (OPSC) as coarse aggregate.

The existing Eurocode 2 (EC2-NS Model) presented a formula for the ultimate shear strength predictions of NWC beam without shear reinforcement. The parameters considered by EC2-NS Model are (1) shear span to effective section depth ratio (a/d), (2) longitudinal steel ratio (ρ), (3) concrete cylindrical compressive strength (f_{ck}), and (4) effective section depth (d).

Since a significant similarity has been observed in Section 4.2.1 for both failure mechanisms of OPSC and NWC beams cast without shear reinforcement, the test results of OPSC beams were therefore compared with the predictions of the existing EC2 Model (Eqn 2.19) to evaluate whether the existing model is relevant (see Column 2 and 3 in Table 7.1). Summary of the comparisons are presented in Table 7.1 (Column 5), which it can be noted that the existing Eurocode 2 design model (EC2-NS Model) underestimated the ultimate shear capacity of OPSC beam specimens cast without shear reinforcement with a mean value of 1.29 and standard deviation of 0.17. As a result, modifications were decided to be carried out to the parameters to reflect the observation derived from the tests. The parameters modified are; span to effective depth ratio (a/d), and effective section depth (d). Such modifications are required to accommodate for the variations observed from tests, such as

underestimations of the parameters span to effective depth ratio, $a/d \leq 2.5$, and effective section depth, $d = 82$ mm.

7.2.2 Modification on parameters

From Section 7.2.1, it was noted that the existing Eurocode 2 model (EC2-NS Model) underestimated the ultimate shear strength of OPSC beam cast without shear reinforcement. As a result, further analyses were carried out to evaluate the relevancy of the parameters: (1) span to effective section depth ratio (a/d), (2) longitudinal steel ratio (ρ), (3) cylindrical concrete strength (f_{ck}), and (4) effective section depth (d), which influence the shear capacity predictions of the beams.

7.2.2.1 Span to effective depth ratio, a/d

It can be noted from Figure 7.1 that as the span to effective depth ratio (a/d) decreases, the rate of increase of ultimate shear strength for both OPSC and NWC beam specimens are more pronounced than the prediction values derived from the existing EC2 design model (EC2-NS Model). That is, the existing EC2 design model (EC2-NS Model) (Eqn 2.22.1) underestimated the increment of the ultimate shear strength with respect to a/d ratio of less than 2.5. It is believed that such discrepancy arose due to the existing expression given by the existing EC2 model (EC2-NS Model), which took into account the increment of ultimate shear strength for the reduction of span to effective depth ratio for beams loaded with $a/d \leq 2$ instead of $a/d \leq 2.5$.

In view from the observations from experiments (Section 4.2.1), it is noted that the failure modes for concrete beams without shear reinforcement, varied for $a/d < 2.5$

and $a/d \geq 2.5$, respectively, which shear compression failure occurred at $a/d < 2.5$ whilst shear failure and diagonal tension failure occurred at $a/d \geq 2.5$. Therefore, the existing expression was revised to be Eqn 7.1.1 to accommodate for both the rate of increase in shear capacity as span to effective depth (a/d) reduces and the two distinct failure modes observed for $a/d < 2.5$ and $a/d \geq 2.5$. With the revised expression for span ratio (Eqn 7.1.1), good agreement with test results are achieved (see Figure 7.1).

$$f\left(\frac{a}{d}\right) = 2.5 \frac{d}{a} \quad \left(\frac{a}{d} < 2.5\right) \quad (\text{Eqn 7.1.1})$$

7.2.2.2 Longitudinal steel ratio, ρ

In general, it can be noted in Figure 7.2 that shear strength of OPSC specimens with respect to longitudinal steel ratio's parameter, $f(\rho)$ were observed to be lower to those of NWC control samples as observations from tests indicate that for beams casted with higher longitudinal steel ratio ($\rho = 3.63\%$) (see Figure 4.44), higher ultimate shear strength were obtained by NWC beam (Specimen NWCE) compared to OPSC beam (Specimen 20E). It is believed such discrepancies occurred due to the higher aggregate impact strength provided by the gravel aggregates (See Table 2.1), and, as a result, higher shear resistance was mobilised by NWC beam.

It can also be noted from Figure 7.2 that the shear failure loads of OPSC beams with respect to the longitudinal steel ratio's are slightly higher in comparison to the predictions derived from the existing EC2 design model (EC2-NS Model) (Eqn 2.22.2). Since the $f(\rho)$ of the ultimate shear strength predictions derived from the existing EC2 design model (EC2-NS Model) marginally underestimated the shear failure loads of the OPSC beams, the existing expression are therefore acceptable. That is, adequate

predictions of the shear strength increment with respect to the increment of longitudinal steel ratio are provided for OPSC beams. Thus, the existing parameter longitudinal reinforcement ratio's equation (Eqn 2.22.2) are adopted into the modified EC2 design model (EC2-I Model) to account for the increment of the ultimate shear strength of OPSC beam as longitudinal steel ratio increases.

7.2.2.3 Cylindrical concrete strength, f_{ck}

In general, it can be observed that the shear strength of OPSC beam specimens without shear reinforcements with respect to cube concrete strength parameter, $f(f_{cu})$ were observed to be lower to those of NWC control samples as observations from tests indicate that the ultimate shear strength obtained by NWC beam specimens (Specimen NWC2 and NWC3) were higher than those of OPSC beam specimens (Specimen 16C and F1) (see Figure 4.46). It is believed that such discrepancy in shear strength between NWC and OPSC beams is due to the differences in the fracture strength of coarse aggregates. That is, higher fracture strength found in the gravel aggregates (see Table 2.1) would have enhance the aggregate interlocking capacity, and, as a result, higher shear resistance was mobilised by NWC beam.

In addition, it can be noted from Figure 7.3 that the shear failure loads of OPSC beams with respect to the cylindrical concrete strength are $f(f_{ck})$, are slightly higher in comparison to the predictions derived from existing Eurocode 2 model (EC2-NS Model) (Eqn 2.22.3). Furthermore, since the predictions derived from the existing EC2 design model (EC2-NS Model) with respect to $f(f_{ck})$ marginally underestimated the shear failure loads of the OPSC beams, the existing expression therefore

satisfactory. Therefore, the existing parameter concrete compressive strength's equation (Eqn 2.22.3) are adopted into the modified EC2 design model (EC2-I Model) to account for the increment in the ultimate shear strength of OPSC beam as concrete compressive strength increases.

7.2.2.4 Beam effective depth, d

In Figure 7.4, it is observed that the predictions derived from the existing EC2 design model (EC2-NS model) (Eqn 2.22.4) with respect to effective section depth, $f(k)$, were lower than the shear failure loads of OPSC specimens with effective section depth, $d = 82 \text{ mm}$ ($h=113 \text{ mm}$). Test observations show that for $d = 82\text{mm}$, the ultimate shear failure loads obtained by both beams (Specimen 12F and NWC5) are comparable with differences of 4% (see Figure 4.49).

Whilst for OPSC specimens with effective depth, $165 \leq d \leq 167$, the shear failure loads were noted to be lower to that of NWC control specimens. Such discrepancy is believed to be attributed to the lower aggregate strength found in Oil Palm kernel Shell (OPS) compared to that found in normal aggregates, which in turn, would have led to lower aggregate interlocking capacity, and as a result, lower ultimate shear resistance could be mobilised. In addition, from Figure 7.5, for effective section depth, $d \geq 165$, it is noted that the predictions of the existing EC2 design model is lower than shear failure loads of OPSC specimens.

Hence, the existing equation was revised to be Eqn 7.1.2 to accommodate for both the rate of increase in shear capacity as the effective section depth, d reduces. With the revised expression for effective section depth (Eqn 7.1.2), good agreement with test results is achieved, as shown In Figure 7.4.

$$f(k) = 1.1 + \frac{200}{d} \quad (d \text{ in mm}) \quad (\text{Eqn 7.1.2})$$

7.2.3 Comparisons with test results

From the modifications of parameters proposed in Section 7.2.2 for the shear strength predictions of OPSC beams without shear reinforcement, the proposing modified EC2 design model (EC2-NS Model) is given as:

For $a/d < 2.5$,

$$V_{Rdc} = [0.18 (1.1 + \frac{200}{d}) (100 \rho f_{ck})^{1/3} + k_1 \sigma_{cp}] b_w d (\frac{2.5d}{a}) \quad (\text{Eqn 7.2})$$

For $a/d \geq 2.5$,

$$V_{Rdc} = [0.18 (1.1 + \frac{200}{d}) (100 \rho f_{ck})^{1/3} + k_1 \sigma_{cp}] b_w d \quad (\text{Eqn 7.3})$$

Where,

$$k_1 = 0.15$$

$$C_{rd,c} = \frac{0.18}{\gamma_c}, \text{ where } \gamma_c = \text{partial factor of concrete}$$

It can be observed from Figure 7.5 to 7.8 that the proposing Eurocode 2 design model (EC2-I Model) (Eqn 7.2 and 7.3 for beams loaded with $a/d < 2.5$ and $a/d \geq 2.5$, respectively) with respect to parameters: shear span to height ratio (a/h), longitudinal steel ratio (ρ), concrete strength (σ_c), and overall section depth (h) exhibit good agreement with the test results, in which a mean value of 1.05 and standard deviation of 0.15 are achieved (see also Table 7.1 Column 6).

7.3 Beams cast with shear reinforcement

7.3.1 Eurocode 2 design model for concrete beam with shear reinforcement, (EC2-II Model)

The proposing “EC2-II” Model is developed to predict for the ultimate shear resistance of a reinforced concrete beam element with shear reinforcement cast using Oil Palm kernel Shell Concrete (OPSC) as coarse aggregate.

The existing Eurocode 2 (EC2-S Model) presented two formulas for the predictions of ultimate shear strength for NWC beam with shear reinforcement (see Eqn 2.48 and Eqn 2.49). Eqn 2.47 considered the yielding of shear reinforcement via the parameters: (1) inclination angle of shear cracks (θ) and (2) the shear reinforcement ratio ($\frac{A_{sw}}{s}$), whilst Eqn 2.48 considered the crushing of concrete compression strut via the parameters: (1) concrete strength (2) inclination angle of shear cracks (θ).

Since a significant similarity has been observed in Section 4.3.1 for both failure mechanisms of OPSC and NWC beams cast with shear reinforcement, hence, further analyses were carried out to examine the relevancy of the existing EC2 model (EC2-S Model) (Eqn 2.48 and 2.49) for the predictions of shear strength of OPSC beam specimens. Comparisons were summarized and presented in Table 7.2. which it is observed that the ultimate shear strength predictions given by the Equation 2.49 achieved good agreement with the test results of OPSC beam specimens with shear reinforcement (see Table 7.2 Column 8) with a mean of 1.02 and standard deviation of 0.21. Whilst for the shear strength predictions given by Equation 2.48 (see Table 7.2 Column 4), it is noted that the existing EC2 design model underestimated the

shear strength of OPSC beam with shear reinforcement (see Table 7.2 Column 7) with a mean of 2.43 and standard deviation of 0.48.

7.3.2 Modification on parameter

It was noted from Section 7.3.1 that the Eqn 2.47 in the existing Eurocode 2 design model (EC2-S Model) underestimated the ultimate shear capacity of OPSC beams with shear reinforcement. Hence, further analysis were carried out to evaluate the relevancy of parameters: (1) inclination angle of shear cracks (θ) and (2) the shear reinforcement ratio ($\frac{A_{sw}}{s}$), governing the shear strength predictions of EC2-S Model and to provide with appropriate modifications (see Section 7.3.2.1 and 7.3.2.2).

7.3.2.1 Inclination angle of shear cracks, θ

In general, it can be noted from Figure 7.9 that the predictions derived from the existing EC2 design model (EC2-S Model) (Eqn 2.50.1) with respect to $f(\theta)$ are in good agreement with the shear failure loads of the OPSC beams. Therefore, the existing expression (Eqn 2.50.1) are acceptable and are adopted into the proposed EC2 design model (EC2-II Model) to account for the increment of the ultimate shear strength of OPSC beam as inclination angle of shear cracks increases.

7.3.2.2 Shear reinforcement ratio, $\frac{A_{sw}}{s}$

It can be noted in Figure 7.10 that the prediction values derived from the existing EC2 design model (EC2-S Model) are observed to underestimate the failure loads of OPSC specimens. Test results indicate that the shear failure loads achieved by OPSC beams

are slightly higher than those of NWC control specimens (see Figure 4.73). It is believed that such discrepancy was attributed to the rougher surface texture observed from the OSPC beams compared to NWC beams (see Figure 4.70 and 4.71). Consequently, this would have led to higher aggregate interlocking resistance, and, as a result, higher shear resistance was mobilised.

In view of the discrepancies noted between the test results and the existing EC2-S Model (Eqn 2.50.2), a revised expression has been proposed to the EC2-S Model (See Eqn 7.4) to account for the increment of shear strength observed, which would be resulted from the increase of shear reinforcement ratio. With the revised expression for shear reinforcement ratio (Eqn 7.4), better agreement with test results are achieved, as shown in Figure 7.10.

$$f\left(\frac{A_{sw}}{s}\right) = 2.2 \frac{A_{sw}}{s} \quad (\text{Eqn 7.4})$$

7.3.3 Comparisons with test results

From the modifications of parameters proposed in Section 7.3.2 for the shear strength predictions of OPSC beams with shear reinforcement, the proposing modified EC2 design model (EC2-II Model) is given as:

$$V_{\text{EC2-II}} = 0.87 \left(2.2 \frac{A_{sw}}{s}\right) f_{yw} z (\cot \theta) \quad (\text{Eqn 7.5})$$

Comparisons between the modified Eurocode 2 design model (EC2-II Model) (Eqn 7.5) and the test results with respect to parameters: (1) inclination angle of shear cracks (θ) and (2) the shear reinforcement ratio $\left(\frac{A_{sw}}{s}\right)$, indicate that agreement are

achieved (see Figure 7.11 and 7.12) (mean value of 1.10 and standard deviation of 0.21 as shown in see Table 7.2, Column 9).

7.4 Summary

Two Eurocode 2 (EC2) design models (EC2-I Model and EC2-II Model) based upon the modification of the existing Eurocode 2 design models have been proposed in this chapter for the ultimate shear strength predictions of OPSC beams cast with and without shear reinforcement, respectively.

The proposed EC2-I Model took into account the parameters: span to effective section depth ratio (a/d), cylindrical concrete strength (f_{ck}), longitudinal steel ratio (ρ) and effective section depth (d), which each parameter were modified for the ultimate shear strength predictions of the OPSC beams without shear reinforcement.

Whilst for OPSC beams with shear reinforcement, the proposed EC2-II Model are the outcomes of the modified parameter of shear reinforcement ratio ($\frac{A_{sw}}{s}$) for the ultimate shear strength predictions.

Generally, the modified EC2 design models (EC2-I Model and EC2-II Model) achieved good agreement with the test results for OPSC beams without and with shear reinforcement, respectively.

Table 7.1 Comparisons of shear strength predictions with respect to the test results of OPSC beam specimens cast without shear reinforcement

1	2	3	4	5	6
Specimen No	V_{OPSC} (kN)	V_{EC2-NS} (kN)	V_{EC2-I} (kN)	$\frac{V_{OPSC}}{V_{EC2-NS}}$	$\frac{V_{OPSC}}{V_{EC2-I}}$
10A	18.95	18.53	20.23	1.02	0.94
S1	21.05	19.46	21.25	1.08	0.99
12A	54.73	42.19	57.68	1.30	0.95
12B	40.00	28.13	38.45	1.42	1.04
12C	27.37	21.09	23.07	1.30	1.19
12D	25.26	21.09	23.07	1.20	1.09
12E	31.58	22.80	24.94	1.38	1.27
12F	26.31	17.22	22.41	1.62	1.17
16A	56.80	48.04	65.87	1.18	0.86
16B	42.10	32.02	43.91	1.31	0.96
16C	29.50	24.02	26.35	1.23	1.12
16D	26.32	24.02	26.35	1.10	1.00
16E	35.79	25.82	28.32	1.39	1.26
20A	73.68	54.08	74.40	1.36	0.99
20B	52.63	37.06	49.60	1.46	1.06
20C	33.68	27.04	29.76	1.25	1.13
20D	27.37	27.04	29.76	1.01	0.92
20E	35.79	28.38	31.23	1.26	1.15
AD1	58.19	51.39	70.47	1.13	0.83
AD2	32.33	25.69	28.19	1.26	1.15
F1	32.67	25.79	28.30	1.27	1.15
F2	47.41	27.70	30.39	1.71	1.56
H2	52.53	37.13	43.52	1.41	1.21
S2	36.64	27.65	29.23	1.38	1.25
			Mean	1.29	1.09
			S.D.	0.17	0.16

V_{OPSC} (kN) = Ultimate shear failure loads of OPSC beam specimens cast without shear reinforcement

V_{EC2-NS} (kN) = Shear resistance of Existing EC2 design model (EC2-I Model)

$$\text{For } a/d \leq 2, V_{Rdc} = [0.18(1 + \sqrt{\frac{400}{d}}) (100 \rho f_{ck})^{1/3} + k_1 \sigma_{cp}] b_w d \left(\frac{2d}{a}\right)$$

$$\text{For } a/d > 2, V_{Rdc} = [0.18(1 + \sqrt{\frac{400}{d}}) (100 \rho f_{ck})^{1/3} + k_1 \sigma_{cp}] b_w d$$

V_{EC2-I} (kN) = Shear resistance of proposing Modified EC2 design model (EC2-I Model)

$$\text{For } a/d < 2.5, V_{Rdc} = [0.18(1.3 + \sqrt{\frac{200}{d}}) (100 \rho f_{ck})^{1/3} + k_1 \sigma_{cp}] b_w d \left(\frac{2.5d}{a}\right)$$

$$\text{For } a/d \geq 2.5, V_{Rdc} = [0.18(1.3 + \sqrt{\frac{200}{d}}) (100 \rho f_{ck})^{1/3} + k_1 \sigma_{cp}] b_w d$$

Table 7.2 Comparisons of shear strength predictions with respect to the test results of OPSC beams cast with shear reinforcement

1	2	3	4	5	6	7	8	9
Specimen No	Measured angle inclination of shear cracks (degree)	Test results V_{OPSC} (kN)	EC2-S Model V_{EC-S} (kN)		EC2-II Model V_{EC2-II} (kN)	$\frac{V_{OPSC}}{V_{EC-S}}$		$\frac{V_{OPSC}}{V_{EC2-II}}$
			$V_{Rd,s}$ (kN) Eqn 2.48	$V_{Rd,max}$ (kN) Eqn 2.49		$\frac{V_{OPSC}}{V_{Rd,s}}$	$\frac{V_{OPSC}}{V_{Rd,max}}$	
3A	34	75.78	36.11	80.11	79.44	2.10	0.95	0.95
3B	35	88.41	34.78	98.37	76.52	2.54	0.90	1.16
3C	40	92.62	29.03	110.65	63.86	3.19	0.84	1.45
4A	41	79.99	42.03	85.56	92.46	1.90	0.93	0.87
4B	41	94.73	42.03	103.66	92.46	2.25	0.91	1.02
4C	45	107.36	36.53	112.35	80.37	2.94	0.96	1.34
5A	38	88.41	58.47	78.63	128.64	1.51	1.12	0.69
5B	42	107.36	50.74	97.64	111.62	2.12	1.10	0.96
5C	44	119.99	47.31	105.31	104.08	2.54	1.14	1.15
4D	50	101.04	36.53	90.76	80.37	2.77	1.11	1.26
4E	53	105.25	36.53	85.49	80.37	2.88	1.23	1.31
Mean						2.43	1.02	1.10
S.D.						0.48	0.21	0.21

V_{OPSC} (kN) = Ultimate shear capacity of the tested OPSC beam with shear reinforcement

V_{EC-S} (kN) = Shear resistance of Existing EC2 design model (EC2-S Model)

$V_{Rd,s}$ (kN) = Shear resistance of Existing EC2 design model (EC2-S Model), which considered the yielding of shear reinforcement

$$V_{EC2-II} = 0.87 \left(\frac{A_{sw}}{s} \right) f_{yw} z (\cot \theta)$$

$V_{Rd,max}$ (kN) = Maximum shear resistance of Existing EC2 design model (EC2-S Model), which considered the crushing of compression struts

$$V_{rd,max} = \frac{\alpha_{cw} b_w v_1 z f_{cd}}{\cot \theta + \tan \theta}$$

V_{EC2-II} (kN) = Shear resistance of proposing Modified EC2 design model of $V_{Rd,s}$ (EC2-II Model)

$$V_{EC2-II} = 0.87 \left(2.2 \frac{A_{sw}}{s} \right) f_{yw} z (\cot \theta)$$

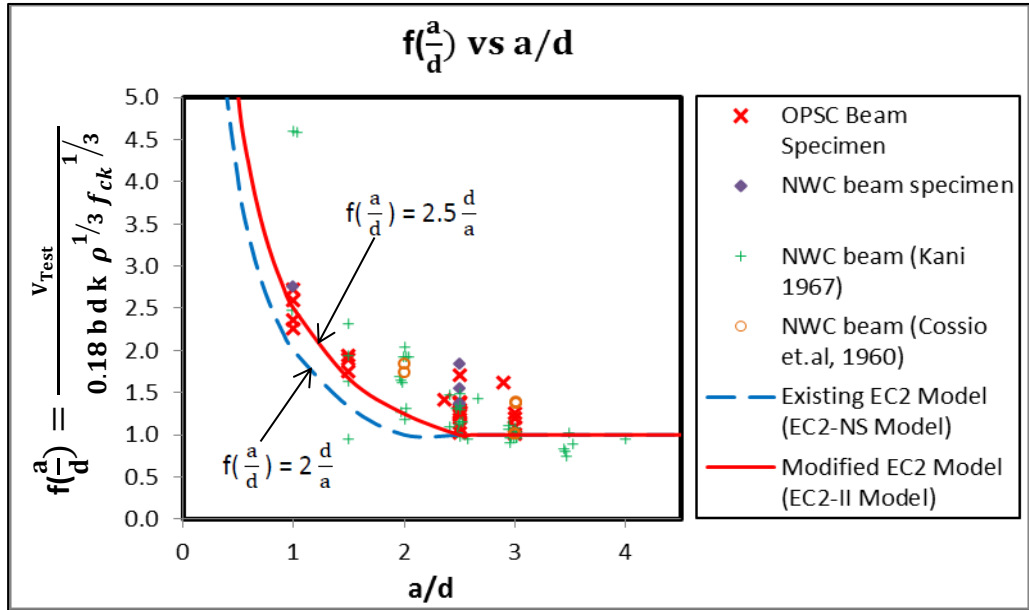


Figure 7.1 $f(a/d)$ vs a/d for Existing EC2 design model (EC2-NS Model) and Modified EC2 design model (EC2-I Model).

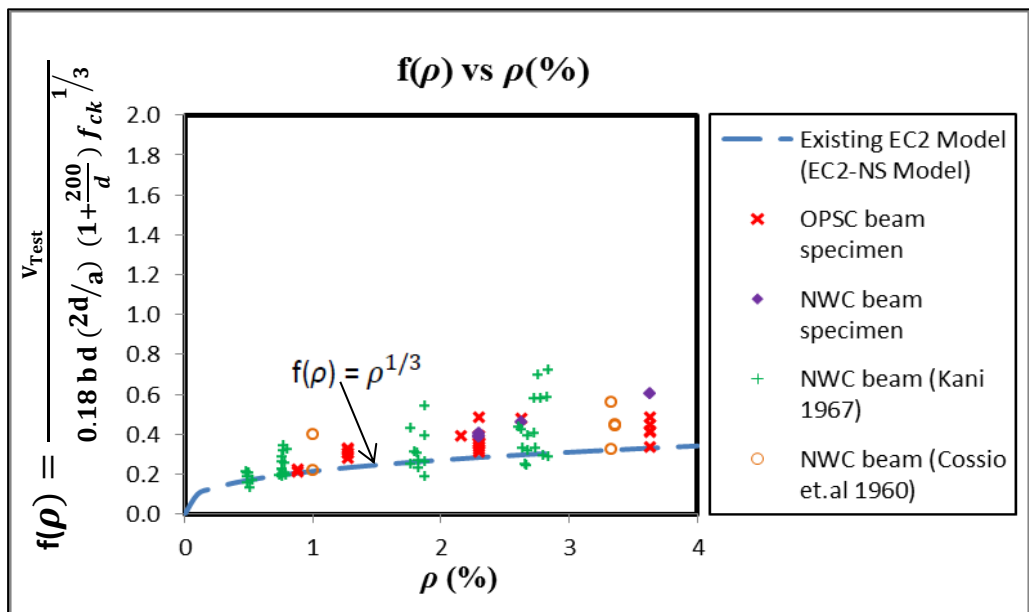


Figure 7.2 $f(\rho)$ vs $\rho(\%)$ for Existing EC2 design model (EC2-NS Model).

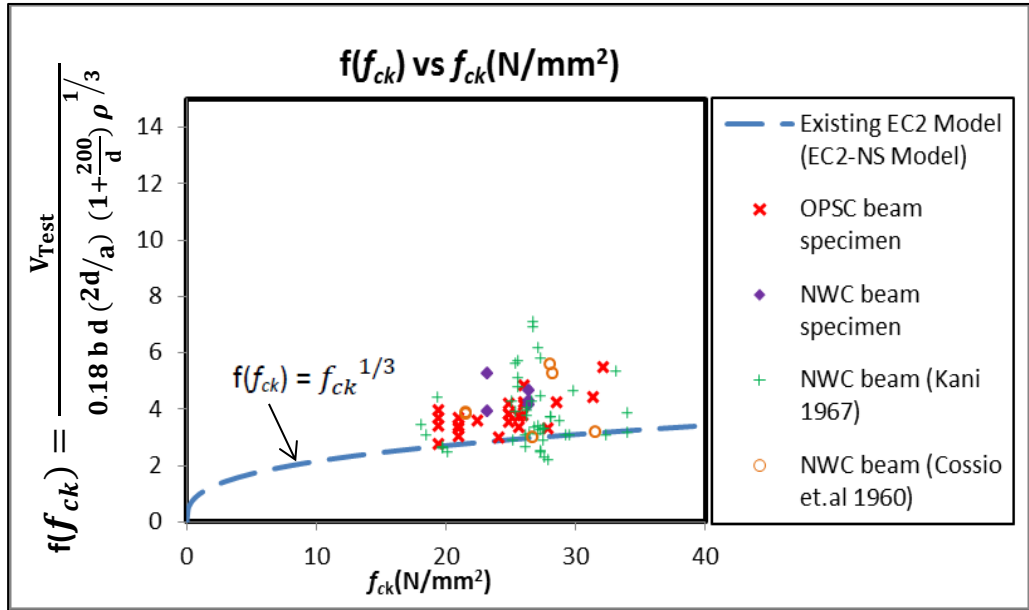


Figure 7.3 $f(f_{ck})$ vs f_{ck} (N/mm²) for Existing EC2 design model (EC2-NS Model).

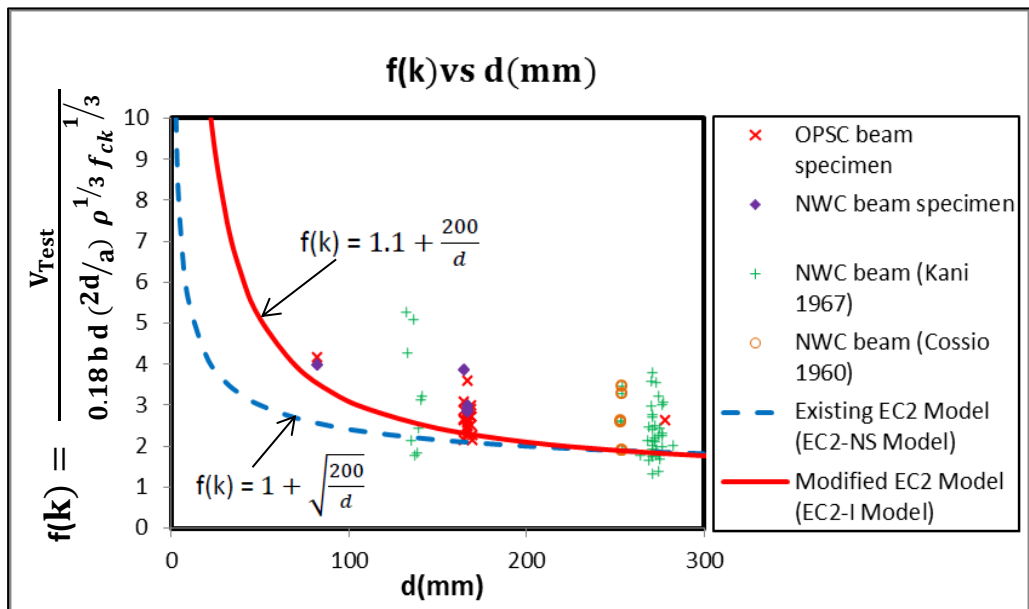


Figure 7.4 $f(k)$ vs d (mm) for Existing EC2 design model (EC2-NS Model) and Modified EC2 design model (EC2-I Model).

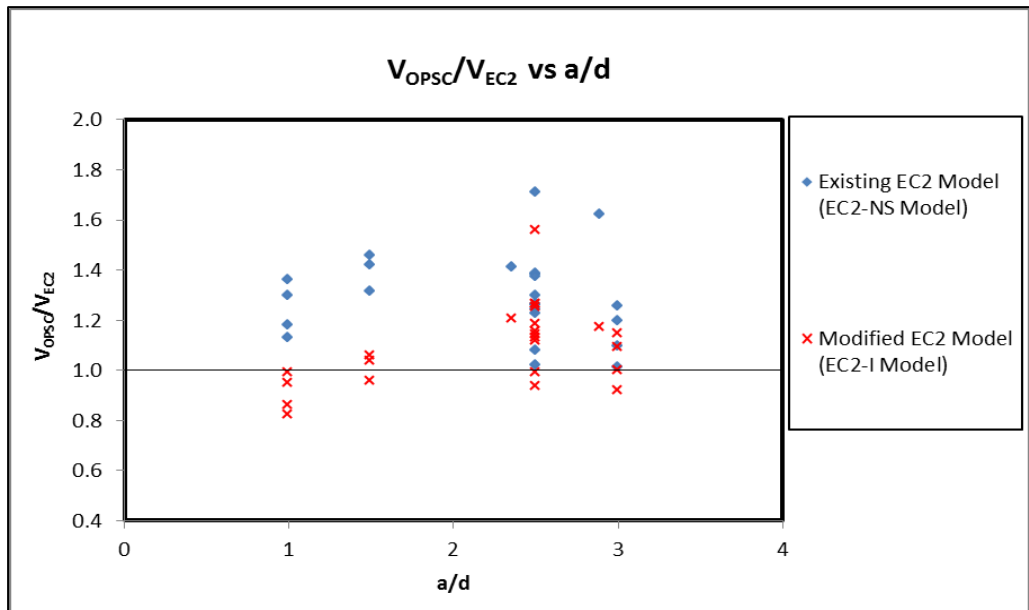


Figure 7.5 V_{OPSC}/V_{EC2} vs Shear span to effective section depth, a/d .

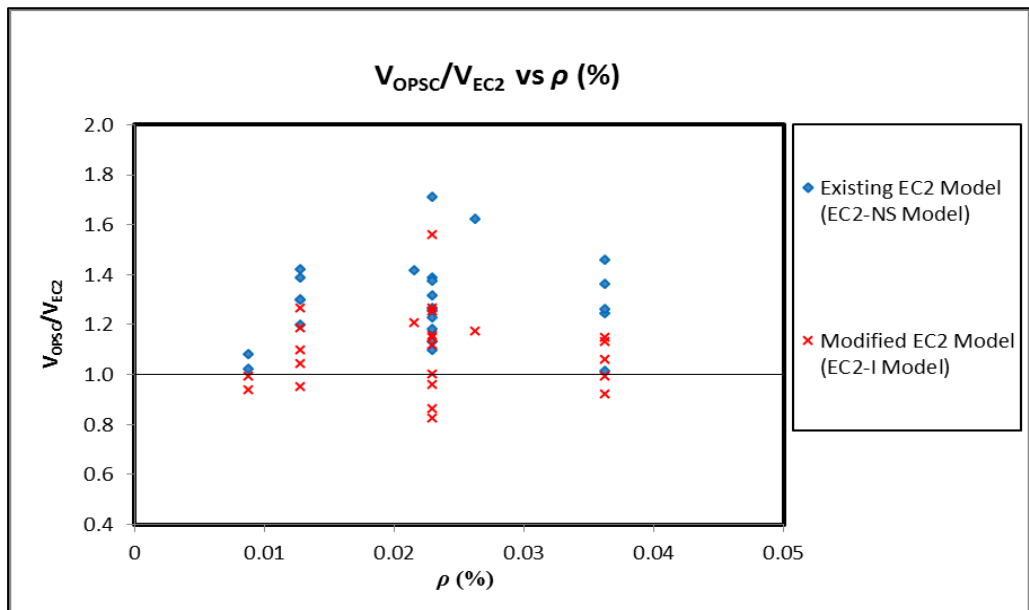


Figure 7.6 V_{OPSC}/V_{EC2} vs Longitudinal steel ratio, ρ (%).

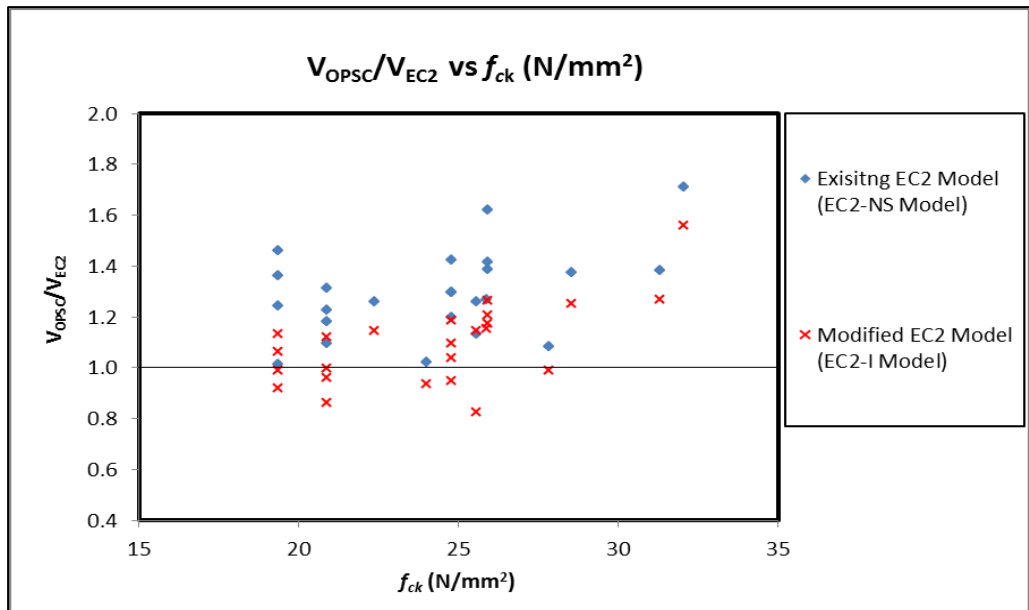


Figure 7.7 V_{OPSC}/V_{EC2} vs Cylindrical concrete strength, f_{ck} (N/mm^2).

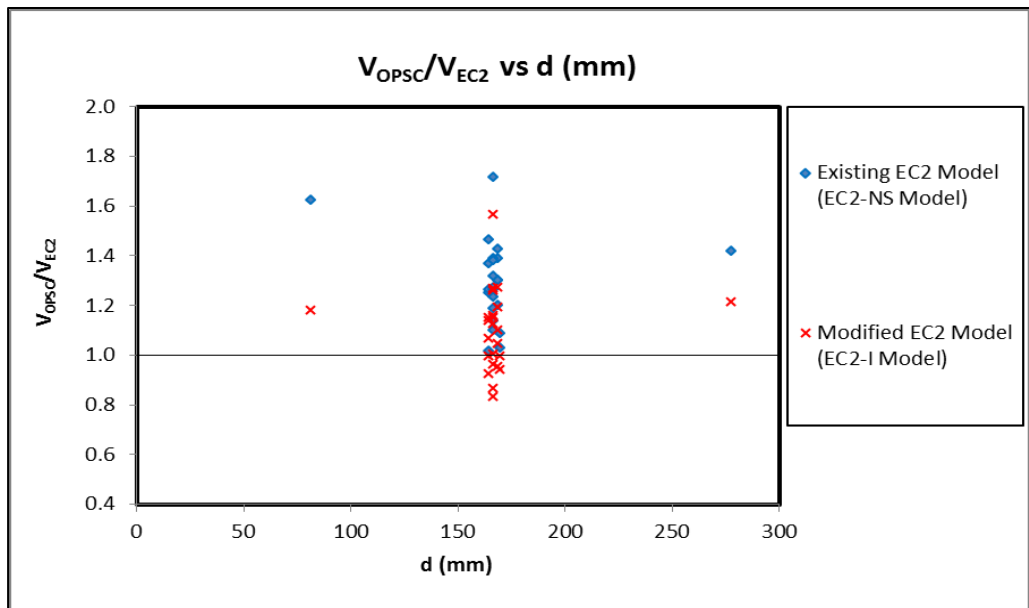


Figure 7.8 V_{OPSC}/V_{EC2} vs Effective section depth, d (mm).

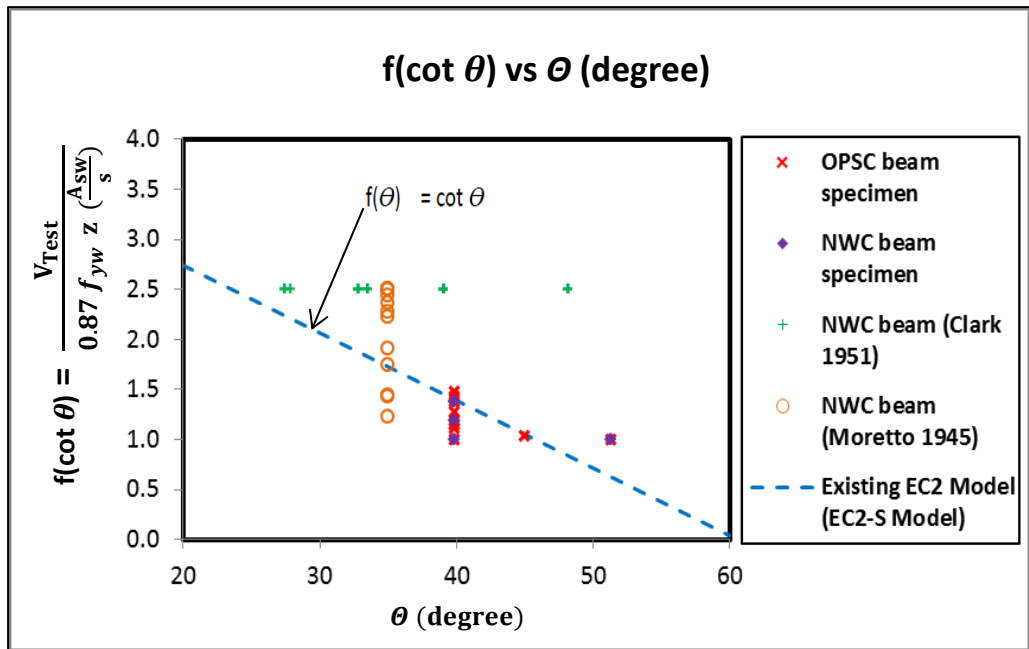


Figure 7.9 $f(\cot \theta)$ vs θ (degree) for Existing EC2 design model (EC2-S Model).

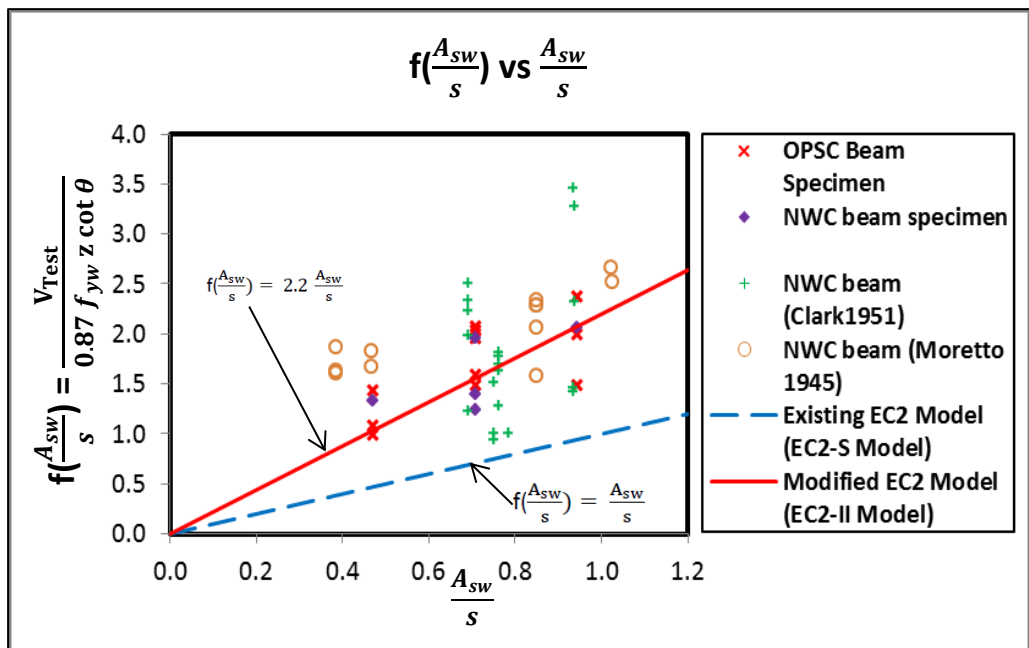


Figure 7.10 $f(\frac{A_{sw}}{s})$ vs $(\frac{A_{sw}}{s})$ for Existing EC2 design model (EC2-S Model) and Modified EC2 design model (EC2-II Model).

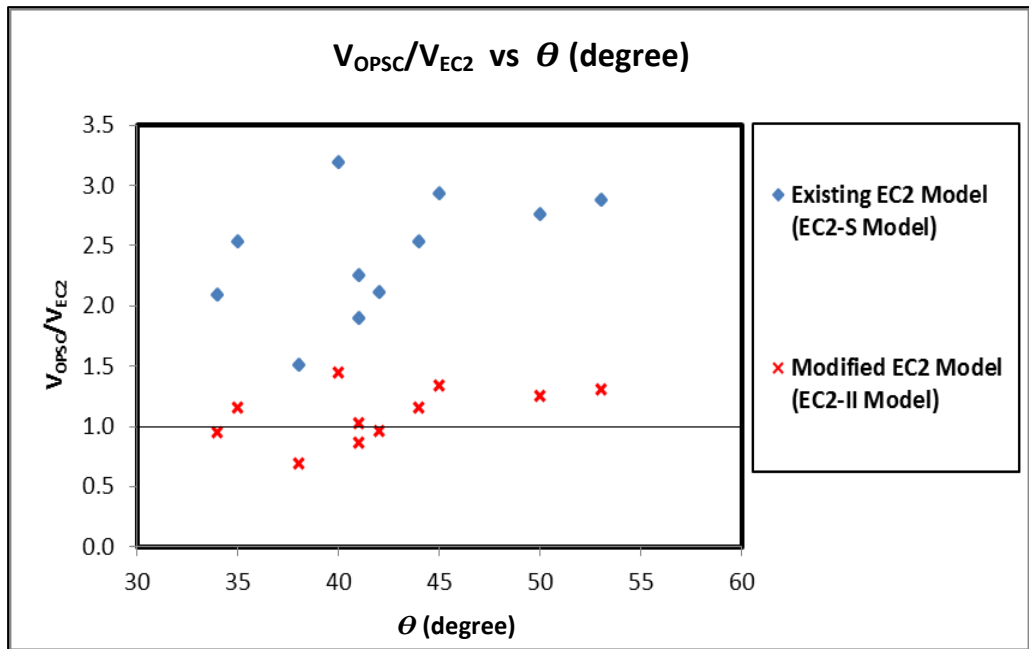


Figure 7.11 V_{OPSC}/V_{EC2} vs Inclination of shear cracks, θ (degree).

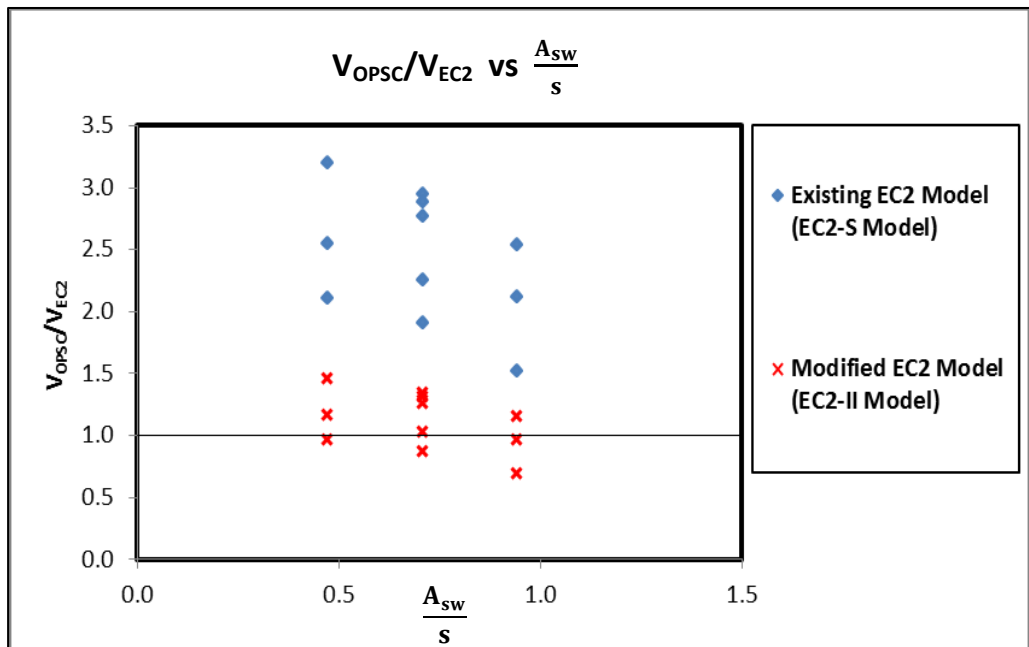


Figure 7.12 V_{OPSC}/V_{EC2} vs Shear reinforcement ratio, $\frac{A_{sw}}{s}$.

Chapter 8

Conclusions and Future Work

8.1 Summary of current study

In recent years, Oil Palm Shell Concrete (OPSC), which use the oil palm kernel shell (OPS) aggregate as the full replacement for coarse aggregate, has received a great deal of attention from researchers. Considerable amount of research have been carried out to aid the understanding of its concrete mixture designs [1-6] and its material properties [7-11]. However, only limited amount of works have been carried out to aid the understanding of the OPSC structural resistance, such as bending resistance [12-14] and shear resistance [15-16]. It is apparent that more research is required to develop a comprehensive understanding for its structural element, particularly in the shear transfer mechanism.

The main objective of this research was to explore the shear resistance of OPSC beams cast with and without shear reinforcement through experimental and analytical study. Mix designs of OPSC were proposed for structural applications. The experimental work carried out in this research involved destructive testing of OPSC beams and NWC beams casted with and without shear reinforcements. Three distinct failure mechanisms were observed from the tests: the shear compression mechanism; the diagonal tension mechanism; and the shear mechanism. The effect of variables on the ultimate shear failure loads of OPSC beams case with and without shear reinforcement were investigated.

Comparisons were carried out on the ultimate shear failure capacities and shear failure mechanisms between the OPSC beams and NWC beams cast with and without shear reinforcements, respectively, which it was found that the shear strength of OPSC beams and NWC beams were comparable when the beams were tested with respect to the variables: effective depth (for beams without shear reinforcements), and shear reinforcement ratio and inclination angle of shear cracks (for beams with shear reinforcements).

Since significant similarity were observed for both OPSC and NWC beams in term of failure mechanism, the test results of OPSC were therefore compared with respect to the theoretical plastic model, Eurocode 2 design model, and BS8110 design model, to investigate the requirement for the model's parameters' modification. As results, two models were developed each from the modification of the existing models with respect to theoretical plastic model, Eurocode 2 design model, and BS8110 design model, for the ultimate shear failure predictions of OPSC beams with and without shear reinforcements, respectively. In all cases, the proposed models achieved good agreement with the test results.

8.2 Mix Design of Oil Palm kernel Shell Concrete (OPSC)

Three mix designs had been proposed for Oil Palm kernel Shell concrete (OPSC) for structural applications. The proposed mix designs include: 3:1:3 and 4:1:3 and 5:1:3 of Ordinary Portland Cement: Sand: OPS aggregate.

8.3 Failure Mechanisms and Effect of Variables on OPSC beams

The experimental work carried out in this research involved destructive testing of twenty-four numbers of OPSC beam specimens casted without shear reinforcement and eleven numbers of OPSC beams casted with shear reinforcement. For OPSC beams casted without shear reinforcements, three distinct failure mechanisms were observed from the tests: the shear compression mechanism; the diagonal tension mechanism; and the shear mechanism. Whilst for OPSC beams casted with shear reinforcements, shear failure mechanism was observed from the tests.

It was observed from tests that all the beam specimens cast without shear reinforcement failed in shear mode of failure. Three modes of shear failure were observed: shear compression failure for $a/d < 2.5$, diagonal tension failure and shear failure, respectively, for $a/d \geq 2.5$ for OPSC beams without shear reinforcement. Whilst for OPSC beams with shear reinforcement, shear compression failure were observed.

The effect of variables to the ultimate failure loads of OPSC beams with and without shear reinforcement were investigated, respectively. For OPSC beams without shear reinforcement, the ultimate failure loads increases with respect to the reduction of span to depth ratio (a/d), increment of concrete strength (f_{cu}), longitudinal steel ratio (ρ) and section depth (h). Whilst for OPSC beams with shear reinforcement, the ultimate failure loads increases with the inclination angle of shear cracks (θ), concrete strength (f_{cu}) and shear reinforcement spacing (s), respectively.

8.4 Comparisons between OPSC and NWC beams

Comparisons were carried out on the ultimate shear failure capacities and the shear failure mechanisms between OPSC beams and NWC beams cast with and without shear reinforcement, respectively. It was found that the ultimate shear strength of OPSC beams and NWC beams are comparable for the parameters: section depth (for beams without shear reinforcement), and shear reinforcement spacing and inclination angle of shear cracks (for beams with shear reinforcement). However, discrepancies in ultimate shear strength between the OPSC beams and NWC beams were observed for the parameters: span to depth ratio, longitudinal steel ratio and concrete strength (for beams without shear reinforcement) and concrete strength (for beams with shear reinforcement).

8.5 Theoretical models

The existing plastic models: CP-NS Model and CP-S Model presented by Braestrup [45] and Neilsen et.al [46] were developed for NWC beams without and with shear reinforcements, respectively. Since significant similarity was observed for OPSC and NWC beams in the failure mechanism, therefore, investigations were carried out using the existing CP models to evaluate the relevancy of the models for the shear resistance predictions of OPSC beams. It was found that the CP-NS Model and CP-S Model underestimated the ultimate shear capacity of the OPSC beams cast with and without shear reinforcements, respectively. Hence, further analytical studies were carried out using the existing models with respect to each tested variables.

As a result, appropriate modifications were carried out as required on the existing parameters to allow for the ultimate shear strength predictions of OPSC beams with

and without shear reinforcement, respectively. Two theoretical models were proposed for predicting the ultimate shear failure load of the OPSC beams: CP-I Model for OPSC beams without shear reinforcements and CP-II Model for OPSC beams with shear reinforcements.

8.5.1 CP-I Model

From the analytical studies carried out by comparisons of test results with the existing concrete plastic Model (CP-NS Model), it was found that the existing plastic model overestimated the ultimate shear failure load of OPSC beams without shear reinforcements with a mean value of 0.89 and standard deviation of 0.19. Therefore, analytical studies were carried out respect to each parameter (span overall depth ratio, longitudinal steel ratio, concrete strength and overall section depth) to determine the requirement for modifications on the parameters.

Hence, CP-I Model, which was the results of the modification on each parameter, was proposed for the ultimate shear strength predictions of OPSC beams without shear reinforcements. The proposed CP-I model achieved good agreement (mean of 1.07 and standard deviation of 0.15) with the test results.

8.5.2 CP-II Model

Comparison studies were carried out between the ultimate shear strength predictions of OPSC beams with shear reinforcements given by the existing CP-S Model and the test results of OPSC beams with shear reinforcements. It was found that the existing plastic model overestimated the ultimate shear failure load of OPSC

beams without shear reinforcements with a mean value of 0.92 and standard deviation of 0.05. Hence, analytical studies were carried out respect to each tested parameters (shear reinforcement ratio, concrete strength and inclination angle of shear cracks) to determine the requirement for the modification of the parameters.

It was found that modification was required for parameter: concrete strength and subsequently, the modified parameter was incorporated into the proposed modified CP design model (CP-II Model) for the ultimate shear strength predictions of OPSC beams with shear reinforcements. It was found that very good agreement between the proposed CP-II model and the test results is achieved (mean of 1.03 and standard deviation of 0.05).

8.6 BS8110 design models

The existing BS8110 design models (BS8110-NS Model and BS8110-S Model) are based on the ultimate shear strength predictions of NWC beams with and without shear reinforcements, respectively. Since significant similarity were observed for both OPSC and NWC beams for its failure mechanism, the test results were therefore compared with the existing BS8110 design models to evaluate the relevancy of the model in predicting the shear failure loads of OPSC beams. It was found that these EC2 models underestimated the ultimate shear strength of OPSC beams cast with and without shear reinforcements, respectively. Therefore, investigations were carried out using the existing BS8110 design models with respect to each tested variables.

Hence, the existing BS8110 design models were modified to allow for the ultimate shear strength predictions of OPSC beams with and without shear reinforcement,

respectively. Two BS8110 design models were proposed for predicting the ultimate shear failure load of the OPSC beams: BS8110-I Model for OPSC beams without shear reinforcements and BS8110-II Model for OPSC beams with shear reinforcements.

8.6.1 BS8110-I Model

Analytical studies were carried out using the existing BS8110 design model (BS8110-NS Model) for the ultimate shear strength predictions of OPSC beams without shear reinforcements, which the predicted values were compared with the test results of OPSC specimens. It was found that the existing BS8110 design model underestimated the ultimate shear failure load of OPSC beams without shear reinforcements with a mean of 1.35 and standard deviation of 0.18. Therefore, further investigations were carried out to identify the requirement for the parameters' modification with respect to parameters considered: (span to effective depth ratio, longitudinal steel ratio, concrete strength and effective section depth).

It was found that modification was required for the parameters: span to effective depth ratio (a/d), and effective section depth (d). The modified BS8110 design model (BS8110-I Model), which incorporated both the modified parameters and unaltered parameters, was proposed for the ultimate shear strength predictions of OPSC beams without shear reinforcements. It was found that the proposed BS8110-I Model achieved good agreement with the test results (mean of 1.03 and standard deviation of 0.15).

8.6.2 BS8110-II Model

Comparison studies were carried out between the ultimate shear strength predictions of OPSC beams with shear reinforcements given by the existing BS8110 design model (BS8110-S Model) and the test results of OPSC beams with shear reinforcements, which it was found that the existing plastic model underestimated the ultimate shear failure load of OPSC beams without shear reinforcements with a mean value of 1.25 and standard deviation of 0.18. Hence, analytical studies were carried out respect to each tested parameter (shear reinforcement ratio, concrete strength and span to effective depth ratio) to determine the requirement for the modification of parameters.

It was found that modification was required for the parameter: span to effective depth ratio and subsequently, the modification was adopted into the proposed BS8110-II Model for the shear strength predictions of OPSC beams with shear reinforcements. A good agreement was found between the proposed BS8110-II model and the test results are achieved (mean of 1.11 and standard deviation of 0.16).

8.7 Eurocode 2 design models

The existing Eurocode 2 design models (EC2-NS Model and EC2-S Model) are based on the ultimate shear strength predictions of NWC beams with and without shear reinforcements. Since significant similarity was observed for OPSC and NWC beams in the failure mechanism, therefore, the relevancy of the existing Eurocode 2 design models for the shear strength predictions of OPSC beams were evaluated. It was found that the models underestimated the ultimate shear strength of OPSC beams

cast with and without shear reinforcements, respectively. Further investigations were carried out with respect to each tested variables to determine the requirement for the shear strength parameters' modification.

Hence, the existing Eurocode 2 design models were modified to allow for the ultimate shear strength predictions of OPSC beams with and without shear reinforcement, respectively. Two Eurocode 2 design models were proposed for predicting the ultimate shear failure load of the OPSC beams: EC2-I Model for OPSC beams without shear reinforcements and EC2-II Model for OPSC beams with shear reinforcements.

8.7.1 EC2-I Model

Investigations were carried out using the existing EC2 design model (EC2-NS Model) for the ultimate shear strength predictions of OPSC beams without shear reinforcements, which the predicted values were compared with the test results of OPSC specimens.

It was found that the existing EC2 design model (EC2-NS Model) underestimated the ultimate shear failure load of OPSC beams without shear reinforcements with a mean of 1.29 and standard deviation of 0.17. Therefore, further investigations were carried out to identify the requirement for modification with respect to the parameters. It was found that modification were required for the parameters' of span to effective depth ratio (a/d) and effective section depth (d).

Upon modification, EC2-I Model, which incorporated both the modified parameters and unaltered parameters, was proposed for the ultimate shear strength predictions

of OPSC beams without shear reinforcements. It was found that very good agreement between the proposed EC2-I Model and the test results is achieved (mean of 1.09 and standard deviation of 0.16).

8.7.2 EC2-II Model

Investigations were carried out using the existing Eurocode 2 design model (EC2-S Model) for the shear strength predictions of OPSC beams without shear reinforcements, which the test results achieved by OPSC beams were compared with the shear strength predictions derived from the EC2-S Model.

It was found that the EC2-S Model, which considered the yielding of shear reinforcement, has underestimated the ultimate shear failure loads of OPSC beams with shear reinforcements (mean of 2.43 and standard deviation of 0.48). Hence, further investigations were carried out on each parameter (shear reinforcement ratio and inclination angle of shear cracks) to determine the requirement for the parameters' modification.

Subsequently, a modified EC2 design model (EC2-II Model) was proposed as the results of the modification on the parameter: shear reinforcement ratio ($\frac{A_{sw}}{s}$) for the ultimate shear strength predictions of OPSC beams with shear reinforcements. It was found that good agreement between the proposed EC2-I Model and the test results is achieved (mean of 1.10 and standard deviation of 0.21).

8.8 Future work

The following work is proposed for the future,

1. Since this study has not involved uniform loading, it is proposed to carry out experimental testing to study the effect of uniform loading on the shear transfer mechanism of OPSC beams cast with and without shear reinforcements.
2. Since this study has only involved small-scale model specimen testing, it is desirable to carry out testing on larger scale model specimens, because it is known that significant size effects are associated with shear failure.
3. Since this study has only carried out on rectangular OPSC beams with and without shear reinforcements and promising results were noted, it is desirable to carry out further testing on other type of structural concrete elements, for example T beams, slabs, columns, and other concrete elements to expand the use of OPS aggregates as coarse aggregates in concrete. With these studies, new design equations specifically for the structural concrete elements can be proposed if required.

References:

1. Okpala D.C., Palm Kernel Shell as Lightweight Aggregate in Concrete. *Construction and Building Materials*, Vol.25, No.4, 1990, pp. 291-296.
2. Basri. H.B., Mannan.M.A., and Zain. M. F. M., Concrete using waste oil palm shells as aggregate. *Cement and Concrete Research*, Vol.29, 1999, pp. 619-622.
3. M.A.Mannan, C. Ganapathy, Mix design for Oil Palm Shell Concrete. *Cement and Concrete Research*, Vol. 31, 2001, pp. 1323-1325.
4. Teo D.C.L., Mannan M. A., and Kurian V.J., Production of Lightweight Concrete Using Oil Palm Shell (OPS) Aggregates. s.l., *4th International Conference on Construction Materials: Performance, Innovations and Structural Implications*.
5. Teo D.C.L., Mannan M. A., Kurian V.J., and Ganapathy C., Lightweight concrete made from oil palm shell (OPS): Structural bond and durability properties. *Building and Environment*, Vol. 42, 2007, pp. 2614-2621.
6. Alengaram U.J., and Muhit B.A.A., and Jumaat M.Z., Utilization of oil palm kernel shell as lightweight aggregate in concrete- A review. *Construction and Building Materials*, Vol. 38, 2013, pp. 161-172.
7. Mannan M.A., and Ganapathy C., Long-term strengths of concrete with oil palm shell as coarse aggregates. *Cement and Concrete Research*, Vol. 31, 2001, pp. 1319-1321.
8. Mannan M.A., and Ganapathy C., Engineering properties of concrete with oil palm shell as coarse aggregate. *Construction and Building Materials*, Vol. 16, 2002, pp. 29-34.
9. Mannan M.A., Basri H.B., Zain M.F.M, and Islam M.N., Effect of curing conditions on the properties of OPS concrete. *Building and Environment*, Vol. 37, pp. 2002, 1167-1171.
10. Mannan M.A., Alexander J., Ganapathy C., and Teo D.C.L. Quality improvement of oil palm shell (OPS) as coarse aggregate in lightweight concrete. *Building and Environment*, Vol. 41, 2006, pp. 1239-1242.

11. Alengaram U.J, Mahmud H., and Jumaat M.Z., Comparison of mechanical and bond properties of oil palm kernel shell concrete with normal weight concrete. *International Journal of the Pyysical Sciences*, Vol.5, No.8, 2010, pp. 1231-1239.
12. Teo D.C.L., Mannan M. A., and Kurian V.J, Structural Concrete Using Oil Palm Shell (OPS) as Lightweight Aggregate, *Turkish J. Eng. Env. Sci*, Vol. 30, 2006, pp. 251-257.
13. Teo D.C.L., Mannan M. A., and Kurian V.J, Flexural Behaviour of Reinforced Lightweight Concrete Beams Made with Oil Palm Shell (OPS). *Journal of Advanced Concrete Technology*, Vol. 4, No.3, 2006, pp. 459-468.
14. Alengaram U.J, Mahmud H., and Jumaat M.Z., Ductility Behaviour of Reinforced Palm Kernel Shell Concrete Beams. *European Journal of Scientific Research*, Vol. 23, No.3, 2008, pp. 406-420.
15. Jumaat M.Z., Alengaram U. J, and Mahmud H., Shear strength of oil palm shell foamed concrete beams. *Materials and Design*, Vol. 30, 2009, pp. 2227-2236.
16. Alengaram U.J., Jumaat M.Z., Mahmud H., and Fayyadh M.M.. Shear behaviour of reinforced palm kernel shell concrete beams. *Construction and Building Mateials*, Vol. 25, 2011, pp. 2918-2927.
17. Choong M.Y., Waste not the palm oil biomass, *The Star Online*, 27 March 2012.
18. Ritter, W. , Die Bauweise Hennebique." *Schweizerische Bauzeitung* , Zurich, Switzerland, 1899, pp-59-61.
19. ACI-ASCE Committee 426 (326), Shear and Diagonal Tension, *ACI Journal*, Vol. 59, No.3, Mar 1962, pp 353-396.
20. Mörsch, E., Der Eisenbetonbau, seine Anwendung und Theorie, 1st Ed., Wayss & Freytag, A.G., *Im Selbstverlag der Firma*, Neustadt, A. D. Hardt, Germany, 1902.
21. Von Emperger F., Einige Versuche über die Würfelfestigkeit von armiertem Beton." *Beton und Eisen*, Vol. 4, 1903, pp -268–269.
22. Von Probst E, Ergebnisse Neuerer Untersuchungen und ein Vergleich mit den bisher bekannten versuchsergebnissen, 1903.
23. Talbot A.N., Tests on Reinforced Concrete Beams, *University of Illinois Engineering Experiment Station*, 1909.

24. Moretto O., An Investigation onof the Strength of Welded Stirrups in Reinforced Concrete Beams, *ACI Journal*, Nov 1945, Proceedings V. 42, No. 2, pp. 141-162.
25. Clark A.P., Diagonal Tension in Reinforced Concrete Beams. *ACI Journal*, Vol.23, No.2, Oct 1951, pp. 145-156.
26. ACI-ASCE Committee 426, Suggested Revisions to Shear Provisions for Building Code, *ACI Journal*, Proceedings Vol. 74, No.9, Sept 1977, pp. 458-469.
27. Kong F.K. and Evans R.H., *Reinforced and Prestressed Concrete*. 3rd Edition ed. Cambiridge: E & FN Spon, 1998.
28. Moody K.G., Viest I.M., Elstner R.C.and Hognestad E., Shear Strength of Reinforced Concrete Beams Part 1-Tests of Simple Beams. *ACI Journal*, Vol. 26, No.4, Dec 1954, pp. 317-332.
29. Moody K.G., and Viest I.M., Shear strength of Reinforced Concrete Beams Part 4- Analytical Studies. *ACI Journal*, Vol.26, No.7, Feb 1964, pp. 697-732.
30. Ferguson P.M., Some Implications of Recent Diagonal Tension Tests, *ACI Journal*, Vol.28, No.2, Aug 1956, pp. 157-172.
31. Taub J., and Neville A.M., Resistance to Shear of Reinforced Concrete Beams Part 1-Beams without Web Reinforcement, *ACI Journal*, Vol. 32, No.2, Aug 1960, pp. 193-298.
32. Mathey R.C. and Watsein D., Shear Strength of Beams Without Web Reinforcement Containing Deformed Bars of Different Yield Strengths, *ACI Journal*, Vol. 60, No.2, Feb 1963, pp.184-206.
33. Acharya D.N. and Kemp K.O., Significance of Dowel Forces on the Shear Failure of Rectangular Reinforced Concrete Beams Without Web Reinforcement, *ACI Journal*, Vol. 62, No. 10, Oct 1960, pp. 1265-1279.
34. Krefeld W.J. andThurston C.W., Studies of the Shear and Diagonal Tension Strength of Simply Supported Reinforced Concrete Beams, *ACI Journal*, Vol.63, No.4, Apr 1966, pp. 451-476.
35. Kani G.N.J., Basic Facts Concerning Shear Failure, *ACI Journal*, Vol.63, No.6, June 1966, pp. 675-692.
36. Rajagopalan K.S. and Ferguson P.M., Exploratory Shear Tests Emphasizing Percentage of Longitudinal Steel, *ACI Journal*, Aug 1968, pp. 634-638.

37. Zsutty T.C., Shear strength prediction for separate categories of simple beam tests, *ACI Journal*, Feb 1971, pp. 138-143.
38. Swamy R.N., Andriopoulos A., and Adepegba D., Arch action and bond in concrete shear failures, *Journal of the Structural Division*, ASCE Proceedings, Vol.96, No. ST6, June 1970, pp.1069-1091.
39. Mphone A.G. and Frantz G.C., Shear Tests of High and Low Strength Concrete Beams Without Stirrups, *ACI Journal*, June 1984, pp. 350-357.
40. Kim W., and White R.N., Initiation of Shear Cracking in Reinforced Concrete Beams with No Web Reinforcement, *ACI Structural Journal*, Vol.88, No.3, June 1991, pp. 301-308.
41. Rebeiz K.S., Shear Strength Prediction for Concrete Members, *Journal of Structural Engineering*, Vol.125, No. 3, Vol.125, No. 3, March 1999, pp. 301-308.
42. Rebeiz K.S., Fente J., and Frabizzio M.A., Effect of Variables on Shear Strength of Concrete Beams, *Journal of Materials in Civil Engineering*, ASCE, Vol. 13, No.6, Dec 2001, pp. 467-470.
43. Russo G., Somma G. and Mitri D., Shear Strength Analysis and Prediction for Reinforced Concrete Beams without Stirrups, *Journal of Structural Engineering*, ASCE, Vol.131, No. 1, Jan 2005, pp. 66-74.
44. Arslan G., Cracking shear strength of RC slender beams without stirrups, *Turkish Journal of Engineering & Environmental Sciences*, 2007.
45. Braestrup M.W., Plastic analysis of shear in reinforced concrete, *Magazine of Concrete Research*, Vol. 26, No. 89, Dec 1974, pp 221-228.
46. Nielsen M.P., Braestrup M.W., Jensen B.C. and Bach F., Concrete Plasticity - beam shear - shear in joints - punching shear, *Copenhagen: Danish Society for Structural Science and Engineering*, Oct 1978.
47. British Standard Institution, BS8110: The structural use of concrete, Part 1, 1997.
48. Eurocode 2, BS EN1992 -1-1: Design of concrete structures. General rules and rules for buildings, 2004.
49. American Concrete Institute Committee, ACI 318, Building code requirement for reinforced concrete, *ACI*, Detroit, 1963.

50. Taub J. and Neville A.M., Resistance to Shear of Reinforced Concrete Beams Part 2-Beams with Vertical Stirrups, *ACI Journal*, Vol. 32, No.3, Sept 1960, pp. 315-336.
51. Bresler B. and Scordelis A.C., Shear Strength of Reinforced Concrete Beams, *ACI Journal*, Vol. 60, No.1, 1963, pp. 51-72.
52. Regan P.E., and Placas A., 1971. Shear Failure Ferguson P.M., Some Implications of Recent Diagonal Tension Tests, *ACI Journal*, Vol.28, No.2, Aug 1956, pp. 157-172.
53. Arslan G., Shear Strength of Reinforced Concrete Beams with Stirrups, *Materials and Structures*, 2008, pp. 113-122.
54. Kani G.N.J., How safe are Our Large Concrete Beams?, *ACI Journal*, Proceedings, Vol.64, No. 3, Mar. 1967, pp. 128-141.
55. Taylor H.P.J., Shear Strength of Large Beams, *Journal of the Structural Division*, Proceedings of the ASCE, Vol.98, No.ST11, Nov 1972, pp. 2473-2490.
56. Leonhardt F. and Walther R., The Stuttgart Shear Tests 1961, C.& .CA, Library Translation No.111: *Cement and Concrete Association*, London, England, 1961.
57. Bazant Z. P. and Kim J.K., Size Effect in Shear Failure of Longitudinally Reinforced Beams, *ACI Structural Journal*, Vol. 81, No.5, Oct 1984, pp. 456-468.
58. Bazant Z.P. and Sun H.H., Size effect in diagonal shear failure: Influence of Aggregate and Stirrups, *ACI Journal*, Aug 1987, pp 259-272.
59. Walraven J. and Lehwalter N., Size Effects in Short Beams Loaded in Shear, *ACI Structural Journal*, Vol. 91, No.5, Oct 1994, pp. 585-592.
60. Bazant Z.P. and Kazemi T., Size Effect on Diagonal Shear Failure of Beams without Stirrups, *ACI Structural Journal*, Vol.88, No.3, June 1991, pp. 268-276.
61. Short A., and Kinniburgh W., *Lightweight Concrete*, Third Edition, *Applied Science Publishers*, London, 1978.
62. Cossio R.D.Z., and Siess C.P., Behavior and Strength in Shear of Beams and Frames Without Web Reinforcement, *ACI Journal*, Vol. 56, No.41, Feb 1960.

Appendix A

OPSC Trial Mixes

Trial Mix no.	Mix Proportion (by volume 400ml) (Ordinary Portland Cement : Sand : Oil Palm Shell)	Water (ml)	Dry Weight (kg)	Saturated Dry Weight (kg)	Compressive Strength (7days) N/mm ²	Remarks
1	2 : 1 : 3.5	500	1.733		17.60	Looked solid.
2	2.5 : 1 : 3.5	500	1.774		18.80	Looked solid.
3	1.5 : 1 : 3	400	1.678		11.60	
4	1.5 : 1 : 4	500	1.571		6.50	Too watery mix
5	1.5 : 1 : 4	425	1.610	1.692	10.55	
6	1.5 : 1 : 3.5	400	1.633	1.715	11.20	
7	1.5 : 1.5 : 3.5	450	1.688	1.762	8.60	
8	2 : 1.5 : 3.5	500	1.735	1.806	15.50	
9	2.5 : 1.5 : 4.5	600	1.705	1.781	14.00	
10	2.5 : 1.5 : 3.5	550	1.765	1.834	17.50	
11	2 : 1 : 4	520	1.660	1.736	12.20	
12	2 : 2 : 4	550	1.719	1.797	11.47	
13	3 : 1 : 4	600	1.714	1.798	16.48	Too watery.
14	3 : 2 : 4	670	1.794	1.866	16.22	
15	2 : 1 : 3	440	1.704	1.776	14.65	Too watery.
16	2.5 : 1 : 3	500	1.767	1.843	19.17	Too watery.
17	1.5 : 1.5 : 3	390	1.723	1.797	11.16	
18	2 : 1.5 : 3	465	1.756	1.838	15.25	Too watery.

19	2.5 : 1.5 : 3	550	1.8	1.866	17.91	Too watery.
21	2 : 2 : 3	470	1.823	1.895	15.5	
22	2.5 : 2 : 3	550	1.841	1.914	17.8	
23	2.5 : 2 : 4	560	1.8	1.881	15.22	
24	2.5 : 1 : 4	500	1.747	1.825	16.34	
25	2 : 2 : 3.5	500	1.815	1.890	15.10	
26	2.5 : 2 : 3.5	570	1.816	1.895	15.24	
27	1.5 : 2 : 3.5	450	1.759	1.841	10.08	Watery
28	3 : 1 : 3	580	1.814	1.878	20.47	
29	1.5 : 1 : 2.5	315	1.757	1.814	16.76	
30	2 : 1 : 2.5	370	1.786	1.852	20.32	
31	2.5 : 1 : 2.5	450	1.818	1.880	20.34	A bit wet
32	3 : 2 : 3.5	600	1.873	1.933	21.34	A bit dry
33	1.5 : 1.5 : 2.5	375	1.778	1.836	12.80	
34	2 : 1.5 : 2.5	400	1.856	1.910	18.54	
35	2.5 : 1.5 : 4	500	1.794	1.855	19.05	
36	2.5 : 1.5 : 2.5	450	1.823	1.872	16.09	
37	3 : 2.5 : 4	700	1.823	1.872	16.09	
38	2.5 : 2.5 : 4	625	1.814	1.855	11.8	
39	4 : 1 : 3	700	1.844	1.901	25.83	
40	5 : 1 : 3	825	1.870	1.928	29.57	

Appendix B

OPS Aggregate Testing



TESTECH SDN. BHD. (207361-H)
Materials, Structures and Geotechnical Testing
 8, Jalan 306/146, Desa Tasik, Sg. Besi, 57000 Kuala Lumpur, West Malaysia.
 Tel: 03-90593587, 90593589 Fax: 03-90593455
 E-mail: inquiry@testech.com.my Website: www.testech.com.my
 North Office: 48, Jalan Perusahaan Jelutong 1, 11600 Pulau Pinang, West Malaysia.
 Tel: 04-2686551, 2686552 Fax: 04-2686550
 E-mail: testech@tm.net.my / penang@testech.com.my




TEST REPORT

ISSUED BY : KUALA LUMPUR OFFICE REPORT NO. : AGE 239/12/R 1360
 DATE : 23-Oct-12 PAGE NO. : 1 OF 4

- 1. Test Requested : 1. Determination of Aggregate Crushing Value Test.
2. Determination of Aggregate Impact Value Test.

- 2. Customer : UNIVERSITY OF NOTTINGHAM MALAYSIA CAMPUS
Jalan Broga
43500 Semenyih
Selangor Darul Ehsan.

- 3. Project : Internal Testing

- 4. Sample Description : OPS (Oil Palm Shell)

- 5. Date of Testing : 16-Oct-12 & 18-Oct-12

- 6. Method of Testing : 1. BS 812 : Part 110 : 1990
2. BS 812 : Part 112 : 1990

- 7. Category of Testing : Laboratory Testing

- 8. Equipment Used : E2/1,E2/9 (Balance), E9/3(Oven) - Traceable to Pyrometro.
E1/2 (Compressive Machine) -Traceable to Unit Test Scientific Sdn. Bhd.

- 9. Remarks : a) The above test is based solely on the sample submitted by customer.
b) No copy of this report is valid without original special red stamp.

The accuracy of test measurements are probability at 95% confidence level.
 Copyright of this test report is owned by the issuing laboratory and may not be reproduced other than in full except with the prior written approval of the Head of the issuing laboratory.

REPORT NO. : AGE 239/12/R 1360

PAGE NO. : 2 OF 4

Customer : UNIVERSITY OF NOTTINGHAM MALAYSIA CAMPUS
 Project : Internal Testing
 Source : OPS (Oil Palm Shell)
 Sample Description : OPS (Oil Palm Shell) Lab. Ref : C828/12

SUMMARY OF LABORATORY TEST RESULTS

Item	Test Requested	Results	Measurement Uncertainty, %
1	Aggregate Crushing Value (%)	5.9	± 0.02
2	Aggregate Impact Value Test (%)	8.4	± 0.06

Certified by,




Yap Seow Keong
Technical Manager

Lab. Ref : C828/12

REPORT NO : AGE 239/12/R 1360

PAGE NO : 3 OF 4

AGGREGATE CRUSHING VALUE TEST

Customer : UNIVERSITY OF NOTTINGHAM MALAYSIA CAMPUS
 Project : Internal Testing
 Sample Description : OPS (Oil Palm Shell)
 Source : OPS (Oil Palm Shell)
 Oven Temperature : 110 °C
 Date Tested : 18-Oct-12
 Tested by : Sharif
 Verified by : Yap S.K
 Test Environmental Condition :- Temperature (Min.) : 28.4 °C (Max.) : 28.4 °C
 Relative Humidity (RH) (Min.) : 63.0% (Max.) : 63.0%

TEST METHOD : BS 812 : Part 110 : 1990

Test No.	1	2	Average
Mass of mould and base plate + Aggregate (g)	13414	13414	
Mass of mould and base plate (g)	12546	12546	
Mass of Aggregate, M_1 (g)	867.6	867.92	
Mass of material passing the designated test sieve size after applying 400kN force in 10 minutes, M_2 (g)	50.91	51.42	
Aggregate Crushing Value $\frac{M_2}{M_1} \times 100$ (%)	5.9	5.9	5.9

AGGREGATE CRUSHING VALUE, ACV = 5.9 %

MEASUREMENT UNCERTAINTY = ± 0.02 %

- Remarks 1. Aggregate size fraction is Smaller than standard size, passing 10.0mm and retained on 6.30mm test sieve.
 2. Aggregate test at dry condition.

Certified by

Yap Seow Keong
Technical Manager



Lab. Ref: C828/12

REPORT NO. : AGE 239/12/R 1360

PAGE NO. : 4 OF 4

AGGREGATE IMPACT VALUE TEST (DRY CONDITION)

Customer : UNIVERSITY OF NOTTINGHAM MALAYSIA CAMPUS
 Project : Internal Testing
 Material : OPS (Oil Palm Shell)
 Source : OPS (Oil Palm Shell)
 Date Tested : 16-Oct-12
 Test Environmental Condition : - Temperature (Min.) : 28.7 °C (Max.) : 28.8 °C
 Relative Humidity (RH) (Min.) : 66.0% (Max.) : 66.0%

Tested by : Sharif
Verified by : Yap S.K

TEST METHOD : BS 812 : Part 112 : 1990

TEST NO.	1	2	AVG
Mass Of Tray + Crushed Aggregate (g)	865.21	861.11	
Mass of Tray (g)	752.99	752.99	
Mass of Aggregate (Initial), M_1 (g)	112.22	108.12	
Mass of Material Passing on the designated test sieve size after crushing, M_2 (g)	9.4	9.0	
Mass of Material Retained on the designated test sieve size after crushing, M_3 (g)	102.8	99.1	
Aggregate Impact Value (AIV) $\frac{M_2}{M_1} \times 100$ %	8.4	8.4	8.4
Measurement Uncertainty %	± 0.06	± 0.06	± 0.06

AGGREGATE IMPACT VALUE (AIV) = **8.4** %

MEASUREMENT UNCERTAINTY (%) = **± 0.06** %

- REMARKS :
- 1) Standard Test Aggregate Sieve Passing 14.0mm and retained on 10.0mm Test Sieve.
 - 2) Aggregate tested at dry condition.
 - 3) The test specimen is subject to 15 such blow and each being delivered at an interval at not less than 1 second.
 - 4) Weight all the mass to the nearest 0.1g.
 - 5) If the total mass of ($M_2 + M_3$) differs from the initial mass M_1 more than 1g, discard the results and test a further specimens.
 - 6) The sample being delivered to TESTECH SDN BHD by customer, therefore TESTECH is not responsible on correctness in sampling

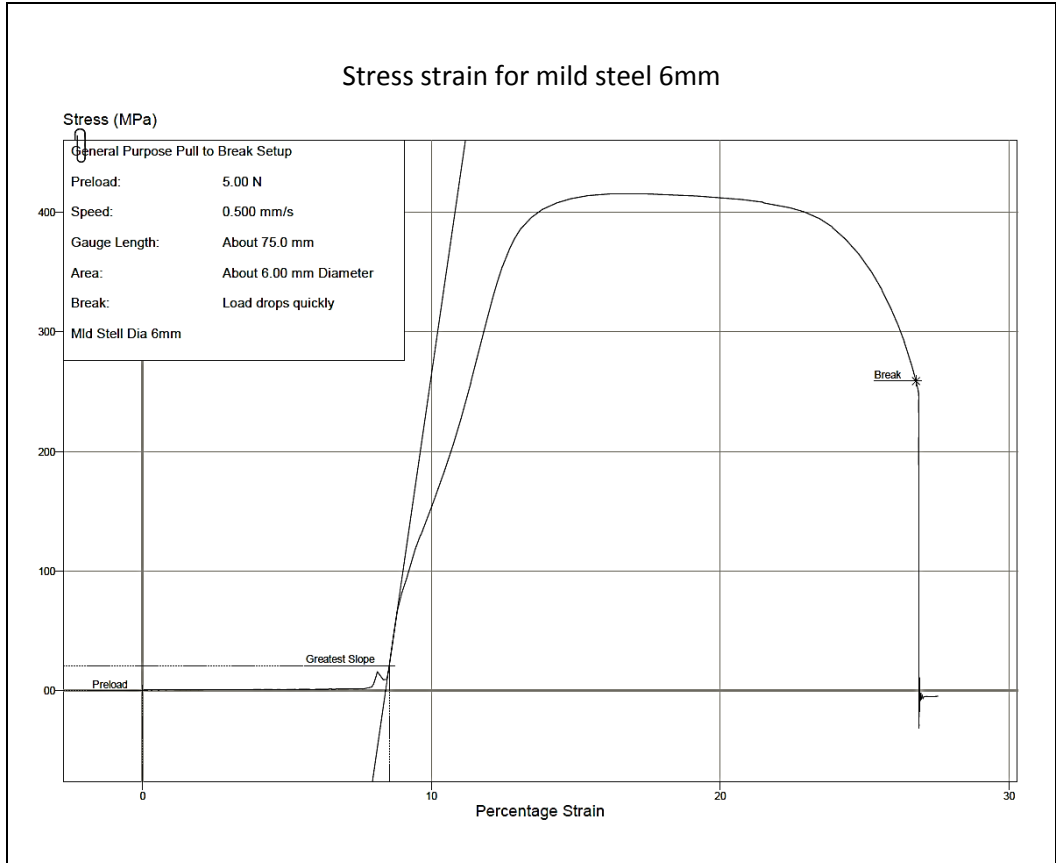
Certified by,



Yap Siew Keong
Technical Manager

Appendix C

Yield strength of Steel Reinforcement



Appendix C

Beam design

Beams were designed to fail in Shear. The beam design is as follow:

1) Beams without shear reinforcement

To ensure the beam to fail in shear, $M_{Rd} > M_{max}$

Beam length = 1.5 m, width = 105 mm and height = 200 mm

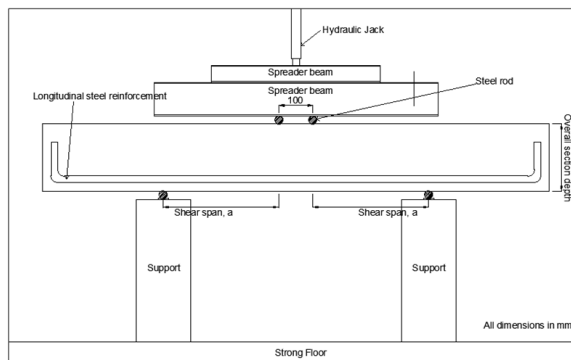
$d = 200 \text{ mm} - 25 \text{ mm} - 0.5 (20 \text{ mm}) = 160 \text{ mm}$

$z = 0.9 d = 144 \text{ mm}$

Using the variable strut inclination method from EC2 [48] for beams without shear reinforcement,

$$V_{Rd \max} = \frac{f_{ck} b_w z v_1}{\beta (\cot \theta + \tan \theta)} = \frac{(25 \text{ MPa} \times 105 \text{ mm} \times 144 \text{ mm} \times 0.54) b_w z v_1}{1 (\cot 22^\circ + \tan 22^\circ)}$$

$$= 70.90 \text{ kN}$$



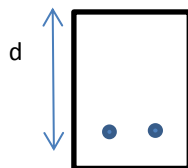
For a/d ratio = 2.5, the shear span length, $a = 425 \text{ mm}$

Self-weight of concrete = $0.2 \text{ m} \times 0.105 \text{ m} \times 25 \text{ MPa} = 0.525 \text{ kN/m} \times 1.5 \text{ m} = 0.75 \text{ kN}$

$$M_{max} = \frac{0.5 (1.5^2)}{8} + 70.90 \text{ kN} \frac{0.425 \text{ m}}{2} = 15.21 \text{ kNm}$$

Using reinforced concrete beam stress block design,

Adopt 2T20 for tension reinforcement,



$$\text{Let say } k = 0.14, z = d \left(0.5 + \sqrt{0.25 - \frac{k}{1.134}} \right) = 137 \text{ mm}$$

$$s = 2 (d-z) = 50 \text{ mm}$$

$$x = s/0.8 = 62.5$$

$$\begin{aligned} M_{Rd} &= 0.87 f_{yk} A_s z \\ &= 0.87 \times 500 \text{ N/mm}^2 \times 2 \pi (10)^2 \times 137 \text{ mm} \\ &= 37449498 \text{ Nmm} = 37.45 \text{ kN m} \end{aligned}$$

$(M_{Rd} = 37.45 \text{ kN}) > (M_{max} = 15.21 \text{ kNm})$, Hence the beam would fail in shear.

2) Beams with shear reinforcement

To ensure the beam to fail in shear, $M_{Rd} > M_{max}$

Beam length = 1.5 m, width = 105 mm and height = 200 mm

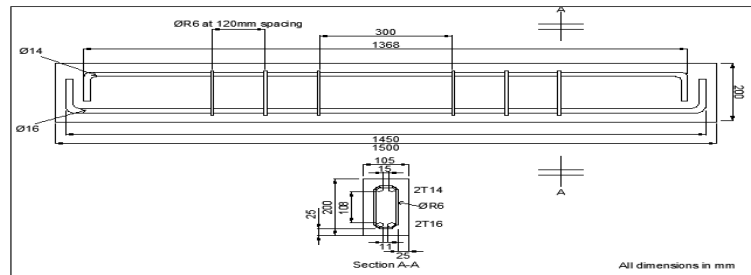
$$d = 200 \text{ mm} - 25 \text{ mm} - 0.5 (16\text{mm}) = 167 \text{ mm}$$

$$z = 0.9 d = 150\text{mm}$$

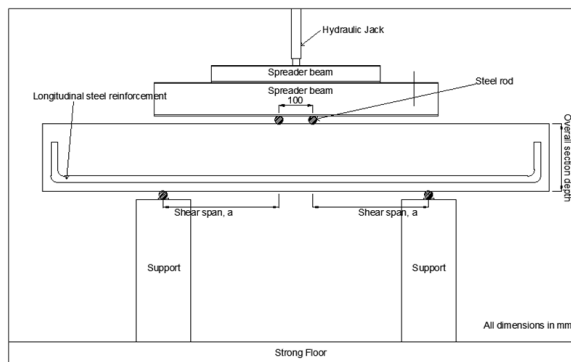
Using the variable strut inclination method from EC2 [48] for beams with shear reinforcement,

$$\begin{aligned} V_{Rd \max} &= \frac{f_{ck} b_w z v_1}{\beta (\cot \theta + \tan \theta)} = \frac{(25 \text{ MPa} \times 105 \text{ mm} \times 150 \text{ mm} \times 0.54) b_w z v_1}{1 (\cot 22^\circ + \tan 22^\circ)} \\ &= 73.85 \text{ kN} \end{aligned}$$

Using R6- 120 mm spacing,



$$V_{Rd s} = 0.87 \frac{A_{sw}}{s} z f_{yk} \cot \theta = 0.87 \frac{2 \pi (3)^2}{120 \text{ mm}} \times 150\text{mm} \times 410\text{MPa} \times \cot 22^\circ = 62.41\text{kN}$$



The shear span length, $a = 240\text{mm}$

Self-weight of concrete = $0.2 \text{ m} \times 0.105 \text{ m} \times 25 \text{ MPa} = 0.525 \text{ kN/m} \times 1.5 \text{ m} = 0.75 \text{ kN}$

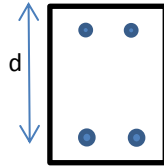
$$M_{max} = \frac{0.5 (1.5^2)}{8} + 73.85 \text{ kN} \frac{0.24\text{m}}{2} + 62.41 \text{ kN} (0.12\text{m}) = 43.08 \text{ kNm}$$

Using reinforced concrete beam stress block design,

Adopt 2T16 for tension reinforcement and 2T14 for compression reinforcement,

$$d = 200 \text{ mm} - 25 \text{ mm} - 0.5 (16\text{mm}) = 167 \text{ mm}$$

$$d' = 25 \text{ mm} + 7 \text{ mm} = 32 \text{ mm}$$



$$A_s = 2 \pi 8^2 = 402.18 \text{ mm}^2$$

$$A_{s'} = 2 \pi 7^2 = 307.72 \text{ mm}^2$$

$$F_{st} = F_{cc} + F_{sc}$$

$$0.87 f_{yk} A_s = 0.567 f_{ck} b s + 0.87 f_{yk} A_{s'}$$

$$s = (0.87 f_{yk} (A_s - A_{s'})) / (0.567 f_{ck} b)$$

$$= (0.87 \times 500 \text{ N/mm}^2 \times (402.18 \text{ mm}^2 - 307.72 \text{ mm}^2)) / (0.567 \times 25 \text{ MPa} \times 105 \text{ mm})$$

$$= 27.6 \text{ mm}$$

Taking moment about the tension steel,

$$M_{Rd} = 0.87 f_{yk} A_{s'} (d - d') + 0.567 f_{ck} b s (d - s/2)$$

$$= [0.87 \times 500 \text{ N/mm}^2 \times 2 \pi (7)^2 \times (167 \text{ mm} - 32 \text{ mm})] + [0.567 \times 25 \text{ MPa} \times 27.6 \text{ mm} \times (167 - 27.6/2)]$$

$$= 18082367 \text{ N mm} + 59936436 \text{ Nmm} = 78.01 \text{ kN m}$$

$(M_{Rd} = 78.01 \text{ kNm}) > (M_{\max} = 43.08 \text{ kNm})$, Hence the beam would fail in shear.

Appendix C

Theoretical Plastic Models

A.1 Beams without Shear Reinforcement

$$f\left(\frac{a}{h}\right) = \frac{V_{\text{Test}} \sin \theta}{0.5 \sigma_c (1 - \cos \theta) b h f(\rho) f(h) f(\sigma_c)}$$

$$f(\rho) = \frac{V_{\text{Test}} \sin \theta}{0.5 \sigma_c (1 - \cos \theta) b h f\left(\frac{a}{h}\right) f(h) f(\sigma_c)}$$

$$f(\sigma_c) = \frac{V_{\text{Test}} \sin \theta}{0.5 \sigma_c (1 - \cos \theta) b h f\left(\frac{a}{h}\right) f(\rho) f(h)}$$

$$f(h) = \frac{V_{\text{Test}} \sin \theta}{0.5 \sigma_c (1 - \cos \theta) b h f\left(\frac{a}{h}\right) f(\rho) f(\sigma_c)}$$

A.2 Beams with Shear Reinforcement

$$f(\sigma_c) = \frac{[V_{\text{Test}} - (f_{yk} b h v \rho_s \frac{1}{\tan \theta})] \sin \theta}{0.5 (1 - \cos \theta) \sigma_c b h}$$

$$f(\rho_s) = \frac{V_{\text{Test}} - \left(\frac{0.5 (1 - \cos \theta) v \sigma_c b h}{\sin \theta}\right)}{f_{yk} b h \left(\frac{1}{\tan \theta}\right)}$$

$$f\left(\frac{1}{\tan \theta}\right) = \frac{V_{\text{Test}} - \left(\frac{0.5 (1 - \cos \theta) v \sigma_c b h}{\sin \theta}\right)}{f_{yk} b h \rho_s}$$

Appendix D

BS8110 Design Models

B.1 Beams without Shear Reinforcement

$$f\left(\frac{a}{d}\right) = \frac{V_{\text{Test}}}{0.79 b d \frac{400^{1/4}}{d} \rho^{1/3} \frac{f_{cu}^{1/3}}{25}}$$

$$f(\rho) = \frac{V_{\text{Test}}}{0.79 b d (2d/a) \left(\frac{400^{1/4}}{d}\right) \frac{f_{cu}^{1/3}}{25}}$$

$$f(f_{cu}) = \frac{V_{\text{Test}}}{0.79 b d (2d/a) \left(\frac{400^{1/4}}{d}\right) \rho^{1/3}}$$

$$f(k) = \frac{V_{\text{Test}}}{0.79 b d (2d/a) \rho^{1/3} \frac{f_{cu}^{1/3}}{25}}$$

B.2 Beams with Shear Reinforcement

$$f\left(\frac{A_{sw}}{s}\right) = \frac{V_{\text{Test}} - \left(0.79 \rho^{1/3} \frac{f_{cu}^{1/3} 4 \sqrt{400}}{25} \right)}{\frac{0.87 f_{yv}}{b s}}$$

$$f(f_{cu}^{1/3}) = \frac{V_{\text{Test}} - \left(\frac{0.87 f_{yv} A_{sw}}{b s}\right)}{0.79 b d (2d/a) \left(\frac{400^{1/4}}{d}\right) \rho^{1/3}}$$

$$f\left(\frac{a}{d}\right) = \frac{V_{\text{Test}} - \left(\frac{0.87 f_{yv} A_{sw}}{b s}\right)}{0.79 \rho^{1/3} \frac{f_{cu}^{1/3} 4 \sqrt{400}}{25}}$$

Appendix E

Eurocode 2 Design Models

C.1 Beams without Shear Reinforcement

$$f\left(\frac{a}{d}\right) = \frac{V_{\text{Test}}}{0.18 b d \rho^{1/3} \left(1 + \frac{200}{d}\right) f_{ck}^{1/3}}$$

$$f(\rho) = \frac{V_{\text{Test}}}{0.18 b d \left(2d/a\right) \left(1 + \frac{200}{d}\right) f_{ck}^{1/3}}$$

$$f(f_{ck}) = \frac{V_{\text{Test}}}{0.18 b d \left(2d/a\right) \left(1 + \frac{200}{d}\right) \rho^{1/3}}$$

$$f(k) = \frac{V_{\text{Test}}}{0.18 b d \left(2d/a\right) \rho^{1/3} f_{ck}^{1/3}}$$

C.2 Beams with Shear Reinforcement

$$f(\cot \theta) = \frac{V_{\text{Test}}}{0.87 f_{ywd} z \left(\frac{A_{sw}}{s}\right)}$$

$$f\left(\frac{A_{sw}}{s}\right) = \frac{V_{\text{Test}}}{0.87 f_{ywd} z \cot \theta}$$